Alternative electron transfer pathways in iron-metabolising bacteria

Laura Gomez Perez

Ph. D. Thesis

School of Biological Sciences, University of East Anglia

September, 2018

Statement

The work submitted in this thesis is my own work, except where due reference is made to other authors, and has not been submitted to this or any other University for any degree.

Abstract

Ferric iron (Fe^{3+}) can be used as a terminal electron acceptor by iron-reducing microorganisms to facilitate cellular respiration under anoxic conditions. In contrast, ferrous iron (Fe^{2+}) is used as an electron donor by iron-oxidising microorganisms. The presence of dissimilatory pathways in iron metabolisers maintain bioavailable iron in the environment for other organisms. Redox reactions between gram-negative bacteria and iron usually occur through an extracellular electron transport (EET) pathway that allows electrons to cross from the inner membrane to the extracellular environment or vice versa. The study of the redox pathway has been thoroughly studied in the iron reducer *Shewanella oneidensis*, however, there is little information about the metabolic pathways used by other iron metabolisers. In this thesis, the environmental isolates *Acinetobacter* and *Citrobacter* have been described as novel iron reducing bacteria by using a combination of techniques including ferrozine assays, cytochrome identification methods and transcriptomic analysis. Results in this thesis suggest that *Acinetobacter* (previously described as a strict aerobic microorganism) in fact is capable of respiring using iron when oxygen is not available. In contrast, *Citrobacter*'s iron reduction pathway seems to involve fermentative processes. These results point out that extracellular electron transport is not the only mechanism in dissimilatory iron metabolism. Moreover, these results suggest that anaerobic environments could be a reservoir for pathogenic strains of *Acinetobacter*, as it has been shown that this species do not require oxygen to survive. In addition to the study of new iron reducers, an overexpression system has been developed to study proteins involved in metal oxidation pathways without the need of culturing the notoriously slow-growing iron oxidising bacteria. The genes *cyc2* and *cyc2*$_{PV-1}$, which encode outer membranes cytochromes from *Acidithiobacillus ferrooxidans* and *Mariprofundus ferrooxydans* respectively, have been transformed into the iron reducer *Shewanella oneidensis* for protein expression optimization. The optimization of this process offers great possibility for the future study and applications of metal oxidation pathways.

Acknowledgements

Firstly, I would like to thank Tom, David and Gary, for giving me the opportunity of doing a PhD and for the supervision during the last four years.

To Richard and Daniel for making the examination process enjoyable and rewarding.

A special thanks to Marcus, for being the best post doc anyone could wish for and helping not just me, but everyone else in the lab, anytime and regardless of how busy you were. A paragraph in this thesis is not enough to thank you.

To all the people in Lab 2.30. I feel really lucky to have spent four years surrounded by such kind, supportive and fun people. Thank you for making me feel welcome from the very first day. I am going to miss you.

To Jon, for being a wonderful English teacher and sharing so many great adventures around England and Spain.

To Raquel, for sharing a bunch of wonderful moments with me as well as making sure that I survived during the bad ones.

To Carlota, Eli, Alfons, Kontxi, Núria and Laura, who have proved that distance is no obstacle to friendship.

To Edu, for pushing me out of my comfort zone when I did not know which path I should follow as well as for his unbroken support.

To my brother, because I know that he really wants to be part of this list.

Finalmente, darles las gracias a mis padres, por haberme apoyado tanto moralmente como económicamente en mis estudios. Sin vosotros no habría llegado hasta aquí.

Le dedico esta tesis a mi yayo, por creer en mi.

Table of Contents

List of Tables and Figures

List of Abbreviations

3PG – 3-Phosphoglyceric acid

AckA – Acetate kinase

ACO – Aconitase

ADP – Adenosine diphosphate

APS – Ammonium persulphate

ATP – Adenosine triphosphate

Car^R – Carbenincillin resistant

cDNA – Complementary DNA

CMC – Critical micelle concentration

CoA – Coenzyme A

Complex I – NADH dehydrogenase

Complex II – Succinate dehydrogenase

Complex III – bc$_1$ complex

Complex IV – Terminal oxidase

Complex V – ATP synthase

CS – Citrate synthase

DDM – n-Dodecyl-beta-Maltoside

DNA – Deoxyribonucleic acid

DNP – 2,4-Dinitrophenol

DNRA – Dissimilatory Nitrate Reduction to Ammonium

E˚ – Potential (V)

EDTA – Ethylenediaminetetraacetic acid

EET – Extracellular electron transfer

ETC – Electron transport chain

FDH – Formate dehydrogenase

Ferrozine – 3-(Pyridin-2-yl)-5,6-bis(4-sulfophenyl)-1,2,4-triazine disodium salt

FH – Fumarase

FPKM – Fragments per kilobase million

G3P – Glyceraldehyde 3-phosphate

HEPES – 4-(2-hydroxyethyl)-1-piperazineethanesulfonic acid

IDH – Isocitrate dehydrogenase

K – Stability constant

Kan^R – Kanamycine resistant

LB – Luria Bertani

LDAO – Lauryldimethylamine oxide

LDH – Lactate dehydrogenase

MALDI-TOF – Matrix Assisted Laser Desorption/Ionization Time Of Flight

MDH – Malate dehydrogenase

ME – Malic enzyme

MFC – Microbial fuel cell

mRNA – Messenger RNA

Mto – Metal oxidation

Mtr – Metal reduction

MWMM – Modified Wolfe's Mineral Media

NADH – Nicotinamide adenine dinucleotide

NADHP – Nicotinamide adenine dinucleotide phosphate

NGS – Next-generation sequencing

NMR – Nuclear magnetic resonance spectroscopy

NTA – Nitrilotriacetic acid

OD – Optical density

OGD – α-ketoglutarate dehydrogenase

OGP – Octyl β-D-glucopyranoside

PAGE – Polyacrylamide gel electrophoresis

PCR – Polymerase chain reaction

PDH – Pyruvate dehydrogenase

PEP – Phosphoenolpyruvate

PEPCK – PEP carboxykinase

PFL – Pyruvate formate-lyase

PKM – Pyruvate kinase

PMF – Proton motive force

Pta – Phosphotransacetylase

PVDF – Polyvinylidene difluoride

Q – Quinone

QH – Quinol

RCF – Relative centrifugal force

RNA – Ribonucleic acid

rpm – Revolutions per minute

rRNA – Ribosomal RNA

RuBP – Ribulose 1,5-bisphosphate

RVG – Raveningham

Sarkosyl – Sodium-lauryl Sarcosinate

SCS – Succinyl-CoA synthetase

SD – Standard deviation

SDS – Sodium dodecyl sulfate

TCA – Tricarboxylic acid

TEMED – Tetramethylethylene-diamine

TMA – Trimethylamine

TMAO – Trymethylamine *N*-oxide

TMBD – 3-3'-5,5'-tetramethyl-benzidine dihydrochloride hydrate

Tris – Tris(hydroxymethyl) aminomethane

Tween 20 – Polysorbate 20

UEA – University of East Anglia

WGB – Withlingham Great Broad

WT – Wild type

General introduction

1.1 Biodiversity

Ecology studies how different organisms interact with each other and with their environment. Recent evidence suggests life began roughly 3.8 billion years ago, ever since then, organisms have adapted to survive in a wide variety of niches on Earth and they have been found in every environment analysed including soil, fresh water, oceans, inside other organisms, air and even in extreme environments such as acidic mines, where the pH is around 0, or hydrothermal vents, where temperature can reach 400 ˚C and 300 bars of pressure (Xu, 2006). In order to survive in an ecosystem, organisms can transform the abiotic components of the environment or interact with other populations that are co-existing with them (Braga *et al.*, 2016).

The three fundamental questions in ecology are "what is there?", "how many are there?" and "what can they do?". To answer these questions, there are three main focuses of study: diversity, abundance and organism activity (Atlas and Bartha, 1998).

The study of diversity focuses on identifying different species that can be found in an ecosystem, from viruses to multicellular organisms, including the Archaea and Bacteria microorganism domains. Some environments, like soil, have a high diversity of species co-existing, while others, including deep sea environments have much less diversity (Atlas and Bartha, 1998).

The study of organism abundance in an environment measures the amount of individuals that are found in an ecosystem and analyse how populations change over time due to the availability of nutrients and due to prey-predator interactions. For example, in a sediment environment there is a high amount of nutrients and the abiotic factors remain constant, therefore, the populations remain very stable. In contrast, in environments such as the atmosphere, air currents regularly disperse

and re-distribute populations creating fluctuations in the abundance of populations (Atlas and Bartha, 1998).

Finally, the study of organism activity focuses on the different processes that organisms can do in order to survive in a specific ecosystem. This ecology area explores biogeochemical cycles, inter-organism communication and metabolic processes that organisms can use in order to adapt to their environment (Atlas and Bartha, 1998).

1.2 Bioenergetics and metabolism

All forms of life need a carbon and an energy source from the environment to survive. The carbon source is transformed into organic macromolecules such as carbohydrates, lipids, amino acids or nucleotides, which are essential to build cellular structures. The set of metabolic pathways required to construct these macromolecules are part of anabolic metabolism, and the reactions involved in these pathways require energy. In order to achieve these endergonic processes and maintain anabolic cellular functions, living organisms need to acquire energy from the environment. This energy can be obtained from the thermodynamically favourable redox reactions that occur as a result of electrons being exchanged between molecules with different electron affinities. Multiple redox reactions can happen in chain reactions to maximise efficiency. The energy produced in these exergonic redox reactions can be stored by cells as ATP and used later on for endergonic reactions (Nelson *et al.*, 2013).

Organisms have evolved to survive in a wide variety of environments with different abiotic and biotic factors limiting their growth conditions. They can be classified according to their tolerance to different abiotic factors such as temperature, pH, pressure or salinity (Rampelotto, 2013). Alternatively, they have been divided in different groups according to the catabolic pathways they use to obtain energy (Table 1-1).

Table 1-1 Catabolism classification for all organisms

Energy source	Carbon source	Types
Chemotrophs: Energy obtained from the oxidation of chemical compounds	**Chemoheterotrophs:** Organic molecules as the carbon source and as the electron donor	**Aerobic respiring organisms:** O_2 as the terminal electron acceptor in respiration
		Anaerobic respiring organisms: O_2 is not used for respiration. Other inorganic or organic molecules as terminal electron acceptors in respiration
		Fermentative organisms: Organic molecules are oxidised to produce ATP without respiring. Endogenous organic molecules as terminal electron acceptors
	Chemoautotrophs: Fixed CO_2 as the carbon source	**Aerobic chemolitotrophs:** Inorganic molecules as electron donors in aerobic respiration
		Anaerobic chemolitotrophs: Inorganic molecules as electron donors in anaerobic respiration
Phototrophs: Energy obtained from photons	**Photoautotrophs:** Fixed CO_2 as the carbon source	**Oxygenic photoautotrophs:** H_2O as the electron donor for CO_2 reduction
		Anoxygenic photoautotrophs: H_2O is not used for CO_2 reduction. Other inorganic or organic molecules are the electron donors
	Photoheterotrophs: Organic molecules as the carbon source and as the electron donors	

Depending on which carbon source they use, organisms can be autotrophs or heterotrophs. Autotrophic organisms can fix CO_2 and produce the organic molecules needed for their cellular functions while heterotrophic organisms have to obtain exogenous organic molecules as they cannot incorporate carbon at the level of CO_2 (Nelson *et al.*, 2013).

According to how they obtain energy, organisms can also be classified as chemotrophs or phototrophs. While chemotrophic organisms use the redox potential difference between chemical compounds at their ground state,

phototrophic organisms absorb light to bring molecules into a higher energy excited state which result in more energetically profitable redox reactions (Bird *et al.*, 2011; Nelson *et al.*, 2013).

Regardless of the pathways used to obtain the energy, all forms of life initiate the energy chain producing redox reactions with an exogenous molecule acting as an electron donor and a molecule acting as the terminal electron acceptor. For each individual redox reaction to be thermodynamically favourable, the molecule to be oxidised (electron donor) has to have a lower affinity for electrons than the molecule to be reduced (electron acceptor), therefore, the redox potential of the electron donor has to be lower than the redox potential of the electron acceptor. Heterotrophs can use exogenous organic molecules both as the carbon source and as the electron donor for their redox reactions. In contrast, autotrophs cannot use CO_2 as the electron donor so they have to use other organic molecules or inorganic molecules such as metals or nitrogen compounds (Nelson *et al.*, 2013; Choi *et al.*, 2015).

Organisms can use either endogenous or exogenous molecules as terminal electron acceptors. Fermentative organisms use endogenous organic molecules while respiring organisms use exogenous terminal electron acceptors. When the terminal electron acceptor is oxygen, it is considered aerobic respiration. However, if there is no oxygen in the environment, other organic or inorganic molecules can be used in anaerobic respiration (Pinchuk *et al.*, 2011; Nelson *et al.*, 2013).

1.3   The iron cycle

With an abundance of 5 %, iron is the fourth most common element in the Earth's crust and the second most abundant metal (Lutgens and Tarbuck, 2000; Weber *et al.*, 2006). This transition metal can exist in different oxidation states, from Fe^{2-} to Fe^{6+}. However, in nature it is mostly found as ferrous iron (Fe^{2+}) and ferric iron (Fe^{3+}) (Hedrich *et al.*, 2011).

The abiotic transition between ferrous iron (Fe^{2+}) and ferric iron (Fe^{3+}) depends on the oxygen concentration and the pH of the environment. Oxygen

spontaneously oxidises iron into different forms of iron(III) oxides (such as hematite, magnetite or goethite). The reaction kinetics of this process directly correlates with the pH. The speed of the iron oxidation decreases the more acidic the media is, until pH 4, where the reaction is so slow that most of the iron remains as ferrous iron (Fe^{2+}) (Morgan and Lahav, 2007; Johnson *et al.*, 2012).

Around 40 % of known enzymes require a metal ion cofactor in order to perform catalysis. Iron is a limiting nutrient for most organisms as it plays a functional role in many biochemical processes. This metal is incorporated in the cells and is bound within hemeproteins. Some of the functions that these types of proteins carry out in the cells are essential for the cell survival, such as oxygen transport, redox reactions or protection against oxidative damage (Schröder *et al.*, 2003; Rosato *et al.*, 2016).

Although very abundant, iron is only bioavailable when it is found in its soluble form. While ferrous iron (Fe^{2+}) can remain soluble both in acidic and circumneutral environments, ferric iron (Fe^{3+}) precipitates in neutral pH. For this reason, iron can be a limiting growth factor for cellular growth (Johnson *et al.*, 2012; Rose, 2012). Moreover, bioavailable iron is not evenly distributed among different environments. In aquatic systems with circumneutral pH, such as fresh water or oceans, iron molecules either form soluble complexes or they precipitate as oxides and sink out of the water column. In soils and sediments, iron is abundant but is commonly found as minerals. In acidic aquatic systems, such hot springs or acid mine drainage systems, iron remains soluble (Emerson *et al.*, 2012).

If the iron cycle was only affected by abiotic factors, acidophilic microorganisms would be the only forms of life able to grow. Fortunately, the oxidation state of iron can be changed by biotic activity too. Some microorganisms can use dissimilatory pathways to reduce or oxidise iron for energy production. Iron reducers use ferric iron (Fe^{3+}) as an electron acceptor, reducing it into ferrous iron (Fe^{2+}), while iron oxidisers use ferrous iron (Fe^{2+}) as an electron donor, oxidising it into ferric iron (Fe^{3+}). Both types of microorganisms still need to assimilate bioavailable iron for anabolic purposes, but they can also transform

soluble and insoluble iron forms, recycling non-available iron, allowing the survival of other species (Emerson *et al.*, 2012).

1.4   Coevolution of organisms and iron

Earth has undergone many biogeochemical changes since it was formed 4.5 billion years ago. The availability and oxidation state changes that iron has presented over time can be correlated with the presence of different microorganisms throughout different eons of Earth's history. Originally, the biosphere was anoxic and soluble ferrous iron was present in the ocean at a concentration of 10^{-9} M (Williams and Fraústo da Silva, 2003; Williams *et al.*, 2011).

It is thought that dissimilatory iron metabolisms have originated independently in different organisms during different periods of time and have evolved convergently (Ilbert and Bonnefoy, 2013). Anaerobic iron oxidisers are thought to be the first organisms able to metabolise iron. They would have used ferrous iron (Fe^{2+}) as an electron donor for anaerobic metabolism. As no oxygen was present in the oceans, the anaerobic respiration would have been coupled to nitrate as the terminal electron acceptor or by coupling it with anoxygenic photosynthesis (Mancinelli and McKay, 1988; Chaudhuri *et al.*, 2001).

Due to the iron oxidation activity, the ferric iron (Fe^{3+}) present in the circumneutral ocean would have precipitated creating Banded Iron Formation (BIF) depositions under anoxic conditions (Ehrenreich and Widdel, 1994). The presence of insoluble iron in anoxygenic environments could justify the subsequent emergence of dissimilatory iron reducing microorganisms (Ilbert and Bonnefoy, 2013).

It is believed that as anoxygenic photosynthesis transitioned to oxygenic photosynthesis in *Cyanobacteria*, the resultant oxygenation of the biosphere caused new BIFs due to the spontaneous iron oxidation produced by its reaction with oxygen (Pierson and Parenteau, 2000). The formation of different BIFs among time could explain the existence of iron reducers with convergent metal reducing pathways (Altermann, 2014). The presence of oxygen in the environment would

also allow aerobic iron oxidising microorganisms to accomplish aerobic respiration using oxygen as the terminal electron acceptor (Ilbert and Bonnefoy, 2013).

In circumneutral aerobic conditions, the ferric iron (Fe^{3+}) either precipitates or forms soluble complexes. The concentration of soluble iron in the ocean is 10^{-19} M, which is 10^{12} times less than when it was anoxic. Nonetheless, despite the decrease in iron bioavailability, organisms still needed iron as a nutrient. Unlike with other metals, proteins which use iron as a cofactor cover redox potentials from -0.5 V to +0.6 V, which represent most of the biological range of redox potentials (Pierre *et al.*, 2002). Various mechanisms have been developed to maximise iron bioavailability. Some organisms can secrete siderophores, which are iron-chelating compounds, to solubilise iron (Varma and Chincholkar, 2007). Other organisms secrete outside the cell iron reductases so they can acquire ferrous iron (Fe^{2+}) which is more soluble than ferric iron (Fe^{3+}) (Dancis *et al.*, 1992). Moreover, to scavenge iron whilst avoiding its toxicity, ferritins can be used to store iron in the cell without letting it precipitate inside the cell or reacting with oxygen (Carrondo, 2003).

1.5   Iron reducers

Respiring chemoheterotrophs obtain their energy from the oxidation of an organic carbon source. Generally, amino acids, monosaccharides and fatty acids are broken down via different catabolic pathways and converted into acetyl-CoA to take part in cellular respiration. Once these organic molecules are transformed into acetyl-CoA, they enter into the tricarboxylic acid (TCA) cycle (Figure 1-1).

A molecule of acetyl-CoA and a molecule of oxaloacetate are transformed by citrate synthase (CS) into citrate. Citrate is turned into isocitrate by aconitase (ACO) and isocitrate dehydrogenase (IDG) transforms it to α-ketoglutarate, gaining a molecule of NADH and producing a molecule of carbon dioxide. α-ketoglutarate is then turned into succinyl-CoA by α-ketoglutarate dehydrogenase (OGD), producing another molecule of NADH and carbon dioxide. Succinyl-CoA is transformed to succinate by succinyl-CoA synthetase, and a GTP molecule is produced. Succinate is oxidised to fumarate at the inner membrane by complex II (succinate dehydrogenase). Fumarate is converted to malate by

fumarase (FH) and finally, malate is transformed back into oxaloacetate by malate dehydrogenase (MDH), producing another molecule of NADH and completing the TCA cycle. The molecule of oxaloacetate obtained can start the TCA cycle again if more molecules of acetyl-CoA are available. To summarise, the TCA cycle catabolises organic molecules, oxidising them into CO_2. During the process, ATP is generated via substrate level phosphorylation and reducing power is produced in the form of NADH (Nelson *et al.*, 2013).
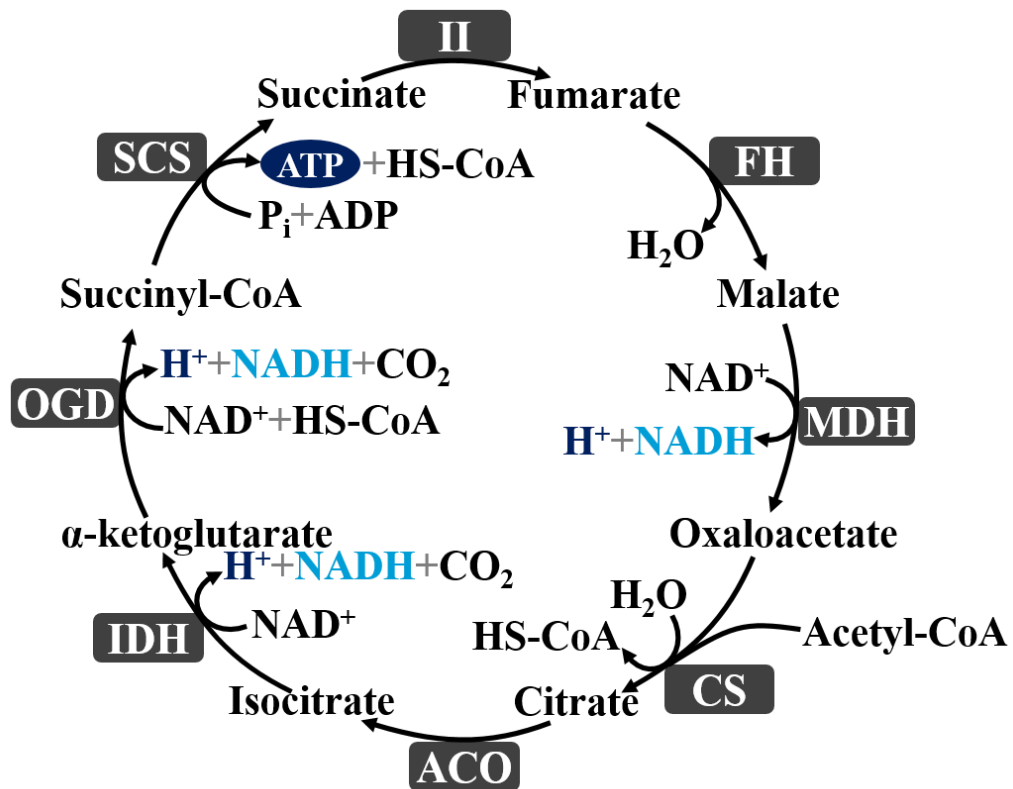
Figure 1-1 Tricarboxylic acid cycle
Overview of the TCA cycle. Enzymes are shown in boxes. Chemical reactions are shown in black arrows. Reducing power is shown in light blue. Processes contributing to energy generation are shown in dark blue.

Despite some ATP being produced in the TCA cycle, most of the ATP obtained during cellular respiration is produced by oxidative phosphorylation in an electron transport chain (ETC).

ETC are protein complexes that couple the energy produced by a chain of redox reactions with the creation of a proton gradient that drives the synthesis of

ATP. For an electron transport chain to be thermodynamically favourable, the electron donor should have a lower redox potential than the redox centres of the proteins involved in the process and in turn these must have a lower redox potential than the terminal electron acceptor.

In aerobic respiration, NADH (-0.32 V) and succinate (+0.03 V) are used as the electron donors and oxygen (+0.82 V) is used as the terminal electron acceptor (Reeve *et al.*, 2017). Different protein complexes (I, II, III and IV) use the energy generated by the redox reaction chain to drive the endergonic process of pumping protons from the cytoplasm to the periplasm across the inner membrane (Figure 1-2). In complex I (NADH dehydrogenase), NADH is oxidised producing NAD^+, a proton and two electrons. The energy produced by the redox reaction of a molecule of NADH is used to pump four protons from the cytoplasm to the periplasm. In addition, succinate is transformed into fumarate by complex II (succinate dehydrogenase). The electrons produced by reactions in complex I and complex II are used to drive the reduction of quinone (Q) into quinol (QH_2) using two cytoplasmic protons. The reduced quinone pool then acts as electron donor for complex III (bc_1 complex). Quinol binds on the periplasmic side of the protein as is reoxidized to quinone. The protons produced in this reaction are released into the periplasm. Finally, electrons are passed from complex III to complex IV (terminal oxidase), where the energy produced by the electron transport is used to pump another four protons to the periplasm and oxygen, acting as the terminal electron acceptor of the ETC, is reduced into water. The chemiosmotic proton gradient generated by complexes I, III and IV allows complex V (ATP synthase) to pump the protons back to the cytoplasm (exergonic reaction). The energy produced by this reaction is used to phosphorylate ADP (endergonic reaction) into ATP. ATP hydrolysis is a very exergonic reaction, allowing cells to use these molecules as a form of energy storage and use them to facilitate cellular endergonic reactions required for diverse metabolic processes (Nelson *et al.*, 2013).
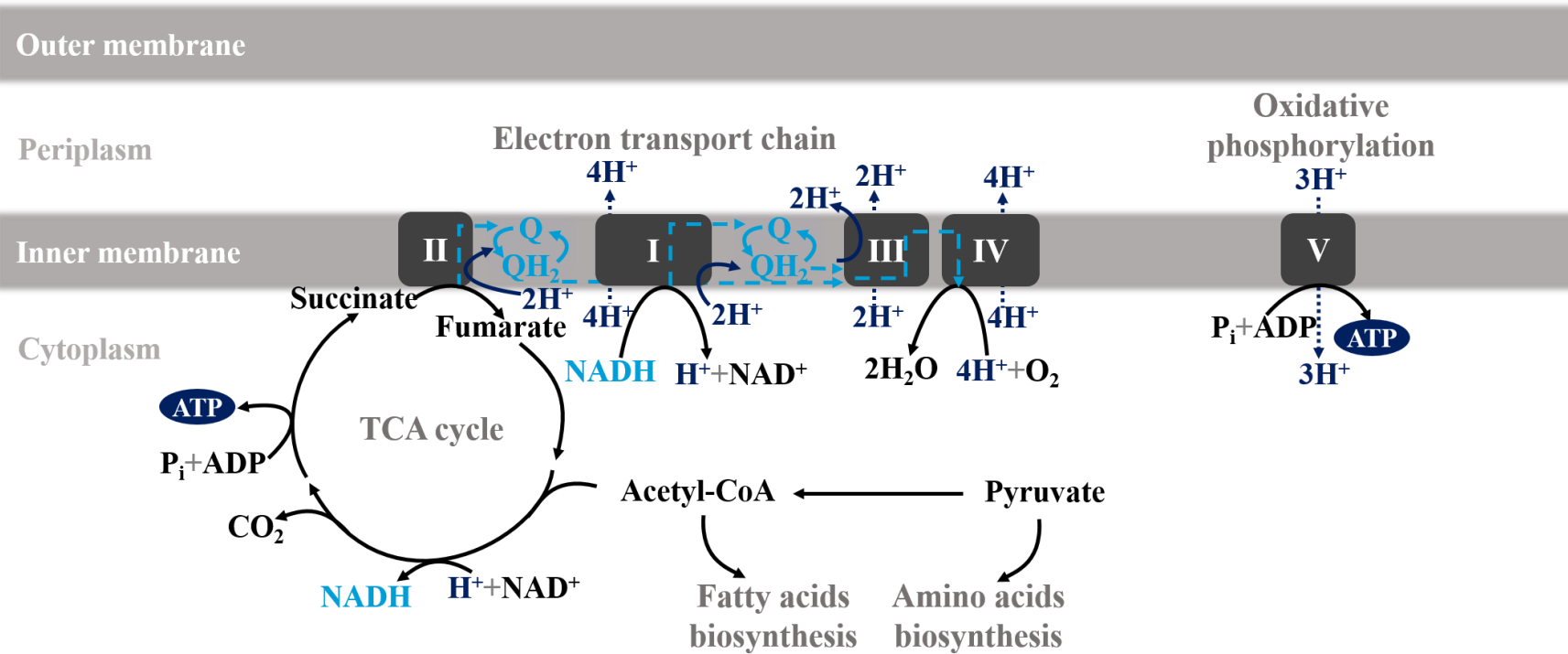
Figure 1-2 Chemoheterotroph aerobic respiration
Overview of aerobic cellular respiration in chemoheterotroph microorganisms. Enzymes are shown in boxes. Chemical reactions are shown in black arrows. Electron transfer is shown in light blue dashed arrows. Molecule transport across the inner membrane is shown in dotted arrows. Processes contributing to energy generation are shown in dark blue.

Iron reducing microorganisms can accomplish cellular respiration when oxygen is not available in the environment by using ferric iron (Fe^{3+}) as the terminal electron acceptor (Myers and Nealson, 1990). In anaerobic conditions, complex IV (terminal oxidase), which reduces oxygen into water, is not necessary for the ECT (White *et al.*, 2016).

Neutrophilic iron reducers can use soluble ferric iron (Fe^{3+}) complexes like Fe(III)citrate (-0.37 V) or insoluble ferric minerals such as goethite (-0.274 V) (Ilbert and Bonnefoy, 2013; Reeve *et al.*, 2017). The difference in the redox potentials between ferric iron (Fe^{3+}) species and NADH is smaller than between oxygen and NADH but still thermodynamically favourable.

During iron reduction respiration, electrons flow from complexes I and II to the quinone pools. From there, instead of going to complex IV, electrons go through a metal-reducing (Mtr) pathway and finally ferric iron (Fe^{3+}) acts as the terminal electron acceptor and is reduced to ferrous iron (Fe^{2+}) (White *et al.*, 2016).

To avoid the accumulation of ferric iron (Fe^{3+}) inside the cells, Mtr pathways in Gram-negatives typically consist on a group of proteins organised in a vertical way, from the inner membrane to the outer membrane so electrons can flow outside the cell and iron can be reduced extracellularly (Ilbert and Bonnefoy, 2013).

The microorganisms typically used as a model for iron reduction respiration are *Shewanella oneidensis* and *Geobacter sulfurreducens*. These two gram-negatives use cytochromes, which are heme-containing proteins able to oxidise and reduce their iron centres, as their electron carriers (Allen *et al.*, 2005). Their Mtr pathways are very similar, where *c*-type cytochromes are located in the inner membrane, the periplasm and the outer membrane, forming an electric cable that allows electron transport and extracellular iron reduction (Lovley, 2006; Shi, Rosso, Clarke, *et al.*, 2012; Liu *et al.*, 2014).

To achieve long distance electron transport, both bacteria are able to form nanowires. *Shewanella* nanowires are extensions of the outer membrane and the periplasm, and their conductivity is correlated with the amount of

c-type cytochromes expressed along the wire (Gorby *et al.*, 2006; Pirbadian *et al.*, 2014). On the other hand, *Geobacter* nanowires are pili with metallic-like conductivity of their own, that allow electron transport without requiring c-type cytochromes across the pili. Still, a c-type cytochrome is necessary at the end of the nanowire to reduce ferric iron (Fe^{3+}) (Y. Liu *et al.*, 2014; Malvankar *et al.*, 2015) By using these nanowires, *Shewanella* and *Geobacter* can reach insoluble metals more easily.

1.5.1. *Shewanella oneidensis* MR-1

Shewanella oneidensis MR-1 was the first isolated microorganism known for being able to achieve dissimilatory metal reduction. It was discovered by Myers and Nealson in 1988 as a bacterium able to reduce manganese oxide as the sole electron acceptor. Further studies discovered that it is a facultative aerobe able to use not just manganese, but also other compounds such as fumarate, dimethyl sulfoxide (DMSO), nitrate, sulphite, chromium, uranium or iron to achieve respiration when oxygen is not available (Marshall *et al.*, 2006; Pinchuk *et al.*, 2011).

Species of the *Shewanella* genus can be found in different aquatic and sediment environments, being more abundant in the sea. As it can inhabit environments with different environmental conditions, this bacterium has mechanisms to resist fluctuations in temperature and pH, it is able to survive with high pressures, it is osmotolerant and can form biofilms (Thormann *et al.*, 2004; Yin and Gao, 2011). Moreover, it can use both chemotaxis and energy taxis to find more energetic environments for anaerobic respiration (Bencharit and Ward, 2005; Schweinitzer and Josenhans, 2010).

As the first iron-metaboliser discovered, *Shewanella* has been thoroughly studied and its Mtr pathway has been characterised. As a chemoheterotroph, *Shewanella* catabolises an organic carbon source to use it both as the carbon source and the electron donor source. As when it is growing aerobically, the carbon source is broken down until acetyl-CoA and its finally oxidised into CO_2 while producing molecules of NADH and some ATP by substrate phosphorylation (Figure 1-1).
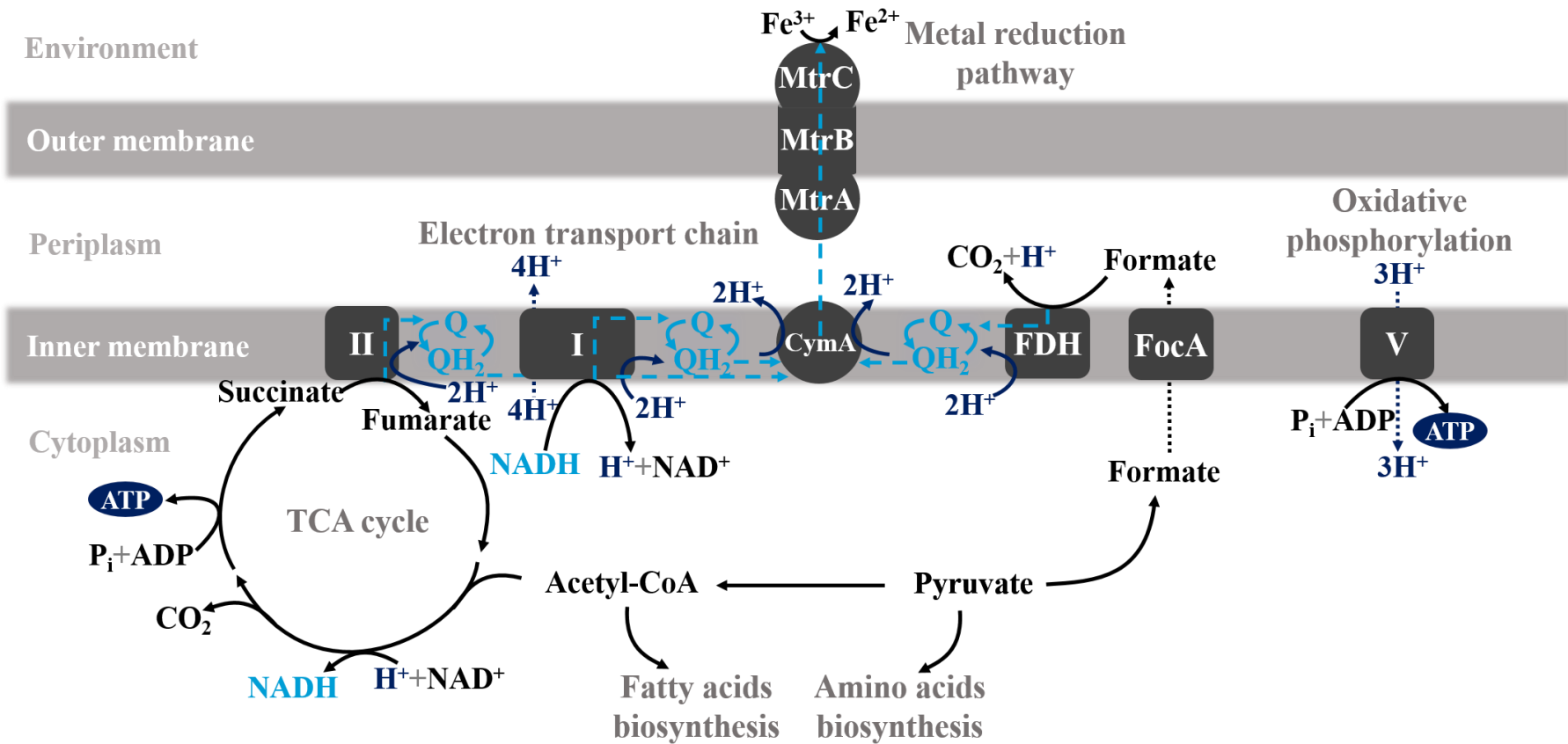
Figure 1-3 Shewanella oneidensis MR-1 chemoheterotroph anaerobic respiration
Overview of Shewanella dissimilatory metal reduction pathway. Enzymes are shown in boxes. Chemical reactions are shown in black arrows. Electron transfer is shown in light blue dashed arrows. Molecule transport across the inner membrane is shown in dotted arrows. Processes contributing to energy generation are shown in dark blue.

In the ETC, NADH (-0.32 V) is oxidised by complex I and succinate (+0.03 V) is oxidised by complex II (Figure 1-3). As in aerobic conditions, the energy obtained by the redox reaction in complex I is used to pump protons from the cytoplasm to the periplasm and the electrons transferred from both complexes go to a quinol pool. The proton gradient force produced by the ETC is used to generate ATP at complex V (Scott, 2017).

Unlike in aerobic respiration, the ETC does not include complexes III and IV, as oxygen is not the terminal electron acceptor. Contrarily, electrons are transferred via the quinone pool to an inner membrane tetraheme *c*-type cytochrome (CymA), the first protein of *Shewanella*'s Mtr pathway. From CymA, electrons are transferred to the periplasm, where a decaheme *c*-type cytochrome (MtrA) is facing the periplasm embedded in an outer membrane porin (MtrB). MtrA transfers the electrons to MtrC, an outer membrane decaheme *c*-type cytochrome located at the other side of MtrB and exposed to the external media. Using the MtrB porin, MtrA and MtrC are connected so electrons can cross the outer membrane (Marritt *et al.*, 2012; McMillan *et al.*, 2012; Shi, Rosso, Clarke, *et al.*, 2012; Beckwith *et al.*, 2015). From the location of the hemes in the resolved structure of MtrC (Figure 1-4) it is thought that the hemes in MtrA and MtrC form an electric wire that facilitate electron transfer across the outer membrane (Edwards *et al.*, 2015).

Although the MtrCAB complex seems to be the vertical electron transfer pathway, *Shewanella* expresses other *c*-type cytochromes in addition to MtrC, to optimise the direct transfer of electrons to the ferric iron (Fe^{3+}) species at the outer membrane (Johs *et al.*, 2010) .

In addition, if direct contact between the cell surface and the terminal electron acceptor is not possible, the cell can secrete flavins to reduce iron indirectly (Shi, Rosso, Clarke, *et al.*, 2012; White *et al.*, 2013).
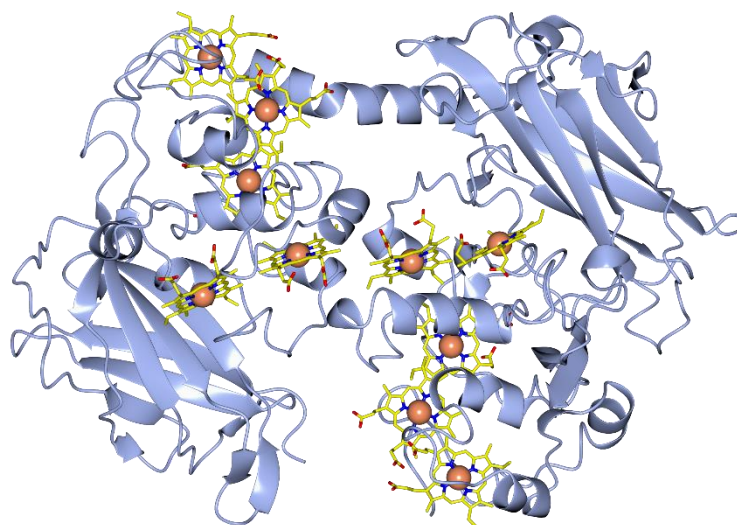
Figure 1-4 Crystal structure of MtrC
Cartoon representation of MtrC. The polypeptide chain is shown in light blue, the iron atoms are represented in orange and the porphyrin rings of the hemes are shown as yellow sticks (Edwards et al., 2015).

Beside *Shewanella*'s importance from a biogeochemical point of view, this iron reducer has a role in some industrial applications. *S. oneidensis* MR-1 is used in bioremediation to decontaminate heavy metal polluted areas. Unlike iron, some heavy metals are more soluble in their oxidised forms than in their reduced forms. Bioremediation using iron reducers is used to precipitate these metals so they can be removed manually from the environment. *S. oneidensis* MR-1 has been used to reduce chromium (VI) to chromium (III), cobalt (III) to cobalt (II), technetium (VII) to technetium (IV) and uranium (VI) to uranium (IV) (Lall and Mitchell, 2007; Cheng *et al.*, 2013).

In addition, due to its ability to transfer electrons to an external electron acceptor, they can be used to produce electricity in microbial fuel cells (Figure 1-5). *S. oneidensis* MR-1 is cultured in an anaerobic chamber, growing as an anaerobic chemoheterotroph. Instead of transferring electrons to ferric iron (Fe^{3+}) through the Mtr pathway, *Shewanella* transfers the electrons to an electrode. The anode, which is soaked in the anaerobic chamber, is connected to a circuit, allowing the electricity generated to be used to power electronic devices. To complete the electrical circuit the electrons flow to the cathode, which is typically found in an aerobic chamber.

Oxygen acts as the terminal electron acceptor, being reduced into water. Both chambers are connected by a selective membrane that allows the protons to flow so oxygen reduction is not limited by the amount of protons available (Ishii et al., 2008; Cheng et al., 2013).
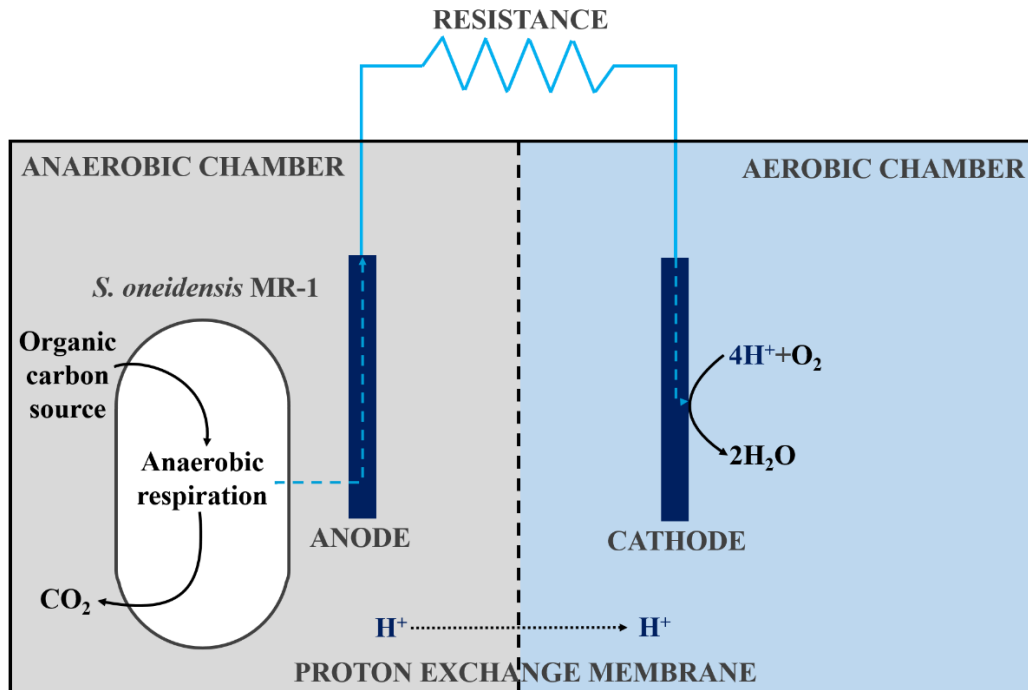
Figure 1-5 Microbial fuel cell
Overview of S. oneidensis MR-1 growing in a MFC. Chemical reactions are shown in black arrows. Electron transfer is shown in light blue dashed arrows. Molecule transport across the inner membrane is shown in dotted arrows.

This method has a high research interest due to the economic impact that could have in the future if the process is optimised and large amounts of energy can be produced by growing this bacterium.

1.6 Iron oxidisers

Iron oxidisers are autotrophic microorganisms, which fix CO_2 and transform it into organic molecules through the Calvin cycle. There are three main steps in this anabolic pathway. Firstly, carbon dioxide is fixed into an organic molecule (RuBP) and transformed into two molecules of 3PG, which are more stable. Secondly, NADPH and ATP are used to reduce 3PG into G3P. G3P takes part both in the Calvin cycle and the metabolism of pyruvate. Consequently, after being anabolised in the Calvin cycle, G3P molecules can be catabolised for energy production through cellular respiration. G3P molecules are also used in the last step of the Calvin cycle, being transformed back into RuBP to be able to start the cycle again. This last process also consumes ATP (Nelson *et al.*, 2013).

G3P can be transformed into pyruvate, and this into acetyl-CoA so the TCA cycle can be driven from CO_2 fixation. The NADH consumed in the Calvin cycle is recovered in the TCA cycle. However, not enough NADH is available to generate ATP through the ETC for the cell to function (Nelson *et al.*, 2013). For this reason, autotrophic organisms require an external electron donor other than the carbon source to accomplish cellular respiration. Iron-oxidising microorganisms use ferrous iron (Fe^{2+}) as the additional electron donor for the ETC. The energy generated from iron oxidation is enough to pump protons to the periplasm to generate ATP. Furthermore, part of the energy is used for an uphill electron transfer where complex I pumps protons from the periplasm to the cytoplasm and reduces NAD^+ back to NADH so more reducing power can be used for CO_2 fixation. A $NAD(P)^+$ transhydrogenase is used to transform NADH into NADPH as this is the form of reducing power used in the Calvin cycle (Bird *et al.*, 2011; White *et al.*, 2016).

Even though the metabolisms of iron reducers and iron oxidisers are very different, there are certain similarities in the way they transport electrons between the cell and the iron source. After *Shewanella*'s Mtr pathway was characterised, Gram-negative iron oxidisers were identified with homologous pathways, where *c*-type cytochromes were located at the outer membrane, the periplasm and the

inner membrane forming a vertical electron transport pathway. *Sideroxydans lithotrophicus*, *Rhodopseudomonas palustris* and *Dechloromonas aromatica* even contain genes in their genome that may encode for outer membrane porins to help the electron transfer between the outer membrane and the periplasm as MtrB does in *Shewanella oneidensis* MR-1 (Shi, Rosso, Zachara, *et al.*, 2012). Gram-positive bacteria and Archaea iron oxidisers would not encode *c*-type cytochromes in the suggested metal-oxidizing (Mto) pathway but produce other electron transport proteins like *b*-type cytochromes, iron-sulfur proteins or copper proteins for an extracellular iron oxidation (White *et al.*, 2016).

According to the environment they are found, iron oxidisers have been classified into 3 different groups: neutrophilic anaerobes, neutrophilic aerobes and acidophilic aerobes (Hedrich *et al.*, 2011).

1.6.1. Neutrophilic anaerobic iron oxidisers

Anaerobic iron oxidisers are thought to be the first group of microorganisms to use iron as an electron donor. In circumneutral conditions, the oxidation of ferrous iron (Fe^{2+}) species (+0.37 V for Fe(II)citrate) can be coupled with the reduction of nitrate (+0.43 V) or anoxygenic photosynthesis (+0.45 V for the midpoint potential of photosystem I) (Widdel *et al.*, 1993; Reeve *et al.*, 2017; Scott, 2017). Anaerobic oxidation is not possible in acidic environments as the redox potential of iron (+0.77 V) is higher than the redox potential of the electron acceptors and the redox reaction would not be thermodynamically favourable (Ilbert and Bonnefoy, 2013). The free energy of anaerobic iron oxidation does not allow microorganisms to grow very fast as the redox potentials of the electron donor and the electron acceptor are very similar (Chakraborty *et al.*, 2011; Pechter *et al.*, 2015)

Rhodopseudomonas palustris is a Gram-negative bacterium that can oxidise iron while growing photoautotrophically. Although ferrous iron (Fe^{2+}) can be used as the sole electron donor, *R. palustris* is commonly grown with a complementary organic carbon source to increase its growth rate, culturing it both as a

photoautotroph and a chemoheterotroph (Bose and Newman, 2011; Pechter *et al.*, 2015).

The Mto pathway of *R. palustris* has been described as a homologous pathway of the Mtr pathway in *S. oneidensis* MR-1 (Figure 1-6). As an autotrophic microorganism, it consumes ATP and NADPH to fix CO_2 in the Calvin cycle and the produced organic molecules enter pyruvate metabolism until they are transformed into acetyl-CoA. Acetyl-CoA is used for the TCA cycle, where some ATP is produced by substrate level phosphorylation and NADH is also produced.

As in iron reducers, NADH is oxidised by complex I resulting in the transport of protons to the periplasm, and succinate is oxidised by complex II. In both reactions electrons are transferred to the quinone pool, transferring protons into the periplasm and electrons to complex III were more protons move from the cytoplasm to the periplasm. The proton gradient produced by complexes I, II and II is used to generate ATP at complex V.

Although ferrous iron (Fe^{2+}) is thought to be oxidised extracellularly, no *c*-type cytochrome facing the outer membrane is predicted for this Mto pathway. Nonetheless, an outer membrane porin (PioB) embeds a *c*-type cytochrome facing the periplasm (PioA). The electrons flow from PioA to an iron-sulfur periplasmic protein (PioC) and from there, to the reaction centre at the inner membrane (Jiao and Newman, 2007; White *et al.*, 2016). As the midpoint potential of the reaction centre (+0.45 V) is higher than the midpoint potential of complex III (+0.2 V), light is required to bring the reaction centre into a higher energy excited state (-1 V) so electrons can be transferred downhill from the reaction centre to complex III, where more protons are pumped to the periplasm. Moreover, an uphill reaction is produced where protons are transported back to the cytoplasm and electrons flow from the quinone pool (+0.113 V) to complex I to produce NADH (-0.32 V) (Widdel *et al.*, 1993; Bird *et al.*, 2011; Reeve *et al.*, 2017; Scott, 2017).
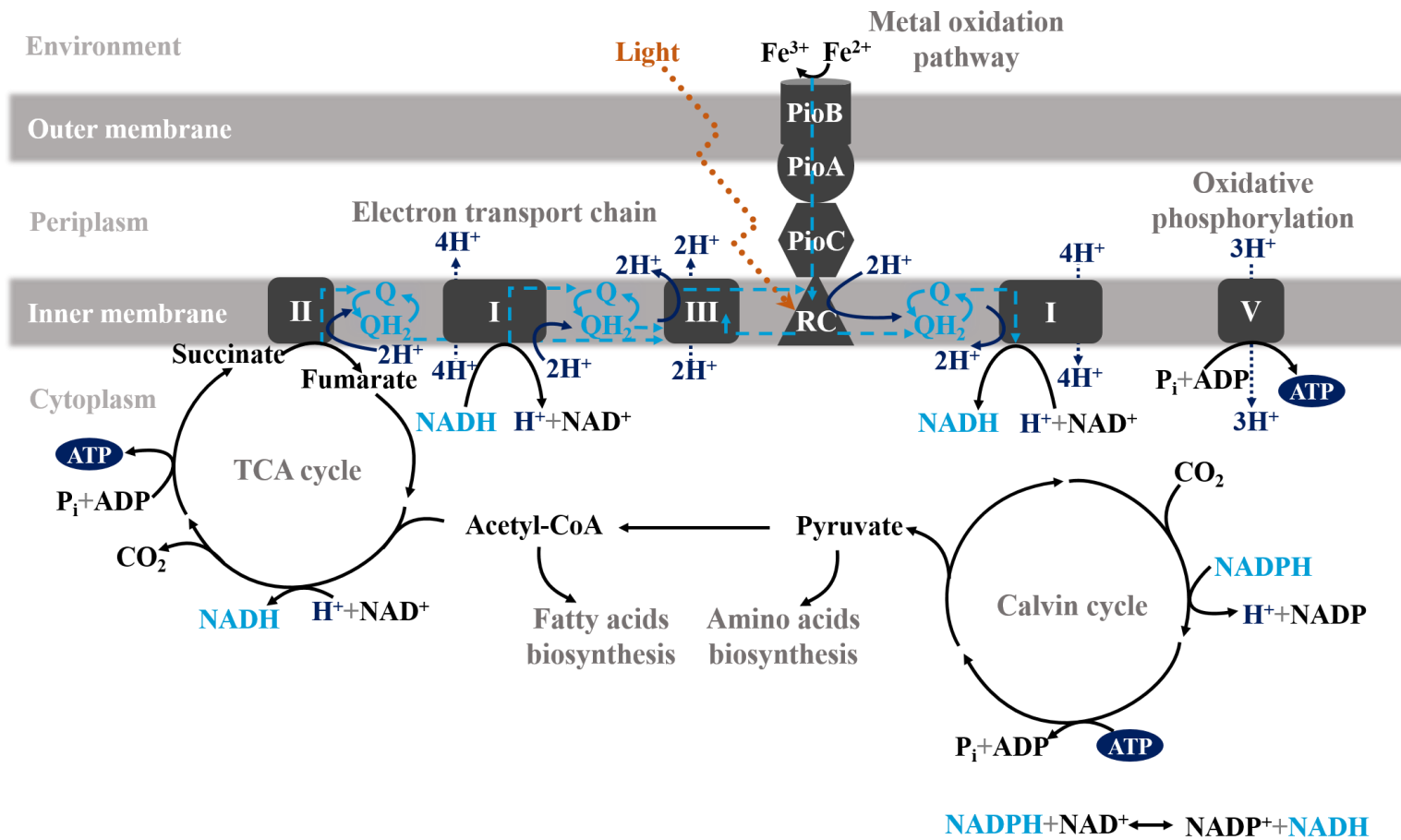
Figure 1-6 Rhodopseudomonas palustris anaerobic photoautotroph metabolism
Overview of Rhodopseudomonas palustris iron oxidation coupled to anoxygenic photosynthesis. Enzymes are shown in boxes. Chemical reactions are shown in black arrows. Electron transfer is shown in light blue dashed arrows. Molecule transport across the inner membrane is shown in dotted arrows. Processes contributing to energy generation are shown in dark blue.

Very little is known about anaerobic iron oxidation coupled to nitrate reduction. It is unclear if the nitrate reduction is directly linked to a thermodynamically favourable enzymatic oxidation of ferrous iron (Fe^{2+}), or if contrarily, there is an abiotic reaction between nitrite and iron during nitrate reduction and iron does not have any energetic function for the cell (Carlson *et al.*, 2012). However, even studies that support the first theory have not been able to couple iron oxidation with nitrate reduction with iron as the sole electron donor, and chemoheterotroph metabolism has been required for these bacteria to grow by the addition of a supplementary organic source (Muehe *et al.*, 2009; Chakraborty *et al.*, 2011).

Dechloromonas aromatica is a Gram-negative bacterium that has been associated with iron oxidation and has a predicted Mto pathway homologous to *Shewanella*'s Mtr pathway. *D. aromatica* has genes associated with CO_2 fixation, but as iron oxidation has not been shown in autotrophic conditions, it is uncertain if this bacterium is able to transform CO_2 into organic molecules (Salinero *et al.*, 2009).

The carbon source is transformed into acetyl-CoA, entering in the TCA cycle and producing reducing power and ATP (Figure 1-7). NADH is oxidised to NAD^+ in complex I and the energy produced is used to pump protons from the cytoplasm to the periplasm. Moreover, succinate is oxidised to fumarate in complex II. The electrons from complex I and II are transported to the quinone pool, translocating more protons from the cytoplasm to the periplasm and allowing electrons to finally pass to a nitrate reductase for the reduction of nitrate. This reaction is thought to occur at the periplasmic side of the inner membrane (White *et al.*, 2016).
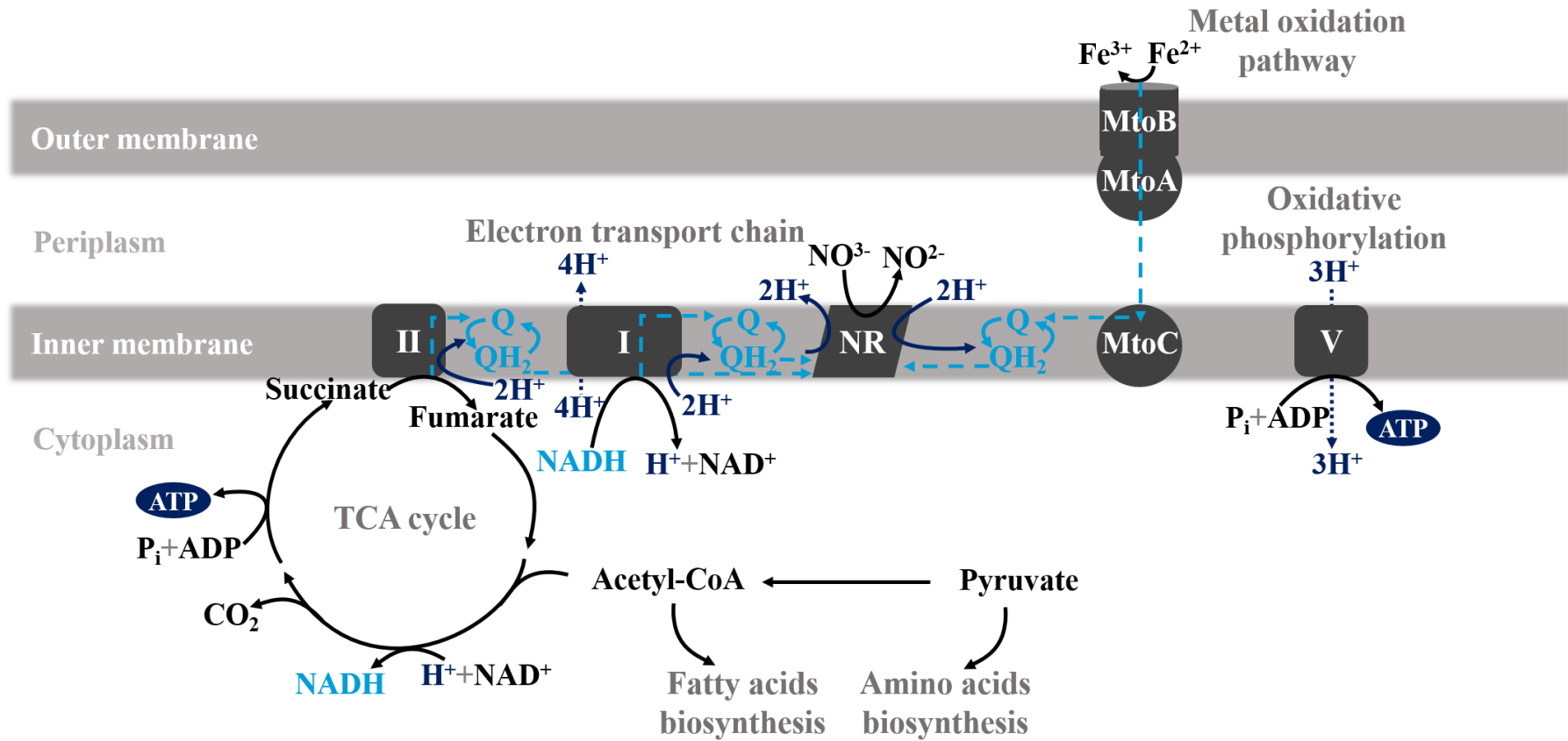
Figure 1-7 Dechloromonas aromatica anaerobic chemolitotroph metabolism

Overview of Dechloromonas aromatica iron oxidation coupled to nitrate reduction. Enzymes are shown in boxes. Chemical reactions are shown in black arrows. Electron transfer is shown in light blue dashed arrows. Molecule transport across the inner membrane is shown in dotted arrows. Processes contributing to energy generation are shown in dark blue.

Ferrous iron (Fe^{2+}) is thought to be oxidised extracellularly and, as in *R. palustris*, no outer membrane *c*-type cytochrome facing the exterior has been identified. However, an outer membrane porin (MtoB) is thought to have a *c*-type cytochrome (MtoA) embedded, facing to the periplasm. At the inner membrane, another *c*-type cytochrome (MtrC) could be receiving the electrons from the periplasm and transferring them to the quinone pool, where more protons would be transferred to the periplasm. Finally, the electrons would reduce nitrate via the nitrate reductase.

The presence of predicted *mto* genes in *D. aromatica* suggests that the Mto pathway could increase the amount of protons transported to the periplasm to create the proton gradient force required to generate ATP. However, it is not clear if the Mto pathway is necessary for the bacteria to survive, or if, anaerobic respiration alone produces enough ATP to cover the energetic requirements of the cell (Chakraborty and Coates, 2005; White *et al.*, 2016).

Both photosynthetic and nitrate reducers microorganisms are predicted to present an extracellular iron oxidation pathway, to avoid the precipitation of oxidised ferric iron (Fe^{3+}) in the cytoplasm that would cause toxicity to the cell (Ilbert and Bonnefoy, 2013).

1.6.2. Acidophilic aerobic iron oxidisers

Once the biosphere became oxygenated, metabolisms evolved to use oxygen as the electron acceptor for cellular respiration due to its high redox potential (+0.82 V at pH 7) (Ilbert and Bonnefoy, 2013; Reeve *et al.*, 2017). In fact, in acidic environments where iron remains soluble with a redox potential higher than at neutral pH (+0.77 V), oxygen is the only electron acceptor available for a thermodynamically favourable electron transfer. Still, the difference of potentials between the electron donor and the electron acceptor is at its thermodynamic limit and, accordingly, these bacteria have a very slow growth (Ilbert and Bonnefoy, 2013).

Acidithiobacillus ferrooxidans was the first isolated iron oxidizing acidophile. This Gram-negative lives in acidified natural environments, growing optimally at pH 2 (Molchanov *et al.*, 2007).

As an autotroph, *A. ferrooxidans* is also able to turn CO_2 into an organic carbon source through the Calvin cycle, by consuming NADHP and ATP. The produced organic molecules can be used to generate acetyl-CoA and start the TCA cycle, which as mentioned previously, produces ATP and NADH (Figure 1-8). As aerobic microorganisms, the ETC works the same way as with aerobic chemoheterotrophs, using the released energy to pump protons into the periplasm using complexes I, III and IV. As aerobic respiring organisms, oxygen acts as the terminal electron acceptor. However, *A. ferrooxidans*, as an anaerobic iron oxidiser, uses part of the NADH produced in the TCA cycle to restore the NADHP consumed in the Calvin cycle, so there is not enough reducing power to generate all the ATP that the cell requires (Nelson *et al.*, 2013).

In *A. ferrooxidans*, ferrous iron (Fe^{2+}) is used as the electron donor and also to reduce NAD^+ into NADH. Like in anaerobic iron-metabolisers, the Mto pathway of aerobic iron oxidisers is organised vertically, not just to avoid iron precipitation inside the cytoplasm (neutral pH), but also to prevent oxidative stress caused by ferric iron (Fe^{3+}) reacting with oxygen (Ilbert and Bonnefoy, 2013).

A. ferrooxidans Mto pathway is slightly different from other pathways homologous to *Shewanella*'s Mtr pathway. Instead of *c*-type cytochromes embedded in a porin, the outer membrane cytochrome (Cyc2) is predicted to function both as an electron transporter and as a porin. Therefore, ferrous iron (Fe^{2+}) (+0.77 V) is oxidised extracellularly by Cyc2 and transported to a periplasmic copper protein (RusA). From RusA, electrons go to two different *c*-type cytochromes (Cyc1 and Cyc42). From Cyc1, a downhill electron transport goes to complex IV, where oxygen (+0.82 V) is reduced to water and protons are transported to the periplasm. With the energy generated in the downhill redox reaction, an uphill electron transport goes from Cyc42 to complex I to restore the concentrations of NADH (-0.32 V), transporting some of the protons from the

periplasm back to the cytoplasm (Yarzábal *et al.*, 2002; Ilbert and Bonnefoy, 2013; White *et al.*, 2016; Reeve *et al.*, 2017).

Although the Mto pathway of *A. ferrooxidans* it is not fully understood yet, the study of this bacterium holds a great interest for industrial applications as it is one of the microorganism used in bioleaching processes. While traditional leaching has been used to extract metals from ores by the use of toxic compounds like cyanide, bioleaching is a cleaner method that uses the ability of iron oxidising microorganisms as part of the mineral extracting process (Kleinman and Crerar, 1979; Valdés *et al.*, 2008).

For example, during the copper extraction from chalcopyrite ($CuFeS_2$) from an acidic mine, ferric iron (Fe^{3+}) spontaneously oxidises the mineral (Zhao *et al.*, 2013):

$$CuFeS_2 + 4\,Fe^{3+} \rightarrow Cu^{2+} + 5Fe^{2+} + 2\,S^0 \quad (spontaneous)$$
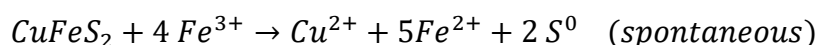
A. ferrooxidans is used to oxidise the iron so it can be reused for more mineral extraction, and also as a sulfur oxidiser to transform elemental sulfur into sulfate so it is solubilised as sulfuric acid:

$$4\,Fe^{2+} + O_2 + 4\,H^+ \rightarrow 4\,Fe^{3+} + 2\,H_2O \quad (iron\ oxidation)$$

$$2\,S^0 + 3\,O_2 + 2\,H_2O \rightarrow 2SO_4^{2-} + 4\,H^+ \quad (sulfur\ oxidation)$$
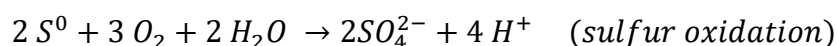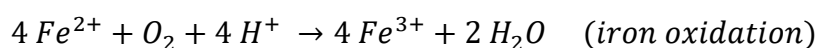
1.6.3. Neutrophilic aerobic iron oxidisers

In circumneutral environments, ferrous iron (Fe^{2+}) is chemically oxidised in the presence of oxygen. For this reason, in order to obtain energy using iron as the sole electron donor, iron oxidisers must inhabit microoxic environments where they can compete with oxygen (Emerson *et al.*, 2012). This group of microorganisms can be found both in fresh water and in marine environments.
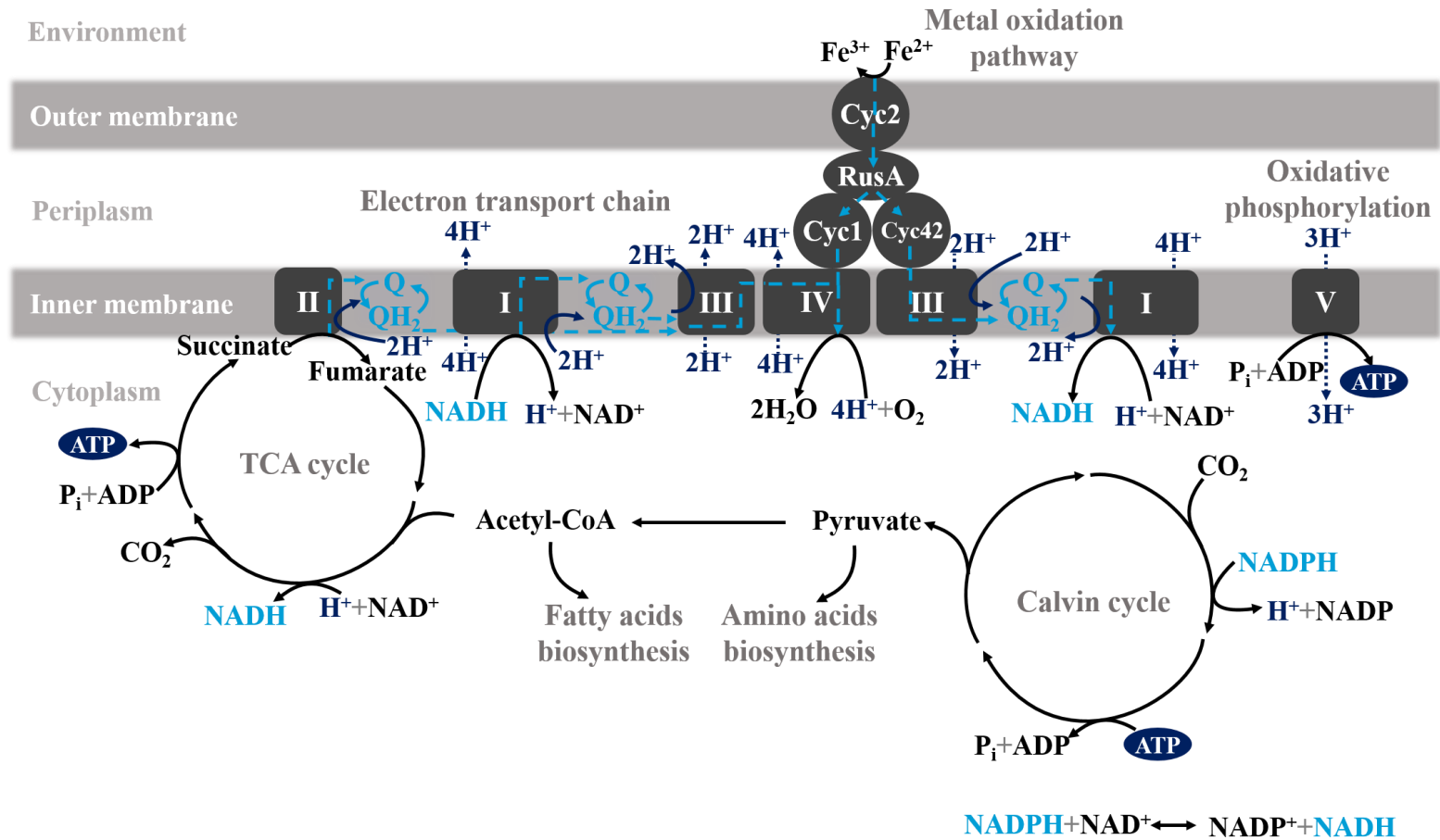
Figure 1-8 Acidithiobacillus ferrooxidans aerobic chemolitotroph metabolism

Overview of Acidithiobacillus ferrooxidans aerobic iron oxidation. Enzymes are shown in boxes. Chemical reactions are shown in black arrows. Electron transfer is shown in light blue dashed arrows. Molecule transport across the inner membrane is shown in dotted arrows. Processes contributing to energy generation are shown in dark blue.

While *Sideroxidans lithotrophicus* and *Gallionella capsiferriformans* are found in fresh water rich in iron, *Mariprofundus ferrooxydans* lives in iron mats in hydrothermal fields (Emerson *et al.*, 2012; Kato *et al.*, 2012).

The metabolic pathway of *Mariprofundus ferrooxydans* used to obtain energy is very similar to the one of *A. ferrooxidans* as both are aerobic autotrophs. However, there are some differences in their Mto pathway. Ferrous iron (Fe^{2+}) oxidation is thermodynamically more favourable for the neutrophilic microorganism as the redox potential of iron complexes at neutral pH (+0.37 V for Fe(II)citrate at pH 7) is lower than at acidic environments (+0.77 V for Fe(II) at pH 2), so the difference of potential between the electron donor and the electron acceptor (+0.82 V for oxygen in the cytoplasm at pH 7) is larger. Like Cyc2 in *A. ferrooxidans*, *M. ferrooxydans* expresses a *c*-type cytochrome that is also thought to function as a porin ($Cyc2_{PV1}$), not requiring a MtrCAB-like protein complex like *Shewanella*. A ferrous iron (Fe^{2+}) species (+0.37 V for Fe(II)citrate) is oxidised extracellularly by $Cyc2_{PV1}$, and the electrons are transported to a periplasmic *c*-type cytochrome ($Cyc1_{PV1}$) (Figure 1-9). From there, a downhill electron transport chain leads to complex IV to reduce oxygen (+0.82 V) into water and pumping protons from the cytoplasm to the periplasm, while an uphill pathway uses part of the energy produced to transform NAD^+ into NADH (-0.32 V) in complex I, transporting back part of the protons from the periplasm to the cytoplasm (Singer *et al.*, 2011; White *et al.*, 2016).
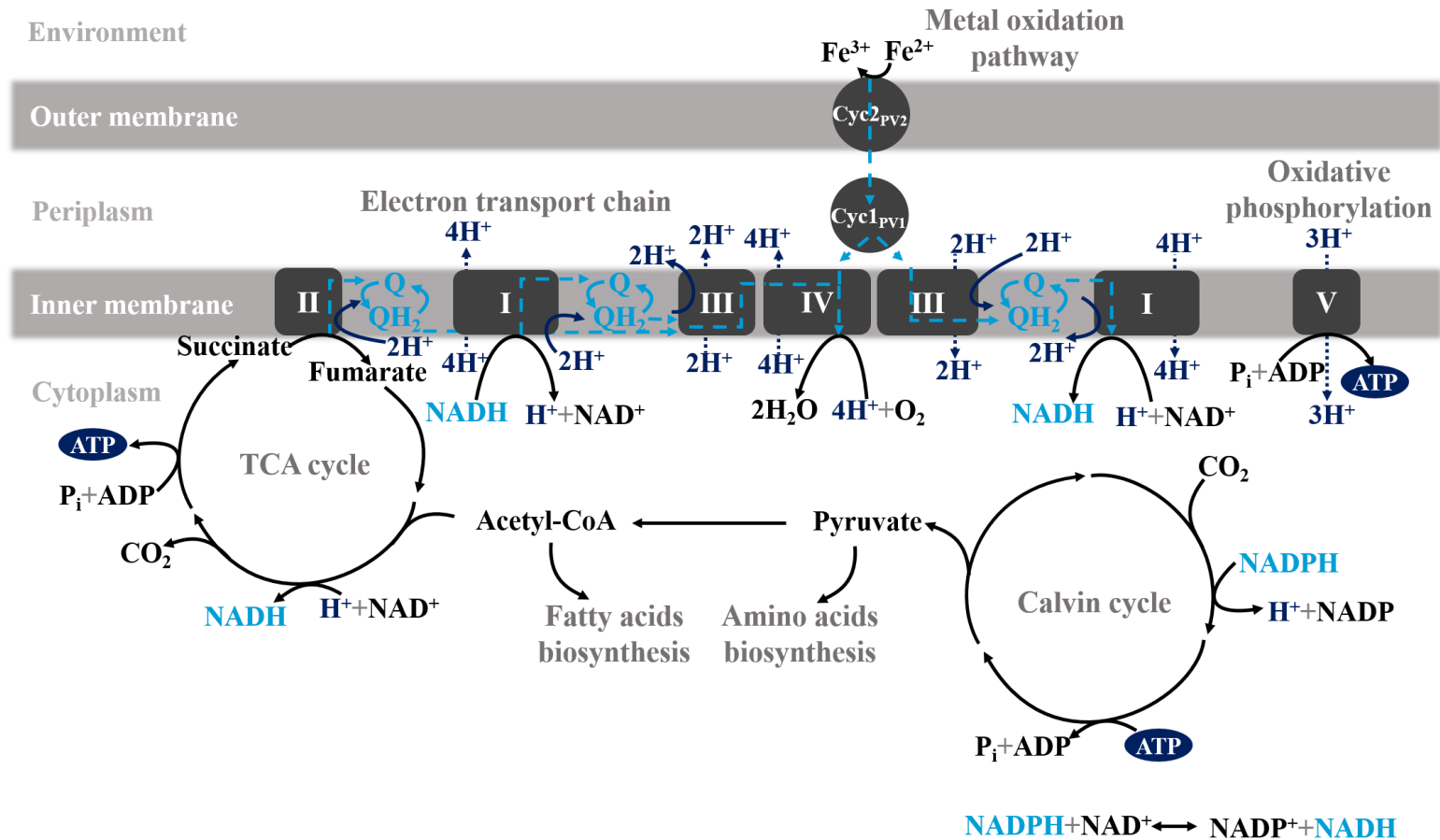
Figure 1-9 *Mariprofundus ferrooxydans* aerobic chemolitotroph metabolism
Overview of Mariprofundus ferrooxydans aerobic iron oxidation. Enzymes are shown in boxes. Chemical reactions are shown in black arrows. Electron transfer is shown in light blue dashed arrows. Molecule transport across the inner membrane is shown in dotted arrows. Processes contributing to energy generation are shown in dark blue.

1.7   Aims of the thesis

From a biogeochemical point of view, iron reducers and iron oxidisers are necessary in many environments to maintain bioavailable iron for other communities. Additionally, their activity can be used for some sustainable industrial applications such as bioremediation, energy production or bioleaching.

Excluding *Shewanella* and *Geobacter*, the model bacteria for dissimilatory iron reduction, there is still a lot to discover about iron-metabolising microorganisms.

The first aim of this thesis is to identify novel iron-reducing microorganisms in environments where, due to abiotic factors, iron bioavailability is limited, and try to identify which mechanisms they use to reduce iron.

The second aim of this thesis is to identify and characterise metal oxidation pathways used by iron oxidisers that have been previously predicted but have not been characterised yet.

1.8 References

Allen, J.W.A., Leach, N., and Ferguson, S.J. (2005) The histidine of the *c-type* cytochrome CXXCH haem-binding motif is essential for haem attachment by the *Escherichia coli* cytochrome *c* maturation (Ccm) apparatus. *Biochem. J.* 389: 587–92.

Altermann, E. (2014) Invited commentary: lubricating the rusty wheel, new insights into iron oxidizing bacteria through comparative genomics. *Front. Microbiol.* 5: 386.

Atlas, R.M. and Bartha, R. (1998) Microbial ecology : fundamentals and applications Benjamin/Cummings.

Beckwith, C.R., Edwards, M.J., Lawes, M., Shi, L., Butt, J.N., Richardson, D.J., and Clarke, T.A. (2015) Characterization of MtoD from *Sideroxydans lithotrophicus*: a cytochrome *c* electron shuttle used in lithoautotrophic growth. *Front. Microbiol.* 6: 332.

Bencharit, S. and Ward, M.J. (2005) Chemotactic responses to metals and anaerobic electron acceptors in *Shewanella oneidensis* MR-1. *J. Bacteriol.* 187: 5049–53.

Bird, L.J., Bonnefoy, V., and Newman, D.K. (2011) Bioenergetic challenges of microbial iron metabolisms. *Trends Microbiol.* 19: 330–340.

Bose, A. and Newman, D.K. (2011) Regulation of the phototrophic iron oxidation (pio) genes in *Rhodopseudomonas palustris* TIE-1 is mediated by the global regulator, FixK. *Mol. Microbiol.* 79: 63–75.

Braga, R.M., Dourado, M.N., and Araújo, W.L. (2016) Microbial interactions: ecology in a molecular perspective. *Brazilian J. Microbiol.* 47: 86–98.

Carlson, H.K., Clark, I.C., Melnyk, R.A., and Coates, J.D. (2012) Toward a mechanistic understanding of anaerobic nitrate-dependent iron oxidation: balancing electron uptake and detoxification. *Front. Microbiol.* 3: 57.

Carrondo, M.A. (2003) Ferritins, iron uptake and storage from the bacterioferritin viewpoint. *EMBO J.* 22: 1959–1968.

Chakraborty, A., Roden, E.E., Schieber, J., and Picardal, F. (2011) Enhanced Growth of *Acidovorax* sp. Strain 2AN during Nitrate-Dependent Fe(II) Oxidation in Batch and Continuous-Flow Systems. *Appl. Environ. Microbiol.* 77: 8548–8556.

Chakraborty, R. and Coates, J.D. (2005) Hydroxylation and carboxylation--two crucial steps of anaerobic benzene degradation by *Dechloromonas* strain RCB. *Appl. Environ. Microbiol.* 71: 5427–32.

Chaudhuri, S.K., Lack, J.G., and Coates, J.D. (2001) Biogenic magnetite formation through anaerobic biooxidation of Fe(II). *Appl. Environ. Microbiol.* 67: 2844–8.

Cheng, Y.-Y., Li, B.-B., Li, D.-B., Chen, J.-J., Li, W.-W., Tong, Z.-H., et al. (2013) Promotion of iron oxide reduction and extracellular electron transfer in *Shewanella oneidensis* by DMSO. *PLoS One* 8: e78466.

Choi, O., Kim, T., Woo, H.M., and Um, Y. (2015) Electricity-driven metabolic shift through direct electron uptake by electroactive heterotroph *Clostridium pasteurianum*. *Sci. Rep.* 4: 6961.

Dancis, A., Roman, D.G., Anderson, G.J., Hinnebusch, A.G., and Klausner, R.D. (1992) Ferric reductase of *Saccharomyces cerevisiae*: molecular characterization, role in iron uptake, and transcriptional control by iron. *Proc. Natl. Acad. Sci. U. S. A.* 89: 3869–73.

Edwards, M.J., White, G.F., Norman, M., Tome-Fernandez, A., Ainsworth, E., Shi, L., et al. (2015) Redox Linked Flavin Sites in Extracellular Decaheme Proteins Involved in Microbe-Mineral Electron Transfer. *Sci. Rep.* 5: 11677.

Ehrenreich, A. and Widdel, F. (1994) Anaerobic oxidation of ferrous iron by purple bacteria, a new type of phototrophic metabolism. *Appl. Environ. Microbiol.* 60: 4517–26.

Emerson, D., Roden, E., and Twining, B.S. (2012) The microbial ferrous wheel: iron cycling in terrestrial, freshwater, and marine environments. *Front. Microbiol.* 3: 383.

Gorby, Y.A., Yanina, S., McLean, J.S., Rosso, K.M., Moyles, D., Dohnalkova, A., et al. (2006) Electrically conductive bacterial nanowires produced by *Shewanella oneidensis* strain MR-1 and other microorganisms. *Proc. Natl. Acad. Sci. U. S. A.* 103: 11358–63.

Hedrich, S., Schlomann, M., and Johnson, D.B. (2011) The iron-oxidizing proteobacteria. *Microbiology* 157: 1551–1564.

Ilbert, M. and Bonnefoy, V. (2013) Insight into the evolution of the iron oxidation pathways. *Biochim. Biophys. Acta - Bioenerg.* 1827: 161–175.

Ishii, S., Shimoyama, T., Hotta, Y., and Watanabe, K. (2008) Characterization of a filamentous biofilm community established in a cellulose-fed microbial fuel cell. *BMC Microbiol.* 8: 6.

Jiao, Y. and Newman, D.K. (2007) The pio operon is essential for phototrophic Fe(II) oxidation in *Rhodopseudomonas palustris* TIE-1. *J. Bacteriol.* 189: 1765–73.

Johnson, D.B., Kanao, T., and Hedrich, S. (2012) Redox Transformations of Iron at Extremely Low pH: Fundamental and Applied Aspects. *Front. Microbiol.* 3: 96.

Johs, A., Shi, L., Droubay, T., Ankner, J.F., and Liang, L. (2010) Characterization of the decaheme *c-type* cytochrome OmcA in solution and on hematite surfaces by small angle x-ray scattering and neutron reflectometry. *Biophys. J.* 98: 3035–43.

Kato, S., Nakamura, K., Toki, T., Ishibashi, J.-I., Tsunogai, U., Hirota, A., et al. (2012) Iron-based microbial ecosystem on and below the seafloor: a case study of hydrothermal fields of the southern mariana trough. *Front. Microbiol.* 3: 89.

Kleinman, R. and Crerar, D. (1979) Thiobacillus ferrooxidans and the formation of acidity in simulated coal mine environments. *Geomicrobiol. J.* 1: 373–388.

Lall, R. and Mitchell, J. (2007) Metal reduction kinetics in *Shewanella*. *Bioinformatics* 23: 2754–9.

Liu, Y., Wang, Z., Liu, J., Levar, C., Edwards, M.J., Babauta, J.T., et al. (2014) A trans-outer membrane porin-cytochrome protein complex for extracellular electron transfer by *Geobacter sulfurreducens* PCA. *Environ. Microbiol. Rep.* 6: 776–85.

Lovley, D.R. (2006) Bug juice: harvesting electricity with microorganisms. *Nat. Rev. Microbiol.* 4: 497–508.

Lutgens, F.K. and Tarbuck, E.J. (2000) Essentials of geology Prentice Hall.

Malvankar, N.S., Vargas, M., Nevin, K., Tremblay, P.-L., Evans-Lutterodt, K., Nykypanchuk, D., et al. (2015) Structural basis for metallic-like conductivity in microbial nanowires. *MBio* 6: e00084.

Mancinelli, R.L. and McKay, C.P. (1988) The evolution of nitrogen cycling. *Orig. Life Evol. Biosph.* 18: 311–25.

Marritt, S.J., Lowe, T.G., Bye, J., McMillan, D.G.G., Shi, L., Fredrickson, J., et al. (2012) A functional description of CymA, an electron-transfer hub supporting anaerobic respiratory flexibility in *Shewanella*. *Biochem. J.* 444: 465–74.

Marshall, M.J., Beliaev, A.S., Dohnalkova, A.C., Kennedy, D.W., Shi, L., Wang, Z., et al. (2006) *c-type* cytochrome-dependent formation of U(IV) nanoparticles by *Shewanella oneidensis*. *PLoS Biol.* 4: e268.

McMillan, D.G.G., Marritt, S.J., Butt, J.N., and Jeuken, L.J.C. (2012) Menaquinone-7 is specific cofactor in tetraheme quinol dehydrogenase CymA. *J. Biol. Chem.* 287: 14215–25.

Molchanov, S., Gendel, Y., Ioslvich, I., and Lahav, O. (2007) Improved Experimental and Computational Methodology for Determining the Kinetic Equation and the Extant Kinetic Constants of Fe(II) Oxidation by *Acidithiobacillus ferrooxidans*. *Appl. Environ. Microbiol.* 73: 1742.

Morgan, B. and Lahav, O. (2007) The effect of pH on the kinetics of spontaneous Fe(II) oxidation by O_2 in aqueous solution--basic principles and a simple heuristic description. *Chemosphere* 68: 2080–4.

Muehe, E.M., Gerhardt, S., Schink, B., and Kappler, A. (2009) Ecophysiology and the energetic benefit of mixotrophic Fe(II) oxidation by various strains of nitrate-reducing bacteria. *FEMS Microbiol. Ecol.* 70: 335–343.

Myers, C.R. and Nealson, K.H. (1988) Bacterial manganese reduction and growth with manganese oxide as the sole electron acceptor. *Science* 240: 1319–21.

Myers, C.R. and Nealson, K.H. (1990) Respiration-linked proton translocation coupled to anaerobic reduction of manganese(IV) and iron(III) in *Shewanella putrefaciens* MR-1. *J. Bacteriol.* 172: 6232–8.

Nelson, D.L and Cox, M.M. (2013) Lehninger principles of biochemistry W.H. Freeman and Company.

Pechter, K.B., Gallagher, L., Pyles, H., Manoil, C.S., and Harwood, C.S. (2015) Essential Genome of the Metabolically Versatile Alphaproteobacterium *Rhodopseudomonas palustris*. *J. Bacteriol.* 198: 867–76.

Pierre, J.L., Fontecave, M., and Crichton, R.R. (2002) Chemistry for an essential biological process: the reduction of ferric iron. *Biometals* 15: 341–6.

Pierson and Parenteau (2000) Phototrophs in high iron microbial mats: microstructure of mats in iron-depositing hot springs. *FEMS Microbiol. Ecol.* 32: 181–196.

Pinchuk, G.E., Geydebrekht, O. V, Hill, E.A., Reed, J.L., Konopka, A.E., Beliaev, A.S., and Fredrickson, J.K. (2011) Pyruvate and lactate metabolism by *Shewanella oneidensis* MR-1 under fermentation, oxygen limitation, and fumarate respiration conditions. *Appl. Environ. Microbiol.* 77: 8234–40.

Pirbadian, S., Barchinger, S.E., Leung, K.M., Byun, H.S., Jangir, Y., Bouhenni, R.A., et al. (2014) *Shewanella oneidensis* MR-1 nanowires are outer membrane and periplasmic extensions of the extracellular electron transport components. *Proc. Natl. Acad. Sci. U. S. A.* 111: 12883–8.

Rampelotto, P.H. (2013) Extremophiles and extreme environments. *Life (Basel, Switzerland)* 3: 482–5.

Reeve, H.A., Ash, P.A., Park, H., Huang, A., Posidias, M., Tomlinson, C., et al. (2017) Enzymes as modular catalysts for redox half-reactions in H_2-powered chemical synthesis: from biology to technology. *Biochem. J.* 474: 215–230.

Rosato, A., Valasatava, Y., and Andreini, C. (2016) Minimal Functional Sites in Metalloproteins and Their Usage in Structural Bioinformatics. *Int. J. Mol. Sci.* 17:.

Rose, A.L. (2012) The influence of extracellular superoxide on iron redox chemistry and bioavailability to aquatic microorganisms. *Front. Microbiol.* 3: 124.

Salinero, K.K., Keller, K., Feil, W.S., Feil, H., Trong, S., Di Bartolo, G., and Lapidus, A. (2009) Metabolic analysis of the soil microbe *Dechloromonas aromatica* str. RCB: indications of a surprisingly complex life-style and cryptic anaerobic pathways for aromatic degradation. *BMC Genomics* 10: 351.

Schröder, I., Johnson, E., and De Vries, S. (2003) Microbial ferric iron reductases. *FEMS Microbiol. Rev.* 27: 427–447.

Schweinitzer, T. and Josenhans, C. (2010) Bacterial energy taxis: a global strategy? *Arch. Microbiol.* 192: 507–520.

Scott, K. (2017) Sustainable and Green Electrochemical Science and Technology John Wiley & Sons Ltd.

Shi, L., Rosso, K.M., Clarke, T.A., Richardson, D.J., Zachara, J.M., and Fredrickson, J.K. (2012) Molecular Underpinnings of Fe(III) Oxide Reduction by *Shewanella Oneidensis* MR-1. *Front. Microbiol.* 3: 50.

Shi, L., Rosso, K.M., Zachara, J.M., and Fredrickson, J.K. (2012) Mtr extracellular electron-transfer pathways in Fe(III)-reducing or Fe(II)-oxidizing bacteria: a genomic perspective. *Biochem. Soc. Trans.* 40: 1261–7.

Singer, E., Emerson, D., Webb, E.A., Barco, R.A., Kuenen, J.G., Nelson, W.C., et al. (2011) *Mariprofundus ferrooxydans* PV-1 the first genome of a marine Fe(II) oxidizing Zetaproteobacterium. *PLoS One* 6: e25386.

Thormann, K.M., Saville, R.M., Shukla, S., Pelletier, D.A., and Spormann, A.M. (2004) Initial Phases of biofilm formation in *Shewanella oneidensis* MR-1. *J. Bacteriol.* 186: 8096–104.

Valdés, J., Pedroso, I., Quatrini, R., Dodson, R.J., Tettelin, H., Blake, R., et al. (2008) *Acidithiobacillus ferrooxidans* metabolism: from genome sequence to industrial applications. *BMC Genomics* 9: 597.

Varma, A. (Ajit) and Chincholkar, S.B. (2007) Microbial siderophores Springer.

Weber, K.A., Achenbach, L.A., and Coates, J.D. (2006) Microorganisms pumping iron: anaerobic microbial iron oxidation and reduction. *Nat. Rev. Microbiol.* 4: 752–64.

White, G.F., Edwards, M.J., Gomez-Perez, L., Richardson, D.J., Butt, J.N., and Clarke, T.A. (2016) Mechanisms of Bacterial Extracellular Electron Exchange. In, *Advances in Microbial Physiology*., pp. 87–138.

White, G.F., Shi, Z., Shi, L., Wang, Z., Dohnalkova, A.C., Marshall, M.J., et al. (2013) Rapid electron exchange between surface-exposed bacterial cytochromes and Fe(III) minerals. *Proc. Natl. Acad. Sci. U. S. A.* 110: 6346–51.

Widdel, F., Schnell, S., Heising, S., Ehrenreich, A., Assmus, B., and Schink, B. (1993) Ferrous iron oxidation by anoxygenic phototrophic bacteria. *Nature* 362: 834–836.

Williams, R.J.P. and Fraústo da Silva, J.J.R. (2003) Evolution was Chemically Constrained. *J. Theor. Biol.* 220: 323–343.

Williams, R.J.P., Teixeira, M., and Louro, R.O. (2011) Iron in evolution.

Xu, J. (2006) Microbial ecology in the age of genomics and metagenomics: concepts, tools, and

Yarzábal, A., Brasseur, G., Ratouchniak, J., Lund, K., Lemesle-Meunier, D., DeMoss, J.A., and Bonnefoy, V. (2002) The high-molecular-weight cytochrome *c* Cyc2 of *Acidithiobacillus ferrooxidans* is an outer membrane protein. *J. Bacteriol.* 184: 313–7.

Yin, J. and Gao, H. (2011) Stress responses of *Shewanella*. *Int. J. Microbiol.* 2011: 863623.

Zhao, X., Wang, R., Lu, X., Lu, J., Li, C., and Li, J. (2013) Bioleaching of chalcopyrite by *Acidithiobacillus ferrooxidans*. *Miner. Eng.* 53: 184–192.

Materials and methods

2.1 Bacterial strains and plasmids

A list of the strains used in this thesis are described in Table 2-1. Strains were stored at -80 ˚C, previously snap-frozen in liquid nitrogen, in 25% (v/v) Glycerol stocks. The stocks were made by adding 1 mL of culture of cells growing in

Table 2-1 Bacterial strains used in this thesis

[1] Pacific Northwest National Laboratory, [2] University of East Anglia, [3] Whitlingham Great Broad, [4] Raveningham field, [5] American Type Culture Collection.

Strain	Characteristics	Source
Shewanella oneidensis MR-1	Wild Type	(David J Richardson
Shewanella oneidensis MR-1	pCyc2-SII	This work
Shewanella oneidensis MR-1	pSII-Cyc2	This work
Shewanella oneidensis MR-1	pCyc2$_{PV-1}$-SII	This work
Shewanella oneidensis MR-1	Δ*mtrB*-Δ*mtrD*	PNNL[1]
Shewanella oneidensis MR-1	Δ*mtrB*-Δ*mtrD*, pCyc2-SII	This work
Shewanella oneidensis MR-1	Δ*mtrB*-Δ*mtrD*, pCyc2$_{PV-1}$-SII	This work
Acinetobacter spp.	Water sample (UEA[2])	This work
Acinetobacter spp.	Water sample (WGB[3])	This work
Acinetobacter spp.	Soil sample (RVG[4])	This work
Acinetobacter baumannii	Wild Type	ATCC[5]
Citrobacter spp.	Sediment sample (WGB)	This work
Acidithiobacillus ferrooxidans ATCC 23270	Wild Type	(Dekker *et al.*, 2016)
Escherichia coli TOP10	Donor cell in tri-parental conjugation	Thermo Scientific
Escherichia coli TOP10	pCyc2-SII	This work
Escherichia coli DH5α	Helper cell in tri-parental conjugation pRK2013	Thermo Scientific
Escherichia coli WM3064	Donor cell in bi-parental conjugation DAP auxotroph pRP4	(Dashiff and Kadouri, 2009)
Escherichia coli WM3064	pCyc2-SII	This work

stationary phase in Luria-Bertani (LB), to 1 mL of sterile 50% (v/v) Glycerol in a pre-sterilised screw-cap tube. Cultures from *Acidithiobacillus ferrooxidans* could not be frozen and liquid subcultures of each strain were routinely prepared in their respective media.

The vectors used for this thesis were suspended in DNase free H_2O and stored at -20 ˚C. A list of the vectors is shown in Table 2-2.

Table 2-2 Vectors used in this thesis
[1]Designed by Dr. Marcus Edwards from University of East Anglia.

Strain	Characteristics	Source
pRK2013	Kan[R], mobilises to the donor cell and helps for the mobilisation of non-self-transmissible plasmids	(Figurski and Helinski, 1979)
pRP4	Kan[R], helps for the mobilisation of non-self-transmissible plasmids	(Dashiff and Kadouri, 2009)
pMEGGA	Kan[R], RBS under L-arabinose operon upstream a constitutively expressed chromophore and strep-tag II sequence downstream it	UEA[1]
pMEGGA_BsmBI	Modified pMEGGA with BsmBI restriction enzymes sites upstream and downstream the chromophore	This work
pMEGGA_Cyc2C	Kan[R], expression of Cyc2 with Strep-tag II at the C-terminus under L-arabinose operon	This work
pMEGGA_Cyc2N	Kan[R], expression of Cyc2 with Strep-tag II at the N-terminus under L-arabinose operon	This work
pEX-K4_Cyc2$_{PV-1}$	Kan[R], *cyc2$_{PV-1}$* (codon optimized for *S. oneidensis* MR-1) with BsmBI restriction enzymes sites flanking it	This work
pMEGGA_Cyc2$_{PV-1}$C	Kan[R], expression of Cyc2$_{PV-1}$ (codon optimized for *S. oneidensis* MR-1) with Strep-tag II at the C-terminus under L-arabinose operon	This work

2.2 Media and growth conditions

2.2.1. Luria-Bertani medium

LB medium (Maniatis *et al.*, 1982) was prepared with 1 % (w/v) Tryptone, 1 % (w/v) NaCl and 1 % (w/v) Yeast extract. For LB agar plates, 1.5 % (w/v) Agar was added to the medium. The media was autoclaved for 15 minutes at 121 ˚C.

From the glycerol stocks, strains were inoculated in 10 mL of LB in 20 mL tubes. Cultures were incubated in a rotary shaker at 200 rpm overnight. *Shewanella oneidensis* and *Citrobacter* spp. were incubated at 30 ˚C, *Acinetobacter* spp. was incubated at 20 ˚C and *Escherichia coli* was incubated at 37 ˚C.

For experiments that required cells at a specific point of their exponential phase, 1% (v/v) of an overnight culture was used as the inoculum. Any required supplement that could not be autoclaved, like antibiotics or gene expression inducers, was filter-sterilised through 0.2 μM filters and added to the LB. Samples were incubated in LB filling up to up to ½ of the capacity of the baffled conical flasks in a rotary shaker at 200 rpm to allow aeration until the cultures reached the required Optical Density (OD). The OD of the culture was measured in 1 cm polystyrene cuvettes in the spectrophotometer at 600 nm.

For goethite reduction assays, 35 mL of the sample were incubated in 50 mL falcon tubes with 50 mM pre-autoclaved goethite. The tubes were sealed with suba-seal® rubber septa and the cultures were sparged with N_2 for 15 minutes. Samples were incubated at 20 ˚C shaking at 200 rpm for 3 days.

To estimate the concentration of viable cells in a sample by counting colony-forming units, serial dilutions of the samples were plated in LB agar with a pre-sterilised glass spreader. The plates were incubated aerobically overnight, each strain at its optimal temperature. Filter-sterilised supplements were added to the autoclaved LB agar once the media had cooled down to 55 ˚C.

2.2.2. Super Optimal Catabolite repression medium

SOC medium is used at the final step of transformation to obtain better efficiency in *Eschericha coli* (Hanahan, 1983). This media contains 2 % (w/v) Tryptone, 0.5 % (w/v) Yeast extract, 8.56 mM NaCl, 2.5 mM KCl, 10 mM $MgCl_2$, 10 mM $MgSO_4$ and 20 mM Glucose.

2.2.3. <u>Minimal medium for ferric iron (Fe^{3+}) respiration</u>

Minimal medium was used to study the electron transfer between bacteria and iron. For iron reduction assays, a basal medium (Table 2-3) supplemented with either 50 mM Formate, 15 mM Acetate, 20 mM Lactate or 30 mM Succinate as a carbon source. The pH of the medium was adjusted at 7 with NaOH before autoclaving.

Table 2-3 Basal medium

Basal medium	
NH_4Cl	17.4 mM
$MgSO_4*7H_2O$	0.8 mM
$CaCl_2*7H_2O$	0.4 mM
K_2HPO_4	0.3 mM

Mineral and vitamin solutions (Table 2-4) were not autoclaved and were added afterwards filter-sterilised in a 0.1 % (v/v) concentration. 0.5 mM of Fe(III)citrate, Fe(III)EDTA or Fe(III)NTA were also added to the media filter-sterilised. When different concentrations of 2,4-Dinitrophenol (DNP) were added to the media, they were also filter-sterilised. For minimal media agar plates, 1.5 % (w/v) Agar was added to the medium and any filter-sterilised solutions were added after the media had cooled down to 55 ˚C.

Shewanella oneidensis MR-1, *Shewanella oneidensis* MR-1 Δ*mtrB*-Δ*mtrD*, the environmental isolates *Acinetobacter* spp. UEA and *Citrobacter* spp. WGB and *Acinetobacter baumannii* were cultivated in 35 mL of this medium in 50 mL falcon tubes. 0.1 mL of LB overnight cultures were centrifuged at 6000 RCF for 2 minutes and cells were washed with minimal media and added to the tubes. The tubes were sealed with suba-seal® rubber septa and the cultures were sparged with N_2 for 15 minutes. Samples were incubated at 20 ˚C shaking at 200 rpm for 6 days.

Table 2-4 Composition of the mineral and vitamins supplement for minimal media

Mineral solution		Vitamin solution	
Nitrilotriacetic acid	7.8 mM	Biotin (B7)	8.2 μM
$MgSO_4$	12.2 mM	Folic acid (B9)	4.5 μM
$MnSO_4$	4.2 mM	Pyridoxine hydrochloride	59.1 μM
NaCl	17.1 mM	Thiamine (B1)	16.6 μM
$FeSO_4*7H_2O$	0.4 mM	Rivoflavin (B2)	13.3 μM
$Co(NO_3)*6H_2O$	0.4 mM	Nicotinic acid (B3)	40.6 μM
$CaCl_2$	0.9 mM	Calcium D-(+)-pantothenate	10.5 μM
$ZnSO_4*7H_2O$	0.3 mM	Cobalamin (B12)	0.1 μM
$CuSO_4*5H_2O$	40.1 μM	p-Aminobenzoic acid (B10)	36.5 μM
$AlK(SO_4)*12H_2O$	21.1 μM	Thioctic acid	24.2 μM
H_3BO_3	0.2 mM		
Na_2SeO_3	5.8 μM		
$NA_2WO_4*2H_2O$	30.3 μM		
$NiCl_2*6H_2O$	84.1 μM		

2.2.4. _Acidithiobacillus ferrooxidans_ iron medium

To grow _Acidithiobacillus ferrooxidans_, iron medium (Table 2-5) adjusted at pH 1.6 with H_2SO_4 was autoclaved and 0.1 % (v/v) of filter-sterilised mineral and vitamin solutions was added afterwards (Table 2-4).

Table 2-5 Iron medium for Acidithiobacillus ferrooxidans

Iron medium	
$FeSO_4$	0.23 mM
$(NH_4)_2SO_4$	3 mM
KH_2PO_4	3 mM
$MgSO_4*7H_2O$	1.62 mM
Trisodium citrate	1.16 mM

250 mL of _A. ferrooxidans_ culture were incubated in 500 mL conical flask aerobically and room temperature and without agitation for at least 14 days. _A. ferrooxidans_ could not be preserved frozen so every 2 weeks a fresh batch was prepared by inoculating ¼ of the previous culture.

2.3 Environment sampling

Water samples of 15 mL fresh-water were collected at two different points of the river Yare: next to the University of East Anglia (UEA) and at the Whitlingham Great Broad (WGB) (Figure 2-1 A and B respectively). A 15 cm^3 core sample was collected from the first 10 cm of sediment in the WGB (Figure 2-1 B).

Samples taken from the environment were stored in 15 mL sterile tubes at -20 °C and they were defrosted at room temperature before being used for further experiments. A soil sample from a field in Raveningham (RVG) (Figure 2-1 C) was brought to the laboratory from a different research group, consequently, the sampling procedure and how the sample was preserved until it was frozen in the laboratory is unknown.
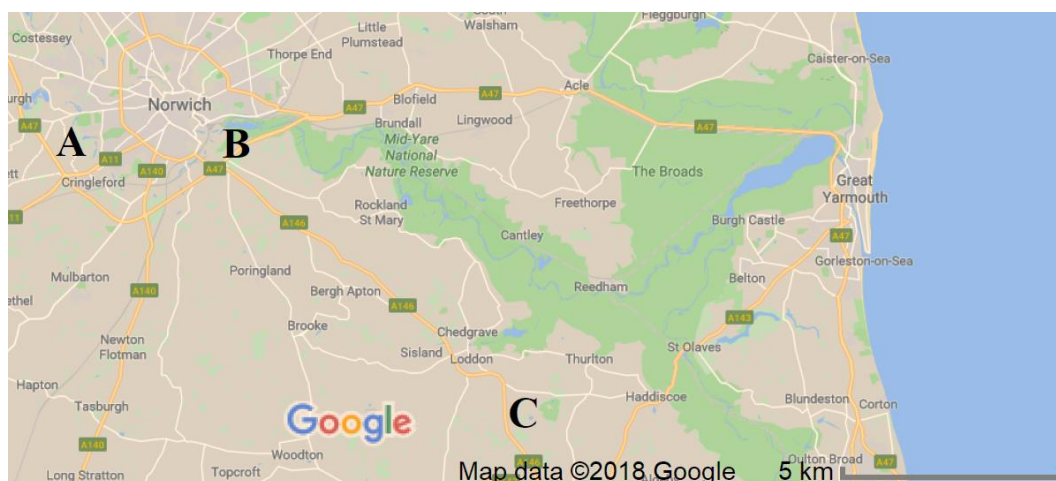
Figure 2-1 Map of sampling locations discussed in this thesis
A) *Yare river at University of East Anglia. B)Yare river at Whitlingham Great Broad. C) Field in Raveningham.*

2.4 Ferrozine assay

Soluble ferrous iron (Fe^{2+}) concentration was measured using the ferrozine assay (Viollier *et al.*, 2000). 1 mL of culture was centrifuged at 20000 RCF for 1 minute to precipitate the cells and the insoluble iron. 30 μL of ferrozine solution (10 mM Ferrozine and 100 mM Ammonium acetate) were added to the supernatant. The absorbance of the samples was measured in 1 cm polystyrene cuvettes in the

spectrophotometer at 562 nm. The concentration of the soluble ferrous iron (Fe^{2+}) was calculated by extrapolating the absorbance of the samples to a standard curve of known concentrations of Fe(II)Cl$_2$.
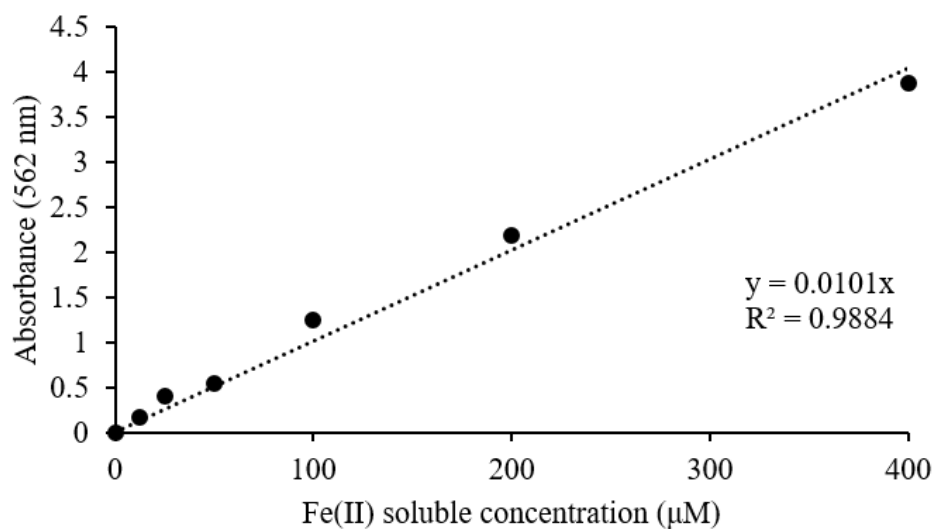
Figure 2-2 Ferrozine standard curve
Standard curve for soluble ferrous iron (Fe^{2+}) concentration. Ferrozine assay with 0 μM, 12.5 μM, 25 μM, 50 μM, 100 μM, 200 μM and 400 μM 1 mL of Fe(II)Cl$_2$.

2.5 DNA extraction

2.5.1. Plasmid

Plasmid extractions were done using the GenElute^{TM} HP plasmid Miniprep Kit (Sigma) according to the manufacturer's instructions but the DNA was eluted with 50 μL of DNase-free H$_2$O instead of the elution buffer provided in the kit.

Plasmids from different *Shewanella oneidensis* MR-1 strains were extracted from culturing cells in 10 mL LB aerobically at 30 ˚C overnight and cultures were centrifuged at 5500 RCF for 15 minutes.

2.5.2. Genomic DNA

Genomic DNA was extracted using the Wizard® Genomic DNA Purification Kit (Promega) according to the manufacturer's instructions but the DNA was eluted with 50 μL of DNase-free H$_2$O instead of the elution buffer provided in the kit.

Genomic DNA from the environmental *Acinetobacter* and *Citrobacter* strains were extracted from culturing cells in 10 mL LB aerobically at 20 ˚C overnight. *Acidithiobacillus ferrooxidans* genome was extracted from 1 L of iron medium. All cultures were centrifuged at 5500 RCF for 15 minutes.

The purity and the concentration of plasmids and genomic DNA samples were measured with the spectrophotometer (Nanodrop One, ThermoScientific).

2.6 RNA extraction

RNA from the environmental *Acinetobacter* (UEA) was extracted for RNA-seq. Through all the process, the area was kept clean to prevent RNAse contamination and, when possible, work was done in a laminar flow cabinet. All surfaces, equipment and material was cleaned with RNaseZap® (Ambion). Pre-sterilised TipOne® filtered pipette tips (Starlab) were used during the whole process.

2.6.1. Cell harvest

A single colony of *Acinetobacter* (UEA) was inoculated from an LB agar plate to 10 mL of LB and it was cultured at 20 ˚C overnight. 1 mL of the culture was centrifuged at 6000 RCF for 2 minutes and cells were washed with minimal media (Chapter 2.2.3) containing succinate as the sole carbon source. Cells were added to 250 mL of the same minimal media (with 0 or 0.5 mM Fe(III)citrate) in 500 mL Duran® bottles. Samples which required anaerobic conditions had open screw tight caps and silicone septum and were sparged with N_2 for 30 minutes. Cultures were incubated overnight at 20 ˚C shaking at 200 rpm.

Samples were transferred to 50 mL falcon tubes and incubated on ice for 1 hour and centrifuged at 6000 RCF for 10 minutes at 4 ˚C. Pellets were resuspended in residual supernatant and samples were transferred to 1.5 mL tubes. Samples were centrifuged at 20000 RCF for 2 minutes at 4 ˚C. All supernatant was removed and cell pellets were snap frozen in liquid nitrogen and stored at -80 ˚C until the next step was done.

2.6.2. <u>RNA extraction</u>

To extract the RNA from the samples, RNA SV Total RNA Isolation Kit (Promega) was used according to the manufacturer's instructions. Isolated RNA was stored at -80 ˚C.

2.6.3. <u>Analysis of RNA</u>

The purity and concentration of the RNA samples was measured in the spectrophotometer (Nanodrop One, ThermoScientific). The absence of genomic DNA was confirmed with a PCR (Chapter 2.8.1) using universal primers to amplify the 16S rRNA (Table 2-8) and visualised with an agarose electrophoresis (Chapter 2.9). The integrity of the RNA was checked using the Experion Automated Electrophoresis System (Biorad) and the Experion RNA Analysis Kit (Biorad) according to the manufacturer's instructions.

2.7 Sequencing

The sequencing of plasmids was done by Eurofins Genomics and the primers used are presented in Table 2-6. The genomic DNA was sequenced and annotated by microbesNG (University of Birmingham). RNA samples were sequenced, aligned and quantified by the Wellcome Centre for Human Genetics (University of Oxford).

Table 2-6 List of primers used for plasmid sequencing

Name	Characteristics	Sequence (5'-3')
27F	Universal 16S rRNA	AGAGTTTGATCATGGCTCA
MEGGA_R	Sequence *cyc2* and *cyc2PV-1* from the C-terminus	GTTCTGATTTAATCTGTATCAGG
cyc2_start_F	Sequence *cyc2* from the N-terminus	CATACCCATGGTGTCATCGTC

2.8 Polymerase chain reaction

2.8.1. 16S rRNA amplification PCR

To identify the environmental strains, a High-Fidelity DNA polymerase was used to have a correct sequence after the amplification. The PCR mix consisted on 10 µL of 5x HiFidelity Buffer (Biolabs), 1 µL of dNTPs (10 mM), 1 µL of the forward primer (10 µM) and 1 µL of the reverse one (10 µM) (Table 2-8), 1 µL of template (100 ng/µL), 35.5 µL of H_2O and 0.5 µL of Phusion Polymerase (Biolabs). Until the start of the PCR, each PCR mix was kept on ice. The PCR was run in a thermocycler and the program used is detailed in Table 2-7. The DNA from the PCR was purified (Chapter 2.8.3) and it was sent for sequencing using the 27S primer (Table 2-6).

Table 2-7 High-Fidelity Phusion PCR cycle for 16S rRNA amplification

Step	Temperature (˚C)	Time (seconds)	Cycles
Initial denaturation	98	120	1
Denaturation	98	15	
Annealing	49	20	35
Elongation	72	60	
Final elongation	72	600	1

Table 2-8 Universal 16S rRNA primers

Name	Sequence (5'-3')
27F	AGAGTTTGATCATGGCTCA
1492R	TACGGTTACCTTGTTACGACTT

Primer	Sequence (5'-3')
MEGGA_BsmBI_F	T**CGTCTCT**TGGAGCCATCCACAATTCGAGAAGTGAGTTTAAA
MEGGA_BsmBI_R	T**CGTCTCT**GGGTATGTATATCTCCTTCTTAAAGTTAAACAAAAT

Primer	Sequence (5'-3')
cyc2_BsmBI _F	T**CGTCTCT**ACCCATGGTGTCATCGTCCGTTGGTTTTAAAAAGAAAAG
cyc2_BsmBI_R	T**CGTCTCT**TTCCAAGTATGATATCCAGGCCAGCAGTTCAAGG
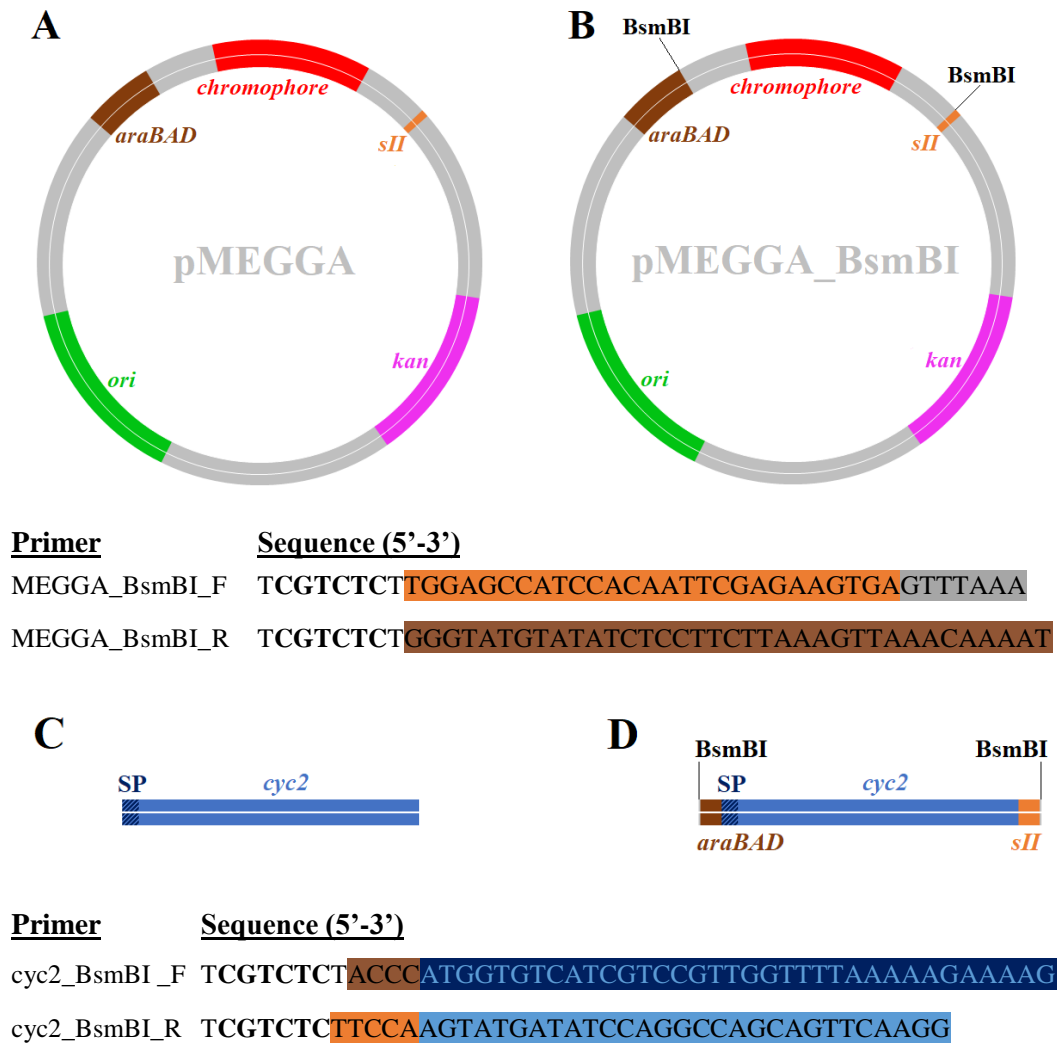
Figure 2-3 PCR site-directed mutagenesis for Golden Gate Assembly
Addition of BsmBI restriction sites in pMEGGA by PCR site-directed mutagenesis. A) Original plasmid before the PCR. B) Modified plasmid with BsmBI restriction sites. C) cyc2 gene from Acidithiobacillus ferrooxidans genome. D) Modified cyc2 gene after adding BsmBI restriction sites and sticky ends complementary to pMEGGA. Origin of replication in green. Kanamycin resistance gene in pink. L-arabinose operon in brown. Chromophore synthesis gene in red. Strep-tag II region in orange. cyc2 in light blue. Signal peptide sequence of cyc2 in dashed dark blue. Primer bases are highlighted in the colour corresponding to each complementary DNA regions. Non highlighted bases contains the mutations added. Restriction sites for BsmBI are in bold.

Primer	Sequence (5'-3')
cyc2_remCter_F	<u>TAA</u>TGGAGCCATCCACAATTCGAGAAGTG
cyc2_remCter_R	GTATGATATCCAGGCCAGCAGTTCAAG
cyc2_addNter_F	CAATTCGAGAAGCTGCCATCCTTTGCGCG
cyc2_addNter_R	TGGATGGCTCCATGCCCAGGCACCGGAA
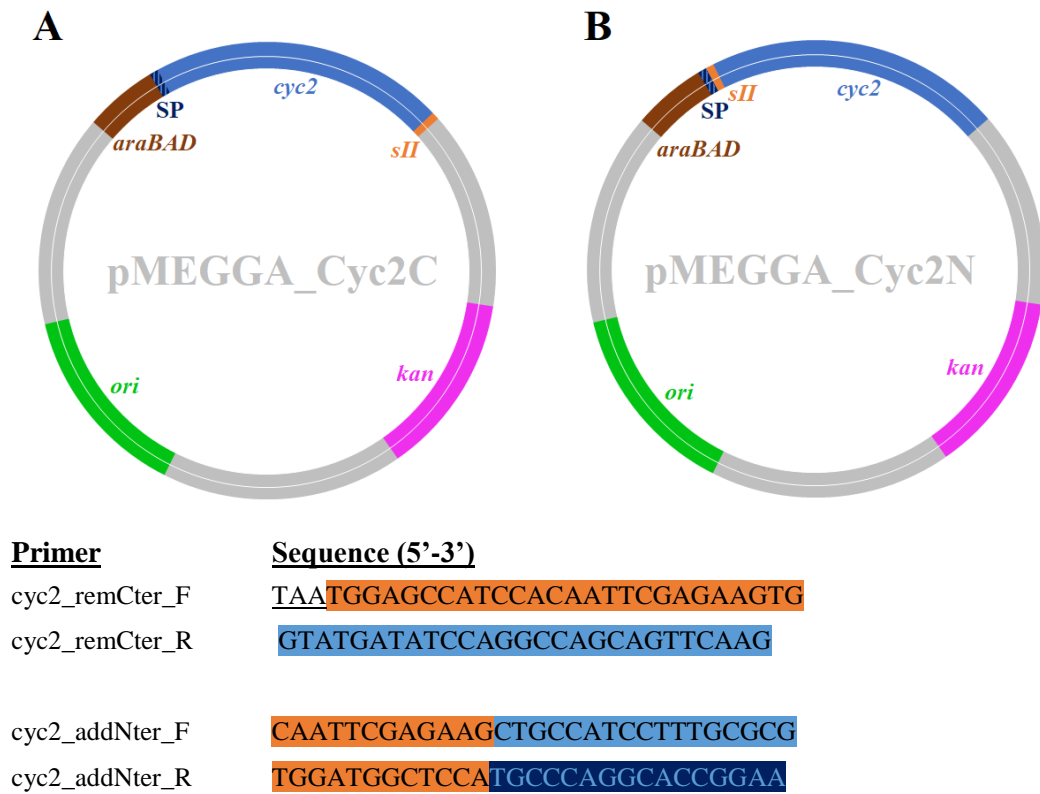
Figure 2-4 PCR site-directed mutagenesis for swapping the strep-tag II from the C-terminus to the N-terminus of cyc2

Addition of a new strep-tag II region after the signal peptide region at the N-terminus of cyc2 and a codon stop between the C-terminus of cyc2 and the previous strep-tag II region. A) pMEGGA_Cyc2C before the PCR. B) pMEGGA_Cyc2N after the mutagenesis. Origin of replication in green. Kanamycin resistance gene in pink. L-arabinose operon in brown. Strep-tag II region in orange. cyc2 in light blue. Signal peptide sequence of cyc2 in dashed dark blue. Primer bases are highlighted in the colour corresponding to each complementary DNA regions. Non highlighted bases contains the mutations added. Stop codon is underlined.

2.8.2. <u>Site-directed mutagenesis PCR</u>

High-Fidelity DNA polymerase was also used to add mutations to a specific region of a DNA sequence. The PCR mix consisted on 21 µL of 2x High-Fidelity PCR Master Mix with HF Buffer (Thermo), 1 µL of the forward primer (100 pM) and 1 µL of the reverse one (100 pM), 2µ template (100 ng/µL) and 21 µL of H_2O. Until the start of the PCR, each PCR mix was kept on ice. The PCR was run in a thermocycler and the program used is detailed in Table 2-9. The primers used for each site-directed mutagenesis PCR are specified in Figure 2-3 and Figure 2-4. Plasmids were re-ligated (Chapter 2.11) and they were sent to sequence to confirm their mutations using the primers MEGGA_R (for pMEGGA_BsmBI) and cyc2_start_F (for pMEGGA_Cyc2N) (Table 2-6).

Table 2-9 High Fidelity Phusion PCR cycle for site-directed mutagenesis

Step	Temperature (˚C)	Time (seconds)	Cycles
Initial denaturation	98	120	1
Denaturation	98	15	
Annealing	65	20	35
Elongation	72	120	
Final elongation	72	600	1

2.8.3. <u>Purification of PCR amplified DNA</u>

Amplified DNA from PCR was purified using GeneElute^{TM} PCR Clean-Up Kit (Sigma) according to manufacturers' instructions but eluting the DNA with 50 µL of DNase H_2O instead of the elution buffer.

2.9 Agarose gel electrophoresis

2.9.1. <u>DNA visualization</u>

DNA was separated by size in an agarose gel (1 % (v/v) agarose, 45 mM Tris-acetate, 1 mM EDTA at pH 8 with HCl, 2 µM ethidium bromide). Loading dye (40 % Sucrose (w/v), 20 % Orange G (w/v)) was mixed in a ratio of 1:10 with the DNA samples. The loading gel Hyperladder^{TM} 1 kb (Bioline) was

used in all gels for size reference. The gel was run in TAE buffer (45 mM Tris-acetate, 1 mM EDTA at pH 8 with HCl) at 120 mA until the orange front reached the bottom of the gel and visualised with an UV-transilluminator.

2.9.2. <u>DNA gel extraction</u>

To extract a band of interest from an agarose gel, GenElute^{TM} Gel Extraction Kit (Sigma) was used according to manufacturers' instructions but eluting the DNA with 50 μL of DNase H$_2$O instead of the elution buffer.

2.10 Golden Gate Assembly

For the expression of Cyc2 and Cyc2$_{PV-1}$ in *S. oneidensis* MR-1, Golden Gate Assembly was used to clone *cyc2* and *cyc2$_{PV-1}$* inside pMEGGA_BsmBI (Figure 2-5). The samples consisted on 1 μL pMEGGA_BsmBI plasmid (50 ng/μL), 4 μL *cyc2* (50 ng/μL), 1.5 μL T4 DNA Ligase Reaction Buffer (Biolabs), 1.5 μL NEBuffer^{TM} 3.1 (Biolabs), 1 μL T4 DNA Ligase (Biolabs), 1 μL BsmBI (Biolabs) and 5 μL DNase free H$_2$O. The program used in the thermocycler is specified in Table 2-10.

Table 2-10 Golden Gate Assembly cycle

Step	Temperature ($^\circ$C)	Time (minutes)	Cycles
Digestion	37	3	25
Ligation	16	4	
Ligase denaturation	50	5	1
BsmBI denaturation	80	5	1

2.11 Phosphorylation and ligation

After a site-directed mutagenesis, 50 μL PCR product (50 nM/μL) was incubated for 2 hours at 37 ˚C with 1 μL DpnI (Biolabs) and 5 μL 1x CutSmart® Buffer to digest the original DNA plasmid for the PCR. A mix of 12.5 μL PCR product (50 nm/μL), 2 μL T4 DNA Ligase Reaction Buffer (Biolabs), 1 μL T4 Polynucleotide Kinase (Biolabs) was incubated at 37 ˚C for 5 minutes and then let

A) Digestion
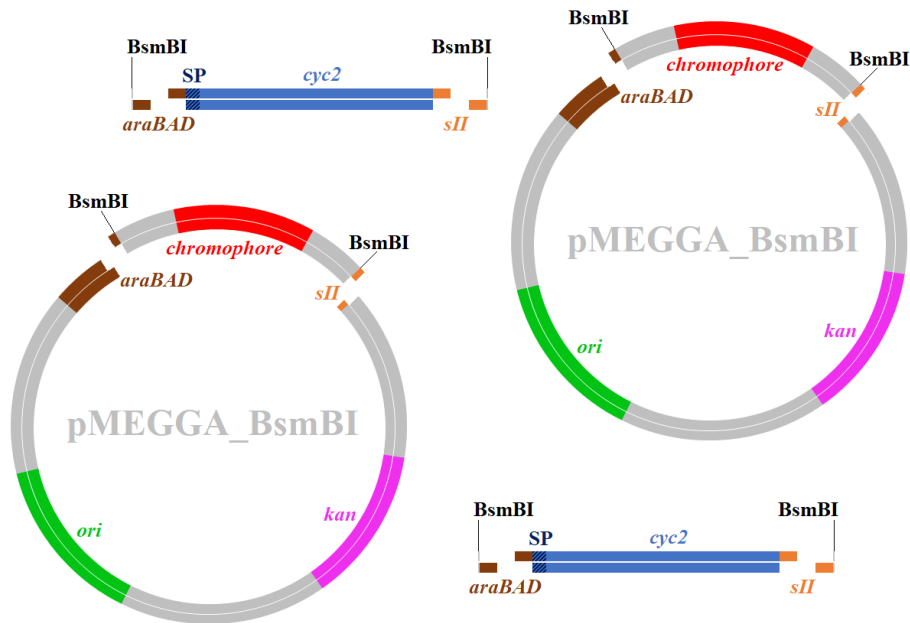
B) Ligation
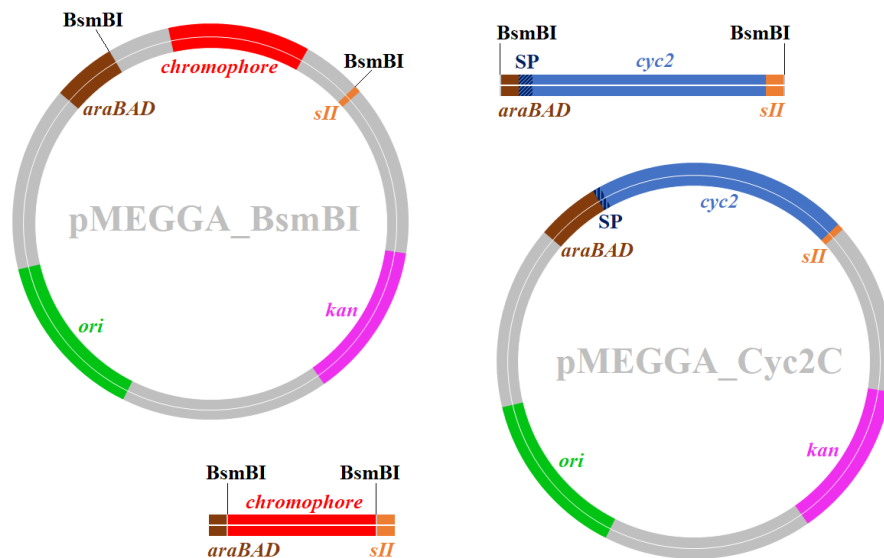
Figure 2-5 Golden gate assembly of cyc2 in pMEGGA
Directional assembling of cyc2 in pMEGGA by cyclic digestion and ligation. A) In the digestion step, BsmBI cleave the DNA in their restriction sites creating cohesive ends B) In the ligation step, cohesive ends are ligated by a T4 DNA ligase. In the second step, pMEGGA_BsmBI can ligate to its original sequence or it can insert cyc2, losing the BsmBI restriction site. Origin of replication in green. Kanamycin resistance gene in pink. L-arabinose operon in brown. Chromophore synthesis gene in red. Strep-tag II region in orange. cyc2 in light blue. Signal peptide sequence of cyc2 in dashed dark blue.

cool down. Finally, 1 μL T4 DNA Ligase (Biolabs) was added to the sample and it was incubated at room temperature overnight.

2.12 Chemical transformation

2.12.1. <u>Preparation of chemically competent cells</u>

Eschericha coli strains TOP10 and WM3064 were used to host pMEGGA_Cyc2C, pMEGGA_Cyc2N and pMEGGA_Cyc2$_{PV-1}$C. To make the cells competent, they were incubated overnight in 10 mL LB at 37 ˚C. The culture of *E. coli* WM3064 had also 100 μg/ml Diaminopimelic acid (DAP) in the media because this strain was auxotrophic for this molecule. 1 mL of the cultures were used to inoculate 100 mL LB or 100 mL LB with DAP and incubated at 37 ˚C shaking at 220 rpm until the OD$_{600}$ reached between 0.4 and 0.6. Cultures were placed in 50 mL tubes on ice for 10 minutes and afterwards, cells were centrifuged at 3500 RCF for 15 minutes at 4 ˚C. Each tube with cell pellets was resuspended in 20 mL of ice cold 0.1 M CaCl$_2$ and incubated in on ice for 1 hour. Cells pelleted again at 3500 RCF for 15 minutes at 4 ˚C and each tube was resuspended in 2.4 mL 0.1 M CaCl$_2$ with 20 % (v/v) Glycerol. Aliquots of 50 μL were stored at -80 ˚C until transformation step.

2.12.2. <u>Transformation of chemically competent cells</u>

Golden Gate Assembly DNA product (Chapter 2.10) was transformed in competent *E. coli* TOP10 and *E. coli* WM3064 by heat shock. 50 μL cell aliquots were mixed with 2.5 μL of Golden Gate Product (20 ng/μL) and incubated on ice for 30 minutes. Afterwards, cells were heat shocked at 42 ˚C for 40 seconds and recovered on ice for another 2 minutes. 200 μL of SOC media or 200 μL SOC with DAP were added to the cells and they were incubated at 37 ˚C for 90 minutes. Cells were pelleted at 4000 RCF for 2 minutes and plated in LB agar or LB with DAP agar. All plates contained 30 μg/ml Kanamycin. Plates were incubated at 37 ˚C overnight.

E. coli colonies that were pink carried pMEGGA_BsmBI vectors that had not changed the chromophore synthesis gene for the insert of interest. White colonies

had pMEGGA_Cyc2C, pMEGGA_Cyc2N or pMEGGA_Cyc2$_{PV-1}$C. White colonies were cultured and the plasmids were extracted to sequence the DNA sequence to confirm the mutation.

2.13 Genetic recombination in *Shewanella oneidensis* MR-1

2.13.1. Tri-parental conjugation

S. oneidensis MR-1 WT (recipient strain) was incubated overnight in 10 mL LB at 30 ˚C. The following day, 1 mL of the culture was incubated in 9 mL LB at 30 ˚C with 50 μg/ml Carbenicillin to increase the antibiotic resistance. Moreover, *E. coli* DH5α (helper strain) and *E. coli* TOP10 with pMEGGA_Cyc2C (donor strain) were incubated overnight in 10 mL LB at 37 ˚C with 30 μg/ml Kanamycin. The three cultures were centrifuged at 5500 RCF for 15 minutes at 4 ˚C and the pellets were washed by resuspending the cells in 10 mL of LB without antibiotics and repeating the centrifugation step. This process was done three times to remove the antibiotics from the media. Each strain pellet was resuspended in 1 mL of LB and the 3 cultures were mixed and poured in a LB agar plate. The plate was incubated for 48 hours at 30 ˚C. 2 mL of LB were added to bacterial layer growing on the plate and cells were resuspended and plated at dilutions 10^{-1}, 10^{-2}, 10^{-3} and 10^{-4} on LB plates with 30 μg/ml Kanamycin and 50 μg/ml Carbenicillin. Plates were incubated at 30 ˚C overnight. *S. oneidensis* MR-1 with pMEGGA_Cyc2C colonies were cultured and the plasmids were extracted to sequence the DNA sequence to confirm the presence of *cyc2* using the primer MEGGA_R (Table 2-6).

2.13.2. Bi-parental conjugation

S. oneidensis MR-1 Δ*mtrB*-Δ*mtrD* (recipient strain) was incubated overnight in 10 mL LB at 30 ˚C. *E. coli* WM3064 with pMEGGA_Cyc2C (donor strain) was incubated overnight in 10 mL LB at 37 ˚C with 30 μg/ml Kanamycin and 100 μg/ml of DAP. Both cultures were centrifuged at 5500 RCF for 15 minutes at 4 ˚C and *E. coli* WM3064 pellet was washed by resuspending the cells in 10 mL of LB without kanamycin and repeating the centrifugation step. This process was done three times to remove the antibiotic from the media. Each strain pellet was resuspended in 1 mL

of LB and *S. oneidensis* MR-1 Δ*mtrB*-Δ*mtrD* and *E. coli* WM3064 with pMEGGA_Cyc2C were mixed and poured in a LB agar plate with 100 μg/ml of DAP. The plate was incubated for 48 hours at 30 ˚C. 2 mL of LB were added to bacterial layer growing on the plate and cells were plated at dilutions 10^{-1}, 10^{-2}, 10^{-3} and 10^{-4} on LB plates with 30 μg/ml Kanamycin without DAP. Plates were incubated at 30 ˚C overnight. *S. oneidensis* Δ*mtrB*-Δ*mtrD* with pMEGGA_Cyc2C colonies were cultured and the plasmids were extracted to sequence the DNA sequence to confirm the presence of *cyc2* using the primer MEGGA_R (Table 2-6).

2.13.3. <u>Transformation by electroporation</u>

Plasmids pMEGGA_Cyc2N and pMEGGA_Cyc2$_{PV}$-1C were transformed into *S. oneidensis* MR-1 WT and *S. oneidensis* MR-1 Δ*mtrB*-Δ*mtrD* by electroporation. Strains were incubated overnight in 10 mL LB at 30 ˚C. 2 mL of the overnight were inoculated in 100 mL of LB and incubated 30 ˚C shaking at 200 rpm until the OD_{600} was 0.4. Cells were placed in 50 mL falcon tubes and centrifuged at 3220 RCF for 15 minutes at 4 ˚C. All supernatant was removed to avoid arcing and each pellets was resuspended in 8 mL 1 M Sorbitol. Samples were centrifuged at 3220 RCF for 15 minutes at 4 ˚C and resuspended in 2 mL 1 M Sorbitol. Cells were distributed in 390 μL aliquots. 0.25 μL Golden Gate Product (20 ng/μL) were mixed to the cells and samples were transferred to an ice cold 0.2 cm Gene Pulser®/Micropulser^{TM} Electroporation Cuvettes and were electroporated at 1.10 kV in the micropulser. Cells were immediately transferred to a 1.5 mL tube and 800 μL of SOC were added. Cells were recovered overnight at 30 ˚C shaking at 200 rpm. The following day samples were centrifuged at 4000 RCF for 2 minutes and 200 μL were plated on LB agar plates with 30 μg/ml Kanamycin. Plates were incubated at 30 ˚C overnight. *S. oneidensis* MR-1 colonies were cultured and the plasmids were extracted to sequence the DNA sequence to confirm the presence of *cyc2* and *cyc2$_{PV-1}$* using the primer cyc2_start_F and MEGGA_R respectively (Table 2-6).

2.14 Expression of Cyc2 and Cyc2$_{PV-1}$

To express Cyc2 and Cyc2$_{PV-1}$ in *S. oneidensis* MR-1, strains of the WT and Δ*mtrB*-Δ*mtrD* mutants with the plasmids pMEGGA_Cyc2C, pMEGGA_Cyc2N and pMEGGACyc2$_{PV-1}$C were incubated overnight in LB with 30 μg/ml Kanamycin at 30 ˚C. 10 mL of the overnight culture were inoculated in 100 mL of LB with 30 μg/ml Kanamycin in baffled conical flasks and incubated at 30 ˚C shaking at 200 rpm until the OD$_{600}$ was 0.4. The expression of the cytochromes Cyc2 and Cyc2$_{PV-1}$ was induced by adding 5 mM L-arabinose to the cultures and cells were incubated at 16 ˚C shaking at 200 rpm for 4 hours. Cells were centrifuged at 6000 RCF for 30 minutes at 4 ˚C. To escalate the amount of biomass, 1 L cultures were induced with the same conditions.

2.15 Separation of cell fractions

To separate the periplasm from the other fractions, cell pellets from 100 mL cultures were resuspended in 1 mL 0.2 M Tris, 1 M Sucrose and 1 mM EDTA at pH 8 with HCl. 1 mg/ml Lysozyme was added and cells were incubated at room temperature for 15 minutes. 4 mL of H$_2$O were added and samples were incubated on ice for another 15 minutes. The periplasm fraction was separated from the cells by being centrifuged at 200000 RCF for 45 minutes. The supernatant contained soluble proteins from the periplasm fraction and the pellet the spheroplasts.

Spheroplasts were resuspended in 5 mL 100 mM Tris pH 7.8 with HCl. To lyse the samples, tubes were placed on ice and sonicated with 3 pulses of 30 seconds were done, with 2 minutes of recover on ice between each pulse. Cell lysates were centrifuged at 5500 RCF for 20 minutes at 4 ˚C to remove cell debris. To separate the cytoplasm fraction from the membranes, cell lysates were ultracentrifuged at 200000 RCF for 45 minutes at 4 ˚C. The supernatant contained soluble proteins from the cytoplasm and the pellet contained the membrane proteins.

To separate the inner membrane from the outer membrane, membrane pellets were resuspended in 100 mM Tris pH 7.8 (HCl) with 5 mg/ml Sodium lauroyl sarcosinate (sarkosyl) (Brown *et al.*, 2010). The soluble fraction contained the inner membrane and the pellet the outer membrane. To solubilise the outer membrane, different detergents were tested (Table 2-11).

Table 2-11 List of detergents used for membrane solubilisation
All critical micelle concentrations (CMC) are from Sigma product specifications
The final concentration is in 100 mM Tris pH 7.8

Detergent	Type	CMC (mM)	Final concentration (mM)
DDM		0.17	0.85
OGP	Nonionic	20-25	125
Triton X-100		0.2-0.9	18
Tween 20		0.06	0.3
CHAPS	Zwitterionic	6-10	50
LDAO		1	5
SDS	Anionic	7-10	50

2.16 Polyacrylamide gel electrophoresis

2.16.1. SDS-PAGE

Sodium dodecyl sulphate polyacrylamide gel electrophoresis (SDS-PAGE) was used to separate proteins by their mass. Components of the gel are described in Table 2-12. APS and TEMED were added at the end to prevent an early polymerisation of the acrylamide.

Table 2-12 Composition of SDS-PAGE

Reagent	Separating % (v/v)	Stacking % (v/v)
ProtoGel (37.5:1 Acrylamide to Bisacrylamide Stabilized Solution)	50	16.7
1 M Tris pH 8.8 (HCl)	37	-
1 M Tris pH 6.8 (HCl)	-	12.5
10% (w/v) APS	0.7	0.5
20% (w/v) SDS	0.5	0.5
TEMED	0.1	0.1

10 µL of cellular fraction sample was mixed with 5 µL SDS-PAGE loading buffer (125 mM Tris pH 6.8 (HCl), 4 % (w/v) SDS, 20 % (v/v) Glycerol, 0.002 % (w/v) Bromophenol blue and 5 M Urea) and samples were incubated at 100 ˚C for 10 minutes before they were loaded in the wells of the gel. Each gel had a well with a protein standard (Table 2-13). Gels run in SDS-PAGE running buffer (25 mM Tris, 52 mM Glycine and 2.4 mM SDS) at 140 V until the dye front reached the bottom of the gel.

Table 2-13 Molecular weight protein standards used in this thesis

Protein Standard	Characteristics
Precision Plus Protein™ Unstained Protein Standard, Strep-tagged (Biorad)	Unstained. For coomassie stain and western-blot. Strep-tag II positive
Precision Plus Protein™ Dual Color Standards (Biorad)	Stained. For heme stain and western-blot.
ACTGene™ Prestained Protein Marker (ACTGene)	Stained. For heme stain and western-blot.

2.16.2. Native gels

Native polyacrylamide gel electrophoresis (native-PAGE) was used to separate the proteins by mass and charge without denature them. Components of the gel are described in Table 2-14. APS and TEMED were added at the end to prevent an early polymerisation of the acrylamide.

Table 2-14 Composition of native-PAGE

Reagent	Separating %	Stacking %
ProtoGel (37.5:1 Acrylamide to Bisacrylamide Stabilized Solution)	18.6	16.6
1 M Tris pH 8.8 (HCl)	35.3	36.45
10% (w/v) APS	0.6	0.6
Triton X-100	0.2	0.2
TEMED	0.1	0.1

10 µL of cellular fraction sample was mixed with 5 µL native-PAGE loading buffer (125 mM Tris pH 6.8 (HCl) and 20 % (v/v) Glycerol). Samples were loaded to the wells and one well contained native-PAGE loading buffer with 0.002 % (w/v) Bromophenol blue. Gels run in native-PAGE running buffer (25 mM Tris and 192 mM Glycine) at 25 mA until the dye front reached the bottom of the gel.

2.16.3. <u>Coomassie stain</u>

To stain all the proteins of a gel, Instant Blue (Expedeon) was poured on a tray until the gel was fully covered and it was incubated while shaking at 20 rpm for 1 hour.

2.16.4. <u>Heme stain</u>

To stain proteins with heme groups, gels were incubated for 10 minutes in 0.25 M Sodium acetate pH 4 (HCl). Afterwards, 15 mL 100 % (v/v) Methanol with 0.1% (w/v) TMBD were added to the solution and it was incubated in the darkness, while shaking at 20 rmp for another 10 minutes. To reveal the bands with the heme groups, 1 mL Hydrogen peroxide was added and incubated while shaking at 20 rpm until bands showed up. The reaction stopped when the gel was washed with H_2O.

2.17 Peptide mass fingerprinting

To confirm the presence of Cyc2 and $Cyc2_{PV-1}$, protein bands from SDS-PAGE gels were sent to analyse by peptide mass fingerprinting at the John Innes Centre Proteomics Facility (Norwich Research Park).

Protein bands could not be cut from a gel stained from a heme stain, and cytochromes do not stain very well with Coomassie stain. For this reason, samples were loaded in a gel in duplicate, and half of the gel was treated with heme stain and the other half with Coomassie stain (Chapter 2.16.3 and 2.16.4). The bands were cut from the second part of the gel doing an estimation of the location of the bands comparing it with the heme stain part. A sterile scalpel was used to cut the bands from the gel to avoid protein contamination.

To send the samples to analyse, bands were de-stained with 30 % (v/v) Ethanol at 65 ˚C in low binding tubes LoBind microcentrifuge tubes (Eppendorf®). This process was repeated until the band had lost all the coomassie stain. Bands were then mixed with a solution containing 50 % (w/v) Acetonitrile and 50 mM Ammonium bicarbonate. Bands were then transferred to a fresh tube with 10 mM Dithiothreitol and incubated at 55 ˚C for 30 minutes. Afterwards, the solution was removed and 50 mM Ammonium was added to the tube. Samples were kept in the darkness shaking at 1000 rpm for 30 minutes. Bands were washed with a solution containing 50 % (w/v) Acetonitrile and 50 mM Ammonium bicarbonate and then a wash of 50 mM Ammonium bicarbonate.

Bands were cut in 1 mm^2 pieces and washed with a solution containing 50 % (w/v) Acetonitrile and 50 mM Ammonium bicarbonate following a wash of 50 mM Ammonium bicarbonate. Finally gel fragments were washed in 100 % (v/v) Acetonitrile. Any liquid was removed from the tubes and samples were sent to be tryptic digested and Matrix-Assisted Laser Desorption/Ionization Time Of Flight (MALDI-TOF).

Mascot 2.4 server was used to search in the UniProt Swiss-Prot/TrEMBL database, comparing the resulted peptide masses with digestions by trypsin/P enzyme and common contaminants. Protein scores had to be greater than 85 to be considered significant ($p < 0.05$).

2.18 Western-blot

To check if the strep-tag II was being expressed with Cyc2 and Cyc2$_{PV-1}$, a western blot was done to identify the tag with specific antibodies. After the SDS-PAGE electrophoresis (Chapter 2.16.1), the gel was transferred to a tray containing Cathode Transfer Buffer (25 mM Tris, 10 % (v/v) Methanol, 40 mM Glycine at pH 8.4 using HCl). 6 filter papers of the size of the gel were soaked in Cathode Transfer Buffer, 4 sheets with Anode Transfer Buffer 1 (300 mM Tris, 10 % (v/v) Methanol) and 2 sheets with Anode Transfer Buffer 2 (25 mM Tris, 10 % (v/v) Methanol). A polyvinylidene difluoride (PVDF) membrane, also of the

same size of the gel, was activated by incubating it with 100 % (v/v) methanol for 15 seconds, rinsed with H_2O and incubated with Anode Transfer Buffer 2 for 5 minutes.

In the western blotting transfer system, carefully trying to prevent bubble formation, 4 sheets incubated with Anode Transfer Buffer 1 were placed on the cathode, then 2 sheets incubated with Anode Transfer Buffer 2, then the PVDF membrane was placed, the SDS-PAGE gel and finally 6 sheets incubated with Cathode Transfer Buffer. The transfer was run at 90 mA for 85 minutes.

After the transfer, the membrane was blocked in TBST (20 mM Tris ph 7.5 (HCl), 150 mM NaCl and 0.1 % (v/v) Tween 20) with 5 % (w/v) skimmed milk powder shaking at 20 rpm for 80 minutes. 0.6 µg/mL of Rabbit Anti Strep-tag II IgG antibody were added to the blocking solution and it was incubated at 4 ˚C shaking at 20 rpm overnight. The following day, the membrane was washed with TBST for 5 minutes shaking at 20 rpm 5 times to remove the primary antibody from the solution. After the final wash, the membrane was incubated with TBST and 0.15 µg/mL of Goat Anti Rabbit IgG conjugated to alkaline phosphatase for 60 minutes. The membrane was washed again 5 times with TBST to remove the secondary antibody from the solution. The membrane was finally placed in an empty tray and 1-Step^{TM} NBT/BCIP Substrate Solution (ThermoFisher Scientific) until the colour change allowed to visualise the bands. The reaction was stopped by pouring away the substrate and washing the membrane with H_2O.

2.19 Purification using the Strep-tag II

Because Cyc2 could not be solubilised with any of the tested non-ionic or zwitterionic detergents, 1 L culture membrane fractions from *S. oneidensis* MR-1 expressing Cyc2 were resuspended with 35 mL 1.2 % (v/v) Triton X-100 and ultracentrifuged at 200000 RCF for 45 minutes. Cyc2 remained in the pellet and it was resuspended with 10 mL 1.5 % (w/v) SDS.

To purify Cyc2, 5 mL StrepTrap HP (GE Healthcare) was used to attach the proteins with the Strep-tag II to the column. All the process was done with an

ÄKTAprime plus (Ge Healthcare) at a flow rate of 0.3 mL/min at 4 ˚C. To regenerate the column, 5 column volumes of 10 mM NaOH went through the column. Afterwards, the column was washed with 5 column volumes of Buffer W (100 mM Tris pH 8 (HCl), 150 mM NaCl and 1 mM EDTA) with 0.1 % (w/v) SDS. Samples were diluted with 100 mL of Buffer W and loaded to the column. The column was washed with 5 column volumes of Buffer W with 0.1 % (w/v) SDS and eluted with 2 column volumes of Buffer W with 0.1 % (w/v) SDS and 50 mM Biotine. At this step, the pH had to be adjusted with NaOH due to the Biotine. 0.5 mL fractions were collected during the whole elution step.

2.20 Redox spectroscopic assay

The spectra of the *c*-type cytochromes were measured in a glovebox with a concentration of O_2 bellow 0.5 ppm to avoid spontaneous oxidation. All reagents were sparged with N_2 and pipette tips and 1 cm polystyrene cuvettes were there for a minimum of 24 hours in the glovebox before being used. After expressing the cytochrome for 4 hours at 16 ˚C aerobically (Chapter 2.14), cells were transferred into the glovebox and diluted in 100 mM HEPES pH 7.2 (NaOH) until the absorbance at 600 nm was 1.6. With the spectrophotometer, the cell spectrum from 510 nm to 570 nm was measured. Cells were reduced by adding 1 mM Formate to the samples, and after 1 minute of incubation the spectrum was measured again. Finally, cells were re-oxidised by adding 3 mM Fe(III)citrate and after 1 minute of incubation the spectrum was measured for a third time.

2.21 Data analysis and bioinformatic tools

2.21.1. Spectrophotometry analysis

Spectrophotometer data was analysed with Microsoft Excel as well as the graphic representation of the results.

2.21.2. Protein analysis

Cyc2 and Cyc2$_{PV-1}$ amino acid sequences where obtained the UniProt database. The molecular weight of the proteins were estimated using the Sequence

Manipulation Suite (Stothard, 2000), the location of the peptide signals where predicted using the SignalP 4.1 Server (Petersen *et al.*, 2011) and the presence of beta-barrel topology was predicted with BOCTOPUS2 (Hayat *et al.*, 2016).

2.21.3. Golden Gate Assembly

In order to design the right primers for inserting *cyc2* and *cyc2$_{PV-1}$*, Genome Compiler was used for a virtual digestion and ligation of the insert in the vector to detect if the DNA fragments had other BsmBI recognition sites that could affect the cloning and check that the cohesive ends formed were going to insert the vector in the right place. *cyc2$_{PV-1}$* from *Mariprofundus ferrooxydans* PV-1 was synthesised with the regions for the golden gate already as part of the sequence. Moreover, it was codon optimised for *S. oneidensis* MR-1.

2.21.4. Genomic analysis

All sequenced fragments from PCR products and plasmid extractions were aligned against the NCBI database using BLAST (Altschul *et al.*, 1990).

The presence of *c*-type cytochrome motifs was analysed using MAST (Bailey and Gribskov, 1998). Because this data base had a limited number of genomes available, the search was done with *Acinetobacter baumannii* and *Citrobacter rodentium* (Table A-1). Later on, the matches were contrasted with the environmental samples to confirm that they also got the genes of interest.

The alignment of the reads in contigs and the genome annotation of the isolated environmental strains were done by microbesNG (University of Birmingham).

The mapping of the contigs in *Acinetobacter* (UEA) and the identification of housekeeping genes was done using SnapGene Viewer (GSL Biotech) and BLAST (Altschul *et al.*, 1990).

For the taxonomical analysis, the 16S rRNA analysis and the multilocus sequence analysis (MLSA) were done using BLAST (Altschul *et al.*, 1990), the

average nucleotide identity (ANI) analysis was done using the ANI Calculator (EZ BioCloud) (Yoon *et al.*, 2017).

2.21.5. Transcriptomic analysis

To analyse the differential expressed genes between two or more culture conditions, three bioinformatic tools are used: Tophat, Cufflinks and Cuffdiff.

Tophat: aligns the cDNA fragments from the RNAseq to a reference genome from a database provided, in this case NCBI. This step was done by the Wellcome Centre for Human Genetics (University of Oxford).

Cufflinks combines and quantifies the number of transcripts from a region. This step was also done by the Wellcome Centre for Human Genetics (University of Oxford).

Cuffdiff compares the amount of transcripts between regions and contrasts the regions with an annotated reference genome to know which genes are being upregulated and downregulated compared to another culture condition. This analysis was done using Galaxy (Afgan *et al.*, 2018). Genes were considered significantly upregulated of downregulated if the q-value was less than 0.05. The results were plotted on a graph using Microsoft Excel.

2.21.6. Metabolic functions

The Kyoto Encyclopedia of Genes and Genomes (KEGG) (Kanehisa Laboratories) was used to analyse the predicted protein functions of the studied genes, and the metabolic pathways were they could have a role in.

2.22 References

Afgan, E., Baker, D., Batut, B., van den Beek, M., Bouvier, D., Čech, M., et al. (2018) The Galaxy platform for accessible, reproducible and collaborative biomedical analyses: 2018 update. *Nucleic Acids Res.* 46: W537–W544.

Altschul, S.F., Gish, W., Miller, W., Myers, E.W., and Lipman, D.J. (1990) Basic local alignment search tool. J. Mol. Biol. 215:403-410.

Bailey, T.L. and Gribskov, M. (1998) Combining evidence using p-values: application to sequence homology searches. *Bioinformatics* 14: 48–54.

Brown, R.N., Romine, M.F., Schepmoes, A.A., Smith, R.D., and Lipton, M.S. (2010) Mapping the Subcellular Proteome of *Shewanella oneidensis* MR-1 using Sarkosyl-Based Fractionation and LC−MS/MS Protein Identification. *J. Proteome Res.* 9: 4454–4463.

Dashiff, A. and Kadouri, D.E. (2009) A new method for isolating host-independent variants of *Bdellovibrio bacteriovorus* using *E. coli* auxotrophs. *Open Microbiol. J.* 3: 87–91.

Dekker, L., Arsène-Ploetze, F., and Santini, J.M. (2016) Comparative proteomics of *Acidithiobacillus ferrooxidans* grown in the presence and absence of uranium. *Res. Microbiol.* 167: 234–239.

Figurski, D.H. and Helinski, D.R. (1979) Replication of an origin-containing derivative of plasmid RK2 dependent on a plasmid function provided in trans. *Proc. Natl. Acad. Sci. U. S. A.* 76: 1648–52.

Hanahan, D. (1983) Studies on transformation of *Escherichia coli* with plasmids. *J. Mol. Biol.* 166: 557–580.

Hayat, S., Peters, C., Shu, N., Tsirigos, K.D., and Elofsson, A. (2016) Inclusion of dyad-repeat pattern improves topology prediction of transmembrane β-barrel proteins. *Bioinformatics* 32: 1571–1573.

Maniatis, T., Fritsch, E.F., and Sambrook, J. (1982) Molecular cloning : a laboratory manual Cold Spring Harbor Laboratory.

Petersen, T.N., Brunak, S., von Heijne, G., and Nielsen, H. (2011) SignalP 4.0: discriminating signal peptides from transmembrane regions. *Nat. Methods* 8: 785–786.

Richardson, D.J., Edwards, M.J., White, G.F., Baiden, N., Hartshorne, R.S., Fredrickson, J., et al. (2012) Exploring the biochemistry at the extracellular redox frontier of bacterial mineral Fe(III) respiration. *Biochem. Soc. Trans.* 40: 493–500.

Stothard, P. (2000) The sequence manipulation suite: JavaScript programs for analyzing and formatting protein and DNA sequences. *Biotechniques* 28: 1102, 1104.

Viollier, E., Inglett, P.., Hunter, K., Roychoudhury, A.., and Van Cappellen, P. (2000) The ferrozine method revisited: Fe(II)/Fe(III) determination in natural waters. *Appl. Geochemistry* 15: 785–790.

Yoon, S., Sanford, R.A., and Löffler, F.E. (2013) *Shewanella* spp. Use acetate as an electron donor for denitrification but not ferric iron or fumarate reduction. *Appl. Environ. Microbiol.* 79: 2818–22.

Isolation and identification of iron-reducing bacteria

3.1 Introduction

Shewanella oneidensis MR-1 was the first microorganism identified as a dissimilatory metal reducer. It was isolated by Myers and Nealson in 1988 in Lake Oneida (United States) and since its discovery, there has been a lot of interest in understanding how its extracellular electron transport system works. The proteins involved in the metal reducing pathway of this gram-negative bacteria have been identified and, with the use of genomic analysis, homologous proteins have been predicted in other environmental microorganisms (Shi, Rosso, Zachara, *et al.*, 2012).

Although dissimilatory iron reduction has been thoroughly studied in the laboratory, there is little known about the diversity of microorganisms able to use ferric iron (Fe^{3+}) as a respiratory terminal electron acceptor in the environment, or the impact they have in the ecosystem. The objective of this chapter was to use classic microbiology techniques to isolate iron reducers from different environments where these microorganisms could have an important role in iron bioavailability, and to characterise their metabolic pathways by biochemical analysis.

3.2 Identification of iron-reducers

3.2.1. Environmental samples

When it comes to isolating iron reducing microorganisms from the environment, the first places that come to mind are anoxic soils and sediments, rich in iron, where aerobic respiration cannot be achieved. However, dissimilatory iron reduction is a key process in any environment, as iron is resolubilised and becomes bioavailable for other microorganisms, allowing their survival. For this reason, iron reducers might be also found in aerobic environments, such as fresh water or the ocean, where the concentration of iron is lower and aerobic respiration is possible.

With the aim of isolating novel species that could have a role in iron recycling, fresh water, sediment and soil samples were taken from different locations in Norfolk (United Kingdom) (Chapter 2.3). The soluble iron content in each sample was measured to determine how much iron was bioavailable in each specific environment (Table 3-1).

Table 3-1 Concentration of bioavailable ferrous and ferric iron in the sampled environments
Fresh water samples were taken at two different points of the river Yare: at the University of East Anglia (UEA) and from the Whitlingham Great Broad (WGB). A sediment sample was also taken from the Whitlingham Great Broad. Finally, a soil sample was taken from a field in Raveningham (RVG). The amount of soluble ferrous iron (Fe^{2+}) was measured using a ferrozine assay (Chapter 2.4). Following this, samples were fully reduced using sodium dithionite to measure the total soluble iron concentration and calculate the amount of soluble ferric iron (Fe^{3+}).

Sample	Soluble Fe^{2+}	Soluble Fe^{3+}
Water (UEA)	0 μM	0.4 μM
Water (WGB)	0 μM	0.7 μM
Sediment (WGB)	16.3 μmol/kg	55.8 μmol/kg
Soil (RVG)	2.5 μmol/kg	16.8 μmol/kg

While the sediment and soil samples had soluble iron both in the oxidised and reduced state, fresh water samples had much less bioavailable iron and the found that was present was in its oxidised state, probably forming complexes with organic ligands otherwise they would precipitate as iron oxides.

3.2.2. Enrichment, isolation and identification

To isolate microorganisms that were able to use ferric iron (Fe^{3+}) as an electron acceptor, selective growth conditions for iron reduction were developed in the laboratory. The samples were enriched in minimal media for ferric iron (Fe^{+3}) respiration (Chapter 2.2.3) under anaerobic conditions, with Fe(III)citrate as the sole terminal electron acceptor, to select for iron-reducing microorganisms. Once iron-reducing bacteria were enriched, the cultures were inoculated on solid minimal media under anaerobic conditions with Fe(III)citrate as the sole terminal electron acceptor with the aim of isolating colonies.

Single colonies were restreaked on LB plates multiple times to decrease the risk of satellite colonies surviving due to proximity to iron-reducing isolates in minimal media. A single colony from LB agar was used to amplify the 16S rRNA and the PCR products were sequenced to identify which microorganisms had been enriched from the environmental samples. As Table 3-2 shows, isolated colonies from fresh water samples and from the soil sample were identified as species from the genus *Acinetobacter*. The isolated colony from the sediment sample was identified as *Citrobacter*.

Table 3-2 16S rRNA identification of isolated colonies from environmental samples
Identification of river water isolates from the river Yare at the University of East Anglia (UEA) and from the Whitlingham Great Broad (WGB), a sediment isolate from the Whitlingham Great Broad and a soil isolate from a field in Raveningham (RVG). The alignment was done against the NCBI database using BLAST as the alignment tool (Altschul *et al.*, 1990).

Colony	Highest Hit	Query Cover %	Identity %
Water (UEA)	*Acinetobacter johnsonii*	98	99
Water (WGB)	*Acinetobacter kyonggiensis*	98	99
Sediment (WGB)	*Citrobacter freundii*	98	97
Soil (RVG)	*Acinetobacter guillouiae*	99	99

Acinetobacter is a genus of gram-negative bacteria, from the *Pseudomonadales* order. It is ubiquitous in the environment, being found in soil, fresh water, marine water, food and animals (Al Atrouni et al., 2016). The most studied species of this genus is *Acinetobacter baumannii*, which is an opportunistic pathogen that causes nosocomial infections in hospitals such as wound infections, pneumonia, meningitis, urinary tract infections or osteomyelitis. The pathogenic *A. baumannii* has become multidrug resistant and it has been placed at the top of the list of bacteria for which new antibiotics are urgently needed by The World Health Organization (Lee et al., 2017). It has been described as an strictly aerobic bacterium (Chan et al., 2012), and as a result it has not been considered in the context of iron respiration in previous literature.

Citrobacter is a genus of gram-negative bacteria, from the *Enterobacteriales* order. It is also ubiquitous in the environment, found in soil, fresh water, food and in the gut microbiota of animals. Some species of this genus are opportunistic pathogens in humans that can cause infections such as diarrhea, septicemia,

meningitis or urinary tract infections (Zhou et al., 2017). *Citrobacter* has been described as a facultative aerobic and can grow by fermentation in anaerobic environments (Peter et al., 2014). It is able to oxidize ferrous iron (Fe^{2+}) to use it as an electron donor (Li et al., 2014) but it has not been previously described as an iron-reducing bacterium.

All further experiments to study the activity of the environmental iron-reducing bacteria were performed with the *Acinetobacter* strain isolated from the University of East Anglia (UEA) fresh water sample, and with the *Citrobacter* strain isolated from the Whitlingham Great Broad (WGB) sediment sample.

3.2.3. Soluble iron reduction

The ability of microbial colonies to reduce iron can be confirmed using a plate-based ferrozine assay (Hirayama and Nagasawa, 2017). This method is based on the fact that when ferrozine is combined with soluble ferric iron (Fe^{3+}) there is no reaction, but when it is combined with soluble ferrous iron (Fe^{2+}) they react forming a purple complex:

$$3 \text{ Ferrozine} + \text{Fe}(H_2O)_6^{2+} \rightarrow \text{Fe}(\text{Ferrozine})_3^{4-} + 6H_2O.$$
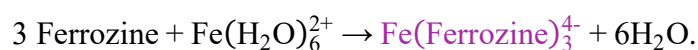
Iron reducing activity can be observed in bacteria growing on plates that contain ferric iron (Fe^{3+}) as an electron acceptor and ferrozine (Figure 3-1). When *Acinetobacter* spp. UEA and *Citrobacter* spp. WGB grew under anaerobic conditions with ferric iron (Fe^{3+}) in LB plates with ferrozine, the plate turned purple suggesting that under these conditions the isolates were able to reduce the available iron. As a positive reference of an iron-reducing bacterium, *S. oneidensis* MR-1 WT was tested and it also turned the media purple. However, the negative control *E. coli* JM101 did not change the colour of the media.

The intensity of the ferrozine-ferrous iron complex can be detected using a spectrophotometer. Therefore, a quantitative measurement of the iron reduction activity can be achieved with iron reducers grown in liquid media.
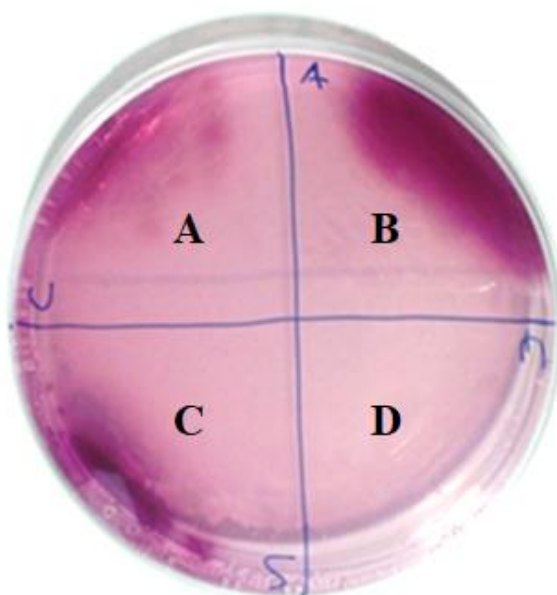
Figure 3-1 Qualitative detection of iron reduction
A) Citrobacter spp. WGB. B) Acinetobacter spp. UEA. C) S. oneidensis MR-1 WT.
D) E. coli JM101. 24 hours after plated anaerobically on a LB plate at 25 ˚C with 0.5 mM
Fe(III)citrate as the only electron acceptor source and with 30 μL ferrozine solution/mL LB. The
presence of iron reducing activity can be detected by the presence of a purple colour in the media
where there is bacterial growth. S. oneidensis MR-1 WT was used as a positive reference of
iron-reducer bacterium and E. coli JM101, that can grow on LB plate but it cannot reduce ferric
iron (Fe^{3+}) used as a negative control.

3.3 Iron reduction by chemoheterotrophic gram-negative bacteria

3.3.1. Iron reduction using different carbon sources

As chemoheterotrophs, iron-reducing bacteria obtain their energy from the oxidation of organic molecules. Depending on what carbon source they use to accomplish anaerobic respiration, variable amounts of ATP are produced by substrate level phosphorylation and variable amounts of NADH are oxidised by electron transport chain to produce ATP by oxidative phosphorylation (Nelson *et al.*, 2013).

In addition to energy production, cells need to use catabolic processes to produce lipids, amino acids, carbohydrates and nucleotides to grow and increase their biomass. Acetyl-CoA and pyruvate are two molecules that are part of both of

the cellular respiration pathway and the central catabolism of the cell. For this reason, the carbon source used for anaerobic respiration must be linked to the production of acetyl-CoA and pyruvate for cell survival (Tang *et al.*, 2007; Kane *et al.*, 2016).
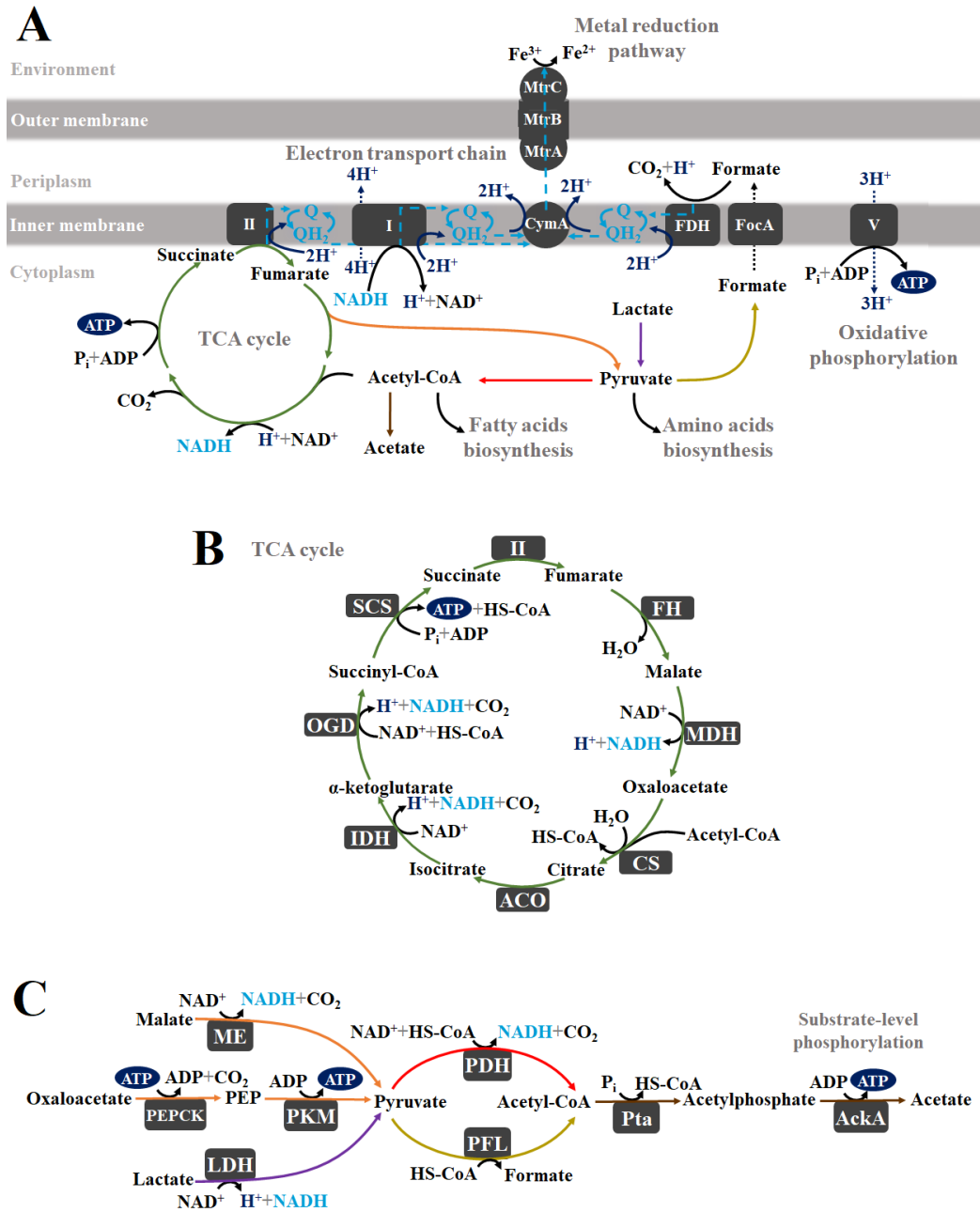
Figure 3-2 Iron respiratory pathway of S. oneidensis MR-1
A) *Overview of the cellular respiration pathways in S. oneidensis MR-1 when ferric iron is used as the electron acceptor. B) Tricarboxylic acid cycle. C) Pyruvate metabolism. Enzymes are shown in boxes. Chemical reactions are shown in black arrows. Electron transfer is shown in light blue dashed arrows. Molecule transport across the inner membrane is shown in dotted arrows. Processes contributing to energy generation are shown in dark blue.*

In Figure 3-2 there is an overview of the pathways that can be used to achieve iron reduction from different carbon sources in *S. oneidensis* MR-1. To achieve iron reduction, *Shewanella* is not able to use acetate as the sole carbon source because the transformation from acetate to acetyl-CoA is not energetically favourable (Figure 3-2 A and C and Table 3-3) (Yoon *et al.*, 2013). Without acetyl-CoA, cellular respiration cannot be achieved since this molecule is essential for the TCA cycle, and therefore, cells do not have enough energy to survive.

Table 3-3 ATP produced using different carbon sources in S. oneidensis MR-1 during anaerobic respiration
Formate cannot be transformed to acetyl-CoA or pyruvate because it is oxidised directly to CO_2. The use of acetate in energy-constrained conditions, like anaerobic respiration, do not allow to the transformation of acetate to acetyl-CoA because it requires ATP to produce it. The ATP molecules produced for each pathway have been calculated from one molecule of the studied carbon source

Carbon source	Biosynthesis pathway		Cellular respiration pathway
	Acetyl-CoA	Pyruvate	
Formate	-	-	1 ATP
Acetate	-1 ATP	-3 – 6.6 ATP	6.6 ATP
Lactate	1 – 2 ATP	2 ATP	10.6 – 11.6 ATP
Succinate	4 ATP	2 ATP	2.6 ATP

When formate is the sole carbon source, it is transported to the periplasm across a membrane transporter (FocA) and oxidised to CO_2 (Figure 3-2 A). The electrons are shuttled across the quinone pool to the cytochrome CymA, and they cross the outer membrane through the metal reducing complex CAB (MtrCAB) where ferric iron (Fe^{3+}) is reduced to ferrous iron (Fe^{2+}). Although the use of formate as the carbon source produces enough proton motive force to allow ATP synthesis by oxidative phosphorylation, no other organic molecules are produced during this process, and no acetyl-CoA nor pyruvate are produced and consequently cells cannot grow (Table 3-3).

When lactate is the sole carbon source, it is oxidised to pyruvate by lactate dehydrogenase (LDH) and from there, it can either form formate and acetyl-CoA by pyruvate formate-lyase (PFL) or just acetyl-CoA by pyruvate dehydrogenase (PDH) (Figure 3-2 A and C). Acetyl-CoA can either continue cellular respiration by entering the TCA cycle, or it can be used as a lipid precursor

to support cell growth or it can be transformed to acetate to generate ATP by substrate level phosphorylation. NADH molecules reduced during the TCA cycle are reoxidized by complex I and the electrons are shuttled to the quinone pool and transported to the extracellular ferric iron (Fe^{3+}) though the Mtr pathway. ATP generation by oxidative phosphorylation is supported by the proton motive force created both by the NADH dehydrogenases and the FDH when the produced formate is oxidised to CO_2 (Table 3-3) (Pinchuk *et al.*, 2011).

Whether *Shewanella* can grow with succinate as the sole carbon source is controversial. Genomic analysis indicates that it has all the genes required to complete the TCA cycle (Table 3-3) (Yang *et al.*, 2010). However, a previous metabolic flux analysis using lactate as the sole carbon source suggests that malate and phosphoenolpyruvate (PEP) cannot be transformed to pyruvate by malic enzyme (ME) and phosphoenolpyruvate carboxykinase (PEPCK), respectively (Figure 3-2 B and C) (Tang *et al.*, 2007). It is unknown if, when succinate is the sole carbon source these enzymes would remain inactive. It is also unclear if unlike when lactate is used as the carbon source, their activity would be essential to produce acetyl-CoA and support cell growth.

There are no previous references in the literature about the ability of *Acinetobacter* and *Citrobacter* to obtain energy from iron reduction. According to the gene database from NCBI, the pyruvate metabolism and the TCA cycle of the environmental bacteria are the same as pyruvate metabolism in *Shewanella* (Figure 3-2), which suggests that they could use the same pathways to achieve anaerobic respiration. The only difference is that *Acinetobacter* genus do not have pyruvate formate-lyase (PFL) so pyruvate has to be transformed to acetyl-CoA by pyruvate dehydrogenase (PDH) and formate is not formed in this process (Figure 3-2 A and C). On the other hand, *Acinetobacter* do have formate dehydrogenase so when formate is the main carbon source, it could be oxidised to reduce ferric iron (Fe^{3+}) (Figure 3-2 A).

To test the iron reduction activity of $S.$ $oneidensis$ MR-1 WT and the isolated strains $Acinetobacter$ spp. UEA and $Citrobacter$ spp. WGB, cultures were grown in minimal media anaerobically, with 0.5 mM Fe(III)citrate as the electron acceptor. The four different carbon sources were tested to see how able they were to reduce ferric iron (Fe^{3+}): 50 mM Formate, 15 mM Acetate, 20 mM Lactate and 30 mM Succinate.

$S.$ $oneidensis$ MR-1 WT reduced over 50 % of the available ferric iron within the first 24 hours of incubation with formate, lactate or succinate as the sole carbon sources. However, ferrous iron (Fe^{2+}) was not detected after 144 hours cultured with acetate as the sole carbon source (Figure 3-3 A).

$Acinetobacter$ spp. UEA strain reduced over 50 % of the ferric iron (Fe^{3+}) when cultured with lactate after 96 hours of incubation. After 144 hours, almost 50 % of the ferric iron (Fe^{3+}) was reduced when succinate was the only carbon source, 20 % with acetate and just 10 % with formate (Figure 3-3 B).

$Citrobacter$ spp. WGB strain reduced over 50 % of the ferric iron (Fe^{3+}) within the first 24 hours incubated with lactate and after 96 hours with succinate. After 144 hours, 15 % of the ferric iron (Fe^{3+}) was reduced when cultured with acetate, and no ferrous iron (Fe^{2+}) was detected when formate was the sole carbon source (Figure 3-3 C).
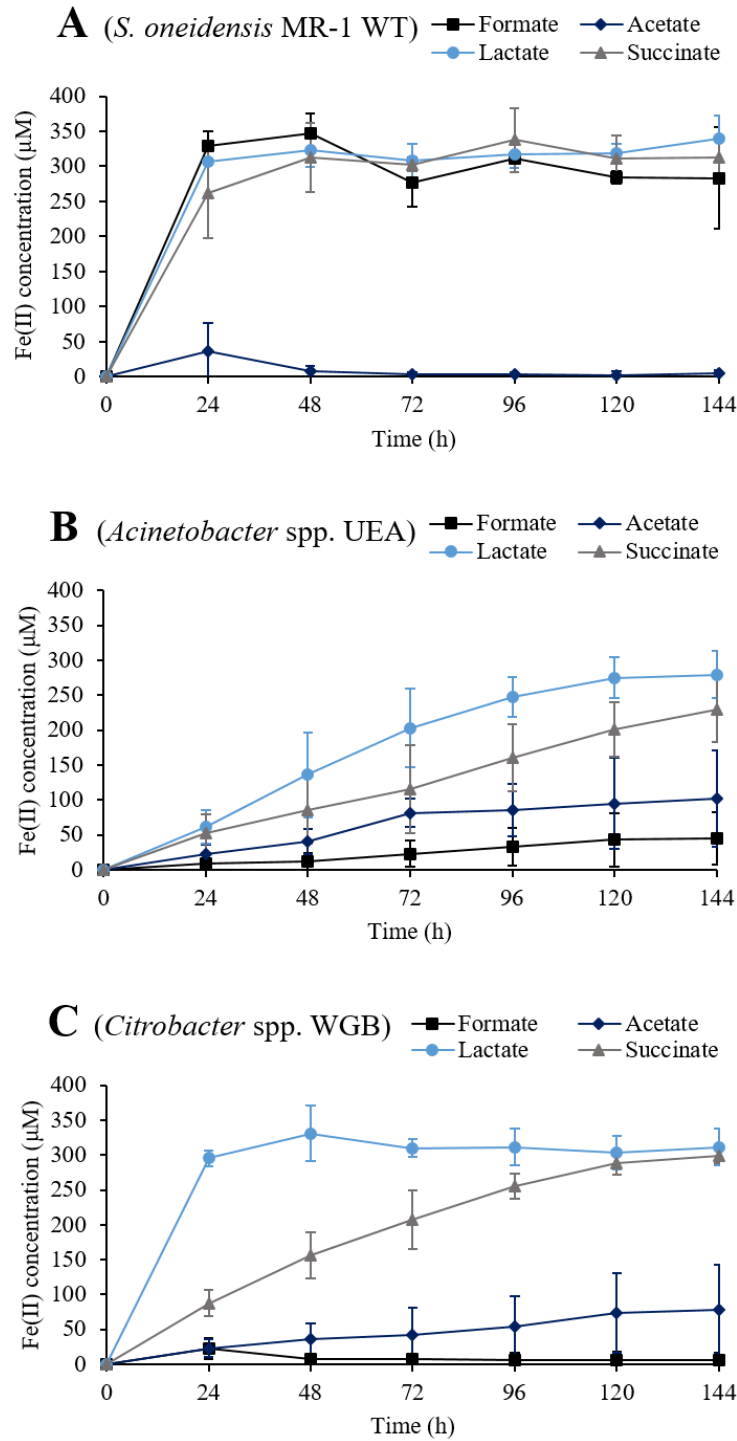
Figure 3-3 Bacterial soluble iron reduction using different carbon sources
Ferrous iron (Fe^{2+}) measurement by ferrozine assay (Chapter 2.4) of cells cultured anaerobically in minimal media at 25 ˚C with 0.5 mM Fe(III)citrate as the electron acceptor source and either 50 mM Formate, 15 mM Acetate, 20 mM Lactate or 30 mM Succinate. Figure A: Shewanella oneidensis MR-1 WT. Figure B: Acinetobacter spp. UEA. Figure C: Citrobacter spp. WGB. Each data point represents the average of three biological replicates and the error bars represent the ± standard deviation (SD).

3.3.2. <u>Iron reduction of different ferric iron (Fe^{3+}) species</u>

Ferric iron (Fe^{3+}) at neutral pH water is commonly found in complex with organic molecules. These complexes are soluble and they do not sink out of the water column, so iron remains available in these environments (Emerson *et al.*, 2012).

Three different ferric iron (Fe^{3+}) chelates were tested to see if *S. oneidensis* MR-1 and the environmental strains were able to use them as the terminal electron acceptor.

Cells were cultured in minimal media anaerobically, with either 0.5 mM Fe(III)citrate, 0.5 mM Fe(III)EDTA or 0.5 mM Fe(III)NTA as the electron acceptor and 30 mM succinate. All three strains were able to reduce Fe(III)citrate and Fe(NTA) at similar rates. After 6 days, *S. oneidensis* MR-1 WT and *Citrobacter* spp. WGB had reduced 3 times less Fe(III)EDTA than the other ferric iron (Fe^{3+}) complexes and *Acinetobacter* spp. UEA 5 times less (Figure 3-4).
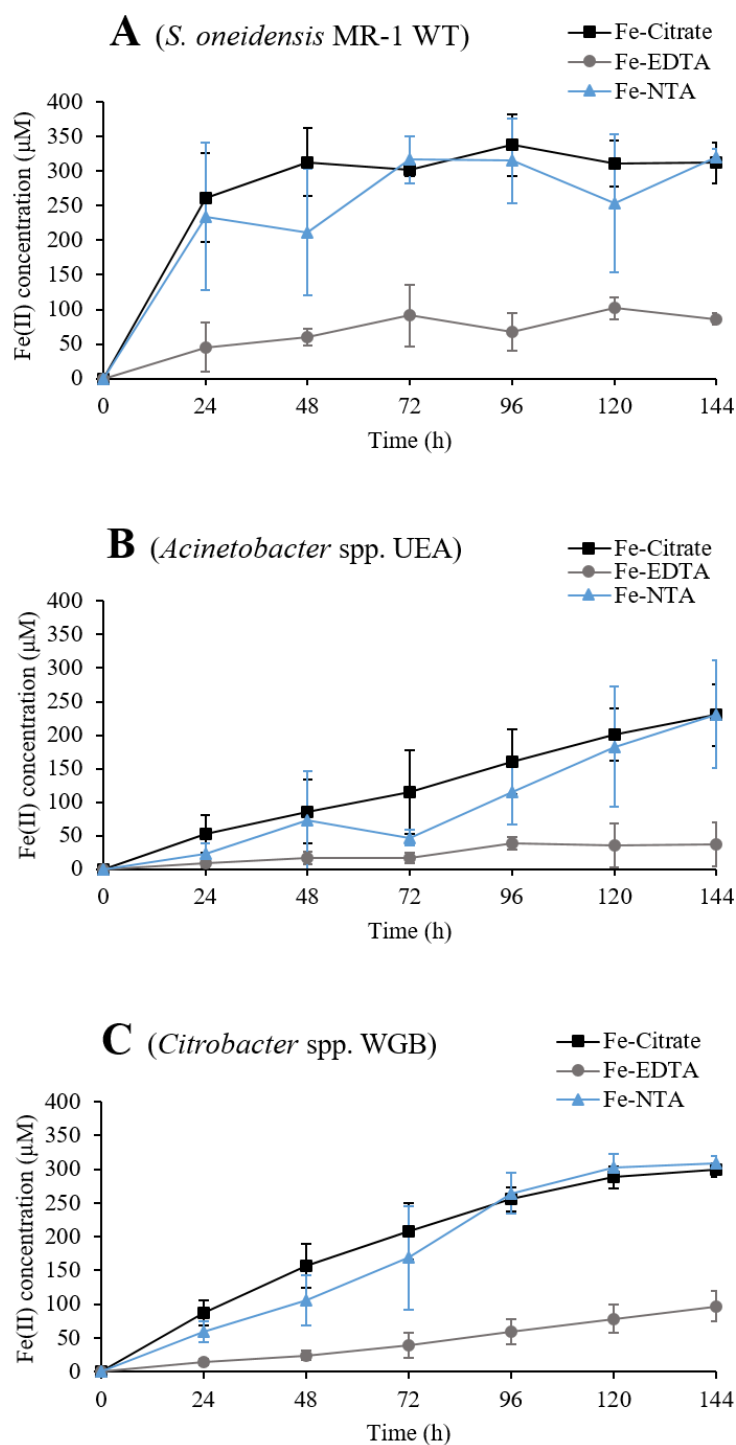
Figure 3-4 Bacterial iron reduction of different ferric iron complexes

Ferrous iron (Fe^{2+}) measurements by ferrozine assay (Chapter 2.4) of cells cultured anaerobically in minimal media at 25 ˚C with either 0.5 mM Fe(III)citrate, 0.5 mM Fe(III)EDTA or 0.5 mM Fe(III)NTA as the electron acceptor source and 30 mM succinate as the carbon source. Figure A: Shewanella oneidensis MR-1 WT. Figure B: Acinetobacter spp. UEA. Figure C: Citrobacter spp. WGB. Each data point represents the average of three biological replicates and the error bars represent the ± standard deviation (SD).

3.3.3. Bacterial growth

To test if *S. oneidensis* MR-1 and the environmental strains were able not just to oxidise succinate for anaerobic respiration, but also use it as the sole carbon source for bacterial growth, cells were cultured in minimal media anaerobically, with 0.5 mM Fe(III)citrate as the electron acceptor and 30 mM Succinate as the sole carbon source.

S. oneidensis MR-1 WT was able to grow using succinate as the sole carbon source and ferric iron (Fe^{3+}) as the terminal electron acceptor (Figure 3-5 A). A mutant of *S. oneidensis* MR-1 without the outer membrane Mtr operon ($\Delta mtrB, \Delta mtrA, \Delta mtrC, \Delta omcA, \Delta mtrF, \Delta mtrE$ and $\Delta mtrD$) was used as a negative control. This strain was unable to use ferric iron (Fe^{3+}) as the terminal electron acceptor as it did not have the required pathway to transport electrons to the extracellular environment. *S. oneidensis* MR-1 $\Delta mtrB$-$\Delta mtrD$ could not reduce ferric iron (Fe^{3+}) to ferrous iron (Fe^{2+}) and therefore, it was not able to grow under anaerobic conditions without another terminal electron acceptor (Figure 3-5 B).

Acinetobacter spp. UEA and *Citrobacter* spp. WGB could also grow at similar rates to *S. oneidensis* MR-1 WT despite reducing ferric iron (Fe^{3+}) slower (Figure 3-5 C, D).

Once confirmed that both *Acinetobacter* spp. UEA and *Citrobacter* spp. WGB were able to not just reduce iron, but also increase their biomass, the next step was to identify which dissimilatory iron reduction pathway they were using.
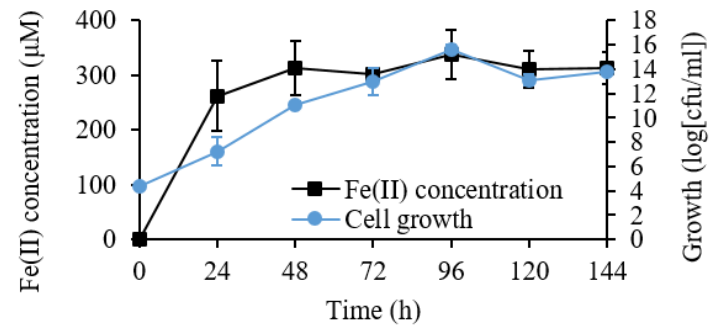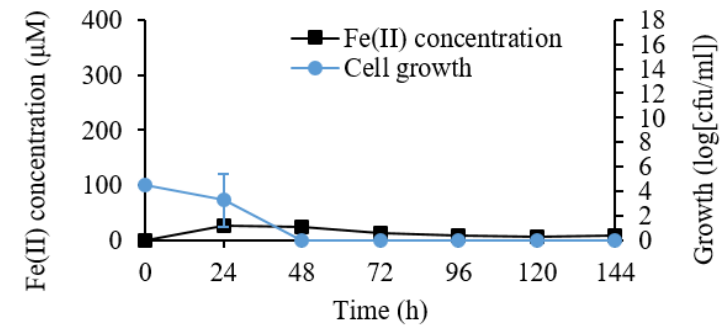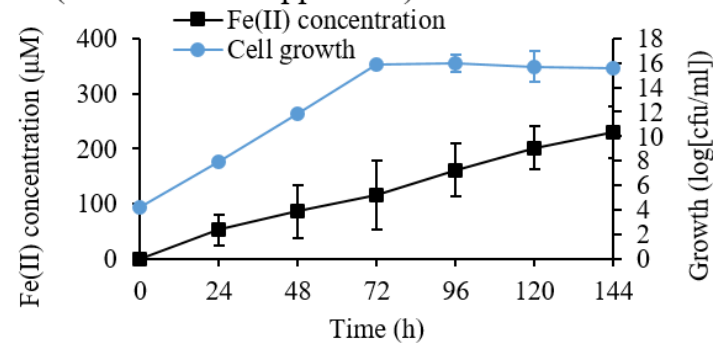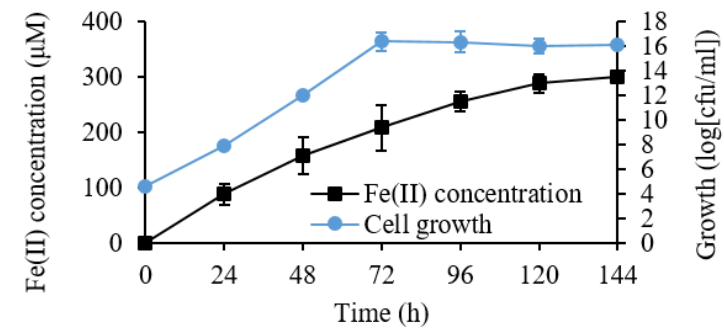
Figure 3-5 Bacterial growth by reducing soluble iron

Bacterial growth quantification by colony forming units and ferrous iron (Fe^{3+}) measurement by ferrozine assay (Chapter 2.4) of cells cultured anaerobically in minimal media at 25 ˚C with 0.5 mM Fe(III)citrate as the terminal electron acceptor and 30 mM Succinate as the sole carbon source. Figure A: S. oneidensis MR-1 WT. Figure B: S. oneidensis MR-1 ΔmtrB-ΔmtrD. Figure C: Acinetobacter spp. UEA. Figure D: Citrobacter spp. WGB. Each data point represents the average of three biological replicates and the error bars represent the ± standard deviation (SD).

If these bacteria were using a homologous pathway to the Mtr pathway in *Shewanella*, electrons would be transported across the membranes by *c*-type cytochromes and ferric iron (Fe^{3+}) would be being reduced extracellularly. For this process, ATP would be produced by oxidative phosphorylation since proton motive force would have been generated by the quinone pool. (Figure 3-6 A).

If the metal-reducing pathways used by the isolated environmental strains was not homologous to *Shewanella*'s, various hypotheses could be considered. The first hypothesis is that electrons could be reducing ferric iron (Fe^{3+}) extracellularly, but without any *c*-type cytochromes involved in the process. In this case, a different protein complex could be involved in the pathway (Figure 3-6 B).

The second proposal is that the bacteria were secreting reduced non-protein molecules to the extracellular environment that would reduce ferric iron (Fe^{3+}) without the need of a specific protein pathway (Figure 3-6 C).

A third hypothesis is that electrons were not crossing the cell membranes to reduce iron, but ferric iron (Fe^{3+}) could be transported inside the cell and reduced intracellularly. In this case, the environmental strains would require the expression of genes to protect the cell from ferric iron (Fe^{3+}) lowering the pH of the cytoplasm and from the free radicals from the ferric oxides (Figure 3-6 D) (Ilbert and Bonnefoy, 2013).

Finally, the last hypothesis is that the microorganism could be transporting the ferric iron (Fe^{3+}) inside the cell but its reduction was independent from energy production and cells were producing ATP from fermentation instead of by oxidative phosphorylation (Figure 3-6 E).

The use of assimilatory ferric reductases for iron reduction was discarded, as they are not energetically favourable and cells would not be able to grow with any energetically favourable metabolic pathway available (Schröder *et al.*, 2003).
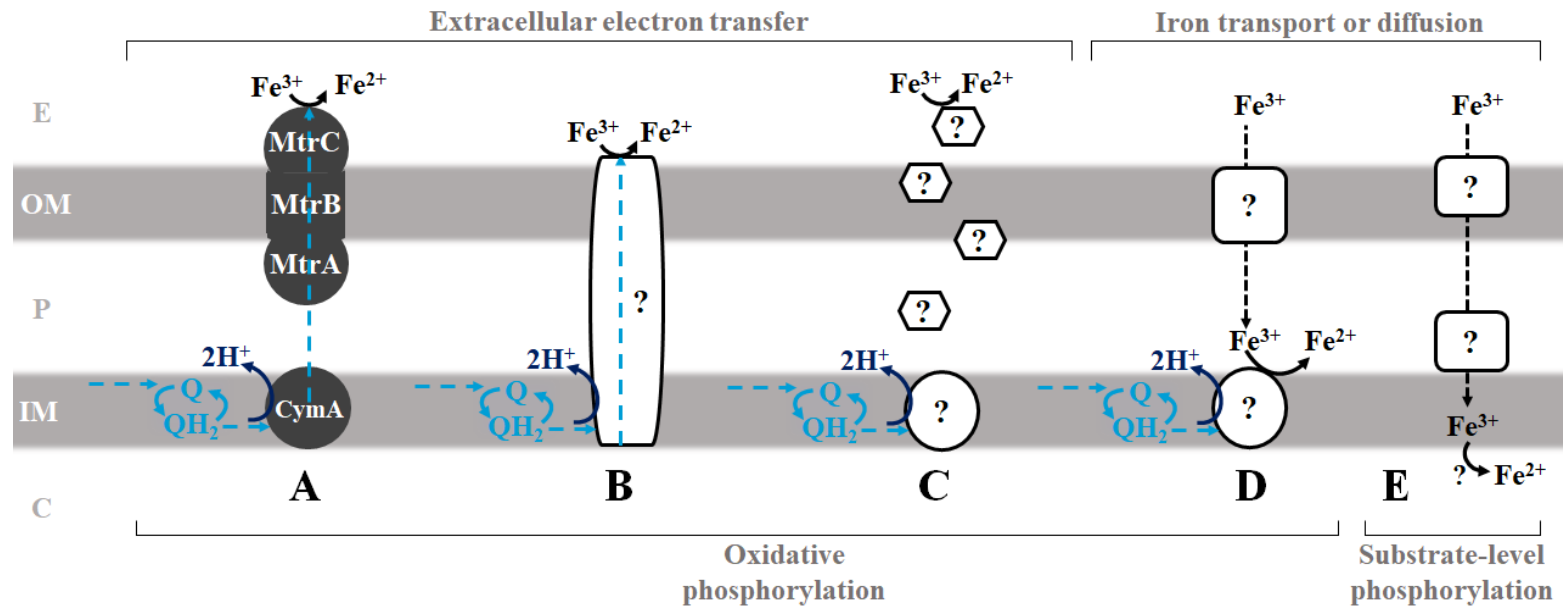
Figure 3-6 Proposed iron reduction pathways for Gram-negative bacteria
A) *Protein complex pathway by c-type cytochromes homologous to Mtr pathway in Shewanella oneidensis MR-1. B) Protein complex pathway not homologous to the one that S. oneidensis MR-1 uses. C) Secretion of reduced non-protein molecules across the membrane. D) Intake of Ferric iron (Fe^{3+}) across the outer membrane. E) Independent iron reduction from ATP production.*

3.4 Characterization of the iron reducing pathway

3.4.1. Cytochrome identification

Once *Acinetobacter* spp. UEA and *Citrobacter* spp. WGB were confirmed as iron-reducing bacteria, the next step was to identify what pathways were involved in this activity.

Most gram-negative bacteria that have been identified as iron-reducing bacteria have gene clusters in their genome that include genes encoding membrane *c*-type cytochromes with the function of transporting electrons across the membranes (Shi, Rosso, Zachara, *et al.*, 2012). *c*-type cytochromes are iron containing proteins where the vinyl group of the heme reacts with the thiol group of cysteine residues forming covalent bonds between the heme and the protein that remain once the protein is denatured (Allen *et al.*, 2003).
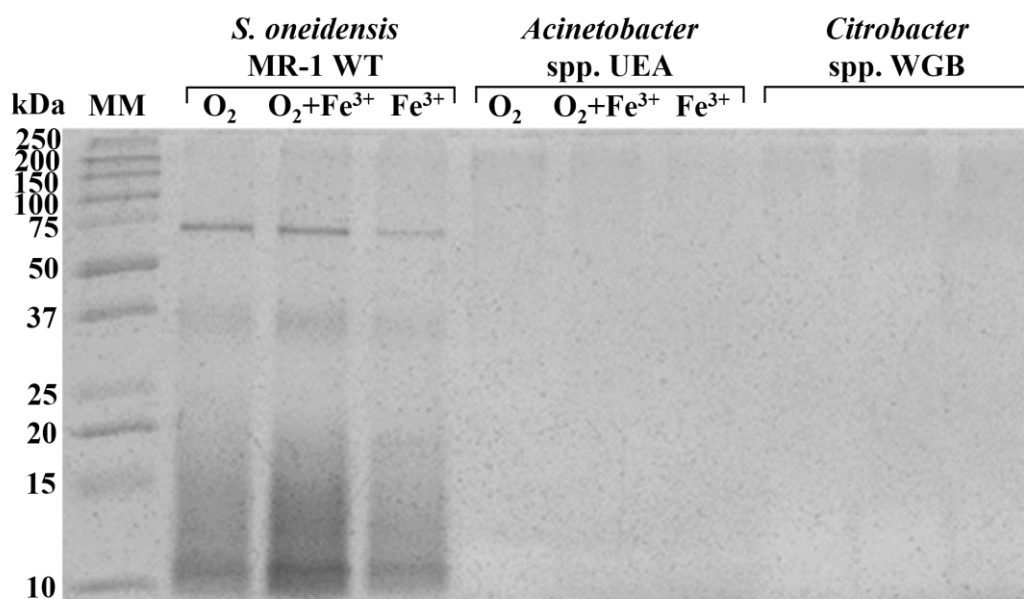
Figure 3-7 c-type cytochrome identification by heme staining in SDS-PAGE
Heme stain of the SDS-PAGE gel (Chapter 2.16.1) containing the total protein content of S. oneidensis MR-1 WT, Acinetobacter spp. UEA and Citrobacter spp. WGB cultured for 24 hours in minimal media at 25 ˚C with 30 mM succinate as the sole carbon source and as a terminal electron acceptor either oxygen, oxygen and 0.5 mM Fe(III)citrate or just 0.5 mM Fe(III)citrate. Cellular concentration (OD_{600}) was normalised between samples before running the SDS-PAGE.

As heme proteins, they can reduce hydrogen peroxide to water. Due to its peroxidase activity, c-type cytochromes can be detected in SDS-PAGE gels if stained with reagents that develop colour when hydrated (Sugano *et al.*, 2007).

Figure 3-7 shows a heme stain of a SDS-PAGE of the total protein content of *S. oneidensis* MR-1 WT, *Acinetobacter* spp. UEA and *Citrobacter* spp. WGB growing in minimal media with 30 mM succinate as the carbon source and as a terminal electron acceptor either oxygen (aerobic conditions), 0.5 mM Fe(III)citrate or both. While bands at different molecular weights could be observed in *S. oneidensis* MR-1 WT, no bands were visible in any condition neither in *Acinetobacter* spp. UEA nor *Citrobacter* spp. WGB.

Although all the Gram-negative bacteria that have been previously associated with iron reduction express c-type cytochromes in their outer membranes, some Gram-positive and Archea use b-type cytochrome for electron transport (White *et al.*, 2016). The main difference between c-type and b-type cytochromes is that in the first, the heme is covalently attached to the protein but it is not in the second. To check if *Acinetobacter* spp. UEA or *Citrobacter* spp. WGB could be using a non c-type cytochrome for the electron transport, a native-PAGE was stained for heme detection. Running a native gel, the proteins would not denature and the non-covalent bounds between the protein and the heme would remain.

Figure 3-8 shows the native-PAGE after being stained for heme detection. Because proteins have not been denatured, they migrate through the gel not just according to their size but also according to their charge. Both the soluble and the insoluble fractions of *S. oneidensis* MR-1 showed bands that could correspond to c-type cytochromes or other cytochromes. *Acinetobacter* spp. UEA did not show any band in any of its fractions. *Citrobacter* spp. WGB showed a band in its soluble fraction but no band in its insoluble fraction, suggesting that it was not using a protein pathway involving cytochromes for transmembrane extracellular iron reduction.
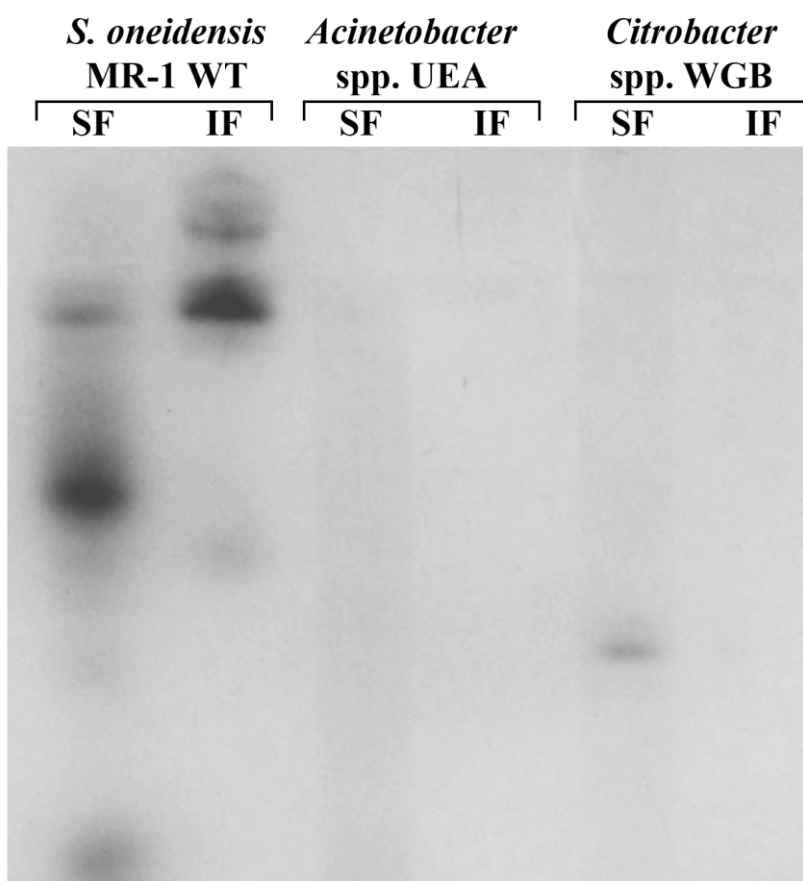
Figure 3-8 Cytochrome identification by heme staining in native-PAGE
Heme stain of the native-PAGE gel (Chapter 2.16.2) containing the soluble fraction (SF) and the insoluble fraction (IF) of S. oneidensis MR-1 WT, Acinetobacter spp. UEA and Citrobacter spp. WGB cultured 24 hours in minimal media anaerobically at 25 ˚C with 30 mM succinate as the sole carbon source and 0.5 mM Fe(III)citrate. Cellular concentration (OD$_{600}$) was normalised between samples before running the native-PAGE.

3.4.2. Insoluble iron reduction

Without cytochromes to transport the electrons across the membranes, *Acinetobacter* spp. UEA and *Citrobacter* spp. WGB could be either reducing ferric iron (Fe^{3+}) extracellularly though an unknown pathway or taking the iron inside the cell where it can be used as a terminal electron acceptor.

To see if the studied strains could reduce insoluble ferric iron (Fe^{3+}), cells were cultured anaerobically with 50 mM goethite (iron(III)oxide-hydroxide) as the terminal electron acceptor. LB instead of minimal media was used for this experiment because the positive control, *S. oneidensis* MR-1 WT, reduced very little goethite when growing in minimal media.
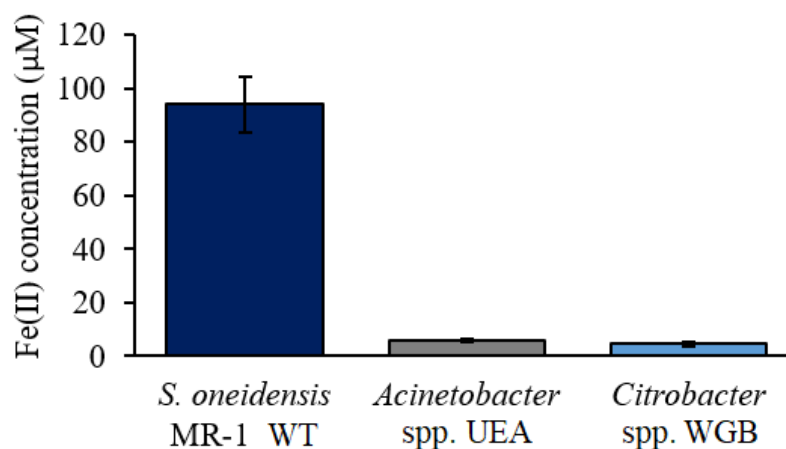
Figure 3-9 Bacterial insoluble iron reduction
Ferrous iron (Fe^{2+}) measurement by ferrozine assay (Chapter 2.4) of S. oneidensis MR-1 WT, Acinetobacter spp. UEA and Citrobacter spp. WGB cultured 48 hours at 25 ˚C in LB anaerobically with 50 mM goethite. Each data point represents the average of three biological replicates and the error bars represent the ± standard deviation (SD).

Figure 3-9 shows that *S. oneidensis* MR-1 WT, after 48 hours, had 100 μM of soluble ferrous iron (Fe^{2+}) in the media (0.2 % of the goethite). *Acinetobacter* spp. UEA and *Citrobacter* spp. WGB had 5 μM soluble ferrous iron (Fe^{2+}). This would correspond to a 0.01 % of the goethite available. However, LB medium contains 13.4 μM of iron (Grant and Pramer, 1962) therefore, there is no proof that the environmental strains could reduce insoluble iron.

3.4.3. ATP production

Since *Acinetobacter* spp. UEA and *Citrobacter* spp. WGB did not show expression of *c*-type cytochromes and they were not able to reduce goethite, the use of an electron transport pathway was discarded and also the secretion of siderophores able to solubilise goethite (Schröder *et al.*, 2003).

If iron reduction in these strains was due to anaerobic respiration or indirectly related to a different metabolic process remains unknown. To know if these strains were producing energy from respiration and not from fermentation, 2,4-Dinitrophenol (DNP) was used as an uncoupling agent. An uncoupling agent is a molecule that is soluble in the lipid membrane and increases its permeability,

conducing protons across it and therefore, preventing the generation of a proton motive force that will allow the production of ATP by oxidative phosphorylation (Hopfer *et al.*, 1968). However, when uncoupling agents are present in the cell, ATP can still be produced by substrate level phosphorylation, so bacteria using fermentation can survive.

Figure 3-10 shows the bacterial growth of *S. oneidensis* MR-1 WT, *Acinetobacter* spp. UEA and *Citrobacter* spp. WGB growing under anaerobic conditions in minimal media with 0.5 mM Fe(III)citrate as electron acceptor, 30 mM succinate as the sole carbon source and with either 0 mM, 0.01 mM, 0.1 mM, 1 mM or 2 mM of DNP.
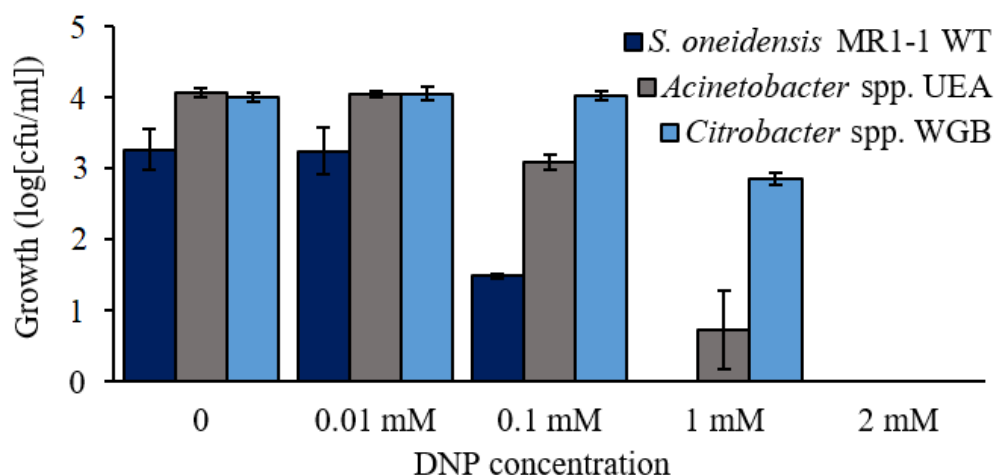
Figure 3-10 Bacterial growth with different concentrations of DNP
Bacterial growth quantification by colony forming units of S. oneidensis MR-1 WT, Acinetobacter spp. UEA and Citrobacter spp. WGB cultured 24 hours in minimal media at 25 ˚C with 0.5 mM Fe(III)citrate as the terminal electron acceptor and 30 mM succinate as the sole carbon source under anaerobic conditions with 0 mM, 0.01 mM, 1 mM or 2 mM of DNP. Each data point represents the average of three biological replicates and the error bars represent the ± standard deviation (SD).

S. oneidensis MR-1 WT growth decreased with 0.1 mM of DNP, and it was unable to grow via anaerobic respiration with 1 mM of DNP. *Acinetobacter* spp. UEA growth decreased slightly with 0.1 mM of DNP but it was still able to survive with 1 mM of DNP. *Citrobacter* spp. WGB growth decreased slightly with 1 mM of DNP. No strain was able to survive with over 2 mM of DNP in the media. Previous literature has measured that in *E. coli*, cells are not able to

survive with aerobic respiration when there is more than 0.5 mM DNP in the media (Lambert *et al.*, 1997).

3.5 Discussion

3.5.1. <u>The role of iron-reducing microorganisms in the environment</u>

This chapter shows significant evidence of iron-reducing activity by *Acinetobacter* and *Citrobacter*, two genus that have been isolated from fresh water, sediment and soil samples and were not previously identified as iron-reducing bacteria (Table 3-2).

As is shown in Table 3-1, the amount of bioavailable iron between samples is very different, however, despite the abiotic differences in these environments, iron-reducing bacteria have been isolated from all of the samples, suggesting that their biological activity could have an important role in each ecosystem.

The role of iron-reducing microorganisms in sediment and soil ecosystems is very clear. Oxygen is not present in the environments and therefore, organisms unable to perform fermentative processes have to survive using anaerobic cellular respiration. As iron concentrations are very high in these environments, iron-reducing microorganisms have a selective advantage to colonise these ecosystems (Emerson *et al.*, 2012).

On the other hand, in fresh water environments where the pH is neutral and the concentration of oxygen is high, some iron molecules are forming ligands with chelates and remain soluble, but most react with oxygen forming iron oxides, precipitating and sinking out of the water column. Although iron-reducing microorganisms could use aerobic respiration in these environments, many organisms survive in nature by symbiotic relationships and keeping iron bioavailable for other organisms to survive could be positive for themselves (Chaffron *et al.*, 2010; Emerson *et al.*, 2012).

3.5.2. <u>Succinate as the sole carbon source in *Shewanella oneidensis* MR-1</u>

The experiments measuring bacterial growth (Figure 3-5) confirmed that *S. oneidensis* MR-1 WT was able to grow when succinate was used as the sole carbon and electron donor source. Besides using the succinate as an electron donor source for cellular respiration, this molecule is also the sole source of carbon for cells to grow. In order to produce biomass, some molecules of succinate need to be transformed to acetyl-CoA and pyruvate to enter the lipids and amino acid synthesis pathways. For this process, *S. oneidensis* MR-1 WT uses malic enzyme (ME) or phosphoenolpyruvate carboxykinase (PEP) (Figure 3-2 C).

These results vary from the published metabolic flux by Tang *et al.*, 2007, where it was suggested that *S. oneidensis* MR-1 WT is not able to use malic enzyme (ME) nor phosphoenolpyruvate carboxykinase (PEP) to produce pyruvate from succinate. A possible justification for these differences is the carbon source used in the experiments. Tang *et al.*, 2007 performed metabolic flux analysis using lactate instead of succinate. To use lactate for cellular respiration, it needs to be transformed first into pyruvate by lactate dehydrogenase (LDH). The pyruvate can be transformed to acetyl-CoA to continue cellular respiration, or it can be used for amino acid synthesis. Likewise, the produced acetyl-CoA can be used for the TCA cycle or for lipid synthesis. The acetyl-CoA that goes through the TCA cycle is transformed into succinate, before completing the TCA cycle and starting the ETC. As pyruvate has been previously produced, there would be no need for the cell to use malic enzyme (ME) nor phosphoenolpyruvate carboxykinase (PEP) to produce more pyruvate from succinate.

It would be possible that the presence of pyruvate in the cell would inhibit the genes encoding for malic enzyme (ME) and phosphoenolpyruvate carboxykinase (PEP), as the cell would already have the molecules needed to synthesise lipids and amino acids, but in the absence of pyruvate, the genes would express those enzymes to allow the cells to grow and multiply.

To contrast this information, it would be interesting to perform metabolic flux analysis of *S. oneidensis* MR-1 WT using succinate as the sole carbon and electron

source or knock-out the genes encoding for malic enzyme (ME) and phosphoenolpyruvate carboxykinase (PEP) to see if *S. oneidensis* MR-1 WT would be able to grow in these conditions.

3.5.3. Soluble iron reduction

When cultured anaerobically in minimal media, *Acinetobacter* spp. UEA was able to reduce iron progressively when lactate, succinate, acetate or formate were used as the sole carbon source (Figure 3-3 B), confirming its ability to reduce iron in anaerobic conditions. However, when DNP was present in the media, acting as an uncoupling agent, the cell growth rate decreased (Figure 3-10). These results suggest that despite *Acinetobacter* spp. UEA being able to produce some ATP by substrate level phosphorylation, most of the energy produced is through oxidative phosphorylation. Consequently, this isolated strain could be using ferric iron (Fe^{3+}) as the terminal electron acceptor to accomplish anaerobic respiration.

Citrobacter spp. WGB was able to reduce iron when cultured with lactate, succinate or acetate but not with formate (Figure 3-3 C). Unlike *Acinetobacter* spp. UEA and *S. oneidensis* MR-1 WT, it was able to grow when the uncoupling agent was present in the media, suggesting that it is able to obtain energy through fermentative pathways (Figure 3-10).

3.5.4. Ferric iron (Fe^{3+}) species

In ferric iron (Fe^{3+}) complexes, the iron reduction rate should be directly proportional with the weakness of the complex (Haas and Dichristina, 2002). Table 3-4 shows the equilibrium constant of the three studied ferric complexes. The reaction of Fe(III)EDTA is further to the right than the ones of Fe(III)citrate and Fe(III)NTA, accordingly, the Fe(III)EDTA complex is stronger and it prevents iron reduction.

This agrees with the results obtained in Figure 3-4, where Fe(III)EDTA was reduced at least 3 times slower than Fe(III)citrate or Fe(III)NTA by the studied strains, while Fe(III)citrate and Fe(III)NTA had similar reduction rates.

Table 3-4 Equilibrium stability constants and redox potentials of ferric iron (Fe³⁺) complexes

Equilibrium	E°(V)	log K
Fe^{3+} + citrate^{3-} = Fe(III)citrate	+0.372	11.5
Fe^{3+} + EDTA^{4-} = Fe(III)EDTA$^-$	+0.096	25.0
Fe^{3+} + NTA^{3-} = Fe(III)NTA	+0.385	15.9

In addition, considering that the redox potential of Fe(III)EDTA (+0.096 V) is much lower than those ones of Fe(III)citrate (+0.372) and Fe(III)NTA (+0.385), it could be that the pathway involving redox reactions starting at the quinone pool (-0.05 – -0.1 V), require proteins with redox midpoint potentials higher than the one for Fe(III)EDTA, being the reduction of Fe(III)EDTA the least thermodynamically favourable (David J. Richardson *et al.*, 2012; Scott, 2017).

3.5.5. <u>Future work</u>

As neither *Acinetobacter* spp. UEA nor *Citrobacter* spp. WGB were able to reduce goethite nor expressed any cytochromes in their membranes that could give any hint on how they reduce iron (Figure 3-7, Figure 3-8 and Figure 3-9), the strongest hypothesis is that these bacteria are reducing iron intracellularly, and *Citrobacter* spp. WGB could be growing using fermentation.

Nonetheless, there are still a lot of questions to be answered. If the isolated bacteria are reducing iron intracellularly, iron might be being reduced via a specific iron reducing pathway, or contrarily, iron could be accepting electrons released in the cytoplasm or the periplasm by many different metabolic reactions. Moreover, the presence of intracellular iron represents a threat for the bacteria, as it would cause toxicity to the cell. Therefore, the isolated iron reducers should have a defense mechanism against iron when growing in anaerobic conditions.

As future work, it would be interesting to do a metabolic flux profile to study the pathways involved in the consumption of the carbon source to identify each intermediate by stable-isotope HPLC-MS to have a better understanding as to how iron reduction is related with the metabolism of the isolated environmental strains (Vergano *et al.*, 2014).

The next chapter of this thesis is focused on the genome and transcriptome of the isolated strains to have a better understanding of their genomic information and how their metabolism changes under anaerobic conditions with ferric iron (Fe^{3+}) as the sole electron acceptor.

3.6   References

Allen, J.W.A., Daltrop, O., Stevens, J.M., and Ferguson, S.J. (2003) *c-type* cytochromes: diverse structures and biogenesis systems pose evolutionary problems. *Philos. Trans. R. Soc. Lond. B. Biol. Sci.* 358: 255–66.

Altschul, S.F., Gish, W., Miller, W., Myers, E.W., and Lipman, D.J. (1990) Basic local alignment search tool. *J. Mol. Biol.* 215: 403–410.

Al Atrouni, A., Joly-Guillou, M.-L., Hamze, M., and Kempf, M. (2016) Reservoirs of Non-*baumannii Acinetobacter* Species. *Front. Microbiol.* 7: 49.

Chaffron, S., Rehrauer, H., Pernthaler, J., and von Mering, C. (2010) A global network of coexisting microbes from environmental and whole-genome sequence data. *Genome Res.* 20: 947–59.

Chan, J.Z.-M., Halachev, M.R., Loman, N.J., Constantinidou, C., and Pallen, M.J. (2012) Defining bacterial species in the genomic era: insights from the genus *Acinetobacter*. *BMC Microbiol.* 12: 302.

Emerson, D., Roden, E., and Twining, B.S. (2012) The microbial ferrous wheel: iron cycling in terrestrial, freshwater, and marine environments. *Front. Microbiol.* 3: 383.

Grant, C.L. and Pramer, D. (1962) Minor element composition of yeast extract. *J. Bacteriol.* 84: 869–70.

Haas, J.R. and Dichristina, T.J. (2002) Effects of Fe(III) Chemical Speciation on Dissimilatory Fe(III) Reduction by *Shewanella putrefaciens*. *Environ. Sci. Technol.* 36: 373–380.

Hirayama, T. and Nagasawa, H. (2017) Chemical tools for detecting Fe ions. *J. Clin. Biochem. Nutr.* 60: 39–48.

Hopfer, U., Lehninger, A.L., and Thompson, T.E. (1968) Protonic conductance across phospholipid bilayer membranes induced by uncoupling agents for oxidative phosphorylation. *Proc. Natl. Acad. Sci. U. S. A.* 59: 484–90.

Ilbert, M. and Bonnefoy, V. (2013) Insight into the evolution of the iron oxidation pathways. *Biochim. Biophys. Acta - Bioenerg.* 1827: 161–175.

Kane, A.L., Brutinel, E.D., Joo, H., Maysonet, R., VanDrisse, C.M., Kotloski, N.J., and Gralnick, J.A. (2016) Formate Metabolism in *Shewanella oneidensis* Generates Proton Motive Force and Prevents Growth without an Electron Acceptor. *J. Bacteriol.* 198: 1337–46.

Lambert, L.A., Abshire, K., Blankenhorn, D., and Slonczewski, J.L. (1997) Proteins Induced in *Escherichia coli* by Benzoic Acid. *J. Bacteriol.* 179: 7595–7599.

Lee, C.-R., Lee, J.H., Park, M., Park, K.S., Bae, I.K., Kim, Y.B., et al. (2017) Biology of *Acinetobacter baumannii*: Pathogenesis, Antibiotic Resistance Mechanisms, and Prospective Treatment Options. *Front. Cell. Infect. Microbiol.* 7: 55.

Li, B., Tian, C., Zhang, D., and Pan, X. (2014) Anaerobic nitrate-dependent iron (II) oxidation by a novel autotrophic bacterium, *Citrobacter freundii* strain PXL1. *Geomicrobiol. J.* 31: 138–144.

Nelson, D.L. and Cox, M.M. (2013) Lehninger principles of biochemistry W.H. Freeman and Company.

Peter, S., Wolz, C., Kaase, M., Marschal, M., Schulte, B., Vogel, W., et al. (2014) Emergence of *Citrobacter freundii* carrying IMP-8 metallo-β-lactamase in Germany. *New microbes new Infect.* 2: 42–5.

Pinchuk, G.E., Geydebrekht, O. V, Hill, E.A., Reed, J.L., Konopka, A.E., Beliaev, A.S., and Fredrickson, J.K. (2011) Pyruvate and lactate metabolism by *Shewanella oneidensis* MR-1 under fermentation, oxygen limitation, and fumarate respiration conditions. *Appl. Environ. Microbiol.* 77: 8234–40.

Richardson, D.J., Edwards, M.J., White, G.F., Baiden, N., Hartshorne, R.S., Fredrickson, J., et al. (2012) Exploring the biochemistry at the extracellular redox frontier of bacterial mineral Fe(III) respiration. *Biochem. Soc. Trans.* 40: 493–500.

Schröder, I., Johnson, E., and De Vries, S. (2003) Microbial ferric iron reductases. *FEMS Microbiol. Rev.* 27: 427–447.

Scott, K. (2017) Sustainable and Green Electrochemical Science and Technology John Wiley & Sons Ltd.

Shi, L., Rosso, K.M., Zachara, J.M., and Fredrickson, J.K. (2012) Mtr extracellular electron-transfer pathways in Fe(III)-reducing or Fe(II)-oxidizing bacteria: a genomic perspective. *Biochem. Soc. Trans.* 40: 1261–7.

Sugano, Y., Muramatsu, R., Ichiyanagi, A., Sato, T., and Shoda, M. (2007) DyP, a unique dye-decolorizing peroxidase, represents a novel heme peroxidase family: ASP171 replaces the distal histidine of classical peroxidases. *J. Biol. Chem.* 282: 36652–8.

Tang, Y.J., Hwang, J.S., Wemmer, D.E., and Keasling, J.D. (2007) *Shewanella oneidensis* MR-1 fluxome under various oxygen conditions. *Appl. Environ. Microbiol.* 73: 718–29.

Vergano, S.S., Rao, M., McCormack, S., Ostrovsky, J., Clarke, C., Preston, J., et al. (2014) In *vivo* metabolic flux profiling with stable isotopes discriminates sites and quantifies effects of mitochondrial dysfunction in *C. elegans*. *Mol. Genet. Metab.* 111: 331–341.

White, G.F., Edwards, M.J., Gomez-Perez, L., Richardson, D.J., Butt, J.N., and Clarke, T.A. (2016) Mechanisms of Bacterial Extracellular Electron Exchange. In, *Advances in Microbial Physiology*., pp. 87–138.

Yang, Y., McCue, L., Parsons, A., Feng, S., and Zhou, J. (2010) The tricarboxylic acid cycle in *Shewanella oneidensis* is independent of Fur and RyhB control. *BMC Microbiol.* 10: 264.

Yoon, S., Sanford, R.A., and Löffler, F.E. (2013) *Shewanella* spp. Use acetate as an electron donor for denitrification but not ferric iron or fumarate reduction. *Appl. Environ. Microbiol.* 79: 2818–22.

Zhou, G., Peng, H., Wang, Y.-S., Huang, X.-M., Xie, X.-B., and Shi, Q.-S. (2017) Complete genome sequence of *Citrobacter werkmanii* strain BF-6 isolated from industrial putrefaction. *BMC Genomics* 18: 765.

Genomic and transcriptomic analysis of the isolated iron reducing bacteria

4.1 Introduction

With the use of classic microbiology, *Acinetobacter* spp. and *Citrobacter* spp. strains were isolated from the environment and grown anaerobically using ferric iron (Fe^{3+}) as the terminal electron acceptor. Biochemical analysis discounted the possibility that these microorganism were using a homologous metal reducing pathway to the one that *Shewanella* uses to obtain energy. However, this analysis could not determine the alternative mechanisms that were being used to obtain energy. In this chapter, the genus *Acinetobacter* and *Citrobacter* have been analysed by bioinformatic tools to provide a better understanding of their metabolism, with the aim of identifying how iron is used by these environmental bacteria when they are growing under anaerobic conditions.

4.2 Omics

By using bioinformatics, the data obtained from DNA and RNA sequencing can be analysed and used to provide additional information on a wide range of an organism's metabolic processes (Ohashi *et al.*, 2015). Next-Generation Sequencing (NGS) tools generate a large amount of data that can be analysed in many different ways, therefore the same data can be used by a wide range of different scientific fields.

4.2.1. Genomics

Genomics focuses on studying genetic information. By analysing the DNA of the genome or the exome of an organism, it is possible to know if it has the genes required to express proteins for certain metabolic processes, or to compare its genome with other species (Ohashi *et al.*, 2015).

Moreover, the epigenome can be also analysed to study the regulation of the genes, by detecting methylation and targets of transcription factors in the DNA sequences (Ohashi *et al.*, 2015).

4.2.2. Transcriptomics

Transcriptomics measures the mRNA sequences of an organism, to understand which genes are being expressed in a particular condition at a specific time of the growth of an organism (Zhang *et al.*, 2010).

4.2.3. Proteomics

Proteomics analyses the secondary and tertiary structures of the proteins expressed in an organism, in order to determine their function in the cell. This field combines the information obtained from DNA and RNA sequencing with biochemical techniques to determine the mass and the charge of the protein, as well as the shape (Zhang *et al.*, 2010).

Interactomics is a field within proteomics that studies the interaction between a protein and other proteins, or a protein with DNA or RNA molecules. The methods to study protein interactions are a combination of bioinformatic analysis of the structural motifs of the amino acid sequences, and experimental approaches, such as genomic libraries or the study of protein complexes (Kandpal *et al.*, 2009).

4.2.4. Metabolomics

The analysis of the metabolites in a cell is another approach to understand protein function in an organism, as the concentration of different substrates and products can give information on the metabolic pathways that are being used (Ohashi *et al.*, 2015).

4.2.5. Bioinformatics in environmental microbiology

The use of bioinformatics does not just allow a better understanding of how a pathway works in an isolated microorganism. Once a specific pathway is identified in a cultured microorganism, a metagenomic analysis can be used to study

communities in more detail, giving more accurate results about the diversity and abundance of the species able to use that pathway, and the impact they have on other populations (Hiraoka *et al.*, 2016).

Because just 1 % of bacteria are cultivable and communities behave different ways in the environment than in the laboratory (Boughner and Singh, 2016), the use of bioinformatics is essential to compare an isolated microorganism with other microorganisms that could be using the pathways of interest.

4.3 Genomic analysis

For its analysis, a genome has to be sequenced and then the sequences corresponding to its genes have to be annotated. One of the main obstacles to this process is that most of the new sequencing technologies can only sequence short molecules of DNA, so the genome has to be fragmented prior to be sequenced. After sequencing, the DNA reads have to be reassembled in the right order to identify the genes in the genome (Zerbino and Birney, 2008).

Figure 4-1 shows one of the most common approaches for assembling a genome. First, the sample genome is fragmented for sequencing. Then, the read sequences are overlapped to assemble the genome *de novo*. Usually, this technique does not allow 100 % coverage of the genome, due to the Next-Generation Sequencing error rate. The sequences obtained by the *de novo* assembly are called contigs. To know the orientation and the location in the genome of the contigs, a read mapping can be done, using a previously annotated sequence from an organism of the same species as the sample one. The sample contigs are aligned against the reference genome and mapped to the genome. When the gap between two contigs has a known length but its sequence is not known, the gap can be filled using the reference genome sequence, the combination of contigs and joining reference genome sequence are collectively called a scaffold. Ideally, the resulting sequence of a genome mapping consists of only one scaffold, corresponding to the whole genome (Zerbino and Birney, 2008).

Once the genome is assembled, the DNA sequence structure is analysed with software tools to identify elements of the sequence that could correspond to promoters or coding regions of a gene and predict the function of the genes by analysing their amino acid sequences. Moreover, the annotated genes can be compared those of the annotated reference genome (Dominguez Del Angel *et al.*, 2018).
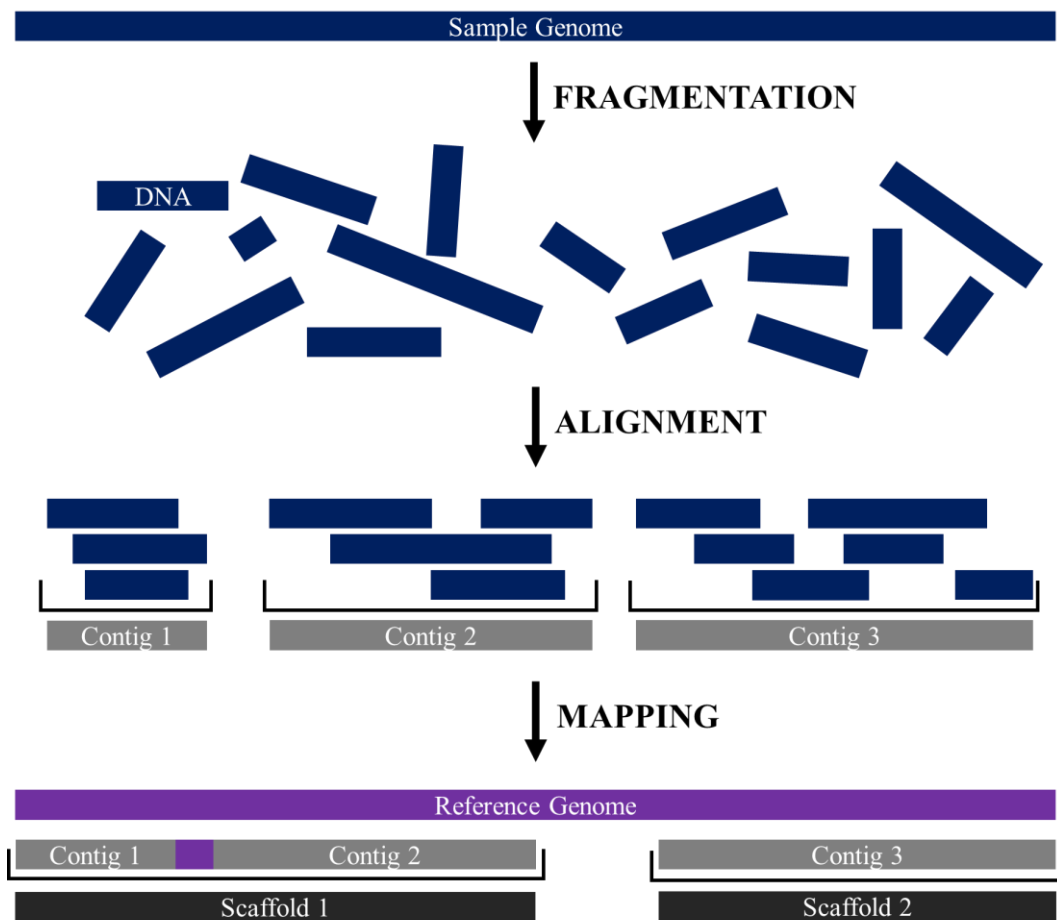
Figure 4-1 Genome sequencing, de novo assembly and read mapping of a genome.

The genomes of the isolated iron-reducing bacterium *Acinetobacter* spp. UEA and *Citrobacter* spp. WGB were sequenced and annotated by microbesNG (Chapter 2.21.4). The reference genomes used to align the isolated iron reducers were *Acinetobacter johnsonii* for *Acinetobacter* spp. UEA and *Citrobacter freundii* for *Citrobacter* spp. WGB, their closest species according to

the 16S rRNA analysis (Chapter 2.21.4). The sequences of both reference genomes were taken from the NCBI public database.

245 contigs were obtained from *Acinetobacter* spp. UEA which covered 83 % of its reference genome and 98 contigs from *Citrobacter* spp. WGB which covered 85 % of its reference genome. All contigs were annotated comparing their genes with the predicted gene function of their respective reference genomes.

4.3.1. Cytochrome identification

Previously identified Gram-negative iron reducing microorganisms expressed membrane associated *c*-type cytochromes to transfer electrons across the membranes (Ilbert and Bonnefoy, 2013). In the previous chapter, the protein content of *Acinetobacter* spp. UEA and *Citrobacter* spp. WGB was stained to identify hemes and no bands were identified. However, it cannot be discounted that the environmental strains expressed the proteins needed to accomplish anaerobic respiration in concentrations below the detectable limit of the heme stain. Consequently, a bioinformatic approach was used to confirm the lack of involvement of *c*-type cytochromes in the iron reduction process.

With the annotated genomes available, genes that encode *c*-type cytochromes were searched for using MAST (Chapter 2.21.4). To do this, the DNA of the environmental strains was translated into amino acid sequences and the program searched for regions with the CXXCH motif. This motif is characteristic of proteins covalently bound to a heme, where the thiol group of the cysteines forms thioether bonds with the vinyl group of the heme and the histidine is an axial ligand to the heme iron. Any amino acid can be found in the positions symbolised by X (Figure 4-2) (Allen *et al.*, 2003).
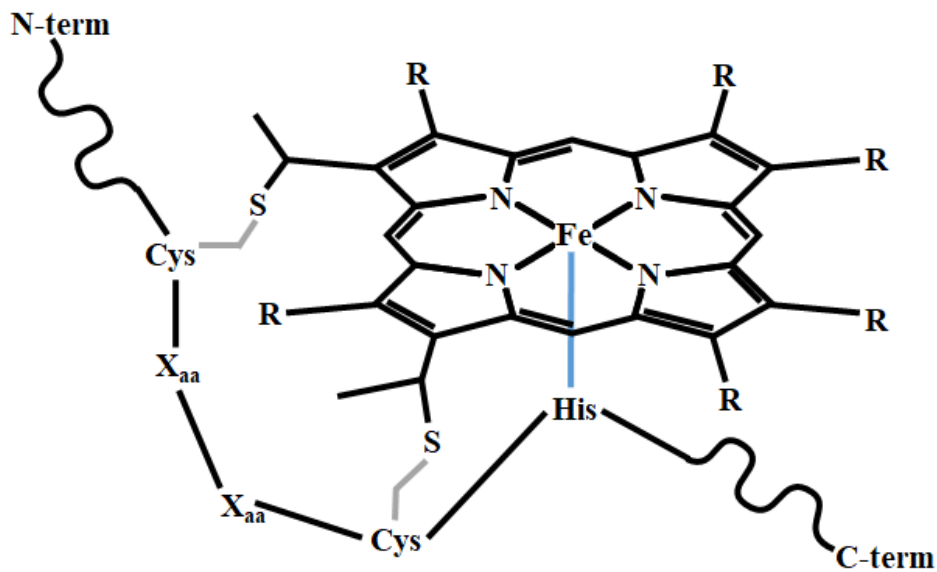
Figure 4-2 Structure of a heme covalently bound to a protein
The bonds between the thiol group of the cysteines and the vinyl groups of the heme are shown in grey. The axial ligand between the histidine and the iron is shown in blue. Any amino acid can be found in the XX position.

Acinetobacter was found to encode 15 proteins with CXXCH motifs, but none of those corresponded to known *Acinetobacter c*-type cytochromes. The full list of genes encoding for proteins with CXXCH motifs in their sequence can be found in Table A-1. In comparison, *Citrobacter* was found to encode 41 genes with CXXCH motifs and 5 of them corresponded to the known *c*-type cytochromes NapC, NapB, NrfA (in duplicate) and TorC. The first four genes are predicted to have a role in the Dissimilatory Nitrate Reduction to Ammonium (DNRA), pathway in which nitrate is reduced to ammonium (Domangue and Mortazavi, 2018). NapC and NapB are involved in the transformation of nitrate to nitrite, and NrfA of nitrite to ammonium. On the other hand, TorC is part of the trimethylamine *N*-oxide (TMAO) pathway, in which TMAO is reduced to trymethylamine (TMA) (Velasquez *et al.*, 2016).

NapC and TorC have been previously described as inner membrane *c*-type cytochromes which transfer electrons from a quinol pool to the periplasm (Gon *et al.*, 2001; Gescher *et al.*, 2008). This role is very similar to the one that CymA has in *Shewanella oneidensis* MR-1 and therefore, they could be considered as potential pathways for *Citrobacter* to transfer electrons from the electron transport chain to the final electron acceptor during anaerobic respiration by iron reduction.

Nonetheless, *Shewanella oneidensis* MR-1 also encodes NapC and TorC as well as CymA (Breuer *et al.*, 2015), and when the Mtr operon of *S. oneidensis* is knocked out, cells are not able to reduce iron, suggesting that NapC and TorC do not have a role in iron reduction.

Due to the combined observations that no bands were observed in the heme stained SDS-PAGE gel, and that *Shewanella* does not seem to be able to reduce ferric iron (Fe^{3+}) using NapC and TorC, it seems unlikely that *Citrobacter* could be using an equivalent system using only elements of the DNRA or the TMAO pathways to reduce ferric iron (Fe^{3+}).

Although unlikely, if *Citrobacter* was actually using these pathways, it would be interesting to study why Fe(III)citrate can be reduced intracellularly via cytochrome complexes in *Citrobacter* whilst it only seems possible in *Shewanella* by extracellular reduction. One possibility could be that intracellular iron does not damage *Citrobacter* species as they can accumulate heavy metals in the periplasm in form of metal phosphatases, to avoid metal toxicity (Macaskie *et al.*, 1994).

4.3.2. <u>Taxonomic classification</u>

As first suggested by Fox *et al.*, 1977, the 16S rRNA gene has been used to classify Archaea and Bacteria taxonomically. 16S rRNA sequences are present in all prokaryotes and the DNA sequences are very conserved among species. This method is still considered the best approximation to classify prokaryotes by many microbiologists (Zuo *et al.*, 2015).

However, this gene can present heterogeneity between multiple copies in the same organisms, as well as being very conserved between organisms that are functionally different (Větrovský and Baldrian, 2013). As an example, *Acinetobacter* pan-genome includes DNA deletions, insertions and horizontal transfer (Chan *et al.*, 2012) Therefore, an innocuous strain of *Acinetobacter* could be considered the same species as a virulent one due to their similarities in the 16S rRNA gene.

Additional techniques can be used in order to compensate for the lack of resolution that the 16S rRNA has from a physiological and morphological point of view (Zhu *et al.*, 2015). If the whole genome is available, there are methods that can be used to define if a strain is part of a species other than using the similarity of the 16S rRNA. Multilocus sequence analysis (MLSA) allows the comparison between housekeeping genes, which are conserved genes necessary for diverse functions in the cell (Oton *et al.*, 2015). Average nucleotide identity (ANI) measures the similarity between the coding regions of whole genomes and provides a comparison not just of the core genome but also the variable parts (Goris *et al.*, 2007).

Table 4-1 shows the differences between using 16S rRNA, MLSA and ANI to classify the environmental strains. 16S rRNA and MLSA were aligned by BLAST and ANI was aligned by EZBioCloud. MLSA was done by concatenating 20 housekeeping genes identified on the annotated genomes. Their functions and their individual percentage of similarity can be found in Table 4-2. The consensual percentage of similarity to define two strains as the same species used were 97 % for 16S rRNA and MLSA, and 95 % for ANI (Goris *et al.*, 2007; Gomila *et al.*, 2015; Nguyen *et al.*, 2016).

Table 4-1 Taxonomical classification of the isolated environmental strains.
16S rRNA, Multilocus sequence analysis (MLSA) and Average nucleotide identity (ANI) have been used to classify the environmental strains taxonomically. Acinetobacter spp. UEA identity has been compared with Acinetobacter johnsonii and Citrobacter spp. WGB compared with Citrobacter freundii, their highest similarity hits in the NCBI database respectively. Identity values that are considered above the threshold to be classified in the same genus but not in the same species are highlighted in grey.

Method	Species	Query cover %	Identity %
16S rRNA	*Acinetobacter* spp. UEA	98	99
	Citrobacter spp. WGB	98	97
MLSA	*Acinetobacter* spp. UEA	100	96
	Citrobacter spp. WGB	100	98
ANI	*Acinetobacter* spp. UEA	67	95
	Citrobacter spp. WGB	63	98

All methods agreed that *Citrobacter* spp. WGB should be considered as a *Citrobacter freundii* strain. However, it is uncertain if *Acinetobacter* spp. UEA should be considered to be classified an *Acinetobacter johnsonii* strain.

According to the 16S rRNA, the environmental strain would be similar enough to *A. johnsonii* to classify as part of the same species. In contrast, the alignment of the housekeeping genes would not consider the two strains as part of the same species. The results of ANI agrees with the 16S rRNA result, classifying the isolated *Acinetobacter* as *A. johnsonii*. However, the recommended percentage of query cover for ANI to be reliable is higher than 70 % and because the environmental isolates did not had all their genome sequenced, the query cover was below the recommended standards (Goris *et al.*, 2007).

The results of this analysis highlight how taxonomic classifications can be biased depending on which method each author decides to use. In the specific case of MLSA, the chosen housekeeping gene can determine the classification of a specific strain. When the 20 identified housekeeping genes of *Acinetobacter* spp. UEA and *Citrobacter* spp. WGB were aligned against their reference genomes individually, just 1 of the *Citrobacter* spp. WGB had a lower identity than 97 % but almost half of the genes in *Acinetobacter* spp. UEA suggested that the environmental strain could be a new species (Table 4-2). In fact,

if *pnp* was the only housekeeping gene used for the alignment, the isolated bacterium would not even be considered as part of the *Acinetobacter* genus.

Even though it is not clear if *Acinetobacter* spp. UEA should be considered a new species or classified as *A. johnsonii*, it can be suggested that the strain isolated from the river Yare in this study, is phylogenetically distant from the other strains of *A. johnsonii* registered in the database (Figure 4-3).
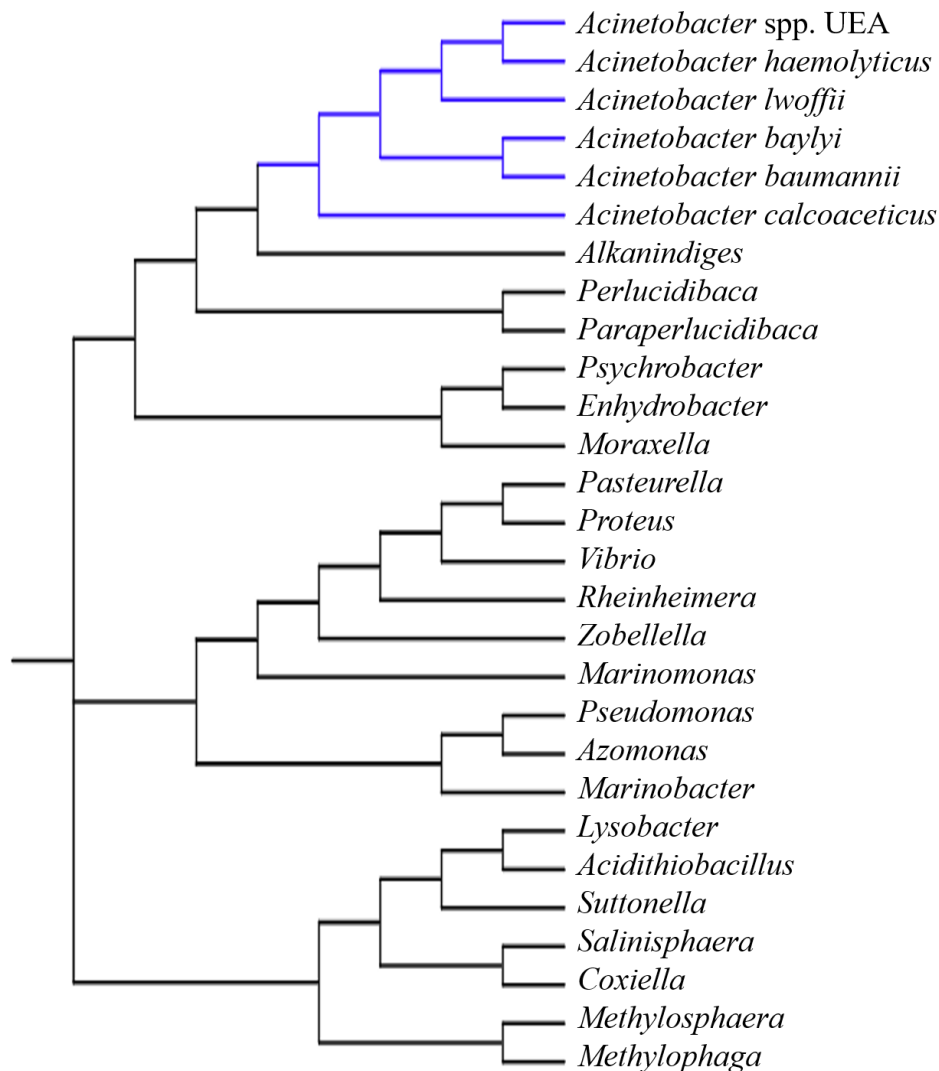
Figure 4-3 Phylogenetic distance of Acinetobacter spp. UEA compared with other Gammaproteobacteria species.
Taxonomical tree using the 16S rRNA. Species of the Acinetobacter genus are highlighted in blue.

Table 4-2 Housekeeping gene homology between the environmental strains and their taxonomical closest match.

Acinetobacter spp. UEA identity compared with Acinetobacter johnsonii and Citrobacter spp. WGB with Citrobacter freundii, their highest similarity hits in the NCBI database respectively. All genes had 100% query cover between the environmental sequence and the database reference. Identity values that are considered above the threshold to be classified in the same genus but not in the same species are highlighted in grey. Identity values that are considered below the genus threshold are highlighted in blue.

Gene	Function	*Acinetobacter* spp. UEA (%)	*Citrobacter* spp. WGB (%)
holA	DNA replication	96	98
polA	DNA modification modification	96	98
deaD	DNA transcription	98	99
hisS	RNA translation	97	99
mnmA	tRNA modification	98	99
rplW	Ribosomal protein	99	100
era	Ribosome modification	96	97
fusA	Translation factors	98	99
pnp	RNA degradation	93	99
pepA	Post translational modification	96	97
dnaK	Protein folding	95	99
ffh	Protein transport	98	98
ftsZ	Cell division	97	99
pitA	Molecule transport	95	99
eno	Glycolysis	95	99
atpG	Proton motive force generation	99	99
rpe	Pentose phosphate pathway	98	99
fadD	Lipid metabolism	97	96
adk	Nucleotide biosynthesis	99	99
coaE	Cofactors biosynthesis	95	99
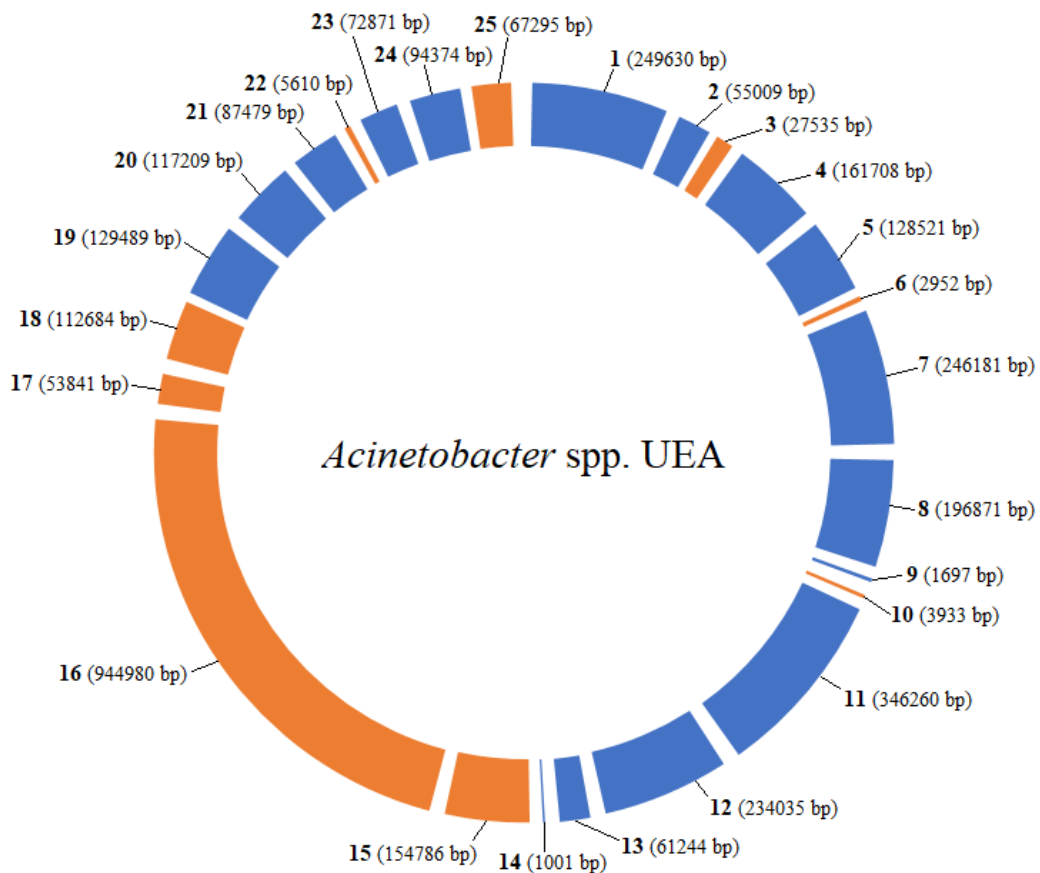
Figure 4-4 Circular assembly of the Acinetobacter spp. UEA genome
98.8% of the contigs obtained from sequencing the genomic DNA have been mapped using Acinetobacter johnsonii as a reference genome resulting in 25 scaffolds covering 82% of the total genome. Sequences aligned in the same direction as the reference genome are represented in orange and in the opposite direction in blue. The length of each scaffold is proportional to the size of the genome but the gaps between them are unknown and have been represented equitably.

Due the possibility of *Acinetobacter* spp. UEA being a novel species, the genome was mapped using SnapGene Viewer and BLAST (Chapter 2.21.4) to provide further information and to determine other differences from existing strains. Since the genome of *Acinetobacter* spp. UEA was not fully covered the first time that it was sent for sequencing, its genomic DNA was sent for a second time. Unfortunately, some of the gaps between contigs were consistent in both analysis. The resulting mapped genome consisted of 25 final scaffolds covering 82 % of the reference genome (98.8% of the obtained contigs were mapped) (Figure 4-4).

4.4   Iron reduction in *Acinetobacter baumannii*

As the *Acinetobacter* genus has not been described before as an iron reducer, and previous literature describes it as a strict aerobe (Chan *et al.*, 2012), it was considered interesting to know if the ability to reduce iron was only from the isolated strain or as a trait shared with other members of the *Acinetobacter* genus. To test the iron reduction activity of other member of this genus, the most studied strain, *Acinetobacter baumannii*, was compared with the environmental isolate.

As Figure 4-5 shows, the iron reduction rates of both strains were very similar, suggesting that *Acinetobacter* species are able to reduce iron and survive anaerobically. The ability of this genus to grow anaerobically in the laboratory together with the fact that different *Acinetobacter* species have been isolated from different environments that would not be thought to support aerobic growth (Table 3-2) suggests that ferric iron (Fe^{3+}) could be one of the factors that allows *Acinetobacter* to grow in anaerobic environments suggesting a much larger role for the environment as a reservoir of this opportunistic pathogen.
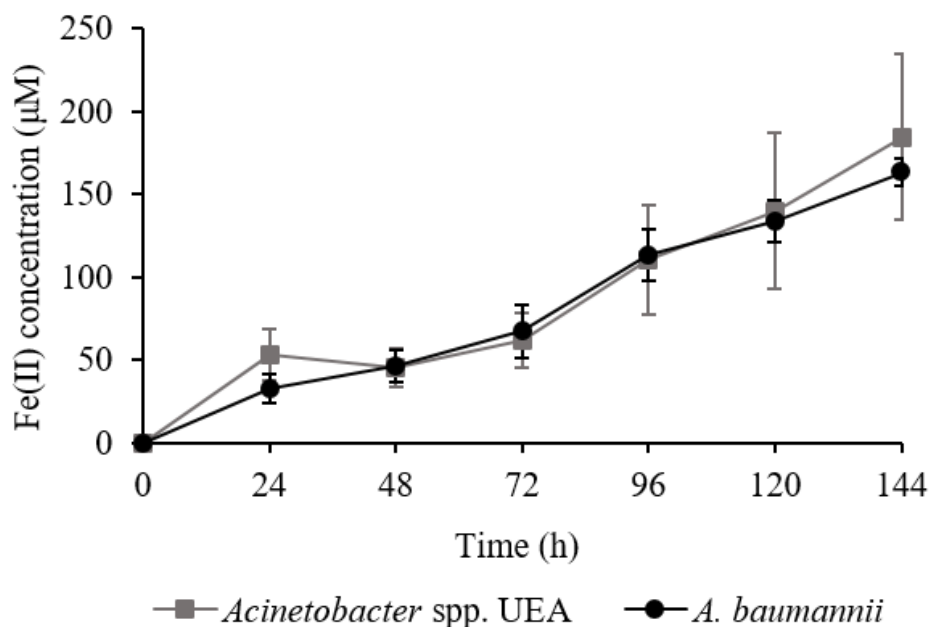
Figure 4-5 Iron reduction in Acinetobacter spp. UEA and Acinetobacter baumannii.
Ferrous iron (Fe^{2+}) measurements by ferrozine assay (Chapter 2.4) of cells cultured anaerobically in minimal media at 25 ˚C with 0.5 mM Fe(III)citrate as the electron acceptor source and 30 mM succinate as the carbon source. Each data point represents the average of three biological replicates and the error bars represent the ± standard deviation (SD).

4.5 Transcriptomic analysis

To have a better understanding of how *Acinetobacter*'s metabolism works during anaerobic respiration, the transcriptome of *Acinetobacter* spp. UEA growing using iron as the sole electron acceptor was compared with the transcriptome of *Acinetobacter* spp. UEA growing using oxygen.
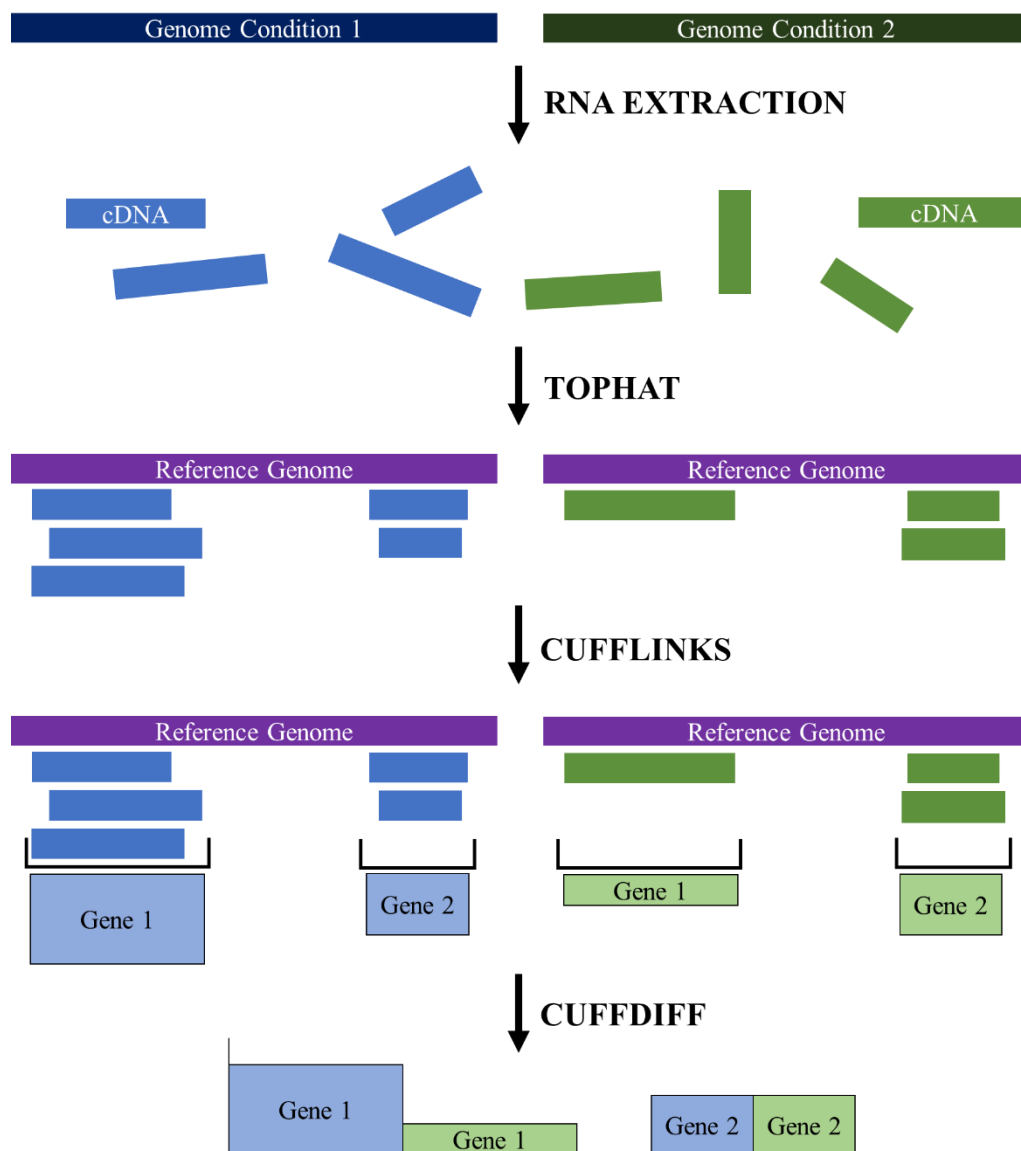
Figure 4-6 Differential gene expression analysis from RNA-seq data

125

To analyse the transcriptome of an organism for differential gene expression, its mRNA is extracted and converted to cDNA through reverse transcription. In order to be sequenced, cDNA has to be fragmented in short sequences and consequently, the reads have to be assembled afterwards.

Once the data of the sequencing is obtained, three bioinformatic tools can be used to analyse differential gene expression: Tophat, Cufflinks and Cuffdiff (Figure 4-6).

To associate the cDNA reads with genes, Tophat is used to align the cDNA fragments with a reference genome already annotated. Then, using Cufflinks, the transcripts corresponding to the same genes are combined and quantified. Finally, Cuffdiff compares the amount of gene expression between samples growing in different condition (Trapnell *et al.*, 2012).

Acinetobacter spp. UEA cells were grown in three different conditions. All three conditions were in minimal media containing 30 mM Succinate but varied in available electron acceptors. The first was grown aerobically without other terminal electron acceptors than oxygen. The second was also grown aerobically but with the addition of 0.5mM Fe(III)citrate. The final growth condition was with 0.5mM Fe(III)citrate but under anaerobic conditions so no oxygen was available as a terminal electron acceptor.

Cultures in the anaerobic condition grew three times slower than the cultures in the other two conditions. The biomasses of the cultures were normalised before the RNA was extracted and the samples were sent to sequence by Wellcome Centre for Human Genetics (Chapters 2.6 and 2.21.5). Because the genome of *Acinetobacter* spp. UEA was not 100 % covered, the cDNA reads were aligned to the genome of *Acinetobacter johnsonii* to determine which reads corresponded to each genes. Once the reads had been assigned a gene, they were quantified to know how much expression there was for each gene in the genome.

A (O$_2$ + Fe(III)citrate compared to O$_2$)

- Non significant
- Upregulated
- Downregulated

y-axis: -log10 q value

x-axis: log2 fold change

B (O$_2$ + Fe(III)citrate compared to Fe(III)citrate)

- Non significant
- Upregulated
- Downregulated

y-axis: -log10 q value

x-axis: log2 fold change
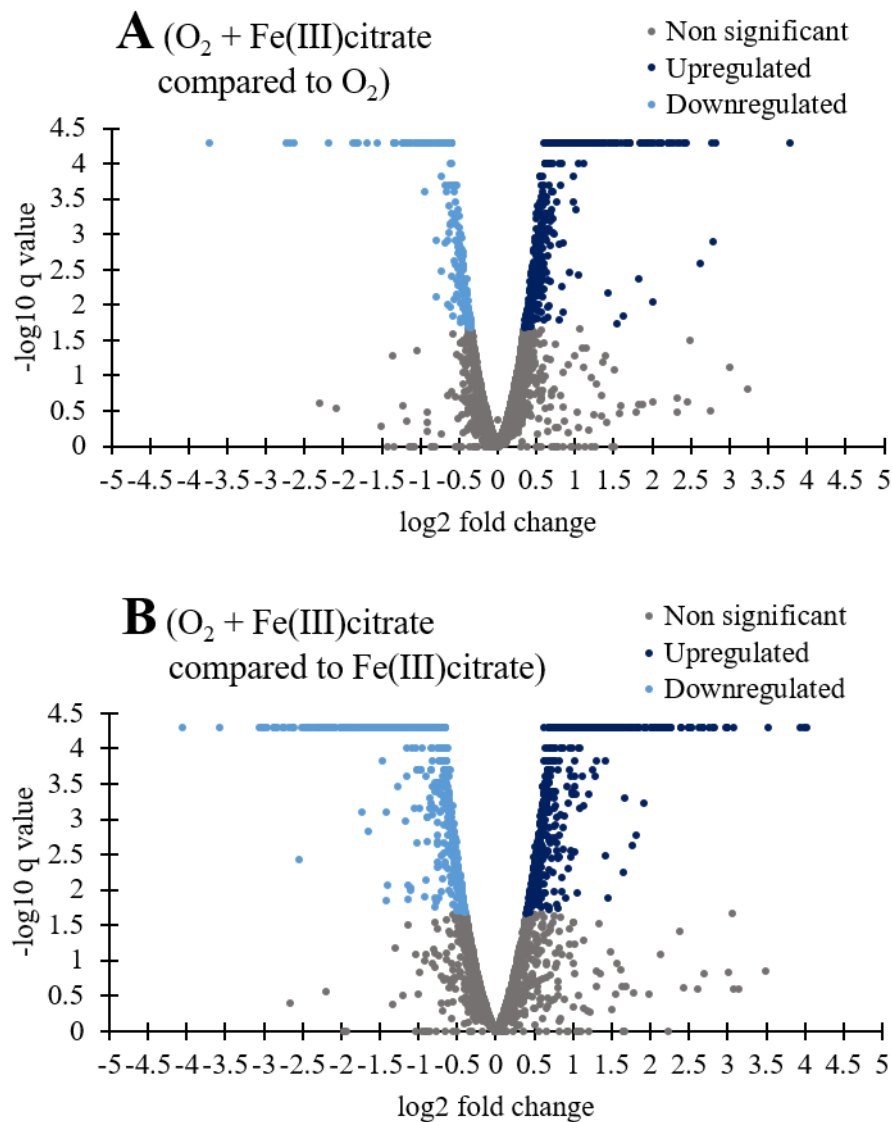
Figure 4-7 Differentially expressed genes in Acinetobacter spp. UEA growing aerobically, aerobically with iron and anaerobically with iron.

A) Comparison between Acinetobacter spp. UEA growing aerobically with 0.5 mM Fe(III)citrate or without iron. Genes which are downregulated when cultures are growing with iron are represented in light blue. Genes which are upregulated when cultures are growing with iron are represented in dark blue. B) Comparison between Acinetobacter spp. UEA growing anaerobically with 0.5 mM Fe(III)citrate or aerobically with 0.5 mM Fe(III)citrate. Genes which are downregulated when cultures are growing without oxygen are represented in light blue. Genes which are upregulated when cultures are growing without oxygen are represented in dark blue. In all conditions 30 mM Succinate is the sole carbon source. Fold change is the ratio of Fragments Per Kilobase Million (FPKM) of the control divided by FPKM of the sample to study. Genes in which differences are non-significant (q-value > 0.05) are represented in grey.

Both Tophat and Cufflink analysis were done by Wellcome Centre for Human Genetics (Chapter 2.21.5). Cuffdiff analysis for differentially expressed genes was done using Galaxy, as it was a public web-based platform that allowed to perform analysis using large amount of data without the need to use a supercomputer (Afgan *et al.*, 2018).

To know which genes were differentially expressed by the presence of ferric iron (Fe^{3+}) in the media, the reads of *Acinetobacter* spp. UEA growing aerobically with Fe(III)citrate were compared with the reads from *Acinetobacter* spp. UEA growing aerobically without iron (Figure 4-7 A). A total of 413 genes were significantly upregulated when Fe(III)citrate was present in the media and 194 genes were significantly downregulated. The full list of genes can be found in Table A-2 in the appendix of this thesis.

In addition to investigating the regulatory effects of the presence of ferric iron, the effects of the presence of oxygen were also studied. To determine which genes were differentially expressed by the absence of oxygen in the media, the reads of *Acinetobacter* spp. UEA growing anaerobically with Fe(III)citrate were compared with the reads of *Acinetobacter* spp. UEA growing aerobically with Fe(III)citrate (Figure 4-7 B). In this analysis 620 genes were significantly upregulated when oxygen was absent in the media and 812 genes were significantly downregulated. The full list of genes can be found in Table A-3 in the appendix of this thesis.

Combining the differentially expressed genes by the presence of Fe(III)citrate and by the absence of oxygen, over two thousand genes were differentially expressed when *Acinetobacter* spp. UEA grew using ferric iron (Fe^{+3}) instead of oxygen as the sole terminal electron acceptor. The most differentially expressed genes (those with a log Fold Change with an absolute value equal or higher than 2) were analysed to determine their function. Because the genome of *Acinetobacter* spp. UEA was not 100 % available, this analysis was done by comparing the predicted functions of the corresponding genes in the annotated genome of *Acinetobacter johnsonii*.

Table 4-3 Functions of the differentially expressed genes in Acinetobacter spp. UEA growing aerobically with iron compared to aerobically without iron.
Comparison between Acinetobacter spp. UEA growing aerobically with 0.5 mM Fe(III)citrate or without iron. In both conditions 30 mM Succinate is the sole carbon source. The table shows the predicted function of the most relevant differentially expressed genes (log2FC > 2 or log2FC < -2). Genes predicted to be part of the same operon grouped by grey divides. Genes in grey have a log2FC lower than 2 but are predicted to be part of the same operon.

A	Downregulated (O_2 + Fe(III)citrate compared to O_2)		
Gene (NCBI)	**log2FC**	**Description**	**Function**
RZ95_RS12380	-2.63	PAP2 family protein	Lipid anabolism

B	Upregulated (O_2 + Fe(III)citrate compared to O_2)		
Gene (NCBI)	**log2FC**	**Description**	**Function**
RZ95_RS05460	2.09	CoA transferase subunit A	
RZ95_RS05465	2.11	hydroxymethylglutaryl-CoA lyase	
RZ95_RS05470	1.84	acetyl/propionyl/methylcrotonyl-CoA carboxylase subunit alpha	
RZ95_RS05475	1.7	enoyl-CoA hydratase	
RZ95_RS05480	2.27	methylcrotonoyl-CoA carboxylase	
RZ95_RS05485	2.82	isovaleryl-CoA dehydrogenase	Lipid and protein catabolism
RZ95_RS05490	2.08	TetR/AcrR family transcriptional regulator	
RZ95_RS05495	2.24	fatty acid--CoA ligase	
RZ95_RS06155	2.40	3-hydroxyacyl-CoA dehydrogenase	
RZ95_RS06160	2.03	acyl-CoA dehydrogenase	
RZ95_RS12480	2.35	fumarylacetoacetase	
RZ95_RS12460	2.43	4-hydroxyphenylpyruvate dioxygenase	Metal ion binding protein

Table 4-3 shows the predicted functions of the genes differentially expressed in aerobic conditions in the presence of Fe(III)citrate compared to aerobic conditions without Fe(III)citrate. Results indicate that cultures growing aerobically with Fe(III)citrate in the media were increasing their degradation of lipids and proteins and lowering their biosynthesis. In addition, a gene encoding a metalloprotein was also upregulated.

Table 4-4 shows the predicted functions of the genes differentially expressed in anaerobic conditions in presence of Fe(III)citrate compared to aerobic conditions in presence of Fe(III)citrate. In the absence of oxygen, more genes involved in the degradation of lipids and proteins were overexpressed, and less in their biosynthesis. Genes involved in aerobic respiration or in protecting the cell against oxidative stress were also downregulated. Genes encoding metalloproteins and cation transporters were also overexpressed.

In addition to the genes with a log Fold Change with an absolute value equal or higher than 2, five genes previously shown to be related with iron homeostasis (Frawley and Fang, 2014) were identified from the significant differentially expressed genes when cultures were growing anaerobically with Fe(III)citrate compared to aerobically with Fe(III)citrate (Figure 4-7 B). Two ferritins (proteins used to sequester iron inside the cell to avoid its toxicity) were downregulated (RZ95_RS03560 and RZ95_RS01565 (Table A-3) and two iron siderophores (proteins used to transport iron inside the cell) were upregulated (RZ95_RS00200, RZ95_RS00625 and RZ95_RS08790 (Table A-3).

Table 4-4 Functions of the differentially expressed genes in Acinetobacter spp. UEA growing anaerobically with iron compared to aerobically with iron.

Comparison between Acinetobacter spp. UEA growing anaerobically with 0.5 mM Fe(III)citrate or aerobically with 0.5 mM Fe(III)citrate. In both conditions 30 mM Succinate is the sole carbon source. The table shows the predicted function of the most relevant differentially expressed genes (log2FC > 2 or log2FC < -2). Genes predicted to be part of the same operon grouped by grey divides. Genes in grey have a log2FC lower than 2 but are predicted to be part of the same operon.

A	Downregulated (Fe(III)citrate compared to O_2 + Fe(III)citrate)		
Gene (NCBI)	**log2FC**	**Description**	**Function**
RZ95_RS00780	-2.27	acetate--CoA ligase	
RZ95_RS12210	-2.34	C4-dicarboxylate ABC transporter substrate-binding protein	
RZ95_RS14750	-2.45	3-isopropylmalate dehydrogenase	
RZ95_RS14755	-2.38	hypothetical protein	
RZ95_RS14760	-3.05	3-isopropylmalate dehydratase small subunit	Lipid and protein anabolism
RZ95_RS16735	-2.43	aliphatic sulfonate ABC transporter substrate-binding protein	
RZ95_RS16740	-2.87	alkanesulfonate monooxygenase, FMNH(2)-dependent	
RZ95_RS16745	-2.20	ABC transporter permease	
RZ95_RS16750	-2.75	ABC transporter ATP-binding protein	
RZ95_RS16765	-2.83	C4-dicarboxylate ABC transporter	
RZ95_RS01215	-2.10	aquaporin Z	
RZ95_RS02980	-2.87	peroxiredoxin	
RZ95_RS07690	-2.18	universal stress protein	Protection against oxidative stress
RZ95_RS07695	-2.31	universal stress protein	
RZ95_RS13755	-2.22	organic hydroperoxide resistance protein	
RZ95_RS02445	-2.18	cytochrome b562	
RZ95_RS03330	-2.01	NADH:flavin oxidoreductase/NADH oxidase	
RZ95_RS07395	-2.12	alcohol dehydrogenase	
RZ95_RS09725	-2.26	SfnB family sulfur acquisition oxidoreductase	Aerobic respiration
RZ95_RS09730	-2.00	FMN-dependent monooxygenase	
RZ95_RS13310	-2.86	hemerythrin	

B	Upregulated (Fe(III)citrate compared to O$_2$ + Fe(III)citrate)		
Gene (NCBI)	**log2FC**	**Description**	**Function**
RZ95_RS09075	3.00	acyl-CoA desaturase	
RZ95_RS09080	3.99	hypothetical protein	
RZ95_RS12480	2.81	fumarylacetoacetase	
RZ95_RS12485	3.00	maleylacetoacetate isomerase	
RZ95_RS12755	2.02	alanine racemase	
RZ95_RS12760	2.82	amino acid transporter	Lipid and protein catabolism
RZ95_RS12765	2.76	succinylglutamate desuccinylase	
RZ95_RS12770	2.49	N-succinylarginine dihydrolase	
RZ95_RS12775	2.20	succinylglutamate-semialdehyde dehydrogenase	
RZ95_RS12780	2.19	arginine N-succinyltransferase	
RZ95_RS12785	1.84	aspartate aminotransferase family protein	
RZ95_RS12790	2.07	Glu/Leu/Phe/Val dehydrogenase	
RZ95_RS01940	2.02	metal-dependent hydrolase	
RZ95_RS01955	2.63	YihA family ribosome biogenesis GTP-binding protein	Metal ion binding protein
RZ95_RS12490	2.68	transcriptional regulator	
RZ95_RS15680	2.20	NO-inducible flavohemoprotein	
RZ95_RS04510	2.39	ABC transporter substrate-binding protein	
RZ95_RS05105	2.26	cation transporter	
RZ95_RS07705	2.16	quaternary ammonium transporter	
RZ95_RS08030	2.10	porin	
RZ95_RS08800	2.39	efflux RND transporter periplasmic adaptor subunit	Cation transport
RZ95_RS08805	2.50	TolC family protein	
RZ95_RS11515	4.02	copper-translocating P-type ATPase	
RZ95_RS12040	2.22	inorganic iron transporter	
RZ95_RS09975	2.09	ferredoxin reductase	Electron transport

It is worth highlighting the large volume of data obtained from the sequencing of a whole transcriptome. A full in depth analysis is time and resource consuming and has not been performed in this thesis. However, some hypotheses can be made analysing the function of the studied differentially expressed genes (Table 4-3 and Table 4-4). This hypotheses can then, be used as the basis for further investigation.

4.5.1. Anaerobic growth

Under anaerobic conditions there would be no need for proteins involved in the aerobic respiration pathway, for this reason they were seen to be downregulated in the absence of oxygen in the media. Moreover under anaerobic conditions the cell does not need protection against reactive oxygen species so genes encoding proteins preventing oxidative stress are also downregulated (Table 4-4).

4.5.2. Lipid and protein metabolism

Lipids and proteins can be degraded by microorganisms in order be used as an energy source via cellular respiration or fermentation (Wilkinson, 1963). When, in the previous chapter, uncoupling agents were used to see if *Acinetobacter* spp. UEA was obtaining energy by anaerobic respiration or by fermentation, results suggested that most of its energy would be provided by anaerobic respiration (Chapter 3).

When *Acinetobacter* grew aerobically, oxygen was used as the terminal electron acceptor, which is very efficient for energy production and therefore, more succinate molecules could be used for biomass and cultures grew fast. In contrast, when cultures grew anaerobically using Fe(III)citrate as the terminal electron acceptor it is less energetically favourable than the use of oxygen due to the difference of potential. For this reason, some lipids and proteins may have to be used to support energy production and therefore, gene regulation in cultures growing anaerobically with Fe(III)citrate lowered the production of biomass (increased the catabolism of lipids and amino acids) so cells were still able to grow but as a result they divided slower (Table 4-4).

Despite there being a clear relation between the absence of oxygen and the regulation of biomass production, oxygen does not seem to be the only factor for the regulation of lipid and protein metabolism. Table 4-3 shows how the presence of Fe(III)citrate also activates some genes involved in the degradation of lipids and proteins. It is not clear why the presence of Fe(III)citrate has an effect on the biomass in aerobic conditions when the cultures growing aerobically with Fe(III)citrate grew as fast as the cultures growing aerobically without Fe(III)citrate.

4.5.3. Iron acquisition

While the regulation of protein and lipid degradation seemed to be linked both to the absence of oxygen and to the presence of Fe(III)citrate, the cation transporters were overexpressed only when Fe(III)citrate was present under anaerobic conditions which suggests that iron reduction was essential only in the absence of oxygen and cation transporters were required for the uptake of ferric iron (Fe^{3+}) for use as a terminal electron acceptor within the cell.

It has been previously described that species of the *Acinetobacter* genus express different types of iron chelating siderophores to assimilate iron (Mortensen and Skaar, 2013). To survive in iron limiting environments, microorganisms express siderophores to obtain as many molecules of iron as possible and when iron is in excess, ferritins are used to sequester the iron inside the cell avoiding its toxicity (Frawley and Fang, 2014). In anaerobic conditions when iron is in excess, the role of these proteins seems to change for *Acinetobacter* spp. UEA. Ferritins were downregulated and siderophores were upregulated. This could be for the need of *Acinetobacter* to have a large amount of available iron inside the cell, rather than in a sequestered from, to accomplish anaerobic respiration.

With no oxygen available, Fe(III)citrate would be essential for energy production as the only available electron acceptor, and more siderophores would be required to transport this cation inside the cell. However, an excess of iron inside the cell in aerobic conditions could damage the cell due the interaction of iron with reactive oxygen species leading to the production of hydroxyl radicals. As a result,

this could explain why the expression of siderophores in aerobic conditions is repressed (Andrews *et al.*, 2003).

4.5.4. Soluble electron transfer protein

The overexpression of a ferredoxin (RZ95_RS09975 Table 4-4) during anaerobic conditions could be a hint at how iron reduction is happening in *Acinetobacter*. Previous results in this thesis suggest that ferric iron (Fe^{3+}) is not being reduced extracellularly. For this reason, this soluble iron-sulfur protein could be acting as a ferric oxidoreductase in the periplasm or the cytoplasm of the cell where iron could be reduced (Goss and Hanke, 2014).

4.5.5. Other metalloproteins

In addition, the upregulation of metalloproteins without an apparent role in cellular respiration of *Acinetobacter* spp. UEA could be upregulated by the presence of the iron, which is required as a cofactor for these proteins.

4.6 Discussion

4.6.1. *Acinetobacter* spp. UEA

Since *Acinetobacter* spp. UEA was not behaving differently to other *Acinetobacter* species and the taxonomic classification was not conclusive, the isolated environmental strain has not been registered as a new species. Even so *Acinetobacter baumannii* was able to reduce iron under anaerobic conditions, which suggests that several members of the *Acinetobacter* genus are iron reducing bacteria.

These results are novel as no one has described *Acinetobacter* as anything other than a strict aerobe before. This could be because most of the studies that are focused on *A. baumannii* are related with clinical research, where this bacterium is cultured in anaerobic conditions to replicate the conditions that has in its host, where it grows under iron limiting conditions (Eijkelkamp *et al.*, 2011)

By analysing the genome of *Acinetobacter* spp. UEA, it has been confirmed that this bacterium lacks any *c*-type cytochromes that could take part in an extracellular electron transfer (EET) pathway.

Its transcriptomics analysis gives a better understanding of how ferric iron (Fe^{3+}) and succinate metabolism are related. It seems that both the presence of Fe(III)citrate and the absence of oxygen regulate the degradation of lipids and proteins to allow their use as an energy source. In the absence of oxygen, the use of iron as the terminal electron acceptor becomes essential and the expression of a soluble ferredoxin as well as siderophores and ferritins was induced. As expected, under anaerobic conditions all the genes involved in aerobic respiration and protection against oxidative stress were no longer required and a downregulation of those genes was observed.

These results suggest that there is not a specific pathway in *Acinetobacter* to achieve anaerobic respiration, but there is a group of metabolic regulations in the cell that allows the use of ferric iron (Fe^{3+}) as the final electron acceptor when oxygen is not available for aerobic respiration. Besides knowing how iron is related with anaerobic metabolism, it would be interesting to recognise how intracellular iron affects the environmental isolates and which mechanisms they have to protect the cell against iron toxicity.

As future work, it would be worth to repeat the genome sequencing to obtain 100 % coverage of the genome of *Acinetobacter* spp. UEA to have the full genome annotated and complete the transcriptomic analysis identifying all the genes differentially expressed.

4.6.2. *Citrobacter* spp. WGB

There is still a lot to understand about *Citrobacter* metabolism. It was previously shown to be able to grow under uncoupling agent conditions, suggesting that it could be surviving by fermentation instead of anaerobic respiration (Figure 3-10) yet its genome presented genes that could express *c*-type cytochromes potentially capable to reduce ferric iron (Fe^{3+}), suggesting role for iron coupled respiration.

Due to cost limitations, the analysis of *Citrobacter* spp. WGB transcriptome was not possible, and therefore, it remains unknown if iron reduction is directly related to succinate metabolism in this bacterium. As future work, this analysis would be necessary to understand its metabolism more, in a study similar to that performed here with *Acinetobacter* spp. UEA.

4.6.3. Metagenomics

Once the iron reducing pathways used by these two isolated microorganisms are identified, metagenomics could be used to study if these pathways are also present in other microorganisms in an ecosystem, with the aim of understanding the impact that iron reducers have in different environments.

4.7 References

Afgan, E., Baker, D., Batut, B., van den Beek, M., Bouvier, D., Čech, M., et al. (2018) The Galaxy platform for accessible, reproducible and collaborative biomedical analyses: 2018 update. *Nucleic Acids Res.* 46: W537–W544.

Allen, J.W.A., Daltrop, O., Stevens, J.M., and Ferguson, S.J. (2003) *c-type* cytochromes: diverse structures and biogenesis systems pose evolutionary problems. *Philos. Trans. R. Soc. Lond. B. Biol. Sci.* 358: 255–66.

Andrews, S.C., Robinson, A.K., Rodríguez-Quin, F., and Ones (2003) Bacterial iron homeostasis.

Boughner, L.A. and Singh, P. (2016) Microbial Ecology: Where are we now? *Postdoc J. a J. Postdr. Res. Postdr. Aff.* 4: 3–17.

Breuer, M., Rosso, K.M., Blumberger, J., and Butt, J.N. (2015) Multi-haem cytochromes in *Shewanella oneidensis* MR-1: structures, functions and opportunities. *J. R. Soc. Interface* 12: 20141117.

Chan, J.Z.-M., Halachev, M.R., Loman, N.J., Constantinidou, C., and Pallen, M.J. (2012) Defining bacterial species in the genomic era: insights from the genus *Acinetobacter*. *BMC Microbiol.* 12: 302.

Domangue, R.J. and Mortazavi, B. (2018) Nitrate reduction pathways in the presence of excess nitrogen in a shallow eutrophic estuary. *Environ. Pollut.* 238: 599–606.

Dominguez Del Angel, V., Hjerde, E., Sterck, L., Capella-Gutierrez, S., Notredame, C., Vinnere Pettersson, O., et al. (2018) Ten steps to get started in Genome Assembly and Annotation. *F1000Research* 7:.

Eijkelkamp, B.A., Hassan, K.A., Paulsen, I.T., and Brown, M.H. (2011) Investigation of the human pathogen *Acinetobacter baumannii* under iron limiting conditions. *BMC Genomics* 12: 126.

Fox, G.E., Magrum, L.J., Balch, W.E., Wolfe, R.S., and Woese, C.R. (1977) Classification of methanogenic bacteria by 16S ribosomal RNA characterization. *Proc. Natl. Acad. Sci. U. S. A.* 74: 4537–41.

Frawley, E.R. and Fang, F.C. (2014) The ins and outs of bacterial iron metabolism. *Mol. Microbiol.* 93: 609–16.

Gescher, J.S., Cordova, C.D., and Spormann, A.M. (2008) Dissimilatory iron reduction in Escherichia coli: identification of CymA of *Shewanella oneidensis* and NapC of *E. coli* as ferric reductases. *Mol. Microbiol.* 68: 706–719.

Gomila, M., Peña, A., Mulet, M., Lalucat, J., and García-Valdés, E. (2015) Phylogenomics and systematics in Pseudomonas. *Front. Microbiol.* 6: 214.

Gon, S., Giudici-Orticoni, M.T., Méjean, V., and Iobbi-Nivol, C. (2001) Electron transfer and binding of the *c-type* cytochrome TorC to the trimethylamine N-oxide reductase in *Escherichia coli*. *J. Biol. Chem.* 276: 11545–51.

Goris, J., Konstantinidis, K.T., Klappenbach, J.A., Coenye, T., Vandamme, P., and Tiedje, J.M. (2007) DNA-DNA hybridization values and their relationship to whole-genome sequence similarities. *Int. J. Syst. Evol. Microbiol.* 57: 81–91.

Goss, T. and Hanke, G. (2014) The end of the line: can ferredoxin and ferredoxin NADP(H) oxidoreductase determine the fate of photosynthetic electrons? *Curr. Protein Pept. Sci.* 15: 385–93.

Hiraoka, S., Yang, C.-C., and Iwasaki, W. (2016) Metagenomics and Bioinformatics in Microbial Ecology: Current Status and Beyond. *Microbes Environ.* 31: 204–12.

Ilbert, M. and Bonnefoy, V. (2013) Insight into the evolution of the iron oxidation pathways. *Biochim. Biophys. Acta - Bioenerg.* 1827: 161–175.

Kandpal, R.P., Saviola, B., and Felton, J. (2009) The era of 'omics unlimited. *Biotechniques* 46: 351–355.

Macaskie, L.E., Bonthrone, K.M., and Rouch, D.A. (1994) Phosphatase-mediated heavy metal accumulation by a *Citrobacter* sp. and related enterobacteria. *FEMS Microbiol. Lett.* 121: 141–146.

Mortensen, B.L. and Skaar, E.P. (2013) The contribution of nutrient metal acquisition and metabolism to *Acinetobacter baumannii* survival within the host. *Front. Cell. Infect. Microbiol.* 3: 1–10.

Nguyen, N.-P., Warnow, T., Pop, M., and White, B. (2016) A perspective on 16S rRNA operational taxonomic unit clustering using sequence similarity. *npj Biofilms Microbiomes* 2: 16004.

Ohashi, H., Hasegawa, M., Wakimoto, K., and Miyamoto-Sato, E. (2015) Next-generation technologies for multiomics approaches including interactome sequencing. *Biomed Res. Int.* 2015: 104209.

Oton, E.V., Quince, C., Nicol, G.W., Prosser, J.I., and Gubry-Rangin, C. (2015) Phylogenetic congruence and ecological coherence in terrestrial *Thaumarchaeota*. *ISME J.*

Trapnell, C., Roberts, A., Goff, L., Pertea, G., Kim, D., Kelley, D.R., et al. (2012) Differential gene and transcript expression analysis of RNA-seq experiments with TopHat and Cufflinks. *Nat. Protoc.* 7: 562–578.

Velasquez, M.T., Ramezani, A., Manal, A., and Raj, D.S. (2016) Trimethylamine N-Oxide: The Good, the Bad and the Unknown. *Toxins (Basel).* 8:.

Větrovský, T. and Baldrian, P. (2013) The variability of the 16S rRNA gene in bacterial genomes and its consequences for bacterial community analyses. *PLoS One* 8: e57923.

Wilkinson, J.F. (1963) Carbon and Energy Storage in Bacteria. *J . gen. Microbiol* 32: 171–176.

Zerbino, D.R. and Birney, E. (2008) Velvet: algorithms for de novo short read assembly using de Bruijn graphs. *Genome Res.* 18: 821–9.

Zhang, W., Li, F., and Nie, L. (2010) Integrating multiple "omics" analysis for microbial biology: application and methodologies. *Microbiology* 156: 287–301.

Zhu, C., Delmont, T.O., Vogel, T.M., and Bromberg, Y. (2015) Functional Basis of Microorganism Classification. *PLoS Comput. Biol.* 11: e1004472.

Zuo, G., Xu, Z., and Hao, B. (2015) Phylogeny and Taxonomy of Archaea: A Comparison of the Whole-Genome-Based CVTree Approach with 16S rRNA Sequence Analysis. *Life (Basel, Switzerland)* 5: 949–68.

Characterization of the monoheme *c*-type cytochromes Cyc2 and Cyc2$_{PV-1}$

5.1 Introduction

Shewanella oneidensis has been used as a model organism to study extracellular electron transfer (EET). This iron reducer not only synthesizes *c*-type cytochromes to transport electrons across membranes (Pitts *et al.*, 2003), but also grows quickly and easily, having a doubling time of 40 minutes in optimal conditions, which facilitates its biomass generation and consequently, the relatively straightforward study of its proteins (Abboud *et al.*, 2005).

In contrast to this and other well studied iron reduction pathways, there is not much information available about how iron oxidising electron transport pathways work. Homologous proteins from the metal reduction pathway of *S. oneidensis* MR-1 have been previously described in iron oxidising microorganisms by bioinformatic analysis (Shi, Rosso, Zachara, *et al.*, 2012). However, the study of the metal oxidation pathway is limited by the growth rate of the iron oxidisers which typically have very slow doubling times and require conditions that are hard to scale up experimentally.

Aerobic iron oxidisers like the circumneutral *Mariprofundus ferrooxydans* or the acidophilic *Acidithiobacillus ferrooxidans* can be cultured entirely autotrophically whilst expressing the *c*-type cytochromes of interest. However, the doubling time of around 9 hours, which is more than 10 times slower than that of *Shewanella oneidensis* MR-1, results in low final cell density. This typically prevents obtaining enough biomass for unrestricted protein studies (Emerson and Moyer, 1997; Molchanov *et al.*, 2007).

Alternatively some anoxygenic iron oxidisers, like the photoautotroph *Rhodopseudomonas palustris* or the nitrate-dependent *Dechloromonas aromatica*, are often cultured chemoheterotrophically to increase their growth rates. In these conditions, these iron oxidisers do not necessarily express the *c*-type cytochromes required for EET (Bose and Newman, 2011; Chakraborty *et al.*, 2011; Pechter *et al.*, 2015)

The aim of this chapter is to obtain high concentrations of the outer membrane *c*-type cytochromes Cyc2 and Cyc2$_{PV-1}$, from *A. ferrooxidans* and *M. ferrooxydans*, by expressing them in an overexpression system using *S. oneidensis* MR-1 as the host, with the objective of characterising them and understanding their role in the iron oxidation pathway.

5.2   Growth of *Acidithiobacillus ferrooxidans*

Acidithiobacillus ferrooxidans is predicted to have an iron oxidation pathway homologous to *S. oneidensis* MR-1 (Figure 1-8). The genes thought to be responsible for iron oxidation in this bacterium encode a number of proteins. These proteins include a *c-type* cytochrome at the outer membrane (Cyc2), rusticyanin (RusA) in the periplasm that has already been characterised (Yano *et al.*, 1991) and two *c-type* cytochromes in the periplasm (Cyc1 and Cyc42).

Unlike *S. oneidensis* MR-1, this microorganism does not have a *c-type* cytochrome embedded in a porin at the outer membrane. However, the amino acid sequence of *cyc2* contains one heme-binding motif and a transmembrane β-barrel topology region, which suggests that *A. ferrooxidans* could be accepting the electrons from the ferrous iron (Fe^{2+}) with a monoheme *c-type* cytochrome that is also a porin (Figure 5-1).

MVSSSVGFKKKRLIVALAAVGGMALSSSAWALPSFARQTGWSCAACHTSYPQL
TPMGRMFKLLGFTTTNLQRQQKLQAKFGNSVGLLISRVSQFSIFLQASATNVGGGQAVF
GSGNSNANASPNNNVQFPQQVSLFYAGEITPHIGSFLHITYSGGGSGTGGGGFSFDDSSIV
WAHPWKLGTNNLLVTGVDVNNTPTAMDLWNTTPDWQAPFFSSDYSSWGHVPQPFIES
SAGAGYPLAGVGVYGADIFGPNRANWLYADADVYTNGQGTQVNPVGGFTAAGPQGR
LSGGAPYVRLAYQHDWGDWNWEVGTFGMWSSVYDNTLNNPLNNISKAGGPIDTFDD
YDLDTQLQWLDTNDNNNVTIRAAWVNEQQQFGAGNIISSNSSGNLNFFNVNATYWYH
DHYGIQGGYRNVWGSANPGLYTTTYTNSGSPDTSNEWIEASYLPWWNTRFSLRYVVY
NKFNGVGSASSNNLGYGASAYNTLELLAWISY

Figure 5-1 Amino acid sequence of Cyc2 from A. ferrooxidans
*Bioinformatic analysis suggests that this gene expresses a 52.82 kDa monoheme β-barrel protein.
A signal peptide with a cleavage site at the C-terminus of its region is highlighted in blue. A heme-
-binding motif is highlighted in red. The amino acid sequence that could be part of the β-barrel is
highlighted in green.*

Yarzábal *et al.*, 2002 has already described how Cyc2 is located in the
membrane of *A. ferrooxidans*, but the protein has not been fully characterised yet.
Due to its chemolitotroph metabolism, the growth of *A. ferrooxidans* was slow, but
enough cells were cultured (Chapter 2.2.4) to isolate the chromosomal DNA of the
acidophilic bacterium and *cyc2* was amplified using PCR in order to clone it into
S. oneidensis MR-1 with the aim of expressing and characterising the cytochrome.

5.3   Molecular cloning of *cyc2*

Via site directed mutagenesis and golden gate assembly, *cyc2* was inserted
into a vector with kanamycin resistance (Chapter 2.10), where the expression of
Cyc2 was regulated under an L-arabinose operon. *cyc2* was inserted upstream of a
strep-tag II sequence, so that when Cyc2 was expressed, a Strep-tag II would be
located at the C-terminus of the protein. Strep-tag II is a synthetic peptide
(WSHPQFEK) with a high affinity for Strep-Tactin (an engineered streptavidin).

This tag can be used to purify recombinant proteins and it can also be
identified immunologically. The plasmid pMEGGA_Cyc2C was transformed in *E.
coli* TOP10 to replicate before being transformed into *S. oneidensis* MR-1 by tri-
-parental conjugation (Chapter 2.13.1). The plasmid was sequenced by Eurofins to
confirm its sequence.

5.4 Cyc2 expression in *S. oneidensis* MR-1 WT

The expression of Cyc2 in *S. oneidensis* MR-1 pMEGGA_Cyc2C cultures was induced with 5 mM L-arabinose and cells were incubated aerobically in LB at 16 ˚C. Cells were lysed and the cell debris was removed by centrifugation. The total protein fraction was separated using SDS-PAGE (Chapter 2.16.1) subsequently the gel was stained for the heme-associated peroxidase activity (Chapter 2.16.4).
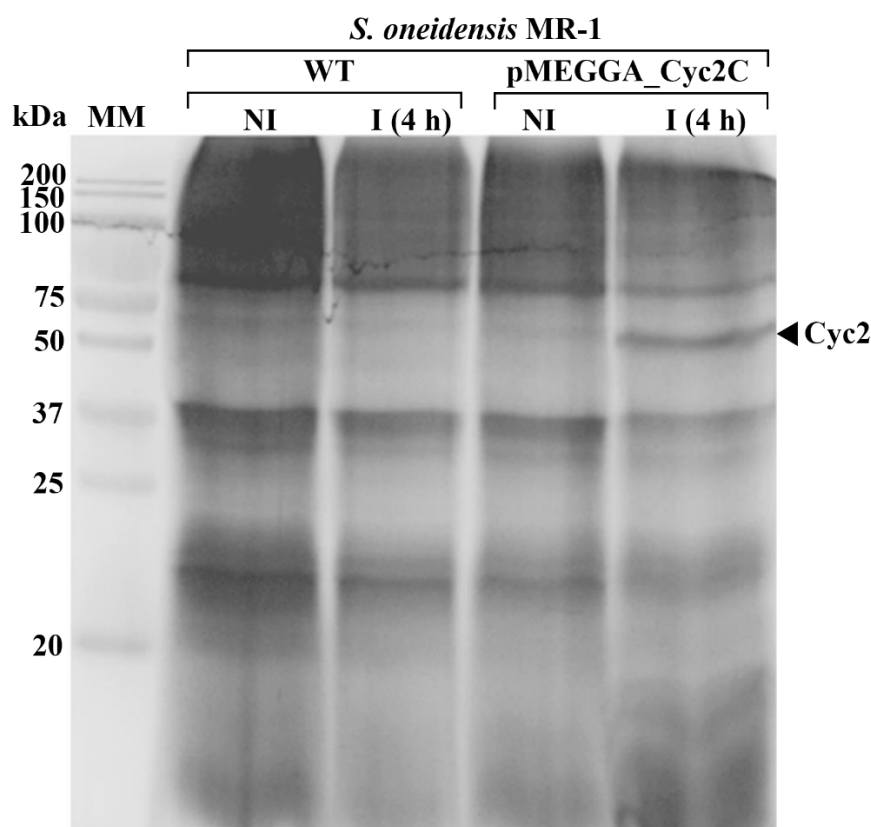
Figure 5-2 Cyc2 expression in S. oneidensis MR-1 pMEGGA_Cyc2C
Heme stain (Chapter 2.16.4) of the total protein content in S. oneidensis MR-1 WT and S. oneidensis MR-1 pMEGGA_Cyc2C not induced (NI) and induced (I) with 5mM of L-arabinose for 4 hours. A band around 50 kDa thought to correspond to Cyc2 is found in the sample were S. oneidensis MR-1 pMEGGA_Cyc2C has been induced but not when it is not induced or if S. oneidensis does not carry the plasmid.

A band corresponding to a heme containing protein was visible at approximately 50 kDa. To confirm that the observed band was due to the induction of pMEGGA_Cyc2C, the results were compared to three negative controls: Firstly *S. oneidensis* MR-1 WT without induction was studied to see if a 50 kDa

144

cytochrome was constitutively expressed in *Shewanella*. Secondly *S. oneidensis* MR-1 WT induced with 5 mM L-arabinose was studied to confirm that no other plasmids with an L-arabinose operon were present and to confirm that the presence of arabinose did not affect the constitutive expression of the native cytochromes. Finally *S. oneidensis* MR-1 pMEGGA_Cyc2C without induction was studied to see if there was any leaky expression of the recombinant cytochrome from the plasmid. No heme band at 50 kDa was found in the negative controls (Figure 5-2).

Cellular fractions were separated to see where Cyc2 was located in the cell when it was expressed by *Shewanella.* The inner membrane was separated from the outer membrane by using sarkosyl (Chapter 2.15).

Bands at 50 kDa on the heme stained gel appeared in both membrane fractions of *S. oneidensis* MR-1 pMEGGA_Cyc2C induced with 5 mM L-arabinose for 4 hours, but no band was found in the soluble fraction (Figure 5-3). Sarkosyl is meant to dissolve just the inner membrane so the results suggest that Cyc2 is located indiscriminately both in the inner and the outer membrane. However, previous authors have found that some parts of the outer membrane can be dissolved by this detergent (Page and Taylor, 1988; Yarzábal *et al.*, 2002). For this reason, Cyc2 in *Shewanella* could be either expressed specifically in the outer membrane as found in *A. ferrooxidans*, or nonspecifically in both membranes.

Interestingly, no 50 kDa band was present in the membrane fraction if the cultures were incubated overnight, possibly suggesting that the protein is being degraded by the cell (Figure 5-3). To confirm that the 50 kDa band corresponded to Cyc2, the band was sent for verification using peptide mass fingerprinting but the concentration of the protein in the gel was insufficient to conclusively confirm the identity.
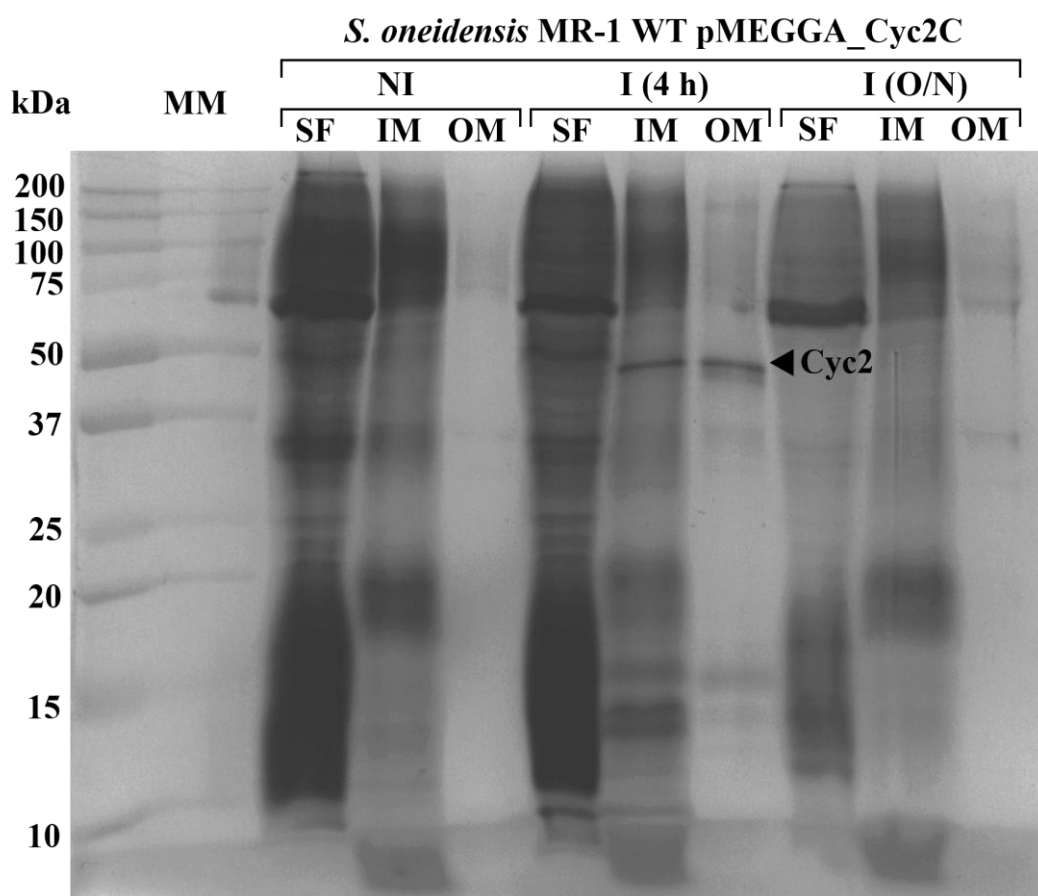
Figure 5-3 Cyc2 location in S. oneidensis MR-1 pMEGGA_Cyc2C
Heme stain (Chapter 2.16.4) of the soluble fraction (SF), the inner membrane fraction (IM) and the outer membrane fraction (OM) of S. oneidensis MR-1 pMEGGA_Cyc2C not induced (NI), induced (I) with 5mM of L-arabinose for 4 hours and induced with 5mM of L-arabinose overnight (O/N). A band around 50 kDa thought to correspond to Cyc2 is found in the membrane fractions where S. oneidensis MR-1 pMEGGA_Cyc2C has been induced for 4 hours but the band was absent after expression overnight.

5.5 Cyc2 purification

To confirm that the 50 kDa protein was indeed Cyc2, *S. oneidensis* MR-1 pMEGGA_Cyc2C cultures were scaled up with the aim of purifying Cyc2 using a Strep-Tactin affinity column. The Strep-tag II attached to the C-terminus of the protein was visualised using western-blotting.

No 50 kDa band appeared when *S. oneidensis* MR-1 pMEGGA_Cyc2C was induced with 5 mM L-arabinose for 4 hours, which suggests that the synthetic peptide had been cleaved from the protein (Figure 5-4). This is also supported by

the observation that when the total protein content was loaded on a Strep-Tactin affinity column (Chapter 2.19), no protein was eluted from the column with the elution buffer.

It is worth noting that all expression conditions, induced or not, contained a band with a lower molecular weight than Cyc2 in their western blot analysis. This band was also present every time that the antibody Anti Strep-tag II was used with *S. oneidensis MR-1* WT, which suggested that a protein of this microorganism interacted non-specifically with the antibody.

Figure 5-4 Strep-tag II detection of Cyc2 expressed in S. oneidensis MR-1 pMEGGA_Cyc2C
Western blot (Chapter 2.18) of the total protein content in S. oneidensis MR-1 pMEGGA_Cyc2C not induced (NI), induced (I) with 5mM of L-arabinose for 4 hours and induced with 5mM of L-arabinose overnight (O/N). In the last lane, a purified MtrC cytochrome from S. oneidensis with a strep-tag II is used as the positive control.

5.5.1. <u>Plasmid recombination</u>

Even though pMEGGA_Cyc2C was sequenced to confirm that no stop codon was located between the end of *cyc2* and *strep-tag II*, it is possible that the synthetic peptide could be cleaved post-expression.

With the continued intention of purifying Cyc2 using the Strep-tag II affinity for the Strep-Tactin column, recombination was used to change the Strep-tag II from the C-terminus to the N-terminus end of the protein to see if the tag remained stable and uncleaved there. Using site-directed mutagenesis (Chapter 2.8.2), a stop codon was added between *cyc2* and *strep-tag II* in pMEGGA_Cyc2C. The original plasmid was digested with DpnI, as plasmids extracted from cells are methylated but not the PCR product (Barnes *et al.*, 2014). The mutated DNA sequence was phosphorylated and ligated (Chapter 2.11) and transformed into *E. coli* TOP10.

A second PCR site-directed mutagenesis was done to add another *strep-tag II* sequence between the signal peptide of *cyc2* and the rest of the gene. Digestion with DpnI, phosphorylation and ligation were repeated and the pMEGGA_Cyc2N was transformed into *E. coli* TOP10. The plasmid was extracted and transformed into *S. oneidensis* MR-1 by electroporation and it was sequenced by Eurofins to confirm the mutation.

The expression of Cyc2 was induced in *S. oneidensis* MR-1 pMEGGA_Cyc2N with 5 mM L-arabinose. A band corresponding to a *c-type* cytochrome appeared when the cells were induced (Figure 5-5). However, the molecular size of the cytochrome expressed when pMEGGA_Cyc2N was induced was slightly lower than the cytochrome expressed using pMEGGA_Cyc2C.
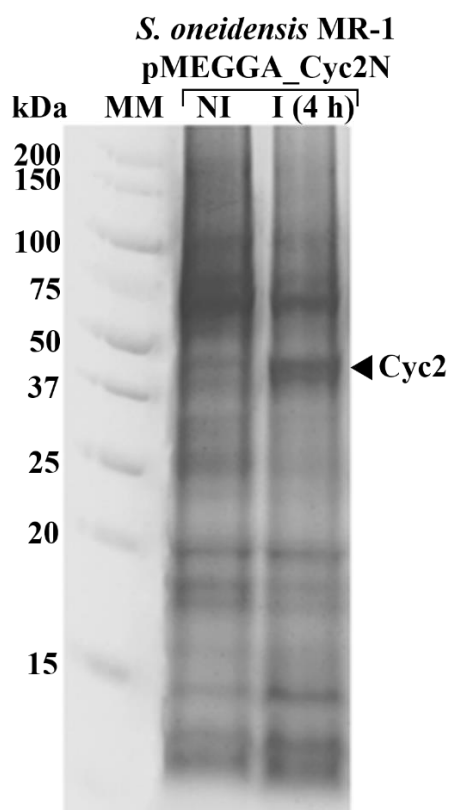
Figure 5-5 Cyc2 expression in S. oneidensis MR-1 pMEGGA_Cyc2N
Heme stain (Chapter 2.16.4) of the total protein content in S. oneidensis MR-1 pMEGGA_Cyc2N not induced (NI) and induced (I) with 5mM of L-arabinose for 4 hours. A band around 50 kDa that could correspond to Cyc2 is found in the sample where cells have been induced but not when they were not induced.

Another western-blot was performed to see if the Strep-tag II was attached at the N-terminus of the cytochrome. Again, in all conditions a protein was expressed with affinity for anti-strep-tag II antibodies (Figure 5-6). Moreover, a very faint band with a higher molecular weight could be seen in the condition where *S oneidensis* MR-1 pMEGGA_Cyc2N was induced with 5 mM L-arabinose for 4 hours (Figure 5-6 A). When the western-blot was repeated separating the soluble fraction from the membrane fraction, the band with the lowest molecular weight could be seen in the soluble fraction while the one with the highest molecular weight was at the membrane fraction, suggesting that it corresponded to Cyc2 with the Strep-tag II (Figure 5-6 A).
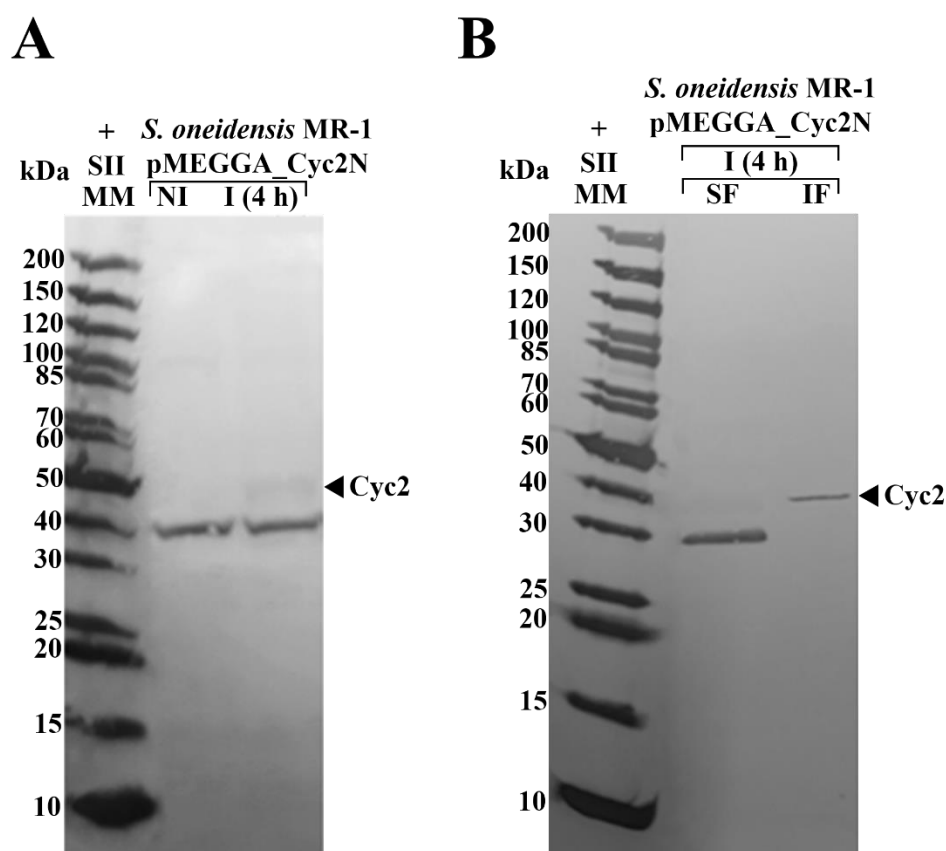
Figure 5-6 Strep tag II detection of Cyc2 expressed in S. oneidensis MR-1 pMEGGA_Cyc2N
A) Western blot (Chapter 2.18) of the total protein content in S. oneidensis MR-1 pMEGGA_Cyc2N not induced (NI) and induced (I) with 5mM of L-arabinose for 4 hours. Both conditions show a band, whose origin is unknown and a very faint band at a higher molecular weight is visible in the induced condition. B) Western blot of the soluble fraction and the membrane fraction of S. oneidensis MR-1 pMEGGA_Cyc2N induced with 5mM of L-arabinose for 4 hours. The lower molecular weight band thought to correspond to non-specific binding is found at the soluble fraction and the higher band (thought to correspond to Cyc2), was found in the membrane fraction. In both images the molecular markers are also strep-tag II positive.

S. oneidensis MR-1 pMEGGA_Cyc2N cultures induced with 5 mM L-arabinose were scaled up to obtain enough protein to purify Cyc2 using a Strep-Tactin affinity column. Different nonionic and zwitterionic detergents at a pH range from 2-8 were tried to solubilise Cyc2 from the membrane fraction (Chapter 2.15). The aim of using only mild detergents was to solubilise the membranes while keeping the tertiary structure of the protein intact (Yang *et al.*, 2014). However, Cyc2 remained insoluble regardless of which mild nonionic or zwitterionic detergents were used and when SDS (strong anionic detergent) was used to solubilise Cyc2 no protein was eluted from the Strep-Tactin affinity column.

5.6　Cyc2 expression in *S. oneidensis* **MR1** Δ***mtrB-***Δ***mtrD***

To test if expressing Cyc2 in *S. oneidensis* would be able to contribute to iron reduction, despite the potential thermodynamic unfavourability (Figure 5-7), the plasmid pMEGGA_Cyc2C was transformed into *S. oneidensis* MR-1 Δ*mtrB-*Δ*mtrD*, a strain with the outer membrane Mtr proteins knocked out. pMEGGA_Cyc2C was sequenced by Eurofins to confirm its sequence. Cyc2 expression was induced by adding 5 mM L-arabinose to the media. After incubating for 4 hours at 16 ˚C, cells were lysed and the total protein fraction was run in a SDS_PAGE and the gel was stained to detect heme-peroxidase activity. A band at 50 kDa appeared on a heme stained gel when *S. oneidensis* Δ*mtrB-*Δ*mtrD* pMEGGA_Cyc2C was induced with 5 mM L-arabinose for 4 hours and no band appeared when cells were not induced (Figure 5-8).
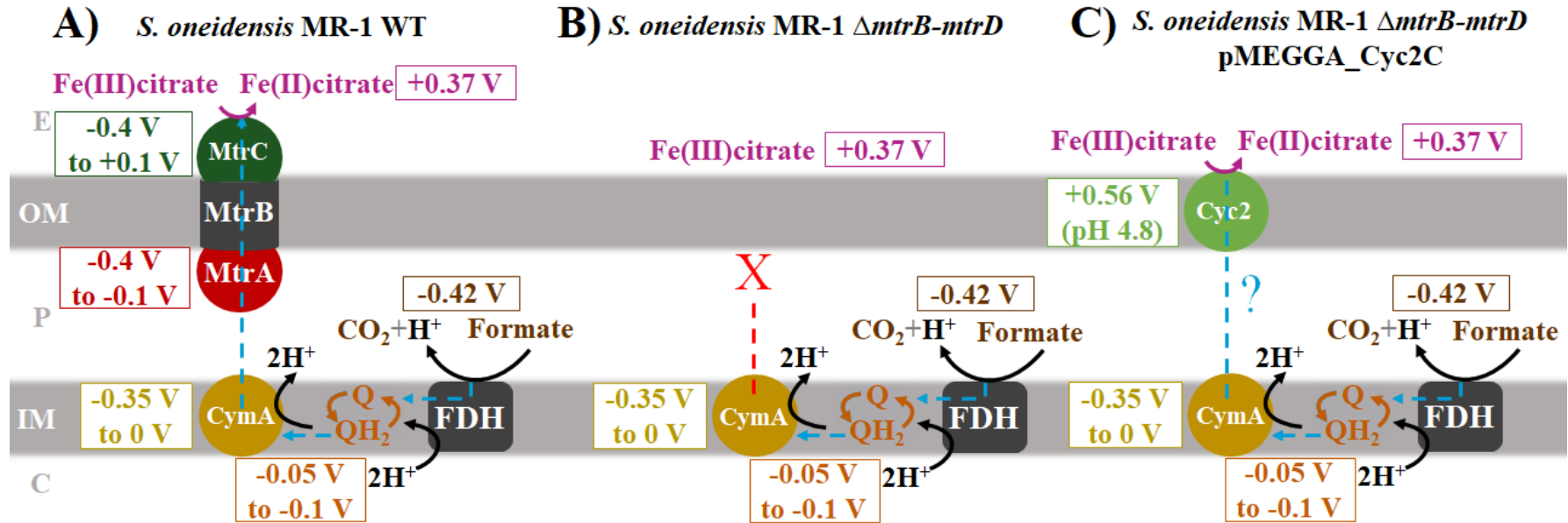
Figure 5-7 Redox potentials in the metal reduction pathway of Shewanella
Redox potentials of the elements involved in the metal reduction pathway in Shewanella using Formate as the electron donor and Fe(III)citrate as the electron acceptor. A) S. oneidensis MR-1. B) S. oneidensis MR-1 ΔmtrB-ΔmtrD. C) S. oneidensis MR-1 ΔmtrB-ΔmtrD pMEGGA_Cyc2C. Electron transfer appears as a dashed arrows. The redox potential of Cyc2 has been determined in A. ferrooxidans by Roger et al., 2012 at pH 4.8 and in Shewanella at pH 7 would be lower but it has not been determined yet. For this reason, it is not known if the electron transfer from Cyc2 to Fe(III)citrate would be thermodynamically favourable.
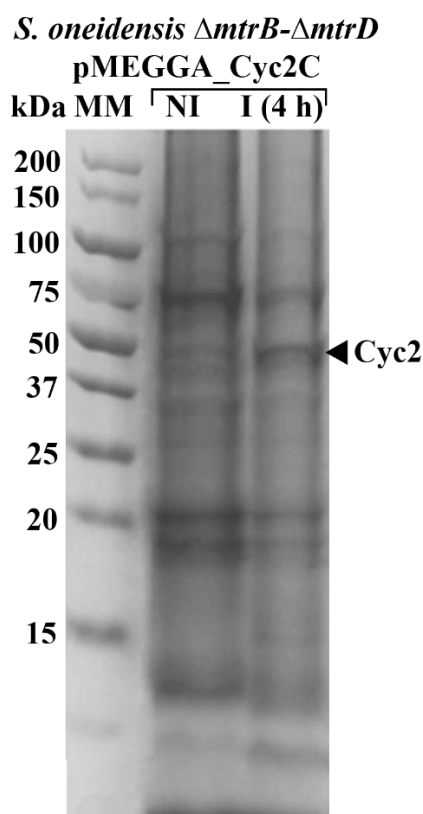
Figure 5-8 Cyc2 expression in S. oneidensis MR-1 ΔmtrB-ΔmtrD pMEGGA_Cyc2C
Heme stain (Chapter 2.16.4) of the total protein content in S. oneidensis MR-1 ΔmtrB-ΔmtrD pMEGGA_Cyc2C not induced (NI) and induced (I) with 5mM of L-arabinose for 4 hours. A band around 50 kDa that could correspond to Cyc2 is found in the sample were cells have been induced but not when they are not induced.

5.7 Activity of Cyc2 in *S. oneidensis* MR-1

Cyc2 does not appear to remain stable for extended amounts of time in *S. oneidensis* MR-1 as previous results suggest it is degraded 16 hours after induction. However, when it is present in the outer membrane, it could still function as an electron transporter for the cell to replace or complement native iron reduction pathway components. To test if the recombinant *c-type* cytochrome could replace part of the metal reduction pathway, the activity was tested by comparing the Fe(III)citrate reduction in minimal media (Chapter 2.2.3) between *S. oneidensis* MR-1 WT (positive control), *S. oneidensis* MR-1 ΔmtrB-ΔmtrD (negative control) and *S. oneidensis* MR-1 ΔmtrB-ΔmtrD pMEGGA_Cyc2C. To have the same growth conditions in all samples, all three cultures were induced with

5 mM L-arabinose for 4 hours at 16 °C in LB. However, not even the positive control *S. oneidensis* MR-1 WT was able to reduce ferric iron (Fe^{3+}) under these conditions.

As the iron reduction measurement was not possible, the electron transfer activity was instead determined by measuring the absorbance spectrum of the cultures under oxidising conditions and under reducing conditions. When cytochromes are reduced, they have an absorption peak at around 550 nm that is absent when the cytochromes are oxidised and can therefore be used to determine the redox state of the proteins using a spectrophotometer (Barton, 2005). This technique can even be used with whole cell cultures if the features in the cytochrome spectra are pronounced enough to be visible over the background absorbance of the cells.

Cells were induced with 5 mM L-arabinose for 4 hours at 16 °C in LB aerobically and then cultures were sparged with N$_2$ and transferred to the glovebox. The spectrum of the cells was measured using LB as the blank (Figure 5-9 A).

To reduce the cytochromes, 1 mM Formate was added to the cultures, acting as the electron donor for the electron transport chain, and the spectrum of each strain was measured again. Theoretically this would lead to the irreversible reduction of all cytochromes on the surface of the cell, which in turn may be observed as a change in absorbance at around 550 nm. Figure 5-9 B shows the increase in absorbance at 541 nm due to the reduction of the hemes.

Finally, 3 mM Fe(III)citrate was added to the cultures, acting as the terminal electron acceptor for the electron transport chain (Figure 5-9 C). If cells were able to transfer the electrons to Fe(III)citrate, the cytochromes would be re-oxidised and the absorbance at 541 nm would be reduced. Just the positive control showed a clear difference between the oxidised and reduced state, suggesting that Cyc2 was not active when it was expressed in *Shewanella* or that the cellular background absorbance prevented this technique from being able to identify the changes in redox state.
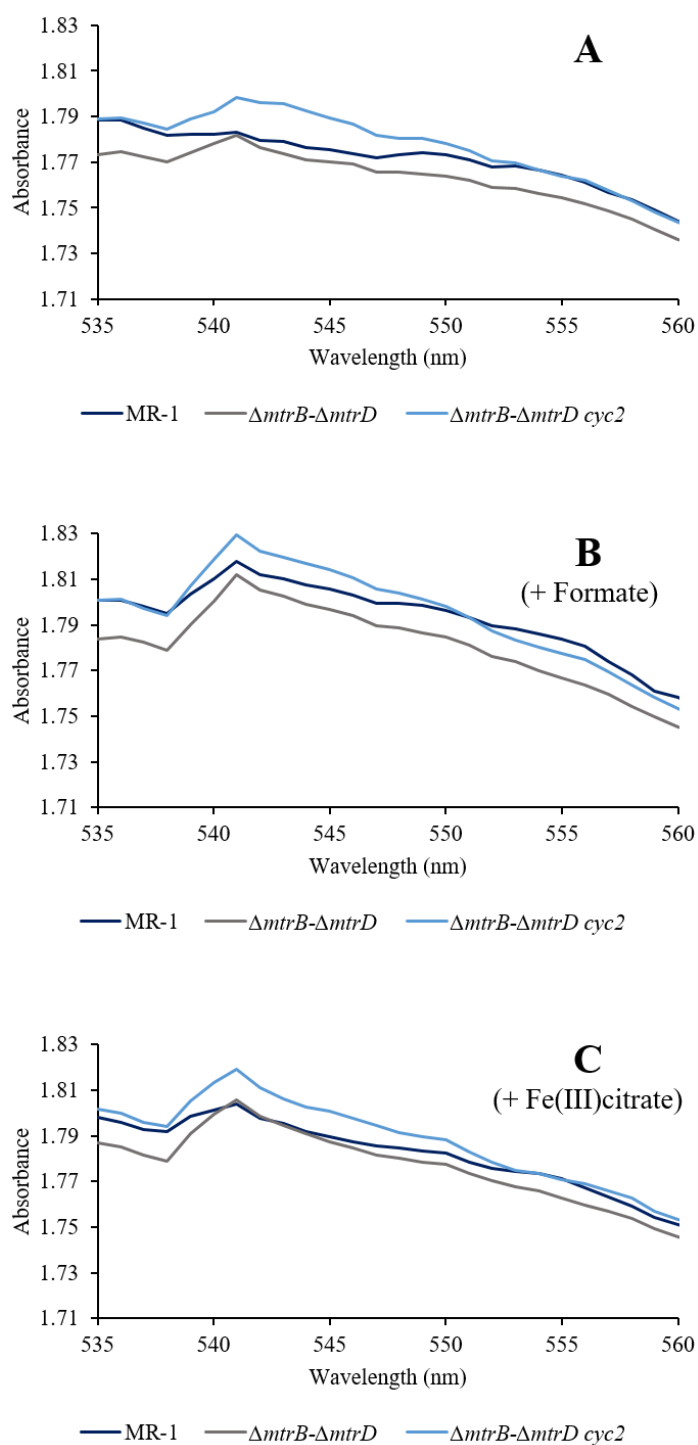
Figure 5-9 Determination of Cyc2 activity by analysing the redox spectrum of S. oneidensis
Absorbance spectrum of S. oneidensis MR-1 WT, S. oneidensis ΔmtrB-ΔmtrD and S. oneidensis ΔmtrB-ΔmtrD pMEGGA_Cyc2C cultures after being induced with 5 mM L-arabinose for 4 hours. A) Spectrum analysis of the three cultures. B) Analysis of the cultures after the addition of 1 mM Formate (electron donor). C) Spectrum analysis of the cultures after the addition of 1 mM Formate (electron donor) followed by 3 mM Fe(III)citrate (electron acceptor). αβ peak associated with hemes are higher when the hemes are reduced. Cell culture concentration was normalised by OD$_{600}$.

5.8   Synthesis of *cyc2PV-1*

Mariprofundus ferrooxydans, is a neutrophilic aerobic iron oxidiser with a predicted metal oxidising pathway homologous to that of *A. ferrooxidans*. Like Cyc2, Cyc2PV-1 is also an outer membrane monoheme *c-type* cytochrome that could also function as a porin (Figure 5-11).

Because *M. ferrooxydans* needs a microoxic environment like *S. lithotrophicus*, the possibility of amplifying *cyc2PV-1* from a *M. ferrooxydans* culture was discarded. Instead the cyc2PV-1 gene was synthetized, having been codon optimised for *Shewanella* with the flanking regions for golden gate cloning added at the ends of the sequence with BsmBI restriction enzyme sites.

MKKMLLSAAAFAVVAVVAVSAVAVAPTTSEAIPAFARQTGAACLSCHFQTFPALN
AFGRAFKMGSFTDVGEQALVEDDNLSLPAVLNATVVIRGNYTNTKTTGVASTGTWNVPS
ETPILIAGRLGSNTGAFIEFANGGAAAGVGGAGAPVSVGNWQIMNSFDMGGFKVGVSAH
NSTFGGSAIMEYSNVFGQHSGKNAGGNLSAIQAAGFANPTLGAGVWAGNEMGNLQFAL
VAPSAAQGTNVGFKLAKLIRGVLTTELGGFDTLVGFGYVTGDAGRPTTVVAPTVPGVGP
VPMSLQFVDLQFQGDVGDMSLGIYADYANAKGKTSTDPAVVGGNFYGAAGLNTAGAKF
DAWSIRADLKPLHNLGVGIGYAYQKQTPGAAAAAGSVAQKITTAQIAAFYEIYQNFEINLI
YNSAKTVNGGLVAGANTTTNTTTIEFEGLL

Figure 5-10 Amino acid sequence of Cyc2PV-1 from M. ferrooxydans
Bioinformatic analysis suggests that this gene expresses a 44.52 kDa monoheme β-barrel protein. A signal peptide with a cleavage site at the C-terminus of its region is highlighted in blue. A heme--binding motif is highlighted in red. The amino acid sequence that could be part of the β-barrel is highlighted in green.

5.9   Molecular cloning of *cyc2PV-1*

pEX-K4_Cyc2PV-1 synthetized by Eurofins was digested with the restriction enzyme BsmBI and the band corresponding to *cyc2PV-1* was purified and used as the insert for the golden gate assembly (Chapter 2.10) in pMEGGA.

The plasmid pMEGGA_Cyc2PV-1C encoded kanamycin resistance, with the expression of *cyc2PV-1* regulated under an L-arabinose operon and a *strep-tag II* upstream *cyc2PV-1*.

The plasmid was transformed into *E. coli* TOP10 to replicate before being transformed into *S. oneidensis* MR-1 by electroporation. The plasmid sequence was then confirmed by Eurofins.

5.10 Cyc2$_{PV-1}$ expression in *S. oneidensis* MR-1 WT

Cyc2$_{PV-1}$ was expressed in *S. oneidensis* MR-1 pMEGGA_Cyc2$_{PV-1}$C by adding 5 mM L-arabinose to the culture. Cells were lysed and the total protein fraction was loaded onto an SDS-PAGE gel. After electrophoresis, the gel was stained for peroxidase associated heme activity. A very intense band at around 40 kDa appeared from the *S. oneidensis* MR-1 pMEGGA_Cyc2$_{PV-1}$C culture and no band was detected in the non-induced culture (Figure 5-11).

The molecular weight of the induced *c-type* cytochrome band corresponds with the theoretical size of Cyc2$_{PV-1}$. When the expression of Cyc2$_{PV-1}$ is compared with the expression of Cyc2, it is noticeable that Cyc2$_{PV-1}$ has a higher heme stain colorimetric signal. The fact that *cyc2$_{PV-1}$* was codon optimised for *Shewanella* could result in higher protein expression which in turn might explain the higher peroxidase activity.
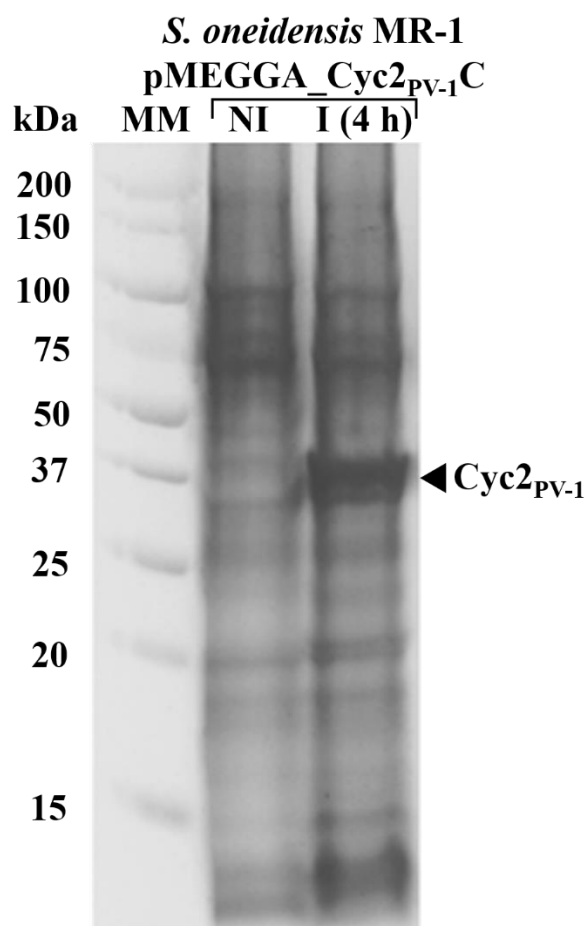
Figure 5-11 Cyc2$_{PV-1}$ expression in S. oneidensis MR-1 pMEGGA_Cyc2$_{PV-1}$C
Heme stain (Chapter 2.16.4) of the total protein content in S. oneidensis MR-1 pMEGGA_Cyc2$_{PV-1}$C not induced (NI) and induced (I) with 5mM of L-arabinose for 4 hours. A band around 40 kDa that could correspond to Cyc2$_{PV-1}$ is found in the sample where cells have been induced but not when they are not induced.

5.11 Cyc2$_{PV-1}$ purification

To confirm that the 40 kDa protein was indeed Cyc2$_{PV-1}$, a western-blot was performed to visualise the Strep-tag II attached to the C-terminus of the protein.

No band appeared when *S. oneidensis* MR-1 pMEGGA_Cyc2$_{PV-1}$C was induced with 5 mM L-arabinose for 4 hours, which suggests that (as previously seen with Cyc2 from *A. ferrooxidans*) the synthetic peptide had been cleaved from the protein. Again, all conditions presented an additional band of an unidentified protein (Figure 5-12).
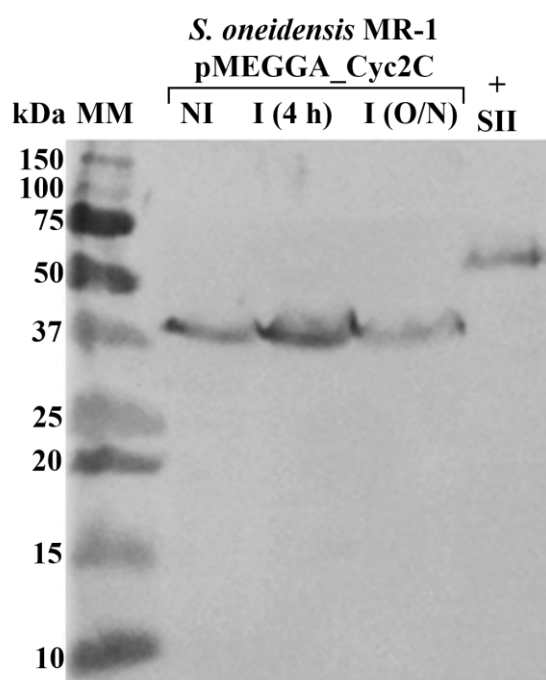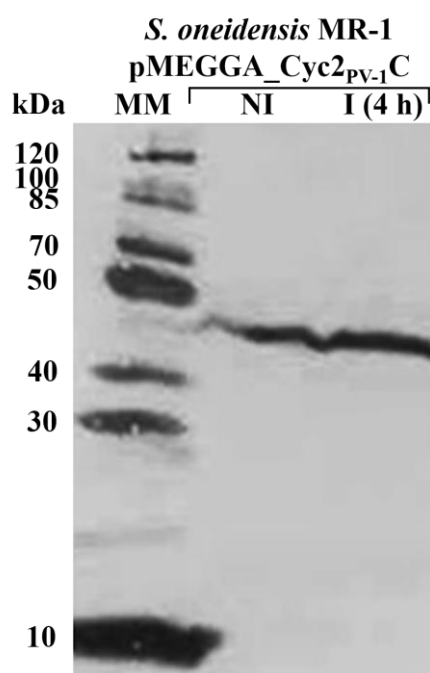
Figure 5-12 Strep-tag II detection of Cyc2$_{PV-1}$ expressed in S. oneidensis MR-1 pMEGGA_Cyc2$_{PV-1}$C

Western blot (Chapter 2.18) of the total protein content in S. oneidensis MR-1 pMEGGA_Cyc2$_{PV-1}$C not induced (NI), induced (I) with 5mM of L-arabinose for 4 hours and induced with 5mM of L-arabinose overnight (O/N). There is a strep-tag II positive protein in all the culture conditions, whose origin is unknown. The molecular markers are also strep-tag II positive

5.12 Cyc2$_{PV-1}$ expression in *S. oneidensis* MR-1 Δ*mtrB*-Δ*mtrD*

Previously redox spectrum assays were used to see if Cyc2 was active in *Shewanella*. Equivalent assays for Cyc2 $_{PV-1}$ could not be attempted because pMEGGA_Cyc2$_{PV-1}$C could not be transformed into *S. oneidensis* MR-1 Δ*mtrB*-Δ*mtrD* despite numerous attempts. Multiple transformation strategies were used including tri-parental conjugation, bi-parental conjugation and transformation by electroporation although none proved successful.

5.13 Discussion

The benefits of studying proteins constitutively expressed by microorganisms rather than using overexpression systems in hosts are that they are being expressed in an environment where they are interacting with other molecules. Consequently, their function can be better evaluated. On the other hand, overexpression systems allow production of higher quantities of proteins, which can be characterised independently to determine their role in the cell. The option of growing iron oxidisers in large quantities was discarded due to their slow metabolism and very specific growth conditions (Emerson and Moyer, 1997; Molchanov *et al.*, 2007). For this reason, it was decided to express the proteins from the metal oxidation pathway in *S. oneidensis* MR-1 as it had been used before by other authors to characterise other cytochromes (Liu *et al.*, 2012; Beckwith *et al.*, 2015).

Golden gate assembly was successfully used to insert *cyc2* from *A. ferrooxidans* and *cyc2$_{PV-1}$* from *M. ferrooxydans* into pMEGGA plasmids. *S. oneidensis* MR-1 was also able to replicate these plasmids and express cytochromes that matched the expected molecular weights of these proteins when the cultures where induced with L-arabinose.

In *Shewanella*, *c-type* cytochrome maturation occurs in the periplasm, where the protein is covalently bound to the heme (Fu *et al.*, 2015). The heme stains performed in this chapter found Cyc2 associated with the membrane fraction of cells. This supports the theory that the protein is, at least temporarily, stable in *Shewanella* even if it was later degraded by the cell. After the cells were lysed, Cyc2 was not found in the debris fraction, but it was found to precipitate when the membranes were solubilised with detergent. This suggests that Cyc2 is not stable in the absence of a lipid environment and, could suggest that the protein needs chaperones or other proteins to be transported stably to the membrane.

When the Strep-tag II of Cyc2 was swapped from the C-terminus to the N-terminus, the plasmid was sequenced to confirm that the open reading frames of the stop codon and the tag encoding sequences were correct after the golden gate

assembly. By swapping the tag, the protein could be detected immunologically by western-blot using anti-strep-tag II antibodies. Nevertheless, when the protein was run on a gel, it migrated different through the gel than when the tag was at the C-terminus, appearing to be around 10 kDa smaller. Size differences were possibly due post-transcriptional modifications. However, those changes did not have any significant impact on the protein structure: it was still located in the cell membrane and was covalently bound to a heme. As future work, it would be interesting to see if the Cyc2$_{PV-1}$ tag is also identifiable if the *strep-tag II* sequence is after the signal peptide of the protein.

Besides the band corresponding to Cyc2, another band appeared in the western-blots with the Strep-tag II antibody. As it is found in the soluble fraction, a possible interaction between the unknown protein and the Strep-Tactin affinity column could be easily avoided by only loading the membrane fraction, Nonetheless, *S. oneidensis* is used as a host for other plasmids by this research group, so it would be convenient to identify the protein to avoid further confusion during Strep-tag II affinity experiments.

When heme stained gels of Cyc2 and Cyc2$_{PV-1}$ were compared, it seemed that *S. oneidensis* could express Cyc2$_{PV-1}$ at higher levels. It would be interesting to see if a codon optimized *cyc2* would increase protein expression and prevent overnight degradation.

The lack of non-denaturing detergents able to solubilise Cyc2 represented a big obstacle to move forward in the characterization of the membrane protein. No more than a 0.1 % SDS can be loaded onto the Strep-Tactin affinity column without damaging it or affecting the structure of the Strep-tag II. It is unclear how the change of SDS concentration affected to Cyc2 when it was already denatured in a 1.5 % SDS buffer, but no protein was eluted from the column. Without a purification method for the expressed cytochromes, it was not possible to confirm that the *c-type* cytochrome seen in the heme stained gels corresponded to the recombinant proteins and no further characterisation could be done at this stage.

With the results obtained, it seems that the best conditions to study these cytochromes in *S. oneidensis* would be with the genes codon optimised and with the Strep-tag II expressed at the N-terminus of the protein. If after trying a wider range of mild nonionic detergents purification of the cytochromes is still not possible, an interactomic study in *A. ferrooxidans* and *M. ferrooxydans* should be considered. This may identify which proteins could be stabilising Cyc2 and Cyc2$_{PV-1}$, and the genes encoding these proteins could be transformed into *S. oneidensis* to ensure expression with all required maturation, assembly and chaperones required for effective expression.

If these proteins can be successfully purified, diverse approaches could be used to characterise them. Firstly, their secondary structure could be confirmed by peptide mass fingerprinting. Secondly, if the tertiary structures were solved by crystallography or nuclear magnetic resonance (NMR), the theory that these proteins work both as cytochromes and porins in the outer membrane could be more definitively confirmed or rejected. Thirdly, if the protein structures were solved, it would be interesting to know how the proteins are arranged within the membrane: is the heme is facing the external environment? Is it facing the periplasm of the cell or is it in the middle of the β-barrel? Finally, the redox potential at neutral pH could be measured to determine if it would be thermodynamically favourable for iron reduction pathways.

When Fe(III)citrate has been added to a culture of *S. oneidensis* MR-1 without the native outer membrane cytochromes used for iron respiration (*S. oneidensis* MR-1 Δ*mtrB*-Δ*mtrD*), no decrease in the peak at 541 nm was detected. If codon optimisation of *cyc2* increased the protein expression it would be interesting to re-visit and improve the method used to test Cyc2 activity. Moreover, the thermodynamic feasibility of this process should be also studied in more detail. The key step in this study would be determining the redox potential of Cyc2 at pH 7. This would allow better predictions as to whether it is theoretically thermodynamically favourable to accept electrons from CymA and transfer them to ferric iron (Fe^{3+}). Alternative experiments could use iron species with a higher

redox potential than Fe(III)citrate (+ 0.37 V), such as potassium ferricyanide (+ 0.46 V), to test more favourable thermodynamics.

The results obtained from the whole cell spectrometry experiments (Figure 5-9) are inconclusive as the resolution of the spectrum is dominated by the background contributions from the cells. To avoid this background noise, the absorbance spectra could be measured with an integrating sphere to avoid losing incident light due to scattering produced by the particles.

Since it was first discovered, *S. oneidensis* MR-1 has become the model organism to study extracellular electron pathway. Bioinformatic analysis have focused the identification of new iron metabolising microorganisms on finding decahemes *c-type* cytochromes homologous to MtrC or MtrA, and porins homologous to MtrB. Proving the viability of iron reduction using a monoheme porin would give another approach to identify novel iron reduction bacteria in the environment.

5.14 References

Abboud, R., Popa, R., Souza-Egipsy, V., Giometti, C.S., Tollaksen, S., Mosher, J.J., et al. (2005) Low-temperature growth of *Shewanella oneidensis* MR-1. *Appl. Environ. Microbiol.* 71: 811–6.

Barnes, H.E., Liu, G., Weston, C.Q., King, P., Pham, L.K., Waltz, S., et al. (2014) Selective microbial genomic DNA isolation using restriction endonucleases. *PLoS One* 9: e109061.

Barton, L. (2005) Structural and functional relationships in prokaryotes Springer.

Beckwith, C.R., Edwards, M.J., Lawes, M., Shi, L., Butt, J.N., Richardson, D.J., and Clarke, T.A. (2015) Characterization of MtoD from *Sideroxydans lithotrophicus*: a cytochrome *c* electron shuttle used in lithoautotrophic growth. *Front. Microbiol.* 6: 332.

Bose, A. and Newman, D.K. (2011) Regulation of the phototrophic iron oxidation (pio) genes in *Rhodopseudomonas palustris* TIE-1 is mediated by the global regulator, FixK. *Mol. Microbiol.* 79: 63–75.

Chakraborty, A., Roden, E.E., Schieber, J., and Picardal, F. (2011) Enhanced Growth of *Acidovorax* sp. Strain 2AN during Nitrate-Dependent Fe(II) Oxidation in Batch and Continuous-Flow Systems. *Appl. Environ. Microbiol.* 77: 8548–8556.

Emerson, D. and Moyer, C. (1997) Isolation and characterization of novel iron-oxidizing bacteria that grow at circumneutral pH. *Appl. Environ. Microbiol.* 63: 4784–92.

Fu, H., Jin, M., Wan, F., and Gao, H. (2015) *Shewanella oneidensis* cytochrome *c* maturation component CcmI is essential for heme attachment at the non-canonical motif of nitrite reductase NrfA. *Mol. Microbiol.* 95: 410–425.

Liu, J., Wang, Z., Belchik, S.M., Edwards, M.J., Liu, C., Kennedy, D.W., et al. (2012) Identification and Characterization of MtoA: A Decaheme *c-type* Cytochrome of the Neutrophilic Fe(II)-Oxidizing Bacterium *Sideroxydans lithotrophicus* ES-1. *Front. Microbiol.* 3: 37.

Molchanov, S., Gendel, Y., Ioslvich, I., and Lahav, O. (2007) Improved Experimental and Computational Methodology for Determining the Kinetic Equation and the Extant Kinetic Constants of Fe(II) Oxidation by *Acidithiobacillus ferrooxidans*. *Appl. Environ. Microbiol.* 73: 1742.

Page, W.J. and Taylor, D.E. (1988) Comparison of methods used to separate the inner and outer membranes of cell envelopes of *Campylobacter* spp. *J. Gen. Microbiol.* 134: 2925–2932.

Pechter, K.B., Gallagher, L., Pyles, H., Manoil, C.S., and Harwood, C.S. (2015) Essential Genome of the Metabolically Versatile Alphaproteobacterium *Rhodopseudomonas palustris*. *J. Bacteriol.* 198: 867–76.

Pitts, K.E., Dobbin, P.S., Reyes-Ramirez, F., Thomson, A.J., Richardson, D.J., and Seward, H.E. (2003) Characterization of the *Shewanella oneidensis* MR-1 Decaheme Cytochrome MtrA. *J. Biol. Chem.* 278: 27758–27765.

Roger, M., Castelle, C., Guiral, M., Infossi, P., Lojou, E., Giudici-Orticoni, M.-T., and Ilbert, M. (2012) Mineral respiration under extreme acidic conditions: from a supramolecular organization to a molecular adaptation in *Acidithiobacillus ferrooxidans*. *Biochem. Soc. Trans.* 40: 1324–1329.

Shi, L., Rosso, K.M., Zachara, J.M., and Fredrickson, J.K. (2012) Mtr extracellular electron-transfer pathways in Fe(III)-reducing or Fe(II)-oxidizing bacteria: a genomic perspective. *Biochem. Soc. Trans.* 40: 1261–7.

Yang, Z., Wang, C., Zhou, Q., An, J., Hildebrandt, E., Aleksandrov, L.A., et al. (2014) Membrane protein stability can be compromised by detergent interactions with the extramembranous soluble domains. *Protein Sci.* 23: 769–89.

Yano, T., Fukumori, Y., and Yamanaka, T. (1991) The amino acid sequence of rusticyanin isolated from *Thiobacillus ferrooxidans*. *FEBS Lett.* 288: 159–162.

Yarzábal, A., Brasseur, G., Ratouchniak, J., Lund, K., Lemesle-Meunier, D., DeMoss, J.A., and Bonnefoy, V. (2002) The high-molecular-weight cytochrome *c* Cyc2 of *Acidithiobacillus ferrooxidans* is an outer membrane protein. *J. Bacteriol.* 184: 313–7.

Final discussion

Although iron is very abundant in nature, microorganisms can only use it as a nutrient when it is found in its soluble form. Oxygen concentration and pH are two abiotic factors that affect the solubility of this metal, hence, iron bioavailability will vary depending on the environment where it is found.

The presence of microorganisms able to metabolise iron in a dissimilatory manner represents an ecological advantage, as other organisms from the same ecosystem can benefit from the solubilisation of iron in their environment.

This thesis has focused on the study of both iron-reducing and iron-oxidising bacteria that, although having very different metabolisms, have an important role in iron recycling. A better understanding of these microorganisms is of considerable interest from a biochemical, ecological and bioremediation perspective.

6.1 Isolation of novel iron-reducing bacteria in the environment

Acinetobacter and *Citrobacter* have been identified as novel iron-reducing species. The isolation of iron reducers from soil, sediment and fresh water samples supports the idea of iron reducers inhabiting not only where iron can be found in excess, but also where iron is a limiting nutrient too.

6.1.2. *Acinetobacter*

Acinetobacter has proved to be able to use iron as the terminal electron acceptor for cellular respiration. However, it is proposed in this thesis that unlike previously described iron reducers, this bacterium does not use extracellular electron transfer mechanisms for this process (White *et al.*, 2016) but transports iron inside the cell. The results of the bioinformatic analysis suggest that *Acinetobacter*, in the absence of oxygen, regulates its metabolism to adapt to a less thermodynamically favourable catabolism using iron as the terminal electron acceptor.

This result represents a new discovery about the *Acinetobacter* genus, which was previously thought to be strictly aerobic (Chan *et al.*, 2012). It also has important implications for studying potential reservoirs that this opportunistic pathogen in environments other than its host or other aerobic environments (Peleg *et al.*, 2012; Pindi *et al.*, 2013; Al Atrouni *et al.*, 2016). The presence of *Acinetobacter* in anaerobic environments could also have an impact of past and future epidemiological studies of *Acinetobacter* infections (Garnacho-Montero and Timsit, 2018).

Moreover, the results obtained in this thesis suggest a broader importance for iron in *Acinetobacter* genetic regulation, which previously had only been studied as a limiting nutrient, but not as a metabolic regulator (Mortensen and Skaar, 2013). A metabolomic analysis could be useful to better understand *Acinetobacter* catabolism under iron respiration. This would give a better appreciation of how iron is being reduced, how the cell is protecting against iron toxicity and oxidative stress, and if iron respiration has a role in pathogenesis.

6.1.3. *Citrobacter*

Citrobacter has previously been described as a facultative aerobic, that is able to couple fermentation to growth (Peter *et al*., 2014). The results in this thesis suggest that it is also able to reduce iron. Like *Acinetobacter, Citrobacter* does not seem to be using extracellular electron transfer mechanisms for iron reduction. However, it remains unclear if it is coupling iron reduction to cellular respiration directly or if it is using fermentation and iron is reduced indirectly. A transcriptomic analysis of this microorganisms could be beneficial to have a better understanding of which genes are being regulated when this bacterium is growing anaerobically with iron as the sole terminal electron acceptor source.

Additionally, it would be interesting to study the importance of iron reduction in microbiota pathogenesis. Iron availability is essential during pathogenic processes (Cherayil *et al.*, 2011) and the presence of *Citrobacter* in the guts of the host could represent an advantage for opportunistic pathogens.

Although both *Acinetobacter* and *Citrobacter* have been proven to be able to reduce soluble iron, they could not reduce it when it was insoluble. These results confirm that these bacteria can survive in anoxic environments but questions if their presence in the environment would be beneficial for other microorganisms as they are not likely to increase the concentrations of bioavailable iron (Emerson *et al.*, 2012). A metagenomic analysis would give further information about the species that are coexisting with *Acinetobacter* and *Citrobacter* in the environment and future experiments with mixed cultures could be done to determine if the presence of these iron reducers which are unable to reduce iron via extracellular electron transfer still have an impact on other species.

6.2 Characterization of proteins involved in the EET metal oxidation pathway

Many iron-oxidising microorganisms have been predicted to have homologous pathways to the one that *Shewanella oneidensis* uses for extracellular electron transfer (EET) iron reduction. However, the study of iron oxidisers is often hindered by difficulties with growing them in the laboratory (Emerson and Moyer, 1997; Molchanov *et al.*, 2007; Bose and Newman, 2011; Chakraborty *et al.*, 2011; Shi, Rosso, Zachara, *et al.*, 2012; Pechter *et al.*, 2015).

In this thesis, a protein overexpression system has been developed to express iron oxidation proteins in *Shewanella*, to overcome the issue of not having enough biomass of iron-oxidising microorganism for protein characterization experiments.

The outer membrane *c*-type cytochromes Cyc2 from *Acidithiobacillus ferrooxidans* and $Cyc2_{PV-1}$ from *Mariprofundus ferrooxydans* have been studied due to their unusually structure and possible function. These proteins seems to function both as cytochromes and as porins, and have been suggested to have a key role in EET.

Via Golden Gate Assembly, these genes of interest were inserted into a cloning vector, using chromophores for a more efficient screening of the transformed colonies.

Shewanella has been able to express the proteins and their heme have been properly incorporated before being transported to the membrane. The codon optimization of the genes for *Shewanella* seems to prevent the cell from degrading the proteins.

The proteins were not successfully purified as they precipitated after cellular lysis and no detergents trialled in this thesis were able to solubilise them. For the future it would be interesting to see if the stability of Cyc2 would improve if expressed together with the periplasmic protein RusA, a periplasmic protein which is part of the same operon of *A. ferrooxidans* as Cyc2 (Yarzabal *et al.*, 2004).

Although there is still a lot of optimization required to use this vector system to study membrane cytochromes, the proposed method could be very suitable for studying periplasmic proteins that make up part of EET pathways, including Cyc1, Cyc2 and RusA from *A. ferrooxidans*, Cyc1$_{PV-1}$ from *M. ferrooxydans*, PioA and PioC from *Rhodopseudomonas palustris* or MtoA from *Dechloromonas aromatica* (White *et al.*, 2016).

6.3   References

Al Atrouni, A., Joly-Guillou, M.-L., Hamze, M., and Kempf, M. (2016) Reservoirs of Non-*baumannii Acinetobacter* Species. *Front. Microbiol.* 7: 49.

Bose, A. and Newman, D.K. (2011) Regulation of the phototrophic iron oxidation (pio) genes in *Rhodopseudomonas palustris* TIE-1 is mediated by the global regulator, FixK. *Mol. Microbiol.* 79: 63–75.

Chakraborty, A., Roden, E.E., Schieber, J., and Picardal, F. (2011) Enhanced Growth of *Acidovorax* sp. Strain 2AN during Nitrate-Dependent Fe(II) Oxidation in Batch and Continuous-Flow Systems. *Appl. Environ. Microbiol.* 77: 8548–8556.

Chan, J.Z.-M., Halachev, M.R., Loman, N.J., Constantinidou, C., and Pallen, M.J. (2012) Defining bacterial species in the genomic era: insights from the genus *Acinetobacter*. *BMC Microbiol.* 12: 302.

Cherayil, B.J., Ellenbogen, S., and Shanmugam, N.N. (2011) Iron and intestinal immunity. *Curr. Opin. Gastroenterol.* 27: 523–8.

Emerson, D. and Moyer, C. (1997) Isolation and characterization of novel iron-oxidizing bacteria that grow at circumneutral pH. *Appl. Environ. Microbiol.* 63: 4784–92.

Emerson, D., Roden, E., and Twining, B.S. (2012) The microbial ferrous wheel: iron cycling in terrestrial, freshwater, and marine environments. *Front. Microbiol.* 3: 383.

Garnacho-Montero, J. and Timsit, J.-F. (2018) Managing *Acinetobacter baumannii* infections. *Curr. Opin. Infect. Dis.* 1.

Molchanov, S., Gendel, Y., Ioslvich, I., and Lahav, O. (2007) Improved Experimental and Computational Methodology for Determining the Kinetic Equation and the Extant Kinetic Constants of Fe(II) Oxidation by *Acidithiobacillus ferrooxidans*. *Appl. Environ. Microbiol.* 73: 1742.

Mortensen, B.L. and Skaar, E.P. (2013) The contribution of nutrient metal acquisition and metabolism to *Acinetobacter baumannii* survival within the host. *Front. Cell. Infect. Microbiol.* 3: 1–10.

Pechter, K.B., Gallagher, L., Pyles, H., Manoil, C.S., and Harwood, C.S. (2015) Essential Genome of the Metabolically Versatile Alphaproteobacterium *Rhodopseudomonas palustris*. *J. Bacteriol.* 198: 867–76.

Peleg, A.Y., de Breij, A., Adams, M.D., Cerqueira, G.M., Mocali, S., Galardini, M., et al. (2012) The success of *Acinetobacter* species; genetic, metabolic and virulence attributes. *PLoS One* 7: e46984.

Peter, S., Wolz, C., Kaase, M., Marschal, M., Schulte, B., Vogel, W., et al. (2014) Emergence of *Citrobacter freundii* carrying IMP-8 metallo-β-lactamase in Germany. *New microbes new Infect.* 2: 42–5.

Pindi, P.K., Yadav, P.R., and Shanker, A.S. (2013) Identification of opportunistic pathogenic bacteria in drinking water samples of different rural health centers and their clinical impacts on humans. *Biomed Res. Int.* 2013: 348250.

Shi, L., Rosso, K.M., Zachara, J.M., and Fredrickson, J.K. (2012) Mtr extracellular electron-transfer pathways in Fe(III)-reducing or Fe(II)-oxidizing bacteria: a genomic perspective. *Biochem. Soc. Trans.* 40: 1261–7.

White, G.F., Edwards, M.J., Gomez-Perez, L., Richardson, D.J., Butt, J.N., and Clarke, T.A. (2016) Mechanisms of Bacterial Extracellular Electron Exchange. In, *Advances in Microbial Physiology*., pp. 87–138.

Yarzabal, A., Appia-Ayme, C., Ratouchniak, J., and Bonnefoy, V. (2004) Regulation of the expression of the *Acidithiobacillus ferrooxidans* rus operon encoding two cytochromes *c*, a cytochrome oxidase and rusticyanin. *Microbiology* 150: 2113–2123.

Appendix

Table A-1 CXXCH motifs for Acinetobacter and Citrobacter genus

List of genes containing sequences for the amino acid motif CXXCH characteristic from heme binding proteins. The sequences used for this analysis do not belong to the environmental Acinetobacter and Citrobacter isolates, but to other species from their corresponding genus available in the MAST database. Highlighted in blue are the genes corresponding to cytochromes c-type, which have been discussed in Chapter 4 of this thesis.

A	*Acinetobacter baumannii* CXXCH motifs						
gene NCBI	**Motif**	**gene NCBI**	**Motif**	**gene NCBI**	**Motif**	**gene NCBI**	**Motif**
CAO99565.1	CTECH	CAP00675.1	CKHCH	CAP01661.1	CVRCH	CAP02882.1	CGLCH
CAO99953.1	CPECH	CAP01185.1	CTTCH	CAP02390.1	CPRCH	CAP02891.1	CHACH
CAP00380.1	CVPCH	CAP01250.1	CSVCH	CAP02562.1	CPYCH		CKTCH
CAP00487.1	CSACH	CAP01313.1	CPNCH	CAP02671.1	CDACH	CAP02970.1	CRDCH

B	*Citrobacter rodentium* CXXCH motifs						
gene NCBI	**Motif**	**gene NCBI**	**Motif**	**gene NCBI**	**Motif**	**gene NCBI**	**Motif**
CBG86790.1	CDVCH	CBG88628.1	CLGCH	CBG90048.1	CGICH	CBG90904.1	CPFCH
	CPTCH		CPRCH	CBG90107.1	CIGCH	CBG90990.1	CDYCH
	CNKCH	CBG88727.1	CAHCH	CBG90172.1	CADCH		CAHCH
CBG87164.1	CGVCH	CBG89080.1	CISCH		CGQCH		CATCH
CBG87437.1	CEKCH		CPDCH		CIDCH	CBG91234.1	CPECH
CBG87738.1	CRYCH		CRNCH		CANCH	CBG91265.1	CPTCH
	CDGCH		CIDCH	CBG90173.1	CLDCH	CBG91449.1	CVSCH
CBG87750.1	CLYCH	CBG89081.1	CLQCH		CTNCH		CADCH
	CIACH		CLQCH		CMSCH		CRSCH
CBG87832.1	CGTCH	CBG89161.1	CLGCH		CASCH		CIDCH
	CSACH	CBG89213.1	CTTCH		CVDCH		CTGCH
CBG88040.1	CLYCH	CBG89357.1	CRECH	CBG90208.1	CTRCH	CBG91586.1	CKNCH
CBG88143.1	CTGCH	CBG89816.1	CIGCH	CBG90252.1	CPHCH	CBG91596.1	CSSCH
CBG88272.1	CEQCH	CBG89830.1	CDLCH	CBG90337.1	CRTCH	CBG91621.1	CGYCH
CBG88334.1	CIGCH	CBG89862.1	CVQCH	CBG90514.1	CGKCH	CBG91659.1	CRQCH
CBG88536.1	CIGCH	CBG89885.1	CCSCH	CBG90885.1	CYICH		CTHCH
CBG88615.1	CPLCH						

Table A-2 Differentially expressed genes in Acinetobacter cultures with Fe(III)citrate

Comparison of the gene expression between Acinetobacter cultures growing in minimal media aerobically (control) and in minimal media aerobically with 0.5 mM Fe(III)citrate (sample). This table shows all the genes differentially expressed with a significant q value (≤0.05). The gene NCBI column shows the gene tag from the reference genome (A. johnsonii XBB1) stored in the National Center for Biotechnology Information. The locus column shows the position of the gene in the genome. The values for the log2 fold change (FC) show if the genes of the sample culture are being upregulated (≥0) or downregulated (≤0). Rows highlighted in blue correspond to the genes that have been mentioned in Chapter 4 of this thesis.

gene NCBI	locus	log2(OF/O)	gene NCBI	locus	log2(OF/O)
RZ95_RS00025	6517-6886	0.81	RZ95_RS00895	197684-198764	-0.67
RZ95_RS00040	10963-11974	1.00	RZ95_RS01075	234450-235749	0.53
RZ95_RS00045	12191-13205	1.44	RZ95_RS01085	236642-237635	0.61
RZ95_RS00075	17038-18979	-0.78	RZ95_RS01200	256409-257018	0.58
RZ95_RS00080	19098-19647	-0.92	RZ95_RS01210	258440-258686	0.71
RZ95_RS00085	20569-20797	1.52	RZ95_RS01215	258767-259454	1.04
RZ95_RS00095	21681-22755	0.46	RZ95_RS01225	260697-261336	0.52
RZ95_RS00100	22802-23471	0.58	RZ95_RS01270	268730-269630	0.58
RZ95_RS00145	31904-33263	3.78	RZ95_RS01355	283628-283952	-0.47
RZ95_RS00150	33404-33968	0.84	RZ95_RS01360	284084-284972	0.44
RZ95_RS00155	34931-36410	1.12	RZ95_RS01405	293775-294774	-0.96
RZ95_RS00220	53326-56011	-0.37	RZ95_RS01510	320582-322004	-0.55
RZ95_RS00260	64344-64992	0.83	RZ95_RS01600	336737-337670	0.63
RZ95_RS00270	65541-66993	-0.74	RZ95_RS01610	338418-338967	-0.40
RZ95_RS00340	77221-77998	0.90	RZ95_RS01615	338993-339734	-0.47
RZ95_RS00345	78006-79406	1.10	RZ95_RS01620	339874-340249	-0.53
RZ95_RS00350	78006-79406	0.91	RZ95_RS01625	340307-341072	1.68
RZ95_RS00355	79491-80277	0.86	RZ95_RS01640	341502-342167	2.21
RZ95_RS00470	103401-104559	-0.41	RZ95_RS01645	342291-343294	1.96
RZ95_RS00485	106603-107138	0.50	RZ95_RS01650	343360-344392	1.36
RZ95_RS00545	120557-121559	0.74	RZ95_RS01680	348977-350210	-0.63
RZ95_RS00555	121654-122404	-1.22	RZ95_RS01690	352126-352498	0.44
RZ95_RS00560	123094-123469	-0.37	RZ95_RS01695	352559-352826	-1.88
RZ95_RS00595	129537-130449	0.55	RZ95_RS01720	357638-358190	0.78
RZ95_RS00600	130604-131042	0.94	RZ95_RS01745	361718-362279	0.60
RZ95_RS00605	131091-131442	1.05	RZ95_RS01825	378874-380248	-0.50
RZ95_RS00675	145769-146966	0.36	RZ95_RS01955	407052-408261	0.67
RZ95_RS00685	148089-148530	0.42	RZ95_RS01980	412746-413385	-0.45
RZ95_RS00690	148638-149322	0.58	RZ95_RS01985	413396-414316	-0.51
RZ95_RS00710	155393-156191	-0.60	RZ95_RS01995	414327-415152	-0.55
RZ95_RS00720	156873-158340	-0.49	RZ95_RS02000	415171-415447	-0.68
RZ95_RS00745	163256-164033	0.39	RZ95_RS02005	415456-415786	-0.62
RZ95_RS00765	167247-168528	-0.40	RZ95_RS02010	415787-416540	-0.57
RZ95_RS00780	170845-172789	1.32	RZ95_RS02015	416543-417408	-0.53
RZ95_RS00800	174952-176059	-0.72	RZ95_RS02030	417500-417869	-0.36
RZ95_RS00805	176086-176815	-0.84	RZ95_RS02035	417878-418196	-0.37
RZ95_RS00815	177901-178669	0.95	RZ95_RS02040	418211-418748	-0.40
RZ95_RS00830	182755-184803	0.66	RZ95_RS02045	418757-419063	-0.36
RZ95_RS00860	188734-189619	-0.99	RZ95_RS02050	419075-419471	-0.37

gene NCBI	locus	log2(OF/O)	gene NCBI	locus	log2(OF/O)
RZ95_RS02055	419484-420018	-0.35	RZ95_RS03415	684907-685573	1.60
RZ95_RS02095	423494-423881	-0.39	RZ95_RS03425	686957-687344	0.54
RZ95_RS02100	423893-424520	-0.40	RZ95_RS03430	687513-687960	0.99
RZ95_RS02105	424536-425544	-0.44	RZ95_RS03435	688019-688370	0.97
RZ95_RS02110	425562-425928	-0.45	RZ95_RS03450	689626-689962	0.82
RZ95_RS02140	431112-432150	0.86	RZ95_RS03460	690617-691022	0.48
RZ95_RS02145	432221-432794	0.60	RZ95_RS03465	691060-693027	0.47
RZ95_RS02150	432976-435259	1.40	RZ95_RS03495	698089-699411	0.76
RZ95_RS02165	436367-438395	-0.50	RZ95_RS03625	728846-730655	0.63
RZ95_RS02180	442103-442193	1.22	RZ95_RS03630	730679-732695	0.44
RZ95_RS02290	460243-461230	-0.41	RZ95_RS03705	744745-745219	1.64
RZ95_RS02295	461403-461664	0.82	RZ95_RS03710	745286-745991	0.70
RZ95_RS02300	461769-462027	0.53	RZ95_RS03755	764345-765062	0.48
RZ95_RS02305	462112-462640	-0.62	RZ95_RS03760	765098-766763	0.50
RZ95_RS02445	486703-487093	0.79	RZ95_RS03780	768986-770774	-0.35
RZ95_RS02450	487153-487603	-0.52	RZ95_RS03895	795305-796112	0.44
RZ95_RS02510	497187-499178	-0.40	RZ95_RS03900	796206-797242	0.66
RZ95_RS02575	514939-516220	0.48	RZ95_RS03945	805474-806719	0.40
RZ95_RS02590	517365-517797	-1.13	RZ95_RS03950	806740-807355	0.46
RZ95_RS02740	543981-545208	-0.48	RZ95_RS03970	811365-811620	-0.41
RZ95_RS02840	569026-569479	0.44	RZ95_RS04025	821851-823036	0.61
RZ95_RS02860	574273-574891	-0.36	RZ95_RS04030	823037-823571	0.52
RZ95_RS02930	590615-591608	1.05	RZ95_RS04080	830808-831108	1.24
RZ95_RS02935	591672-592548	0.57	RZ95_RS04085	831322-832255	-0.60
RZ95_RS03070	617637-618084	0.56	RZ95_RS04095	833002-833617	0.40
RZ95_RS03075	618102-618651	0.43	RZ95_RS04100	833681-834341	-0.38
RZ95_RS03080	618660-619625	0.58	RZ95_RS04105	834874-837258	0.54
RZ95_RS03085	619707-620067	1.53	RZ95_RS04115	837322-837703	-0.45
RZ95_RS03125	625450-625837	-0.43	RZ95_RS04125	838446-838743	-0.50
RZ95_RS03130	625849-626278	-0.43	RZ95_RS04130	838844-839798	-0.49
RZ95_RS03135	626770-627739	-0.37	RZ95_RS04240	858018-858864	0.69
RZ95_RS03235	646932-648051	0.57	RZ95_RS04365	888248-891482	-0.60
RZ95_RS03240	648170-649445	0.95	RZ95_RS04370	891496-892639	-0.51
RZ95_RS03245	649629-652032	0.95	RZ95_RS04375	892947-893394	-0.39
RZ95_RS03260	654637-654991	0.68	RZ95_RS04425	901310-902039	-0.45
RZ95_RS03265	655005-655458	0.88	RZ95_RS04440	903178-904519	1.11
RZ95_RS03270	655641-656817	0.38	RZ95_RS04455	907850-909455	-1.56
RZ95_RS03275	656917-657442	0.86	RZ95_RS04460	909590-909965	-1.33
RZ95_RS03285	659489-660953	-0.43	RZ95_RS04485	916875-917241	0.55
RZ95_RS03300	663597-665436	-0.43	RZ95_RS04505	920861-921245	0.37
RZ95_RS03305	665637-666072	0.84	RZ95_RS04510	921320-922433	0.71
RZ95_RS03320	666582-667718	-0.55	RZ95_RS04570	931346-932588	0.37
RZ95_RS03325	668071-669352	-0.65	RZ95_RS04585	934841-935312	1.28
RZ95_RS03340	671649-672459	0.87	RZ95_RS04590	935381-937268	0.55
RZ95_RS03390	681353-681560	0.68	RZ95_RS04595	937464-938841	-0.61
RZ95_RS03400	682249-682906	0.56	RZ95_RS04650	947871-949212	1.19
RZ95_RS03410	683874-684270	0.60	RZ95_RS04690	951833-952454	-0.56

gene NCBI	locus	log2(OF/O)	gene NCBI	locus	log2(OF/O)
RZ95_RS04715	958016-959378	1.00	RZ95_RS05540	1135120-1135732	0.35
RZ95_RS04720	959709-961113	0.42	RZ95_RS05555	1136837-1137563	0.41
RZ95_RS04775	969624-970233	0.80	RZ95_RS05615	1145286-1146905	0.47
RZ95_RS04815	980513-981470	-0.76	RZ95_RS05635	1148611-1150147	-0.65
RZ95_RS04825	983126-984197	0.71	RZ95_RS05655	1153962-1155402	0.41
RZ95_RS04840	986451-987327	-0.54	RZ95_RS05675	1157972-1158641	1.87
RZ95_RS04910	998658-999309	0.41	RZ95_RS05680	1158801-1159674	0.57
RZ95_RS04945	1004758-1005766	0.41	RZ95_RS05720	1164367-1164931	-1.05
RZ95_RS04950	1006149-1008564	0.93	RZ95_RS05740	1171160-1171439	0.55
RZ95_RS04955	1008651-1009452	0.90	RZ95_RS05780	1183386-1184415	0.56
RZ95_RS05020	1019224-1021066	0.62	RZ95_RS05880	1198513-1198837	-0.52
RZ95_RS05040	1024877-1025096	0.86	RZ95_RS05890	1201930-1203937	0.44
RZ95_RS05090	1035744-1035999	-0.43	RZ95_RS05935	1214495-1215779	-0.66
RZ95_RS05095	1036013-1037414	-0.61	RZ95_RS05960	1220249-1221131	1.27
RZ95_RS05110	1039208-1041980	0.48	RZ95_RS05965	1221175-1222063	1.21
RZ95_RS05180	1056068-1056968	0.42	RZ95_RS05970	1222200-1222551	1.70
RZ95_RS05200	1061040-1061307	-0.63	RZ95_RS06000	1229841-1231220	0.56
RZ95_RS05215	1063275-1064619	0.70	RZ95_RS06005	1231244-1231979	0.44
RZ95_RS05225	1066027-1067170	0.73	RZ95_RS06025	1235326-1235773	-0.60
RZ95_RS05230	1067225-1067744	0.70	RZ95_RS06030	1235782-1236010	-0.54
RZ95_RS05250	1072830-1073208	0.57	RZ95_RS06035	1236021-1236408	-0.65
RZ95_RS05255	1073310-1073751	0.48	RZ95_RS06060	1240422-1241369	-0.43
RZ95_RS05265	1074900-1075680	0.52	RZ95_RS06065	1241373-1243362	-0.45
RZ95_RS05305	1082210-1082588	-0.47	RZ95_RS06070	1243365-1244439	-0.45
RZ95_RS05310	1082726-1083088	0.57	RZ95_RS06095	1250063-1250627	0.54
RZ95_RS05320	1083786-1084041	0.62	RZ95_RS06135	1257828-1258182	0.83
RZ95_RS05325	1084314-1085595	-0.50	RZ95_RS06140	1258662-1259622	0.65
RZ95_RS05360	1091958-1092471	-0.51	RZ95_RS06145	1259631-1260981	0.95
RZ95_RS05380	1095324-1096644	-0.40	RZ95_RS06150	1261255-1262281	0.39
RZ95_RS05410	1101140-1103720	-0.47	RZ95_RS06155	1262424-1263195	2.40
RZ95_RS05415	1103947-1105234	-0.55	RZ95_RS06160	1263442-1264579	2.03
RZ95_RS05430	1108433-1109450	-0.48	RZ95_RS06165	1264838-1266485	2.42
RZ95_RS05440	1110856-1112314	1.34	RZ95_RS06210	1275421-1279939	0.38
RZ95_RS05445	1112469-1113450	0.44	RZ95_RS06220	1280495-1280930	0.36
RZ95_RS05450	1113540-1114950	1.67	RZ95_RS06230	1281517-1281787	1.23
RZ95_RS05455	1115083-1115713	1.98	RZ95_RS06260	1288590-1289955	1.30
RZ95_RS05460	1115716-1116421	2.09	RZ95_RS06275	1291679-1291916	0.85
RZ95_RS05465	1116447-1119338	2.11	RZ95_RS06290	1295142-1296051	0.38
RZ95_RS05470	1116447-1119338	1.85	RZ95_RS06305	1297042-1299620	-0.48
RZ95_RS05475	1119358-1120153	1.70	RZ95_RS06320	1301358-1302087	-0.67
RZ95_RS05480	1120163-1121765	2.27	RZ95_RS06325	1302166-1302721	-0.76
RZ95_RS05485	1121801-1122974	2.82	RZ95_RS06605	1354985-1355231	0.60
RZ95_RS05490	1123122-1123749	2.08	RZ95_RS06645	1362319-1362985	0.63
RZ95_RS05495	1123849-1125538	2.24	RZ95_RS06650	1362993-1363506	0.66
RZ95_RS05500	1125612-1126605	2.00	RZ95_RS06655	1363555-1364335	0.59
RZ95_RS05505	1126675-1127350	0.95	RZ95_RS06675	1368351-1368765	0.52
RZ95_RS05510	1127403-1128201	0.89	RZ95_RS06690	1371229-1371988	-0.57

gene NCBI	locus	log2(OF/O)	gene NCBI	locus	log2(OF/O)
RZ95_RS06725	1377358-1378648	-0.48	RZ95_RS07955	1628940-1630404	0.39
RZ95_RS06755	1382957-1384592	0.51	RZ95_RS07970	1632733-1633249	-0.56
RZ95_RS06775	1389505-1391566	0.42	RZ95_RS07985	1634216-1635434	0.54
RZ95_RS06825	1398402-1398852	0.42	RZ95_RS08115	1657013-1657445	0.53
RZ95_RS06835	1401968-1403108	0.43	RZ95_RS08130	1658548-1658908	0.69
RZ95_RS06885	1411581-1412631	0.47	RZ95_RS08135	1659037-1662256	0.58
RZ95_RS06890	1412710-1413457	0.42	RZ95_RS08195	1673266-1674466	0.51
RZ95_RS06900	1413900-1416177	0.53	RZ95_RS08200	1674483-1675779	0.69
RZ95_RS06930	1420034-1421171	0.59	RZ95_RS08210	1677531-1677837	-0.53
RZ95_RS06945	1422975-1424613	0.75	RZ95_RS08235	1682204-1683449	0.46
RZ95_RS06950	1424892-1425090	1.37	RZ95_RS08240	1683631-1683859	0.62
RZ95_RS06955	1425215-1425452	0.84	RZ95_RS08245	1684114-1685545	0.47
RZ95_RS06960	1425535-1426525	0.36	RZ95_RS08250	1685599-1687090	0.53
RZ95_RS07050	1445671-1446214	0.41	RZ95_RS08255	1687145-1688300	0.46
RZ95_RS07055	1446317-1446539	0.65	RZ95_RS08385	1710936-1713609	0.45
RZ95_RS07080	1449943-1452022	1.30	RZ95_RS08415	1717557-1718061	1.00
RZ95_RS07155	1466137-1466407	0.99	RZ95_RS08750	1796045-1796984	0.59
RZ95_RS07180	1470410-1471664	0.54	RZ95_RS08755	1797187-1800658	2.78
RZ95_RS07230	1483101-1484562	0.99	RZ95_RS08770	1802350-1803409	1.19
RZ95_RS07285	1493126-1493708	-0.59	RZ95_RS08835	1819828-1821106	1.28
RZ95_RS07305	1495712-1496003	0.89	RZ95_RS08840	1821346-1822714	0.62
RZ95_RS07335	1501786-1502383	0.56	RZ95_RS08845	1822995-1823910	0.47
RZ95_RS07360	1505387-1506203	-0.50	RZ95_RS08850	1824025-1825135	1.00
RZ95_RS07365	1506213-1507599	-0.52	RZ95_RS08860	1825600-1826521	0.79
RZ95_RS07370	1507612-1509058	-0.99	RZ95_RS08865	1826599-1828503	0.64
RZ95_RS07380	1509413-1510925	-1.70	RZ95_RS08875	1828593-1829610	0.58
RZ95_RS07385	1511123-1512299	-0.68	RZ95_RS08885	1830464-1831697	0.66
RZ95_RS07390	1512328-1513300	-1.04	RZ95_RS08905	1834625-1835402	0.44
RZ95_RS07395	1513494-1514706	-1.84	RZ95_RS08930	1838823-1839291	0.58
RZ95_RS07435	1523392-1523728	-0.42	RZ95_RS08955	1846010-1847183	0.81
RZ95_RS07580	1549664-1550165	0.42	RZ95_RS09010	1856663-1858397	0.48
RZ95_RS07620	1556014-1557520	1.02	RZ95_RS09045	1865443-1866472	0.82
RZ95_RS07660	1566615-1567347	0.65	RZ95_RS09070	1871375-1873475	0.96
RZ95_RS07675	1569609-1569867	1.04	RZ95_RS09090	1877623-1879177	0.46
RZ95_RS07680	1570291-1572901	-0.35	RZ95_RS09095	1879435-1879873	0.59
RZ95_RS07740	1581352-1581904	0.51	RZ95_RS09115	1881922-1882666	0.71
RZ95_RS07780	1590856-1592017	0.57	RZ95_RS09135	1885930-1886848	0.41
RZ95_RS07805	1595903-1597574	0.37	RZ95_RS09150	1888493-1888985	0.56
RZ95_RS07810	1597872-1600454	1.10	RZ95_RS09155	1889092-1890487	0.80
RZ95_RS07815	1597872-1600454	1.01	RZ95_RS09160	1890598-1891606	0.70
RZ95_RS07825	1601840-1602263	0.54	RZ95_RS09610	1959821-1961018	0.72
RZ95_RS07840	1603494-1604685	-0.62	RZ95_RS09720	1980135-1981338	-1.34
RZ95_RS07850	1605231-1606269	-0.39	RZ95_RS09725	1981348-1983990	-0.80
RZ95_RS07870	1608954-1609182	0.72	RZ95_RS09760	1989017-1989356	-1.80
RZ95_RS07910	1615309-1615534	0.63	RZ95_RS09765	1989413-1989953	1.11
RZ95_RS07925	1617126-1620882	0.56	RZ95_RS09770	1990070-1990766	0.56
RZ95_RS07935	1621558-1623082	0.54	RZ95_RS09795	1994226-1996893	0.39

gene NCBI	locus	log2(OF/O)	gene NCBI	locus	log2(OF/O)
RZ95_RS09800	1996917-1998087	0.47	RZ95_RS11495	2352155-2353737	-1.32
RZ95_RS09815	2001221-2002073	0.50	RZ95_RS11500	2352155-2353737	-1.19
RZ95_RS09820	2002094-2002993	0.57	RZ95_RS11505	2353772-2355005	-1.34
RZ95_RS09835	2004790-2004994	0.84	RZ95_RS11515	2356625-2359589	-0.76
RZ95_RS09855	2007858-2008200	1.35	RZ95_RS11530	2360877-2363307	-0.57
RZ95_RS09875	2011549-2012602	-0.44	RZ95_RS11535	2363435-2363816	1.01
RZ95_RS09905	2016930-2017140	0.86	RZ95_RS11540	2364057-2364999	0.52
RZ95_RS09910	2017574-2018156	0.39	RZ95_RS11575	2370722-2370920	0.83
RZ95_RS09945	2022643-2022853	0.84	RZ95_RS11585	2371739-2373056	0.49
RZ95_RS09950	2023131-2023347	0.92	RZ95_RS11590	2373119-2373638	0.74
RZ95_RS09975	2027250-2028318	-0.35	RZ95_RS11605	2376700-2377435	-0.61
RZ95_RS10005	2034366-2035482	0.45	RZ95_RS11620	2378873-2379350	0.53
RZ95_RS10130	2066470-2067112	-0.94	RZ95_RS11640	2384157-2385792	-1.07
RZ95_RS10145	2068443-2069493	0.45	RZ95_RS11645	2385859-2386150	-1.04
RZ95_RS10390	2111564-2111641	2.62	RZ95_RS11650	2386362-2388041	0.80
RZ95_RS10405	2114602-2115559	0.43	RZ95_RS11655	2386362-2388041	0.92
RZ95_RS10410	2115679-2116698	1.16	RZ95_RS11685	2395792-2396641	-0.44
RZ95_RS10415	2116939-2117242	1.24	RZ95_RS11775	2412053-2412218	0.93
RZ95_RS10420	2117252-2119355	1.12	RZ95_RS11830	2424085-2425117	0.44
RZ95_RS10450	2125870-2126851	-0.62	RZ95_RS11845	2428417-2429056	0.51
RZ95_RS10505	2141529-2143062	-0.59	RZ95_RS11850	2429216-2429834	0.51
RZ95_RS10510	2143064-2144438	-0.40	RZ95_RS11910	2446043-2446553	0.52
RZ95_RS10610	2166469-2167339	0.52	RZ95_RS11940	2450111-2450629	0.43
RZ95_RS10615	2167464-2167887	0.98	RZ95_RS11945	2450924-2451371	0.59
RZ95_RS10620	2168227-2168662	0.54	RZ95_RS11950	2451404-2453284	0.36
RZ95_RS10625	2168731-2169190	0.42	RZ95_RS11970	2455881-2456085	1.71
RZ95_RS10715	2184549-2185560	-0.36	RZ95_RS12010	2463881-2465201	0.72
RZ95_RS10740	2189130-2190054	0.37	RZ95_RS12065	2475045-2475121	2.00
RZ95_RS10745	2190173-2191382	0.51	RZ95_RS12070	2475184-2475261	1.62
RZ95_RS10750	2191441-2192191	1.03	RZ95_RS12080	2475382-2475459	2.78
RZ95_RS10810	2200429-2201183	-0.39	RZ95_RS12085	2475508-2475585	1.55
RZ95_RS10825	2203008-2206845	-0.37	RZ95_RS12090	2475610-2475686	1.83
RZ95_RS10925	2223630-2226051	0.83	RZ95_RS12110	2478021-2478168	1.91
RZ95_RS10930	2226067-2227873	0.94	RZ95_RS12170	2491351-2494456	0.55
RZ95_RS10945	2230068-2231139	-0.46	RZ95_RS12180	2496327-2497680	0.68
RZ95_RS10950	2231144-2231774	-0.37	RZ95_RS12185	2497704-2499990	1.08
RZ95_RS11000	2241415-2242348	-0.76	RZ95_RS12190	2500016-2500700	1.86
RZ95_RS11015	2246152-2248627	1.16	RZ95_RS12195	2500709-2502152	1.30
RZ95_RS11130	2274560-2276222	-0.41	RZ95_RS12210	2504028-2507518	1.07
RZ95_RS11140	2278254-2279517	0.49	RZ95_RS12220	2504028-2507518	1.26
RZ95_RS11160	2281852-2283283	-0.65	RZ95_RS12235	2509533-2509998	0.66
RZ95_RS11260	2303904-2304312	0.80	RZ95_RS12320	2527730-2528930	0.47
RZ95_RS11285	2308783-2309488	0.50	RZ95_RS12325	2529271-2529463	1.04
RZ95_RS11290	2309734-2310889	0.52	RZ95_RS12330	2529524-2531231	1.44
RZ95_RS11345	2318992-2320381	-0.82	RZ95_RS12335	2531395-2531674	1.54
RZ95_RS11485	2348816-2352121	-1.17	RZ95_RS12345	2532944-2533889	1.12
RZ95_RS11490	2348816-2352121	-1.24	RZ95_RS12350	2533957-2536124	0.98

gene NCBI	locus	log2(OF/O)	gene NCBI	locus	log2(OF/O)
RZ95_RS12355	2533957-2536124	1.00	RZ95_RS13350	2751710-2752163	-0.72
RZ95_RS12360	2533957-2536124	1.11	RZ95_RS13435	2769760-2771896	-0.49
RZ95_RS12365	2536186-2536909	0.56	RZ95_RS13470	2778020-2779463	0.66
RZ95_RS12380	2539749-2541766	-2.63	RZ95_RS13485	2781137-2782397	-0.89
RZ95_RS12385	2539749-2541766	-0.63	RZ95_RS13560	2792921-2793977	0.51
RZ95_RS12390	2541767-2542448	-0.88	RZ95_RS13565	2793987-2795097	0.46
RZ95_RS12395	2542451-2544110	-3.73	RZ95_RS13610	2801916-2803836	0.53
RZ95_RS12405	2544533-2545658	-1.04	RZ95_RS13615	2803855-2805073	0.92
RZ95_RS12460	2556436-2557498	2.43	RZ95_RS13620	2805102-2806767	0.85
RZ95_RS12465	2557662-2559063	1.67	RZ95_RS13625	2806780-2807914	1.28
RZ95_RS12470	2559092-2560319	0.76	RZ95_RS13630	2807974-2808808	1.24
RZ95_RS12475	2560575-2561397	0.54	RZ95_RS13635	2808995-2809964	2.21
RZ95_RS12480	2561582-2562866	2.35	RZ95_RS13670	2816764-2817016	0.49
RZ95_RS12485	2562887-2563526	1.94	RZ95_RS13675	2817152-2817485	0.83
RZ95_RS12490	2563547-2564123	1.93	RZ95_RS13680	2817656-2819111	0.36
RZ95_RS12525	2569149-2570868	0.98	RZ95_RS13705	2821185-2822535	-0.68
RZ95_RS12530	2570918-2572364	0.81	RZ95_RS13715	2823353-2826273	0.40
RZ95_RS12535	2572517-2573537	0.40	RZ95_RS13755	2832777-2833203	1.46
RZ95_RS12540	2574437-2575682	0.46	RZ95_RS13760	2833246-2833825	0.42
RZ95_RS12555	2578068-2578803	-0.39	RZ95_RS13885	2860703-2860997	0.65
RZ95_RS12560	2578965-2580345	0.50	RZ95_RS13915	2866165-2867809	0.44
RZ95_RS12640	2594910-2596104	0.67	RZ95_RS13965	2874649-2875417	0.57
RZ95_RS12650	2597204-2597990	1.07	RZ95_RS14000	2884869-2885745	0.41
RZ95_RS12655	2598027-2599452	1.17	RZ95_RS14030	2890029-2891484	-2.20
RZ95_RS12665	2601133-2601838	1.31	RZ95_RS14035	2891487-2891811	-2.73
RZ95_RS12670	2601840-2602488	1.19	RZ95_RS14040	2891822-2892950	-2.68
RZ95_RS12720	2614054-2615410	0.98	RZ95_RS14085	2903803-2905816	-0.59
RZ95_RS12750	2620567-2621392	0.66	RZ95_RS14315	2948169-2950923	0.68
RZ95_RS12755	2621471-2622698	0.43	RZ95_RS14355	2961499-2962375	0.96
RZ95_RS12760	2622754-2624254	0.46	RZ95_RS14360	2962433-2963765	1.49
RZ95_RS12785	2629534-2630752	-0.41	RZ95_RS14415	2976315-2977032	0.45
RZ95_RS12790	2630829-2632101	-0.73	RZ95_RS14590	3009969-3011418	0.52
RZ95_RS12810	2634108-2635557	0.47	RZ95_RS14610	3013898-3014177	-0.58
RZ95_RS12815	2635573-2636836	0.46	RZ95_RS14615	3014282-3014786	-0.39
RZ95_RS12825	2639329-2640775	0.50	RZ95_RS14695	3029702-3030641	0.55
RZ95_RS12835	2642620-2643315	1.20	RZ95_RS14745	3040245-3040674	0.84
RZ95_RS12840	2643866-2646324	1.11	RZ95_RS14750	3040728-3041808	0.97
RZ95_RS12845	2643866-2646324	1.15	RZ95_RS14755	3041845-3042406	0.75
RZ95_RS13075	2689630-2690512	-0.68	RZ95_RS14760	3042505-3043156	0.66
RZ95_RS13220	2722268-2723798	0.62	RZ95_RS14840	3057301-3059494	0.73
RZ95_RS13250	2728941-2729394	0.56	RZ95_RS14970	3085741-3085936	0.64
RZ95_RS13255	2729728-2730706	0.77	RZ95_RS15095	3109048-3109924	-0.48
RZ95_RS13265	2732366-2735963	0.36	RZ95_RS15100	3110125-3110578	-1.18
RZ95_RS13270	2736079-2736814	0.94	RZ95_RS15105	3110721-3111675	1.01
RZ95_RS13280	2737810-2738848	-0.39	RZ95_RS15110	3111685-3112042	0.99
RZ95_RS13310	2742599-2743055	-1.34	RZ95_RS15115	3112114-3112375	1.47
RZ95_RS13345	2750086-2751514	0.43	RZ95_RS15160	3128778-3130206	0.36

gene NCBI	locus	log2(OF/O)	gene NCBI	locus	log2(OF/O)
RZ95_RS15185	3134708-3135785	-0.46	RZ95_RS16210	3349061-3349307	-0.69
RZ95_RS15245	3148201-3151305	-0.47	RZ95_RS16215	3349391-3350267	-0.47
RZ95_RS15450	3190351-3191041	-0.51	RZ95_RS16280	3363294-3364995	0.36
RZ95_RS15455	3191139-3191340	2.13	RZ95_RS16290	3365875-3366160	0.53
RZ95_RS15475	3195893-3197813	-1.13	RZ95_RS16300	3368421-3369024	0.39
RZ95_RS15485	3198414-3199002	-1.00	RZ95_RS16305	3369054-3369654	0.55
RZ95_RS15495	3200789-3201674	0.44	RZ95_RS16310	3369668-3370310	0.49
RZ95_RS15525	3212374-3212740	-0.52	RZ95_RS16315	3370441-3370840	0.55
RZ95_RS15530	3212788-3213295	-0.46	RZ95_RS16320	3370940-3371888	0.41
RZ95_RS15535	3213596-3214292	-0.51	RZ95_RS16335	3374734-3375082	0.52
RZ95_RS15540	3214295-3214724	-0.44	RZ95_RS16435	3393244-3394162	1.00
RZ95_RS15560	3216024-3217216	-0.52	RZ95_RS16455	3399075-3399546	-0.46
RZ95_RS15575	3217571-3217655	1.43	RZ95_RS16460	3399550-3400006	-0.40
RZ95_RS15625	3226116-3227310	0.49	RZ95_RS16730	3456848-3457814	-1.23
RZ95_RS15645	3229986-3230727	0.42	RZ95_RS16735	3457824-3458820	-0.88
RZ95_RS15765	3256513-3257935	-0.35	RZ95_RS16790	3469812-3470355	0.59
RZ95_RS15955	3295861-3296488	1.11	RZ95_RS16840	3479558-3481103	0.39
RZ95_RS15980	3300344-3300872	-0.39	RZ95_RS16900	3493209-3493500	0.56
RZ95_RS15995	3301931-3303611	0.61	RZ95_RS16920	3497027-3497501	-0.79
RZ95_RS16010	3306514-3307834	0.39	RZ95_RS16935	3500072-3500324	1.12
RZ95_RS16065	3319403-3319946	1.07	RZ95_RS16950	3502466-3503420	-0.74
RZ95_RS16070	3320328-3323099	1.10	RZ95_RS16970	3506553-3508317	-0.36
RZ95_RS16120	3333575-3334109	-0.41	RZ95_RS16975	3508322-3508643	-0.46
RZ95_RS16145	3338810-3339365	1.02	RZ95_RS16990	851879-852257	1.30
RZ95_RS16180	3343589-3344009	-0.34	RZ95_RS19965	72033-72192	2.33
RZ95_RS16185	3344035-3345430	-0.60	RZ95_RS20255	2329318-2329502	1.17
RZ95_RS16190	3345456-3346326	-0.60	RZ95_RS20260	2390360-2390689	-0.93
RZ95_RS16195	3346414-3347959	-0.63	RZ95_RS20295	2720207-2720566	0.40
RZ95_RS16200	3348003-3348540	-0.62	RZ95_RS20300	2768482-2769216	-0.49
RZ95_RS16205	3348552-3349023	-0.61			

Table A-3 Differentially expressed genes in an Acinetobacter culture without oxygen

Comparison of the gene expression between Acinetobacter cultures growing in minimal media aerobically with 0.5 mM Fe(III)citrate (control) and in minimal media anaerobically with 0.5 mM Fe(III)citrate (sample). This table shows all the genes differentially expressed with a significant q value (≤0.05). The gene NCBI column shows the gene tag from the reference genome (A. johnsonii XBB1) stored in the National Center for Biotechnology Information. The locus column shows the position of the gene in the genome. The values for the log2 fold change (FC) show if the genes of the sample culture are being upregulated (≥0) or downregulated (≤0). Rows highlighted in blue correspond to the genes that have been mentioned in Chapter 4 of this thesis.

gene NCBI	locus	log2(F/OF)	gene NCBI	locus	log2(F/OF)
RZ95_RS00005	87-1467	1.22	RZ95_RS00375	82997-83897	-0.78
RZ95_RS00010	1577-2726	0.67	RZ95_RS00385	84484-85124	-1.20
RZ95_RS00015	2741-3824	1.07	RZ95_RS00390	85194-86169	-0.76
RZ95_RS00025	6517-6886	-1.26	RZ95_RS00395	86314-88378	0.89
RZ95_RS00030	7525-9466	1.12	RZ95_RS00430	94606-95818	-0.40
RZ95_RS00040	10963-11974	-0.77	RZ95_RS00435	95981-97678	-0.74
RZ95_RS00045	12191-13205	-1.01	RZ95_RS00445	97776-99135	0.94
RZ95_RS00055	13718-14081	-1.03	RZ95_RS00450	99144-99855	0.64
RZ95_RS00075	17038-18979	0.85	RZ95_RS00455	100069-100768	-0.84
RZ95_RS00080	19098-19647	1.12	RZ95_RS00460	100971-101811	0.69
RZ95_RS00100	22802-23471	-0.77	RZ95_RS00470	103401-104559	-0.64
RZ95_RS00120	26131-27676	-1.16	RZ95_RS00475	104671-105979	-0.57
RZ95_RS00135	28352-31269	-1.39	RZ95_RS00480	105995-106565	-0.77
RZ95_RS00145	31904-33263	-1.14	RZ95_RS00485	106603-107138	-1.05
RZ95_RS00155	34931-36410	-1.22	RZ95_RS00490	107363-108941	-0.60
RZ95_RS00175	39474-41738	0.56	RZ95_RS00495	108960-109476	-0.63
RZ95_RS00185	42209-44039	-1.21	RZ95_RS00505	111104-111680	-1.44
RZ95_RS00190	44406-46092	-1.36	RZ95_RS00510	111694-113575	-0.80
RZ95_RS00195	46163-47462	-0.77	RZ95_RS00535	118866-119565	-0.69
RZ95_RS00200	47667-49773	0.55	RZ95_RS00540	119638-120361	-1.42
RZ95_RS00220	53326-56011	-0.40	RZ95_RS00545	120557-121559	-1.03
RZ95_RS00230	56993-58094	0.51	RZ95_RS00550	120557-121559	-0.75
RZ95_RS00235	58096-61234	0.58	RZ95_RS00560	123094-123469	-1.91
RZ95_RS00240	61365-61743	-0.53	RZ95_RS00565	123608-124151	-0.58
RZ95_RS00245	61846-62965	0.94	RZ95_RS00570	124165-124936	-0.77
RZ95_RS00255	63463-64285	-0.51	RZ95_RS00595	129537-130449	-0.51
RZ95_RS00270	65541-66993	0.70	RZ95_RS00600	130604-131042	-1.05
RZ95_RS00275	67023-68046	-0.87	RZ95_RS00605	131091-131442	1.51
RZ95_RS00285	68656-68902	-0.52	RZ95_RS00620	133441-134302	-1.10
RZ95_RS00290	68917-69472	-0.56	RZ95_RS00625	134490-136728	0.78
RZ95_RS00295	69544-70579	0.64	RZ95_RS00635	137122-137575	0.75
RZ95_RS00300	70687-71050	-1.38	RZ95_RS00645	138452-139397	-0.80
RZ95_RS00305	71125-71866	-1.07	RZ95_RS00655	140987-142436	-0.42
RZ95_RS00315	72946-74224	-0.68	RZ95_RS00660	142492-143422	-0.96
RZ95_RS00335	76605-77063	0.64	RZ95_RS00665	143422-144277	-0.54
RZ95_RS00340	77221-77998	-0.62	RZ95_RS00680	147089-147992	0.49
RZ95_RS00345	78006-79406	-0.71	RZ95_RS00705	154635-155211	2.15
RZ95_RS00350	78006-79406	-0.66	RZ95_RS00710	155393-156191	-1.04
RZ95_RS00355	79491-80277	-1.40	RZ95_RS00715	156285-156651	-0.54

gene NCBI	locus	log2(F/OF)	gene NCBI	locus	log2(F/OF)
RZ95_RS00725	158461-159793	-0.90	RZ95_RS01410	295026-296046	-1.33
RZ95_RS00730	159807-160464	-1.13	RZ95_RS01445	303438-304245	0.59
RZ95_RS00750	164562-165612	0.78	RZ95_RS01450	304276-306806	0.89
RZ95_RS00755	165752-167148	0.93	RZ95_RS01455	306971-309947	-0.85
RZ95_RS00760	165752-167148	0.75	RZ95_RS01475	309966-311719	-0.61
RZ95_RS00780	170845-172789	-2.27	RZ95_RS01485	311829-313053	-0.55
RZ95_RS00785	172908-173523	-0.44	RZ95_RS01505	316028-320510	-0.67
RZ95_RS00790	173584-174825	0.69	RZ95_RS01520	323240-323831	-1.40
RZ95_RS00800	174952-176059	-1.95	RZ95_RS01525	323877-325505	-0.94
RZ95_RS00805	176086-176815	-1.25	RZ95_RS01565	330613-331078	-0.64
RZ95_RS00825	182755-184803	-1.41	RZ95_RS01570	331329-331524	0.74
RZ95_RS00830	182755-184803	-1.14	RZ95_RS01580	332132-334232	-0.96
RZ95_RS00835	185052-185742	-0.74	RZ95_RS01585	334455-334737	0.47
RZ95_RS00860	188734-189619	0.56	RZ95_RS01600	336737-337670	0.86
RZ95_RS00865	190702-192412	-0.43	RZ95_RS01605	338132-338390	0.43
RZ95_RS00875	193109-195941	0.62	RZ95_RS01610	338418-338967	0.40
RZ95_RS00880	196261-196636	0.69	RZ95_RS01625	340307-341072	-0.67
RZ95_RS00895	197684-198764	-0.74	RZ95_RS01640	341502-342167	-0.86
RZ95_RS00905	200339-200924	-0.84	RZ95_RS01645	342291-343294	-1.25
RZ95_RS00910	201318-202251	1.44	RZ95_RS01655	344546-345452	-0.75
RZ95_RS01065	231872-233291	-0.91	RZ95_RS01665	346412-346871	-1.18
RZ95_RS01075	234450-235749	-0.67	RZ95_RS01675	347963-348839	2.15
RZ95_RS01085	236642-237635	-0.55	RZ95_RS01680	348977-350210	0.87
RZ95_RS01115	243522-244353	0.91	RZ95_RS01685	350574-351984	0.70
RZ95_RS01125	244673-244901	-1.54	RZ95_RS01690	352126-352498	-1.17
RZ95_RS01200	256409-257018	-1.68	RZ95_RS01695	352559-352826	1.48
RZ95_RS01210	258440-258686	-1.27	RZ95_RS01700	352895-353258	0.65
RZ95_RS01215	258767-259454	-2.10	RZ95_RS01705	353508-354738	1.92
RZ95_RS01220	259585-260587	-0.46	RZ95_RS01720	357638-358190	-1.39
RZ95_RS01225	260697-261336	0.50	RZ95_RS01730	359594-360239	0.43
RZ95_RS01230	261654-262116	1.43	RZ95_RS01750	362497-362830	-1.18
RZ95_RS01240	263062-264013	-0.50	RZ95_RS01755	363219-363597	0.91
RZ95_RS01250	264684-265077	-0.88	RZ95_RS01765	364102-365401	-0.63
RZ95_RS01270	268730-269630	0.73	RZ95_RS01775	365853-367155	0.43
RZ95_RS01280	270346-271078	-0.71	RZ95_RS01785	367842-368997	0.99
RZ95_RS01290	271918-272383	-1.93	RZ95_RS01795	370674-372498	-1.14
RZ95_RS01295	272671-273882	0.92	RZ95_RS01810	376296-377085	1.72
RZ95_RS01300	272671-273882	0.96	RZ95_RS01815	377182-377389	0.90
RZ95_RS01305	273974-274352	-0.67	RZ95_RS01820	377674-378616	-0.56
RZ95_RS01325	275733-276153	-0.69	RZ95_RS01825	378874-380248	-1.17
RZ95_RS01340	279706-280471	-1.12	RZ95_RS01835	381215-383117	-0.55
RZ95_RS01350	283215-283533	1.02	RZ95_RS01840	383233-384064	2.27
RZ95_RS01360	284084-284972	-1.42	RZ95_RS01845	384814-386737	2.98
RZ95_RS01365	285280-286558	-1.57	RZ95_RS01935	403152-404412	-1.17
RZ95_RS01375	288576-289023	1.30	RZ95_RS01940	404465-405410	2.02
RZ95_RS01385	290782-291124	-0.56	RZ95_RS01945	405549-406410	0.94
RZ95_RS01405	293775-294774	-1.77	RZ95_RS01950	406513-406963	2.24

gene NCBI	locus	log2(F/OF)	gene NCBI	locus	log2(F/OF)
RZ95_RS01955	407052-408261	2.63	RZ95_RS02310	462712-463315	0.54
RZ95_RS01960	408410-409994	-1.77	RZ95_RS02315	463430-464288	0.50
RZ95_RS01965	410002-411211	-0.65	RZ95_RS02320	464331-465162	0.58
RZ95_RS01975	412374-412686	1.43	RZ95_RS02330	466697-468242	-1.29
RZ95_RS01980	412746-413385	1.41	RZ95_RS02345	468942-471865	-1.41
RZ95_RS01985	413396-414316	1.37	RZ95_RS02355	472679-474077	-0.40
RZ95_RS01990	413396-414316	1.29	RZ95_RS02370	475165-476062	-0.75
RZ95_RS01995	414327-415152	1.18	RZ95_RS02375	476062-476494	-0.81
RZ95_RS02000	415171-415447	1.09	RZ95_RS02380	476511-476934	-0.44
RZ95_RS02005	415456-415786	1.06	RZ95_RS02390	477675-478176	-0.77
RZ95_RS02010	415787-416540	0.84	RZ95_RS02395	478204-478693	-1.28
RZ95_RS02015	416543-417408	0.79	RZ95_RS02400	478784-479099	-1.60
RZ95_RS02030	417500-417869	0.47	RZ95_RS02440	485352-486627	-0.65
RZ95_RS02045	418757-419063	0.42	RZ95_RS02445	486703-487093	-2.18
RZ95_RS02050	419075-419471	0.48	RZ95_RS02450	487153-487603	1.04
RZ95_RS02055	419484-420018	0.56	RZ95_RS02455	487630-487885	1.10
RZ95_RS02060	420032-420383	0.56	RZ95_RS02460	487904-488312	1.29
RZ95_RS02065	420385-420883	0.58	RZ95_RS02475	490305-491040	-1.29
RZ95_RS02070	420889-421066	0.62	RZ95_RS02505	495768-497178	0.90
RZ95_RS02075	421069-421510	0.66	RZ95_RS02510	497187-499178	0.96
RZ95_RS02080	421522-422875	0.55	RZ95_RS02515	499180-500515	0.75
RZ95_RS02090	423118-423475	0.57	RZ95_RS02525	501628-502138	-0.47
RZ95_RS02095	423494-423881	0.62	RZ95_RS02535	505109-505475	-0.71
RZ95_RS02100	423893-424520	0.59	RZ95_RS02540	506244-508460	-1.32
RZ95_RS02105	424536-425544	0.68	RZ95_RS02545	506244-508460	-1.14
RZ95_RS02110	425562-425928	0.68	RZ95_RS02550	508565-509582	-1.39
RZ95_RS02115	426123-427614	1.37	RZ95_RS02575	514939-516220	1.18
RZ95_RS02120	427752-428544	-0.52	RZ95_RS02580	516412-516964	0.91
RZ95_RS02125	428578-429751	-0.63	RZ95_RS02590	517365-517797	0.46
RZ95_RS02130	429943-430201	-0.50	RZ95_RS02595	517919-519155	1.13
RZ95_RS02140	431112-432150	-1.41	RZ95_RS02605	519171-520739	0.69
RZ95_RS02145	432221-432794	-0.97	RZ95_RS02610	520757-521879	0.74
RZ95_RS02175	439400-441836	-0.63	RZ95_RS02615	521882-523178	0.86
RZ95_RS02180	442103-442193	0.58	RZ95_RS02625	523205-525046	0.64
RZ95_RS02210	444249-445080	0.52	RZ95_RS02630	525215-526625	0.79
RZ95_RS02215	445184-446120	0.48	RZ95_RS02635	526766-527390	0.54
RZ95_RS02220	446201-447452	-0.85	RZ95_RS02650	530361-530691	-0.64
RZ95_RS02225	447567-448161	-0.96	RZ95_RS02655	530795-531926	0.75
RZ95_RS02230	448203-448578	-1.90	RZ95_RS02675	534624-535665	1.21
RZ95_RS02235	448790-449720	-0.96	RZ95_RS02740	543981-545208	-1.05
RZ95_RS02245	450788-451499	-0.42	RZ95_RS02745	545331-548076	-0.99
RZ95_RS02270	454543-455620	-0.50	RZ95_RS02750	548109-549036	-0.70
RZ95_RS02275	455658-457116	1.05	RZ95_RS02755	549087-550257	0.58
RZ95_RS02280	457425-459393	-0.75	RZ95_RS02805	560180-560402	0.71
RZ95_RS02290	460243-461230	-0.86	RZ95_RS02810	560553-561438	0.90
RZ95_RS02295	461403-461664	-0.94	RZ95_RS02820	563692-564457	1.21
RZ95_RS02305	462112-462640	1.58	RZ95_RS02840	569026-569479	0.66

gene NCBI	locus	log2(F/OF)	gene NCBI	locus	log2(F/OF)
RZ95_RS02850	570186-571968	-1.06	RZ95_RS03290	660962-661988	0.81
RZ95_RS02855	572165-573968	-0.89	RZ95_RS03295	662055-663426	1.13
RZ95_RS02860	574273-574891	-0.57	RZ95_RS03300	663597-665436	1.82
RZ95_RS02865	575011-576682	0.61	RZ95_RS03305	665637-666072	-0.89
RZ95_RS02885	580364-581810	1.19	RZ95_RS03325	668071-669352	-1.05
RZ95_RS02890	581888-582249	0.86	RZ95_RS03330	669460-670576	-2.01
RZ95_RS02900	583766-584489	-0.48	RZ95_RS03340	671649-672459	-1.36
RZ95_RS02905	584805-585375	-1.12	RZ95_RS03350	673334-674524	-0.47
RZ95_RS02910	585474-587325	1.66	RZ95_RS03360	675581-678188	-0.92
RZ95_RS02930	590615-591608	-0.63	RZ95_RS03385	680546-681122	-1.16
RZ95_RS02935	591672-592548	0.95	RZ95_RS03390	681353-681560	-3.03
RZ95_RS02945	593758-595090	0.70	RZ95_RS03395	681641-681995	-1.57
RZ95_RS02975	599469-600866	-0.66	RZ95_RS03400	682249-682906	-0.90
RZ95_RS02980	601174-601816	-2.87	RZ95_RS03405	683012-683285	-0.90
RZ95_RS02990	602793-605517	0.93	RZ95_RS03410	683874-684270	-1.58
RZ95_RS02995	605709-606057	-0.88	RZ95_RS03415	684907-685573	-1.74
RZ95_RS03000	606214-607435	-1.10	RZ95_RS03425	686957-687344	-1.93
RZ95_RS03005	607580-608648	-0.75	RZ95_RS03430	687513-687960	-1.86
RZ95_RS03045	612045-613590	-1.06	RZ95_RS03435	688019-688370	-1.02
RZ95_RS03060	614295-617213	-1.40	RZ95_RS03440	688549-688888	-0.97
RZ95_RS03085	619707-620067	-1.13	RZ95_RS03445	689029-689395	-1.58
RZ95_RS03105	622998-623658	-0.62	RZ95_RS03450	689626-689962	-2.21
RZ95_RS03125	625450-625837	1.10	RZ95_RS03455	690072-690519	-1.24
RZ95_RS03130	625849-626278	1.25	RZ95_RS03460	690617-691022	-1.03
RZ95_RS03135	626770-627739	0.46	RZ95_RS03465	691060-693027	-1.09
RZ95_RS03140	627771-628584	0.64	RZ95_RS03475	693110-694697	1.95
RZ95_RS03145	628585-629434	0.75	RZ95_RS03485	695555-696365	0.57
RZ95_RS03150	629476-629926	-0.65	RZ95_RS03495	698089-699411	-0.90
RZ95_RS03155	630205-630649	-0.94	RZ95_RS03520	701880-705333	-0.53
RZ95_RS03175	633522-634380	0.51	RZ95_RS03525	705337-706333	-1.13
RZ95_RS03185	636114-637125	-0.85	RZ95_RS03535	708823-709891	-0.63
RZ95_RS03190	637132-637555	-0.84	RZ95_RS03560	714835-715300	-0.72
RZ95_RS03195	637697-639011	0.72	RZ95_RS03575	716977-719451	1.12
RZ95_RS03200	639154-639796	0.63	RZ95_RS03580	716977-719451	1.10
RZ95_RS03205	639902-641117	-0.65	RZ95_RS03585	719458-720879	0.71
RZ95_RS03220	642172-644305	-0.43	RZ95_RS03620	727044-728829	-0.87
RZ95_RS03225	644316-645522	-0.61	RZ95_RS03625	728846-730655	-1.04
RZ95_RS03235	646932-648051	-0.96	RZ95_RS03630	730679-732695	-1.10
RZ95_RS03240	648170-649445	-0.93	RZ95_RS03635	732706-733645	-0.45
RZ95_RS03245	649629-652032	-0.87	RZ95_RS03640	733652-734798	-0.96
RZ95_RS03250	652412-654534	-2.76	RZ95_RS03650	736703-737810	0.62
RZ95_RS03255	652412-654534	-2.41	RZ95_RS03660	737851-739233	0.83
RZ95_RS03265	655005-655458	-0.75	RZ95_RS03675	740706-741369	0.93
RZ95_RS03270	655641-656817	-0.52	RZ95_RS03680	741466-742024	0.78
RZ95_RS03275	656917-657442	-0.46	RZ95_RS03685	742100-742283	0.72
RZ95_RS03280	657817-658840	-1.04	RZ95_RS03690	742459-744177	0.98
RZ95_RS03285	659489-660953	0.64	RZ95_RS03705	744745-745219	-2.61

gene NCBI	locus	log2(F/OF)	gene NCBI	locus	log2(F/OF)
RZ95_RS03710	745286-745991	-0.66	RZ95_RS04225	854527-856153	0.61
RZ95_RS03715	745994-749597	0.61	RZ95_RS04230	856356-856863	-0.75
RZ95_RS03725	752529-757085	-0.50	RZ95_RS04250	860623-861898	-0.75
RZ95_RS03735	757192-758158	-0.92	RZ95_RS04270	865614-866325	-0.42
RZ95_RS03740	758236-759160	0.80	RZ95_RS04275	867127-869950	-0.62
RZ95_RS03755	764345-765062	-1.08	RZ95_RS04280	869966-871181	-0.47
RZ95_RS03765	766817-767174	-1.77	RZ95_RS04290	872846-874013	-1.29
RZ95_RS03840	783555-783849	-0.69	RZ95_RS04295	874024-874915	-0.98
RZ95_RS03845	783970-784705	-0.53	RZ95_RS04305	875950-877663	-0.55
RZ95_RS03850	784738-785617	-0.60	RZ95_RS04320	880024-880951	-0.99
RZ95_RS03890	794618-795293	-1.10	RZ95_RS04325	880992-881898	-1.60
RZ95_RS03895	795305-796112	-1.17	RZ95_RS04345	884712-885153	-1.63
RZ95_RS03900	796206-797242	-0.83	RZ95_RS04370	891496-892639	0.55
RZ95_RS03925	799923-800361	-0.87	RZ95_RS04375	892947-893394	0.94
RZ95_RS03930	800364-800721	-1.27	RZ95_RS04380	893480-894020	1.29
RZ95_RS03940	800824-805461	-0.75	RZ95_RS04385	894032-894356	0.80
RZ95_RS03945	805474-806719	-0.73	RZ95_RS04405	898372-898684	0.86
RZ95_RS03965	811034-811346	0.71	RZ95_RS04410	898738-899107	0.85
RZ95_RS03970	811365-811620	0.64	RZ95_RS04425	901310-902039	0.74
RZ95_RS03980	813194-813893	0.42	RZ95_RS04445	904755-906084	0.69
RZ95_RS03985	814066-814837	-1.55	RZ95_RS04450	906213-907203	0.80
RZ95_RS03995	816285-817662	0.62	RZ95_RS04455	907850-909455	-1.42
RZ95_RS04000	817694-818174	1.03	RZ95_RS04460	909590-909965	0.81
RZ95_RS04005	818198-818585	1.12	RZ95_RS04470	911573-914678	-0.62
RZ95_RS04010	818685-819483	1.20	RZ95_RS04505	920861-921245	-1.57
RZ95_RS04020	820191-821586	-0.92	RZ95_RS04510	921320-922433	2.39
RZ95_RS04025	821851-823036	-1.88	RZ95_RS04550	927909-928887	-0.69
RZ95_RS04030	823037-823571	-2.00	RZ95_RS04555	928954-929308	-0.50
RZ95_RS04040	824471-824759	0.75	RZ95_RS04560	929386-930082	0.83
RZ95_RS04045	824881-826765	0.99	RZ95_RS04575	932790-933861	-0.43
RZ95_RS04050	827199-827409	-0.75	RZ95_RS04585	934841-935312	-2.25
RZ95_RS04060	828119-828722	0.75	RZ95_RS04605	939343-939898	0.83
RZ95_RS04105	834874-837258	-0.83	RZ95_RS04610	939985-940672	-0.64
RZ95_RS04110	834874-837258	-0.76	RZ95_RS04650	947871-949212	-1.30
RZ95_RS04115	837322-837703	0.63	RZ95_RS04660	949543-950044	2.09
RZ95_RS04120	837846-838428	1.50	RZ95_RS04685	950998-951625	-1.06
RZ95_RS04125	838446-838743	1.03	RZ95_RS04700	953729-954908	-0.88
RZ95_RS04130	838844-839798	1.58	RZ95_RS04710	956481-957873	-0.51
RZ95_RS04155	840272-841103	0.67	RZ95_RS04715	958016-959378	-2.17
RZ95_RS04160	841114-841696	0.61	RZ95_RS04720	959709-961113	-0.54
RZ95_RS04170	843489-844773	0.93	RZ95_RS04760	966535-967141	0.44
RZ95_RS04175	844798-846694	0.74	RZ95_RS04765	967623-968376	-1.25
RZ95_RS04180	846885-847869	-0.44	RZ95_RS04770	968393-969329	-1.20
RZ95_RS04185	847940-848993	0.85	RZ95_RS04775	969624-970233	1.85
RZ95_RS04190	849023-849764	0.67	RZ95_RS04805	977455-978952	-0.69
RZ95_RS04195	849870-850437	0.77	RZ95_RS04815	980513-981470	-0.95
RZ95_RS04210	851589-851853	-0.57	RZ95_RS04830	984525-985353	-0.46

gene NCBI	locus	log2(F/OF)	gene NCBI	locus	log2(F/OF)
RZ95_RS04845	987408-987729	0.80	RZ95_RS05380	1095324-1096644	0.46
RZ95_RS04865	990455-990905	-0.84	RZ95_RS05390	1097337-1098111	-0.69
RZ95_RS04870	990973-991675	0.56	RZ95_RS05395	1098236-1099286	-0.59
RZ95_RS04875	991678-991996	1.30	RZ95_RS05410	1101140-1103720	0.69
RZ95_RS04895	995182-995791	1.33	RZ95_RS05420	1105357-1107562	0.93
RZ95_RS04900	996078-997080	-0.64	RZ95_RS05440	1110856-1112314	-2.21
RZ95_RS04940	1002481-1004619	-0.88	RZ95_RS05445	1112469-1113450	-0.95
RZ95_RS04945	1004758-1005766	-0.82	RZ95_RS05490	1123122-1123749	0.72
RZ95_RS04950	1006149-1008564	-1.78	RZ95_RS05510	1127403-1128201	-0.63
RZ95_RS04955	1008651-1009452	-1.26	RZ95_RS05515	1128291-1129065	-0.97
RZ95_RS04965	1010126-1011601	-0.83	RZ95_RS05520	1129192-1129978	-1.64
RZ95_RS04995	1014131-1014545	-1.42	RZ95_RS05540	1135120-1135732	-2.08
RZ95_RS05005	1015603-1016380	-1.57	RZ95_RS05585	1140890-1141103	0.79
RZ95_RS05010	1016430-1017825	-0.57	RZ95_RS05590	1141200-1142352	0.84
RZ95_RS05020	1019224-1021066	-0.99	RZ95_RS05625	1146995-1148587	1.06
RZ95_RS05040	1024877-1025096	-1.51	RZ95_RS05630	1146995-1148587	1.13
RZ95_RS05050	1026089-1026788	-0.52	RZ95_RS05635	1148611-1150147	0.72
RZ95_RS05065	1030104-1030509	-0.65	RZ95_RS05655	1153962-1155402	0.63
RZ95_RS05070	1030822-1031611	-0.48	RZ95_RS05660	1155569-1156016	0.63
RZ95_RS05075	1031630-1032764	-1.01	RZ95_RS05665	1156049-1156265	0.87
RZ95_RS05090	1035744-1035999	-0.81	RZ95_RS05670	1156410-1157427	0.66
RZ95_RS05095	1036013-1037414	-2.25	RZ95_RS05675	1157972-1158641	-2.48
RZ95_RS05100	1037876-1038308	-0.62	RZ95_RS05680	1158801-1159674	-0.67
RZ95_RS05105	1038384-1039008	2.26	RZ95_RS05710	1162738-1162942	-0.47
RZ95_RS05120	1043537-1044005	0.82	RZ95_RS05715	1163430-1164162	-0.64
RZ95_RS05125	1044321-1045113	1.27	RZ95_RS05720	1164367-1164931	1.17
RZ95_RS05135	1046334-1046901	0.72	RZ95_RS05725	1165275-1169214	0.40
RZ95_RS05145	1048197-1048977	-0.69	RZ95_RS05735	1170363-1171137	0.55
RZ95_RS05155	1049795-1051052	-0.90	RZ95_RS05745	1171709-1172705	0.97
RZ95_RS05190	1057550-1059947	-0.65	RZ95_RS05780	1183386-1184415	-1.06
RZ95_RS05200	1061040-1061307	-0.65	RZ95_RS05785	1184416-1184683	-0.96
RZ95_RS05215	1063275-1064619	-0.49	RZ95_RS05790	1184684-1185182	-0.88
RZ95_RS05230	1067225-1067744	-0.95	RZ95_RS05815	1187080-1189286	-0.71
RZ95_RS05235	1068200-1069310	-0.45	RZ95_RS05820	1189288-1190634	-0.76
RZ95_RS05240	1069377-1070469	-0.60	RZ95_RS05865	1195880-1196723	-1.26
RZ95_RS05245	1070472-1072722	-0.76	RZ95_RS05870	1196864-1197530	0.43
RZ95_RS05250	1072830-1073208	-0.92	RZ95_RS05875	1197661-1198381	0.48
RZ95_RS05260	1074144-1074774	0.86	RZ95_RS05880	1198513-1198837	-1.54
RZ95_RS05265	1074900-1075680	0.50	RZ95_RS05885	1199044-1201678	-0.45
RZ95_RS05285	1078584-1079907	0.49	RZ95_RS05890	1201930-1203937	-0.72
RZ95_RS05290	1079974-1080976	0.53	RZ95_RS05895	1204070-1204973	-0.58
RZ95_RS05310	1082726-1083088	-2.62	RZ95_RS05905	1205096-1206747	0.97
RZ95_RS05315	1083150-1083738	1.21	RZ95_RS05910	1206780-1210350	0.93
RZ95_RS05340	1089895-1090201	-0.67	RZ95_RS05930	1213039-1213912	-1.34
RZ95_RS05350	1090210-1091253	1.06	RZ95_RS05945	1217663-1217933	0.68
RZ95_RS05355	1091416-1091872	0.78	RZ95_RS05960	1220249-1221131	-1.11
RZ95_RS05375	1094088-1095255	1.03	RZ95_RS05970	1222200-1222551	-2.68

gene NCBI	locus	log2(F/OF)	gene NCBI	locus	log2(F/OF)
RZ95_RS05975	1222804-1224685	1.00	RZ95_RS06715	1374768-1376409	0.47
RZ95_RS05985	1227024-1228026	-0.86	RZ95_RS06720	1376440-1377298	0.47
RZ95_RS06015	1232484-1233555	0.65	RZ95_RS06750	1381609-1382884	0.82
RZ95_RS06025	1235326-1235773	0.73	RZ95_RS06775	1389505-1391566	-0.53
RZ95_RS06030	1235782-1236010	0.77	RZ95_RS06785	1392248-1392551	-0.69
RZ95_RS06035	1236021-1236408	0.68	RZ95_RS06795	1392680-1395594	-0.78
RZ95_RS06050	1239533-1240412	1.00	RZ95_RS06800	1392680-1395594	-1.15
RZ95_RS06080	1245850-1248229	-0.58	RZ95_RS06850	1405320-1405815	-1.05
RZ95_RS06085	1248385-1249222	-0.44	RZ95_RS06860	1407501-1408173	-0.46
RZ95_RS06110	1252910-1253336	0.94	RZ95_RS06865	1408301-1408985	0.46
RZ95_RS06130	1255760-1257541	0.54	RZ95_RS06900	1413900-1416177	-0.86
RZ95_RS06135	1257828-1258182	1.46	RZ95_RS06910	1416645-1417119	-0.74
RZ95_RS06150	1261255-1262281	-0.43	RZ95_RS06930	1420034-1421171	-0.80
RZ95_RS06155	1262424-1263195	-0.80	RZ95_RS06945	1422975-1424613	-1.42
RZ95_RS06170	1266780-1267551	0.56	RZ95_RS06950	1424892-1425090	-2.74
RZ95_RS06180	1269051-1269832	1.08	RZ95_RS06955	1425215-1425452	-0.78
RZ95_RS06185	1269051-1269832	1.02	RZ95_RS06960	1425535-1426525	1.03
RZ95_RS06195	1270507-1271143	-0.41	RZ95_RS06965	1426826-1427921	1.33
RZ95_RS06215	1280146-1280350	-1.92	RZ95_RS06970	1427943-1429688	-0.83
RZ95_RS06220	1280495-1280930	-1.09	RZ95_RS06980	1429754-1430237	0.91
RZ95_RS06225	1281038-1281398	-1.12	RZ95_RS07005	1435993-1438225	-0.49
RZ95_RS06230	1281517-1281787	-0.90	RZ95_RS07015	1440069-1440858	1.31
RZ95_RS06245	1285123-1286056	1.10	RZ95_RS07040	1444051-1445588	1.07
RZ95_RS06250	1286432-1287656	-0.77	RZ95_RS07050	1445671-1446214	-0.52
RZ95_RS06255	1287888-1288374	0.80	RZ95_RS07060	1446595-1446814	0.78
RZ95_RS06260	1288590-1289955	-1.32	RZ95_RS07065	1446818-1448114	1.75
RZ95_RS06275	1291679-1291916	-1.26	RZ95_RS07080	1449943-1452022	-1.22
RZ95_RS06280	1292407-1293694	1.38	RZ95_RS07150	1465815-1466043	-1.10
RZ95_RS06285	1294045-1294840	0.70	RZ95_RS07155	1466137-1466407	-1.16
RZ95_RS06295	1296161-1296593	0.67	RZ95_RS07180	1470410-1471664	-1.98
RZ95_RS06315	1299971-1301315	0.69	RZ95_RS07190	1473244-1474447	0.61
RZ95_RS06340	1304310-1305507	0.63	RZ95_RS07195	1474555-1475161	-0.48
RZ95_RS06345	1305509-1306865	0.60	RZ95_RS07205	1476860-1477688	-1.74
RZ95_RS06375	1312346-1313192	-0.89	RZ95_RS07210	1477834-1480612	-0.58
RZ95_RS06380	1314048-1314654	1.77	RZ95_RS07240	1486706-1487090	-1.92
RZ95_RS06605	1354985-1355231	-1.84	RZ95_RS07245	1487608-1488229	-0.65
RZ95_RS06620	1356297-1357152	0.43	RZ95_RS07285	1493126-1493708	1.18
RZ95_RS06625	1357206-1357938	0.66	RZ95_RS07305	1495712-1496003	-0.72
RZ95_RS06630	1358074-1358515	-1.17	RZ95_RS07335	1501786-1502383	-1.46
RZ95_RS06640	1361839-1362106	0.87	RZ95_RS07340	1502481-1503186	-0.57
RZ95_RS06645	1362319-1362985	-0.82	RZ95_RS07355	1504739-1505336	-0.84
RZ95_RS06650	1362993-1363506	-1.41	RZ95_RS07360	1505387-1506203	-1.45
RZ95_RS06655	1363555-1364335	-1.06	RZ95_RS07365	1506213-1507599	-1.37
RZ95_RS06670	1366134-1368159	-1.51	RZ95_RS07370	1507612-1509058	-1.27
RZ95_RS06675	1368351-1368765	-0.97	RZ95_RS07380	1509413-1510925	-1.96
RZ95_RS06685	1370003-1371173	0.71	RZ95_RS07385	1511123-1512299	-1.38
RZ95_RS06690	1371229-1371988	1.42	RZ95_RS07390	1512328-1513300	-1.05

gene NCBI	locus	log2(F/OF)	gene NCBI	locus	log2(F/OF)
RZ95_RS08435	1718616-1722810	1.00	RZ95_RS09560	1947108-1947810	1.02
RZ95_RS08440	1722834-1726659	0.75	RZ95_RS09565	1947829-1949056	1.18
RZ95_RS08485	1735672-1736661	1.42	RZ95_RS09570	1949131-1951396	0.79
RZ95_RS08640	1774059-1774269	0.97	RZ95_RS09575	1951411-1953680	1.65
RZ95_RS08750	1796045-1796984	0.92	RZ95_RS09580	1951411-1953680	1.82
RZ95_RS08755	1797187-1800658	-1.29	RZ95_RS09585	1951411-1953680	2.19
RZ95_RS08770	1802350-1803409	-1.64	RZ95_RS09610	1959821-1961018	1.19
RZ95_RS08790	1807288-1809382	0.50	RZ95_RS09615	1961187-1962120	-0.84
RZ95_RS08795	1809815-1814178	1.37	RZ95_RS09620	1962402-1964607	0.54
RZ95_RS08800	1809815-1814178	2.39	RZ95_RS09625	1964676-1965849	0.44
RZ95_RS08805	1814179-1815502	2.50	RZ95_RS09665	1972586-1973210	-0.50
RZ95_RS08815	1816043-1816952	-0.71	RZ95_RS09710	1978240-1978711	-0.72
RZ95_RS08830	1818675-1819563	-0.86	RZ95_RS09715	1978990-1979755	-0.52
RZ95_RS08835	1819828-1821106	-1.00	RZ95_RS09720	1980135-1981338	-1.69
RZ95_RS08840	1821346-1822714	0.55	RZ95_RS09725	1981348-1983990	-2.26
RZ95_RS08860	1825600-1826521	-0.60	RZ95_RS09730	1981348-1983990	-2.00
RZ95_RS08865	1826599-1828503	-0.59	RZ95_RS09735	1984012-1984855	-1.41
RZ95_RS08930	1838823-1839291	-1.04	RZ95_RS09740	1984864-1985700	-1.66
RZ95_RS08935	1839502-1843108	0.66	RZ95_RS09745	1985711-1987422	-1.54
RZ95_RS08940	1843113-1843764	1.22	RZ95_RS09750	1985711-1987422	-1.16
RZ95_RS08945	1843781-1844522	1.82	RZ95_RS09755	1987735-1988827	0.47
RZ95_RS08950	1844797-1845691	0.66	RZ95_RS09760	1989017-1989356	1.48
RZ95_RS08955	1846010-1847183	-1.14	RZ95_RS09765	1989413-1989953	-1.13
RZ95_RS08965	1848379-1849378	-1.01	RZ95_RS09770	1990070-1990766	-0.63
RZ95_RS09005	1856245-1856563	-1.19	RZ95_RS09780	1991652-1992749	1.84
RZ95_RS09015	1858630-1859824	0.68	RZ95_RS09790	1992992-1994198	-0.80
RZ95_RS09025	1860552-1861089	-0.90	RZ95_RS09795	1994226-1996893	-0.60
RZ95_RS09030	1861352-1862591	-0.72	RZ95_RS09815	2001221-2002073	-0.69
RZ95_RS09050	1866543-1866924	-0.62	RZ95_RS09820	2002094-2002993	-1.92
RZ95_RS09055	1867176-1868355	0.52	RZ95_RS09825	2002094-2002993	-1.88
RZ95_RS09065	1869835-1870897	-0.61	RZ95_RS09835	2004790-2004994	-2.12
RZ95_RS09070	1871375-1873475	-1.19	RZ95_RS09840	2005019-2005625	-0.68
RZ95_RS09075	1873951-1875121	3.00	RZ95_RS09855	2007858-2008200	-1.51
RZ95_RS09080	1875133-1876162	3.99	RZ95_RS09875	2011549-2012602	-0.94
RZ95_RS09085	1876389-1877505	-1.19	RZ95_RS09880	2012642-2013668	-0.85
RZ95_RS09095	1879435-1879873	1.09	RZ95_RS09895	2016342-2016540	3.95
RZ95_RS09100	1879934-1880528	0.78	RZ95_RS09900	2016596-2016824	3.53
RZ95_RS09105	1880558-1881269	1.11	RZ95_RS09905	2016930-2017140	2.67
RZ95_RS09110	1881447-1881771	0.98	RZ95_RS09910	2017574-2018156	0.55
RZ95_RS09130	1884594-1885836	1.17	RZ95_RS09920	2019639-2020011	0.95
RZ95_RS09135	1885930-1886848	0.61	RZ95_RS09930	2020967-2021237	1.42
RZ95_RS09140	1887084-1887639	1.25	RZ95_RS09935	2021492-2021780	0.96
RZ95_RS09145	1887703-1888306	0.54	RZ95_RS09940	2022019-2022501	1.38
RZ95_RS09155	1889092-1890487	-0.96	RZ95_RS09955	2023916-2025745	0.47
RZ95_RS09160	1890598-1891606	-0.81	RZ95_RS09960	2023916-2025745	1.66
RZ95_RS09530	1942103-1942385	0.54	RZ95_RS09970	2026141-2027236	1.22
RZ95_RS09535	1942399-1942711	0.47	RZ95_RS09975	2027250-2028318	2.09

gene NCBI	locus	log2(F/OF)	gene NCBI	locus	log2(F/OF)
RZ95_RS09980	2028458-2029154	0.55	RZ95_RS10730	2186287-2187999	-1.69
RZ95_RS09985	2029192-2030008	0.65	RZ95_RS10735	2188011-2189073	-1.87
RZ95_RS10015	2036642-2038460	-0.44	RZ95_RS10740	2189130-2190054	-1.89
RZ95_RS10030	2039604-2041985	-0.90	RZ95_RS10745	2190173-2191382	1.26
RZ95_RS10060	2046747-2047023	0.97	RZ95_RS10750	2191441-2192191	-0.85
RZ95_RS10145	2068443-2069493	-0.50	RZ95_RS10760	2193410-2194121	0.98
RZ95_RS10150	2069723-2070347	0.56	RZ95_RS10770	2194849-2195257	-0.70
RZ95_RS10155	2070367-2071663	0.81	RZ95_RS10780	2196031-2196490	-0.95
RZ95_RS10165	2072440-2072794	-1.11	RZ95_RS10790	2197282-2198173	0.56
RZ95_RS10415	2116939-2117242	-1.25	RZ95_RS10800	2198850-2199420	-0.44
RZ95_RS10420	2117252-2119355	-1.35	RZ95_RS10805	2199524-2200325	-0.41
RZ95_RS10445	2125437-2125665	0.62	RZ95_RS10865	2214663-2215071	0.68
RZ95_RS10455	2127018-2127420	-1.17	RZ95_RS10880	2216251-2217559	0.70
RZ95_RS10460	2127542-2129684	-0.61	RZ95_RS10885	2217913-2219200	-0.45
RZ95_RS10465	2129865-2132475	-0.73	RZ95_RS10890	2219252-2219822	-0.92
RZ95_RS10470	2132555-2132897	-0.77	RZ95_RS10895	2219883-2220084	-0.89
RZ95_RS10475	2133059-2134271	-1.00	RZ95_RS10910	2221293-2223554	0.57
RZ95_RS10480	2134350-2135313	-0.43	RZ95_RS10945	2230068-2231139	0.64
RZ95_RS10490	2136535-2139303	1.14	RZ95_RS10950	2231144-2231774	0.77
RZ95_RS10495	2136535-2139303	1.33	RZ95_RS10970	2233771-2237132	1.30
RZ95_RS10500	2139407-2140433	1.81	RZ95_RS10985	2239169-2239739	-0.45
RZ95_RS10505	2141529-2143062	-1.23	RZ95_RS11000	2241415-2242348	1.18
RZ95_RS10510	2143064-2144438	-0.53	RZ95_RS11005	2243222-2244638	-0.90
RZ95_RS10515	2144912-2145614	-0.77	RZ95_RS11015	2246152-2248627	-0.99
RZ95_RS10545	2152055-2152907	0.59	RZ95_RS11020	2248721-2248982	-1.13
RZ95_RS10555	2153649-2154366	1.46	RZ95_RS11025	2249255-2249606	1.12
RZ95_RS10570	2157517-2158102	-0.71	RZ95_RS11030	2249613-2251658	0.76
RZ95_RS10575	2158205-2160227	0.67	RZ95_RS11050	2253261-2253795	-0.79
RZ95_RS10580	2160402-2161194	-1.26	RZ95_RS11070	2257374-2260251	0.40
RZ95_RS10585	2161636-2162170	0.60	RZ95_RS11075	2260391-2262671	-0.57
RZ95_RS10590	2162376-2163843	-0.67	RZ95_RS11100	2266808-2267743	2.09
RZ95_RS10610	2166469-2167339	-1.95	RZ95_RS11110	2268421-2270458	-0.87
RZ95_RS10615	2167464-2167887	-1.90	RZ95_RS11115	2270647-2272345	1.07
RZ95_RS10620	2168227-2168662	-0.78	RZ95_RS11120	2272627-2273782	0.91
RZ95_RS10625	2168731-2169190	-1.42	RZ95_RS11125	2273784-2274528	0.99
RZ95_RS10635	2170255-2170909	0.50	RZ95_RS11130	2274560-2276222	1.12
RZ95_RS10640	2170933-2171659	0.58	RZ95_RS11140	2278254-2279517	-0.47
RZ95_RS10645	2171672-2172383	1.17	RZ95_RS11160	2281852-2283283	1.38
RZ95_RS10650	2172393-2172591	0.65	RZ95_RS11170	2283643-2286042	1.26
RZ95_RS10655	2172626-2173655	0.62	RZ95_RS11195	2286550-2287159	0.99
RZ95_RS10660	2173661-2174700	0.55	RZ95_RS11205	2287894-2289139	0.69
RZ95_RS10675	2175569-2177387	0.79	RZ95_RS11230	2294794-2298064	-0.84
RZ95_RS10685	2178121-2179500	-0.97	RZ95_RS11240	2299824-2302244	-0.72
RZ95_RS10710	2183572-2184385	-0.68	RZ95_RS11255	2302286-2303844	-0.97
RZ95_RS10715	2184549-2185560	-2.44	RZ95_RS11260	2303904-2304312	0.62
RZ95_RS10720	2185597-2186203	-2.15	RZ95_RS11265	2304643-2305489	1.10
RZ95_RS10725	2186287-2187999	-1.90	RZ95_RS11275	2306722-2307541	-0.93

gene NCBI	locus	log2(F/OF)	gene NCBI	locus	log2(F/OF)
RZ95_RS11280	2307695-2308466	-0.51	RZ95_RS11805	2418410-2419226	-0.67
RZ95_RS11315	2313877-2314264	-0.99	RZ95_RS11810	2419256-2421746	-0.54
RZ95_RS11355	2321264-2321516	-1.24	RZ95_RS11815	2421748-2422477	-0.48
RZ95_RS11360	2321691-2324141	-1.16	RZ95_RS11820	2422488-2423130	-0.43
RZ95_RS11365	2321691-2324141	-1.24	RZ95_RS11845	2428417-2429056	1.13
RZ95_RS11385	2327683-2328316	-0.43	RZ95_RS11850	2429216-2429834	0.52
RZ95_RS11390	2328380-2328932	-1.45	RZ95_RS11860	2431910-2433530	1.20
RZ95_RS11395	2328934-2329219	-1.21	RZ95_RS11865	2433956-2437643	0.51
RZ95_RS11410	2330244-2331178	1.45	RZ95_RS11905	2444698-2445976	0.76
RZ95_RS11485	2348816-2352121	1.49	RZ95_RS11910	2446043-2446553	1.52
RZ95_RS11490	2348816-2352121	1.40	RZ95_RS11925	2447738-2448536	0.79
RZ95_RS11495	2352155-2353737	1.28	RZ95_RS11930	2448602-2449511	0.56
RZ95_RS11500	2352155-2353737	1.30	RZ95_RS11940	2450111-2450629	-0.82
RZ95_RS11505	2353772-2355005	1.25	RZ95_RS11950	2451404-2453284	-0.81
RZ95_RS11510	2355372-2356284	0.53	RZ95_RS11955	2453415-2453754	-1.30
RZ95_RS11515	2356625-2359589	4.02	RZ95_RS11960	2453802-2454333	-0.53
RZ95_RS11520	2359671-2360067	1.25	RZ95_RS11980	2456330-2456852	-0.55
RZ95_RS11525	2360138-2360729	0.96	RZ95_RS11985	2457161-2458160	-0.64
RZ95_RS11530	2360877-2363307	1.03	RZ95_RS11990	2458298-2459486	0.72
RZ95_RS11565	2369201-2369996	0.77	RZ95_RS12010	2463881-2465201	-1.61
RZ95_RS11570	2369999-2370710	0.69	RZ95_RS12025	2466313-2467513	0.85
RZ95_RS11580	2371002-2371662	-0.64	RZ95_RS12030	2467654-2469829	-0.58
RZ95_RS11585	2371739-2373056	-1.01	RZ95_RS12040	2470648-2473315	2.22
RZ95_RS11590	2373119-2373638	-0.89	RZ95_RS12045	2473410-2474190	0.79
RZ95_RS11595	2373879-2375925	1.17	RZ95_RS12050	2474207-2474669	0.85
RZ95_RS11600	2375927-2376494	0.76	RZ95_RS12110	2478021-2478168	-2.97
RZ95_RS11605	2376700-2377435	1.23	RZ95_RS12115	2478286-2479420	0.45
RZ95_RS11620	2378873-2379350	-0.75	RZ95_RS12125	2479944-2484426	-0.41
RZ95_RS11625	2379460-2380945	0.45	RZ95_RS12130	2484592-2486665	-0.80
RZ95_RS11635	2383093-2383946	2.04	RZ95_RS12135	2486715-2487252	-0.91
RZ95_RS11640	2384157-2385792	1.04	RZ95_RS12140	2487257-2487626	-1.05
RZ95_RS11645	2385859-2386150	0.88	RZ95_RS12145	2487653-2488037	-1.09
RZ95_RS11655	2386362-2388041	-1.05	RZ95_RS12160	2489890-2490145	-1.11
RZ95_RS11660	2388456-2390289	0.89	RZ95_RS12165	2490202-2491330	-0.65
RZ95_RS11665	2390757-2392275	-1.66	RZ95_RS12170	2491351-2494456	-0.42
RZ95_RS11675	2394379-2394808	-1.07	RZ95_RS12210	2504028-2507518	-2.34
RZ95_RS11700	2397101-2398007	0.47	RZ95_RS12215	2504028-2507518	-1.65
RZ95_RS11710	2398586-2399579	-1.03	RZ95_RS12220	2504028-2507518	-1.39
RZ95_RS11725	2400400-2400922	0.61	RZ95_RS12230	2509160-2509490	-0.57
RZ95_RS11740	2402860-2404477	-0.77	RZ95_RS12235	2509533-2509998	-1.44
RZ95_RS11745	2404617-2405532	-0.93	RZ95_RS12260	2515832-2516807	-0.67
RZ95_RS11760	2408649-2410176	0.69	RZ95_RS12275	2517979-2518651	0.56
RZ95_RS11770	2410996-2411539	1.14	RZ95_RS12285	2519828-2521448	-1.47
RZ95_RS11775	2412053-2412218	-1.15	RZ95_RS12300	2523331-2523880	-1.23
RZ95_RS11780	2412286-2413465	-0.50	RZ95_RS12305	2523892-2525542	-0.73
RZ95_RS11790	2414474-2415377	0.50	RZ95_RS12325	2529271-2529463	-1.16
RZ95_RS11795	2415463-2417548	-0.71	RZ95_RS12330	2529524-2531231	-2.29

gene NCBI	locus	log2(F/OF)	gene NCBI	locus	log2(F/OF)
RZ95_RS12335	2531395-2531674	-2.63	RZ95_RS12815	2635573-2636836	1.20
RZ95_RS12340	2531961-2532384	1.36	RZ95_RS12820	2637413-2638916	-0.53
RZ95_RS12345	2532944-2533889	-1.99	RZ95_RS12825	2639329-2640775	1.62
RZ95_RS12350	2533957-2536124	-1.63	RZ95_RS12835	2642620-2643315	-2.29
RZ95_RS12355	2533957-2536124	-1.60	RZ95_RS12840	2643866-2646324	-1.37
RZ95_RS12360	2533957-2536124	-1.38	RZ95_RS12845	2643866-2646324	-1.27
RZ95_RS12370	2537633-2538821	-0.52	RZ95_RS12850	2646540-2647947	-0.44
RZ95_RS12385	2539749-2541766	-0.85	RZ95_RS12855	2648081-2649008	0.62
RZ95_RS12390	2541767-2542448	-0.82	RZ95_RS12860	2649026-2650146	0.69
RZ95_RS12395	2542451-2544110	0.54	RZ95_RS12890	2654661-2655567	0.62
RZ95_RS12405	2544533-2545658	-1.68	RZ95_RS12895	2655726-2656638	0.63
RZ95_RS12415	2546906-2548163	-1.01	RZ95_RS13100	2693741-2694791	-1.30
RZ95_RS12420	2548299-2548929	0.59	RZ95_RS13105	2694799-2695579	-1.45
RZ95_RS12430	2550009-2550483	-0.88	RZ95_RS13110	2695603-2697591	-0.55
RZ95_RS12435	2550498-2551356	-1.26	RZ95_RS13130	2700003-2700552	-1.73
RZ95_RS12450	2554246-2555599	-0.55	RZ95_RS13215	2720696-2722181	-0.92
RZ95_RS12460	2556436-2557498	1.66	RZ95_RS13270	2736079-2736814	-1.36
RZ95_RS12465	2557662-2559063	1.06	RZ95_RS13275	2736998-2737688	-0.46
RZ95_RS12475	2560575-2561397	2.53	RZ95_RS13280	2737810-2738848	-1.20
RZ95_RS12480	2561582-2562866	2.81	RZ95_RS13285	2738874-2739996	-1.02
RZ95_RS12485	2562887-2563526	3.00	RZ95_RS13310	2742599-2743055	-2.86
RZ95_RS12490	2563547-2564123	2.68	RZ95_RS13335	2748156-2749005	-0.63
RZ95_RS12535	2572517-2573537	-0.58	RZ95_RS13340	2749173-2750076	-0.43
RZ95_RS12540	2574437-2575682	-1.38	RZ95_RS13360	2754372-2755023	-1.38
RZ95_RS12545	2576010-2577168	0.87	RZ95_RS13365	2755279-2756212	-1.45
RZ95_RS12550	2577248-2577866	-1.54	RZ95_RS13370	2756222-2757272	-0.82
RZ95_RS12555	2578068-2578803	-0.85	RZ95_RS13375	2757395-2758127	-0.56
RZ95_RS12615	2590714-2591188	0.56	RZ95_RS13380	2758196-2759009	-0.92
RZ95_RS12620	2591412-2591991	-1.96	RZ95_RS13385	2759011-2759284	-0.93
RZ95_RS12625	2592161-2592680	-1.14	RZ95_RS13390	2759405-2759693	-1.23
RZ95_RS12640	2594910-2596104	-0.67	RZ95_RS13405	2764103-2765057	-0.51
RZ95_RS12645	2596553-2596748	-0.94	RZ95_RS13415	2765896-2766712	-1.14
RZ95_RS12650	2597204-2597990	-1.16	RZ95_RS13420	2766741-2767200	-0.61
RZ95_RS12655	2598027-2599452	-0.89	RZ95_RS13425	2767306-2768188	1.69
RZ95_RS12665	2601133-2601838	-0.62	RZ95_RS13435	2769760-2771896	0.68
RZ95_RS12680	2603228-2605355	-1.01	RZ95_RS13440	2772026-2772497	0.55
RZ95_RS12685	2605449-2607873	-0.84	RZ95_RS13445	2772674-2773049	0.56
RZ95_RS12745	2619607-2620288	0.62	RZ95_RS13450	2773203-2774661	-1.37
RZ95_RS12750	2620567-2621392	0.91	RZ95_RS13455	2774939-2776169	-0.54
RZ95_RS12755	2621471-2622698	2.02	RZ95_RS13465	2776726-2777833	0.48
RZ95_RS12760	2622754-2624254	2.82	RZ95_RS13470	2778020-2779463	0.60
RZ95_RS12765	2624657-2625635	2.76	RZ95_RS13480	2780003-2781101	-0.52
RZ95_RS12770	2625656-2626997	2.49	RZ95_RS13505	2784662-2785430	-0.87
RZ95_RS12775	2627020-2629521	2.20	RZ95_RS13515	2786321-2786807	-0.60
RZ95_RS12780	2627020-2629521	2.19	RZ95_RS13525	2787240-2787558	0.57
RZ95_RS12785	2629534-2630752	1.85	RZ95_RS13540	2787791-2790814	0.95
RZ95_RS12790	2630829-2632101	2.07	RZ95_RS13550	2791763-2792450	0.42

gene NCBI	locus	log2(F/OF)	gene NCBI	locus	log2(F/OF)
RZ95_RS13555	2792628-2792904	-0.82	RZ95_RS14050	2895267-2895912	-1.00
RZ95_RS13560	2792921-2793977	-1.03	RZ95_RS14075	2900521-2903170	0.45
RZ95_RS13565	2793987-2795097	-1.07	RZ95_RS14085	2903803-2905816	1.26
RZ95_RS13590	2799233-2799899	0.46	RZ95_RS14090	2905832-2907533	1.43
RZ95_RS13595	2800028-2800559	-1.09	RZ95_RS14175	2922613-2923048	0.85
RZ95_RS13600	2800582-2801185	-0.97	RZ95_RS14210	2927590-2928481	1.92
RZ95_RS13605	2801308-2801857	-1.06	RZ95_RS14220	2929850-2930897	1.09
RZ95_RS13635	2808995-2809964	-1.29	RZ95_RS14235	2931895-2932312	0.93
RZ95_RS13645	2811638-2812730	0.42	RZ95_RS14265	2937549-2938512	1.04
RZ95_RS13665	2814800-2816758	-0.58	RZ95_RS14295	2944351-2945374	0.85
RZ95_RS13670	2816764-2817016	-0.61	RZ95_RS14315	2948169-2950923	-1.55
RZ95_RS13675	2817152-2817485	-3.57	RZ95_RS14320	2951050-2951872	-0.55
RZ95_RS13680	2817656-2819111	-0.65	RZ95_RS14325	2951878-2952829	-0.92
RZ95_RS13685	2819435-2819990	-1.09	RZ95_RS14330	2952876-2953695	-0.43
RZ95_RS13690	2820050-2820362	-0.82	RZ95_RS14340	2955544-2957624	-1.24
RZ95_RS13715	2823353-2826273	-1.46	RZ95_RS14345	2957887-2960083	-1.21
RZ95_RS13730	2826890-2828435	-1.26	RZ95_RS14350	2960324-2961341	-0.99
RZ95_RS13755	2832777-2833203	-2.22	RZ95_RS14360	2962433-2963765	-0.87
RZ95_RS13780	2837338-2840035	-0.43	RZ95_RS14365	2964071-2965337	-0.42
RZ95_RS13785	2840197-2842963	0.51	RZ95_RS14370	2965815-2967033	-0.46
RZ95_RS13800	2844558-2846666	1.20	RZ95_RS14390	2971144-2972050	1.12
RZ95_RS13810	2846696-2848220	-1.18	RZ95_RS14395	2972228-2973098	0.60
RZ95_RS13815	2848483-2848810	-0.64	RZ95_RS14400	2973120-2973399	1.03
RZ95_RS13820	2849140-2850409	1.03	RZ95_RS14405	2974130-2975657	-0.73
RZ95_RS13850	2856238-2856451	-1.47	RZ95_RS14410	2975761-2976310	-1.03
RZ95_RS13855	2856580-2857132	-1.31	RZ95_RS14420	2977190-2978501	-0.54
RZ95_RS13860	2857285-2857645	0.90	RZ95_RS14425	2978529-2979135	-0.98
RZ95_RS13865	2857656-2857851	0.96	RZ95_RS14440	2980932-2983209	0.87
RZ95_RS13870	2858072-2859326	0.77	RZ95_RS14460	2988091-2989789	-0.84
RZ95_RS13880	2860273-2860702	1.61	RZ95_RS14470	2989890-2992231	-0.98
RZ95_RS13885	2860703-2860997	1.09	RZ95_RS14475	2989890-2992231	-1.15
RZ95_RS13895	2861707-2862325	-0.49	RZ95_RS14485	2992968-2993595	-0.55
RZ95_RS13905	2863174-2863726	0.66	RZ95_RS14505	2994994-2996229	0.79
RZ95_RS13910	2863731-2865654	0.53	RZ95_RS14515	2998757-2999540	-0.73
RZ95_RS13915	2866165-2867809	-1.16	RZ95_RS14555	3005024-3005483	-1.83
RZ95_RS13930	2868424-2869542	-0.46	RZ95_RS14560	3005597-3006125	-0.42
RZ95_RS13955	2873352-2873751	-1.03	RZ95_RS14570	3006182-3007210	-0.70
RZ95_RS13960	2873769-2874531	-0.90	RZ95_RS14585	3009150-3009852	-0.41
RZ95_RS13965	2874649-2875417	-0.67	RZ95_RS14595	3011577-3011814	0.93
RZ95_RS13975	2877797-2879186	0.67	RZ95_RS14600	3011826-3011982	1.06
RZ95_RS14010	2886630-2887035	0.63	RZ95_RS14605	3012124-3013840	-0.42
RZ95_RS14015	2887082-2887691	0.77	RZ95_RS14615	3014282-3014786	-1.09
RZ95_RS14020	2887707-2889045	0.75	RZ95_RS14620	3014861-3015251	0.75
RZ95_RS14025	2889230-2889932	-0.99	RZ95_RS14635	3017767-3018919	-1.62
RZ95_RS14030	2890029-2891484	-0.50	RZ95_RS14645	3019959-3020409	-1.29
RZ95_RS14035	2891487-2891811	-2.54	RZ95_RS14650	3020488-3021058	-1.58
RZ95_RS14040	2891822-2892950	-1.27	RZ95_RS14665	3022527-3025170	-0.50

gene NCBI	locus	log2(F/OF)	gene NCBI	locus	log2(F/OF)
RZ95_RS14670	3025206-3025656	-0.97	RZ95_RS15200	3138315-3139818	0.95
RZ95_RS14675	3025726-3026716	0.45	RZ95_RS15210	3141582-3144423	-0.65
RZ95_RS14695	3029702-3030641	0.92	RZ95_RS15220	3144424-3146598	-0.86
RZ95_RS14705	3032226-3033345	-1.37	RZ95_RS15245	3148201-3151305	0.82
RZ95_RS14710	3033486-3034854	-1.51	RZ95_RS15250	3151314-3152799	1.29
RZ95_RS14715	3034919-3036224	-0.94	RZ95_RS15255	3152838-3153363	1.71
RZ95_RS14730	3038137-3039145	-0.72	RZ95_RS15280	3154179-3154264	2.52
RZ95_RS14735	3039375-3039597	1.03	RZ95_RS15285	3154317-3154647	0.78
RZ95_RS14750	3040728-3041808	-2.45	RZ95_RS15290	3154660-3155452	0.71
RZ95_RS14755	3041845-3042406	-2.38	RZ95_RS15295	3155731-3157444	-0.64
RZ95_RS14760	3042505-3043156	-3.05	RZ95_RS15300	3157474-3159561	-0.50
RZ95_RS14765	3043177-3044611	-2.86	RZ95_RS15310	3159567-3160167	0.60
RZ95_RS14775	3045506-3046364	0.57	RZ95_RS15315	3160182-3161097	1.65
RZ95_RS14780	3046422-3046929	-1.20	RZ95_RS15320	3161132-3161882	0.97
RZ95_RS14785	3046999-3047245	-2.09	RZ95_RS15325	3162024-3162348	-0.52
RZ95_RS14795	3048295-3048778	-0.85	RZ95_RS15330	3162739-3164401	-1.14
RZ95_RS14800	3048859-3051157	-1.07	RZ95_RS15335	3164512-3165503	-0.70
RZ95_RS14810	3051541-3052156	-0.74	RZ95_RS15355	3166927-3169009	0.73
RZ95_RS14820	3053041-3054178	-1.31	RZ95_RS15370	3170995-3172798	-0.47
RZ95_RS14840	3057301-3059494	-1.82	RZ95_RS15380	3173545-3174340	0.73
RZ95_RS14855	3062310-3063210	0.66	RZ95_RS15390	3176414-3176759	-0.67
RZ95_RS14865	3064453-3065122	1.17	RZ95_RS15395	3176914-3177322	-0.76
RZ95_RS14875	3067087-3070570	0.51	RZ95_RS15405	3178934-3181088	-0.66
RZ95_RS14900	3073204-3073849	3.07	RZ95_RS15410	3181100-3182273	-0.77
RZ95_RS14905	3074131-3074407	0.89	RZ95_RS15430	3187561-3188260	-1.20
RZ95_RS14910	3074503-3075601	1.45	RZ95_RS15435	3188317-3188590	-0.84
RZ95_RS14950	3082667-3083057	-1.52	RZ95_RS15440	3188702-3189452	-1.11
RZ95_RS14960	3084046-3084610	-1.16	RZ95_RS15455	3191139-3191340	-2.50
RZ95_RS14965	3084660-3085617	-0.65	RZ95_RS15460	3192236-3192416	-1.41
RZ95_RS14985	3088257-3088818	-0.48	RZ95_RS15465	3192426-3194484	-1.14
RZ95_RS14990	3088876-3089287	-1.19	RZ95_RS15470	3194561-3195713	-1.18
RZ95_RS15025	3093622-3094649	-0.66	RZ95_RS15475	3195893-3197813	1.21
RZ95_RS15065	3101905-3102244	0.76	RZ95_RS15480	3197909-3198254	-1.70
RZ95_RS15075	3103022-3103460	-0.59	RZ95_RS15485	3198414-3199002	-4.05
RZ95_RS15085	3104851-3107074	-0.49	RZ95_RS15495	3200789-3201674	-0.93
RZ95_RS15095	3109048-3109924	1.56	RZ95_RS15500	3201756-3202256	-1.03
RZ95_RS15100	3110125-3110578	-0.99	RZ95_RS15505	3202416-3202773	-2.15
RZ95_RS15105	3110721-3111675	-1.21	RZ95_RS15510	3202922-3203462	-2.99
RZ95_RS15110	3111685-3112042	-1.72	RZ95_RS15520	3207984-3212073	0.59
RZ95_RS15115	3112114-3112375	-2.16	RZ95_RS15525	3212374-3212740	0.60
RZ95_RS15125	3113873-3115967	1.12	RZ95_RS15530	3212788-3213295	0.63
RZ95_RS15155	3128181-3128724	-1.17	RZ95_RS15535	3213596-3214292	0.89
RZ95_RS15160	3128778-3130206	-1.48	RZ95_RS15540	3214295-3214724	0.88
RZ95_RS15165	3130402-3131107	-0.79	RZ95_RS15545	3214842-3215376	0.99
RZ95_RS15170	3131274-3132219	-0.49	RZ95_RS15550	3215383-3215824	0.51
RZ95_RS15185	3134708-3135785	1.14	RZ95_RS15575	3217571-3217655	1.26
RZ95_RS15195	3137521-3138304	0.93	RZ95_RS15590	3219488-3220157	-0.76

gene NCBI	locus	log2(F/OF)	gene NCBI	locus	log2(F/OF)
RZ95_RS15620	3225680-3226109	0.46	RZ95_RS16125	3334229-3335384	-0.72
RZ95_RS15640	3228945-3229866	-0.65	RZ95_RS16135	3336585-3337155	0.52
RZ95_RS15645	3229986-3230727	-0.92	RZ95_RS16140	3337554-3338475	1.00
RZ95_RS15650	3230778-3231888	-0.61	RZ95_RS16145	3338810-3339365	-0.74
RZ95_RS15665	3234046-3234763	1.19	RZ95_RS16150	3339488-3340034	-0.77
RZ95_RS15675	3236509-3237514	0.61	RZ95_RS16155	3340231-3340606	1.56
RZ95_RS15680	3237854-3239747	2.20	RZ95_RS16180	3343589-3344009	0.46
RZ95_RS15685	3239822-3240443	-0.96	RZ95_RS16185	3344035-3345430	0.51
RZ95_RS15690	3240453-3241251	-0.53	RZ95_RS16190	3345456-3346326	0.58
RZ95_RS15695	3241460-3241988	0.41	RZ95_RS16195	3346414-3347959	0.52
RZ95_RS15700	3242047-3242911	1.23	RZ95_RS16200	3348003-3348540	0.56
RZ95_RS15705	3243126-3244323	-0.40	RZ95_RS16205	3348552-3349023	0.52
RZ95_RS15710	3244342-3245689	-0.43	RZ95_RS16215	3349391-3350267	0.80
RZ95_RS15720	3246127-3248325	0.49	RZ95_RS16220	3350374-3350773	1.27
RZ95_RS15730	3248423-3249341	-0.47	RZ95_RS16225	3350944-3351784	0.94
RZ95_RS15735	3249467-3250277	-0.52	RZ95_RS16235	3351925-3353187	0.56
RZ95_RS15740	3250406-3251711	-0.89	RZ95_RS16240	3353190-3353991	0.85
RZ95_RS15745	3251776-3252916	-0.45	RZ95_RS16245	3353995-3355097	1.14
RZ95_RS15750	3253001-3254033	-1.42	RZ95_RS16255	3355258-3356179	-0.89
RZ95_RS15755	3254272-3254908	-0.53	RZ95_RS16280	3363294-3364995	-0.60
RZ95_RS15760	3254929-3256498	0.49	RZ95_RS16285	3365267-3365867	-0.59
RZ95_RS15765	3256513-3257935	0.50	RZ95_RS16290	3365875-3366160	-0.89
RZ95_RS15780	3260804-3261875	-0.74	RZ95_RS16300	3368421-3369024	0.41
RZ95_RS15785	3261877-3262978	-0.64	RZ95_RS16310	3369668-3370310	-0.95
RZ95_RS15790	3263136-3264985	-1.22	RZ95_RS16315	3370441-3370840	-1.29
RZ95_RS15800	3265017-3265653	-0.50	RZ95_RS16320	3370940-3371888	-1.69
RZ95_RS15805	3265738-3266287	0.59	RZ95_RS16330	3373018-3374587	1.53
RZ95_RS15810	3266432-3267092	0.72	RZ95_RS16335	3374734-3375082	-1.50
RZ95_RS15815	3267119-3269518	0.77	RZ95_RS16340	3375208-3375623	-1.46
RZ95_RS15820	3267119-3269518	0.73	RZ95_RS16355	3377267-3378508	-1.41
RZ95_RS15825	3269532-3269991	0.69	RZ95_RS16360	3377267-3378508	-0.49
RZ95_RS15830	3270142-3271546	-0.86	RZ95_RS16435	3393244-3394162	1.52
RZ95_RS15835	3271605-3271944	-1.23	RZ95_RS16440	3395360-3396026	0.67
RZ95_RS15975	3298916-3300242	-0.63	RZ95_RS16445	3396028-3397423	0.46
RZ95_RS15990	3301503-3301884	-0.49	RZ95_RS16450	3397941-3399057	0.44
RZ95_RS15995	3301931-3303611	-1.02	RZ95_RS16465	3400018-3401435	1.14
RZ95_RS16000	3303759-3305979	-0.80	RZ95_RS16475	3401455-3402820	0.50
RZ95_RS16015	3307937-3308582	-0.46	RZ95_RS16480	3402832-3404671	0.44
RZ95_RS16035	3311776-3312751	0.84	RZ95_RS16485	3404730-3406101	0.49
RZ95_RS16050	3316550-3317264	0.44	RZ95_RS16510	3411777-3412653	0.91
RZ95_RS16060	3318986-3319343	-0.51	RZ95_RS16580	3427165-3428423	0.83
RZ95_RS16065	3319403-3319946	-0.69	RZ95_RS16605	3429150-3432496	1.06
RZ95_RS16070	3320328-3323099	1.60	RZ95_RS16620	3433171-3434937	1.77
RZ95_RS16090	3325100-3328023	-1.38	RZ95_RS16630	3435986-3437264	0.75
RZ95_RS16105	3328696-3330241	-1.21	RZ95_RS16645	3439182-3441381	0.85
RZ95_RS16110	3330948-3332976	0.58	RZ95_RS16650	3441594-3442299	-0.67
RZ95_RS16115	3333047-3333485	0.49	RZ95_RS16665	3444840-3445413	-0.51

gene NCBI	locus	log2(F/OF)	gene NCBI	locus	log2(F/OF)
RZ95_RS16675	3446516-3447233	1.44	RZ95_RS16865	3488117-3488630	0.78
RZ95_RS16685	3448181-3449816	0.82	RZ95_RS16875	3489416-3490784	-0.51
RZ95_RS16690	3449889-3450507	-1.23	RZ95_RS16880	3490846-3491228	-0.57
RZ95_RS16695	3450687-3452096	-0.56	RZ95_RS16900	3493209-3493500	-1.76
RZ95_RS16705	3452132-3452879	-1.26	RZ95_RS16905	3493898-3494864	1.36
RZ95_RS16715	3454003-3454387	0.51	RZ95_RS16930	3499371-3499899	-0.92
RZ95_RS16725	3455164-3456517	-0.62	RZ95_RS16935	3500072-3500324	-1.68
RZ95_RS16730	3456848-3457814	-2.23	RZ95_RS16950	3502466-3503420	1.39
RZ95_RS16735	3457824-3458820	-2.43	RZ95_RS16960	3503909-3505055	0.59
RZ95_RS16740	3458846-3460837	-2.87	RZ95_RS16970	3506553-3508317	1.03
RZ95_RS16745	3458846-3460837	-2.20	RZ95_RS16975	3508322-3508643	1.59
RZ95_RS16750	3460847-3461648	-2.75	RZ95_RS16980	3508652-3509042	1.46
RZ95_RS16760	3462704-3463265	-0.97	RZ95_RS16985	3509075-3509210	0.82
RZ95_RS16765	3463397-3464534	-2.83	RZ95_RS16990	851879-852257	-0.89
RZ95_RS16790	3469812-3470355	-1.54	RZ95_RS19965	72033-72192	-1.61
RZ95_RS16825	3475934-3478854	-1.38	RZ95_RS20005	532241-532433	-1.02
RZ95_RS16840	3479558-3481103	-1.56	RZ95_RS20010	680284-680428	1.01
RZ95_RS16855	3484918-3486202	-0.67	RZ95_RS20025	852459-853453	0.73
RZ95_RS16860	3486980-3488102	0.71	RZ95_RS20255	2329318-2329502	-0.88